Identification and Roles of Cell Substrates of Intracellular Mono-ADP-Ribosylation

Thesis

Identification and Roles of Cell Substrates of Intracellular Mono-ADP-Ribosylation

Giovanna Grimaldi, MSc

Discipline: Life and Biomolecular Sciences

Affiliated Research Centre Programme:

Telethon Institute of Genetics and Medicine and Consorzio Mario Negri Sud

Thesis submitted in accordance with the requirements of the Open University

for the degree of Doctor of Philosophy

August 2011

DATE OF SUBMISSION: 25 AUGUST 2011

DATE OF AWARD: 2 FEBRUARY 2012

PAGE

NUMBERING

AS ORIGINAL

To my parents

Considerate la vostra semenza:

fatti non foste a viver come bruti, ma per seguir virtute e canoscenza

Dante Alighieri

La Divina Commedia, L'inferno, canto XXVI

Abstract

Mono-ADP-ribosylation is a reversible post-translational modification that is catalysed by either bacterial pathogenic toxins or endogenous cellular ADP-ribosyltransferases (ARTs), and that can modulate the functions of target proteins. This latter aspect has only recently emerged as an important mechanism in mammalian cells for the control of a vast array of cellular processes. Some of the members of the poly-ADP-ribosyl-polymerase (PARP) family are among the mammalian enzymes that can catalyse mono-ADP-ribosylation. Here, based on biochemical data, I provide evidence that the PARP family member PARP12 is a mono-ART (mART) that can modify acidic amino acid residues. Using an affinity purification method based on a protein module that recognises ADP-ribosylated proteins (the macro domain), together with liquid chromatography coupled to tandem mass spectrometry, I have identified 25 putative PARP12 substrates that are involved in different cellular processes. The identification of this range of substrates suggests that PARP12 is involved in multiple cellular functions, ranging from regulation of small-GTPases to the control of newly synthesized RNA. To determine its biological role, I analysed its intracellular localisation. Data reported here show that PARP12 is a mART that is localised to the Golgi complex, where it can use the NAD^+ pool present on this organelle to modify Golgi-localised proteins. In line with these findings, among the PARP12 substrates, I identified Rab1A, a small GTPase that controls both transport from the endoplasmic reticulum to the Golgi complex, and the structure of the Golgi itself. My data suggest a role for PARP12 in maintenance of Golgi structure, potentially through ADP-ribosylation of Rab1A. A further aspect I have analysed is

the ADP-ribosylation of the dual function protein C-terminal binding protein 1/ BFA-dependent ADP-ribosylated substrate (CtBP1/BARS) as a mechanism of action of the toxin brefeldin A (BFA). BFA-induced ADP-ribosylation of CtBP1/BARS occurs through a novel mechanism that comprises two steps: (i) synthesis of a BFA-ADP-ribose conjugate (BAC); and (ii) covalent binding of the BAC into the NAD^+-binding pocket of CtBP1/BARS. Here, I demonstrate that this reaction requires the involvement of ADP-ribosyl-cyclases, such as CD38. Importantly, this modification abolishes CtBP1/BARS fissioning activity, while it increases CtBP1/BARS co-repressor activity, in a promoter-dependent context. As with sumoylation and phosphorylation, ADP-ribosylation thus represents a new mechanism for the regulation of the functions of CtBP1/BARS.

Table of contents

List of figures

List of tables

Abbreviations

3-AB	3-aminobenzamide
AADPR	Acetyl-ADPR
AcMNPV	Autographa californica multiple nuclear polyhedrosis virus
Acyl-CoA	Acyl-coenzyme A
ADP	Adenosine diphosphate
ADPR	ADP-ribose
ADPRC	ADP-ribosylcyclase
ADPRTs	ADP-ribosylating toxins
ALC1	Amplified in liver cancer 1
AMD	Auto-modification domain
AMP	Adenosine monophosphate
AMPK	AMP protein kinase
APC	Adenomatous polyposis coli
APS	Ammonium persulphate
ARFs	ADP-ribosylation factor
ART	ADP-ribosyltransferase
ARTC	ART DTX-like
ARTD	ART CLX-like
ATM	Ataxia telengiectasica-mutated
ATP	Adenosine triphosphate
BAC	BFA-ADP-ribose conjugate
BAL	B-aggressive lymphoma
BER	Base excision-repair
BFA	Brefeldin A
BRCA	Breast cancer
BSA	Bovine serum albumin

cAMP	cyclic AMP
CD	Catalytic domain
CD	Cluster of differentiation
CdK1	Cyclin dependent kinase 1
cDNA	Complementary DNA
CLL	Chronic lymphocytic leukaemia
CoaSt6	Collaborator of STAT6
COP	Coat protein complex
Cpm	Counts per minute
Crk	CT10-regulator of kinase
CtBP1/BARS	C-terminal binding protein 1/BFA ADP-ribosylated substrate
CTCF	CCCTC binding factor
CTX	Cholera toxin
DBD	DNA binding domain
DLBCL	Diffuse large B-cell lymphoma
DMEM	Dulbecco's modified eagle's medium
DMP	Dimethylpimelidate
DMSO	Dimethylsulfoxide
DNA	Deoxyribonucleic acid
DNA-PK	DNA protein kinase
Dnmt1	DNA methyltransferase 1
DSB	Double-strand break
dsDNA	Double strand DNA
DTT	DL-dithiothreitol
DTX	Diphtheria toxin
ECL	Enhnaced chemiluminescence
ECM	Extra-cellular matrix
EDTA	Ethylenediaminetetraacetic acid

EF-2	Elongation factor 2
EGF	Epidermal growth factor
EGFR	EGF receptor
EMT	Epithelial-to-mesenchymal transition
ER	Endoplasmic reticulum
ERES	ER exit sites
ERGIC	ER-Golgi intermediate compartment
ERM	Ezrin/Radixin/Moesin
ESI	Electrospray ionisation
EST	Expressed sequence tag
FBS	Foetal bovine serum
FGF	Fibroblast growth factor
FGFR	Fibroblast growth factor receptor
g	Gravity
G protein	Guanine nucleotide-binding proteins
GAP	GTPase activating protein
GAPDH	Glyceraldehyde 3-phosphate dehydrogenase
GDH	Glutamate dehydrogenase
GDP	Guanosine diphosphate
GEF	Guanine nucleotide exchange factor
GFP	Green fluorescent protein
Giα	α subunit of inhibitory G protein
GM1	Monosialotetrahexosylganglioside1
GPI	Glycosylphosphatidylinositol
GST	Glutathione S-transferase
Gsα	α subunit of stimulatory G protein
GTP	Guanosine triphosphate
Gtα	α subunit of G protein transducin

HAT	Histone acetyl transferase
HB-EGF	Heparin-binding EGF-like growth factor
HDACs	Histone deacetylases
HEPES	4-(2-Hydroxy-ethyl)-piperazine-1-ethanesulfonic acid
HIF1α	Hypoxia inducible factor 1α
His	Histidine
HMGB1	High mobility group box-1 protein
HMTases	Histone lysine methyl transferases
HNP	Human neutrophil peptide
HPLC	High performance liquid chromatography
HPRT1	Homo Sapiens Hypoxanthine Phosphoribosyltransferase 1
HR	Homologous recombination
HRP	Horse radish peroxidase
IC	Intermediate compartment
IC_{50}	Half maximal inhibitory concentration
IL	Interleukin
IPTG	Isopropyl-C-D-1-thiogalactopyranoside
KDM5B	Lysine (K)-specific demethylase 5B
K_m	Michaelis-Menten constant
LARII	Luciferase Assay Reagent II
LB	Lysogen broth
LC-MS/MS	Liquid chromatography-tandem mass spectrometry
LR	att L sites- att R sites recombination
LSD1	Histone lysine-specific demethylase
LTX	Heat-labile enterotoxin
MALDI	Matrix-assisted laser desorption/ ionisation
mARTs	mono-ADP-ribosyltransferases
MEFs	Mouse embryo fibroblasts

MEM	Minimum Essential Medium
MIBG	*meta*-iodobenzylguanidine
mRNA	messenger RNA
MVP	Major vault protein
NA	Nicotinic acid
NAADP	Nicotinic acid adenine dinucleotide phosphate
NAADPR	Nicotinic acid-ADPR
NAD	Nicotinamide-adenine dinucleotide
NADP	NAD phosphate
NBD	Nucleotide binding domain
NES	Nuclear-export sequence
Nf-kB	Nuclear Factor Kappa-light-chain-enhancer of activated B cells
NHEJ	Non-homologous end-joining
NICD	NAD^+-induced cell death
NLS	Nuclear localisation signal
nNOS	Neuronal nitric-oxide synthase
NOXA	NADPH oxidase activator
O/N	Over-night
OD	Optical density
PAK1/6	p21-activated kinase 1/6
PARG	Poly-ADPR-glycohydrolases
PARPs	Poly-ADP-ribose polymerases
pART	Poly-ADP-ribosyltransferase
PBS	Phosphate-buffered saline
PBZ	Poly-ADPR-binding zinc finger
PCR	Polymerase chain reaction
PDGF	Platelet-derived growth factor
PDGF-BB	BB isoform of platelet-derived growth factor

PGC-1α	PPARγ co-activator-1α
PH	Polyhedron promoter
PLB	Passive lysis buffer
PPARγ	Peroxisome-proliferator activated receptor-γ
PTB	Phosphotyrosine binding
PTM	Post-translational modifications
PTX	Pertussis Toxin
qRT-PCR	Quantitative reverse transcription polymerase chain reaction
RAR	Retinoic acid receptor
RepI/II	Reporter I/II
RIPA	Radio-immuno-precipitation-assay
RNA	Ribonucleic acid
RNP	Ribonucleoprotein
Rpm	Revolutions per minute
RRB1	Ras responsive element binding protein 1
RT	Room temperature
SBD	Substrate binding domain
SDS	Sodium dodecyl sulphate
SDS-PAGE	SDS-polyacrylamide gel electrophoresis
SH2	Src Homology domain 2
SH3	Src Homology domain 3
Sir2	Silent information regulator 2
siRNA	Short-interfering RNA
SIRT	Sirtuin
SSBs	Single strand breaks
STAT1/6	Signal transducer and activator of transcription 1/6
SUMO	Small ubiquitin-like modifier
TAE	Tris/acetic acid/EDTA

TBA	tetrabutylammonium
TBE	Tris/boric acid/EDTA
TCA	Trichloroacetic acid
TCDD	2,3,7,8-tetrachlorodibenzo-p-dioxin
TE	Tris/EDTA
TEMED	N,N,N',N'-tetramethylethylenediamine
TEP1	Telomerase-associated protein 1
TFF1	Trefoil factor 1
TGN	*trans*-Golgi network
TLE	Trasducin-like enhancer
TNFα	Tumour necrosis factor α
TRF1	Telomeric repeat binding factor 1
TRIS	Tris-[hydroxymethyl]-aminomethane
VIP2	Vegetative insecticidal protein
V_{max}	Maximal velocity of an enzymatic reaction at saturating substrate concentration
VTCs	Vesicular tubular clusters
X-Gal	5-bromo-4-chloro-3-indolyl-D-galactoside
YFP	Yellow fluorescent protein
ZAP	Zinc-finger CCCH-type antiviral protein
ZEB	Zinc finger E-box-binding homeobox
Znf217	Zinc finger protein 217

CHAPTER 1. Introduction

1.1 Post-translational modifications: regulators of protein function and signal integration

The complex physiology of eukaryotic cells is regulated by a number of multilayered and interconnected mechanisms. Transcription of new mRNA, alternative RNA splicing, and translation into a protein, which can then be followed by post-translational modifications (PTMs) of a protein, create a continuously fine-tuned regulatory network. Of the various regulatory mechanisms available to the cell, PTMs serve a particular purpose, as they are both highly dynamic and largely reversible. As a result of improved detection technologies, the list of protein modifications in the literature has risen to well over 200 (Mann and Jensen, 2003). This extensive array that includes many reversible PTMs creates signalling diversity and is particularly suitable for relaying rapid messages in the cell. Some PTMs, including glycosylation, lipidation and disulphide bridge formation, are stable and are important for maturation and correct folding of newly synthesized proteins. Others, such as phosphorylation, are more transient, and thus have essential roles in intracellular signalling. A crucial aspect of signalling through PTMs is the presence of modular protein domains that recognise particular types of PTMs located on specific amino-acid residues. This coupling of PTMs with PTM-recognition domains creates an attractive 'decoding' mechanism for monitoring and responding to alterations in the cellular microenvironment (Sims and Reinberg, 2008).

The classical example of PTMs is phosphorylation, which involves the transfer of the γ-phosphate group from ATP to specific amino acids. The first protein kinase activity was reported in 1954 for the phosphorylation of casein (Burnett and Kennedy, 1954). Over the next few decades, a rapidly growing body of evidence revealed the importance of reversible phosphorylation as a versatile tool to regulate protein function. Phosphatases removing the phosphate group from modified residues were also discovered, and were shown to have specificity towards individual phosphorylated residues (Barford et al., 1998). To date, besides phosphorylation, a variety of further important PTMs have been identified and are under study, including in particular, methylation, ubiquitination and acetylation, to name just a few. ADP-ribosylation is another PTM, which is the focus of the present thesis.

The ADP-ribosylation reaction

The modification of proteins by ADP-ribosylation is a phylogenetically ancient mechanism (Corda and Di Girolamo, 2003). It involves the transfer of ADP-ribose (ADPR) from NAD^+ to target proteins, and it is accompanied by the release of nicotinamide (Figure 1.1). As with phosphorylation, this reaction is reversible and thus the extent of protein modification by ADP-ribosylation depends on the activity of cellular ADP-ribosylhydrolases that reverse the reaction by hydrolysing the protein ADP-ribose linkage (Figure 1.1) (Corda and Di Girolamo, 2003). The consumption of NAD^+ by ADP-ribosylating enzymes connects them not only to energy metabolism, but also to other NAD^+-consuming enzymes, including the histone deacetylases (HDACs) of the Sirtuin family and ADP-ribosyl cyclases (Ying, 2006) (see sections 1.3.1 1.3.3).

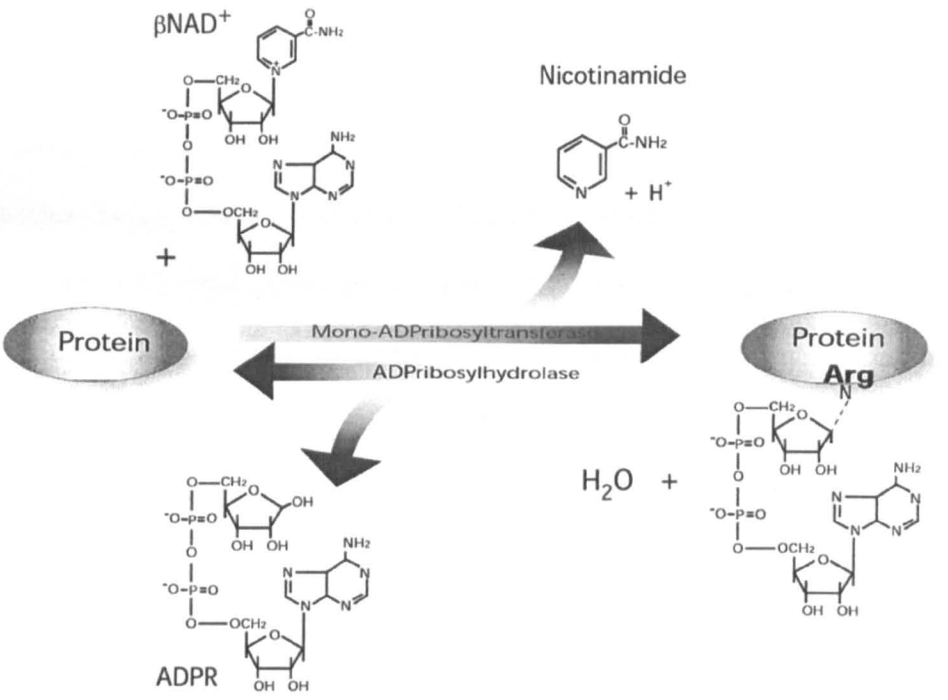

Figure 1.1: The ADP-ribosylation reaction

A schematic representation of the reversible mono-ADP-ribosylation reaction. An arginine-specific mono-ADP-ribosyltransferase catalyses the transfer of an ADP-ribose moiety from NAD^+ to an arginine residue of an acceptor protein, with the simultaneous release of nicotinamide. Specific ADP-ribosylhydrolase can reverse the reaction, by hydrolysing the N-glycoside linkage between ADP-ribose and the arginine residue. Other amino-acid residues that can be modified by this reaction are cysteine, glutamic acid, diphthamide and asparagine. From (Di Girolamo et al., 2005).

NAD^+ has a cytosolic concentration of about 500 μM, with a half-life of about 1-2 h (Rechsteiner et al., 1976; Williams et al., 1985). Its reduced form, NADH, acts as a coenzyme in numerous redox reactions, and has pivotal roles in many fundamental cellular processes, including mitochondrial oxidative phosphorylation, where it acts as a co-factor for three rate-limiting enzymes of the tricarboxylic-acid cycle. In addition, NAD^+ has been implicated in cell death, in regulation of calcium homeostasis, and in controlling gene expression (Ying, 2006). Thus, the consumption of NAD^+ by NAD^+-consuming enzymes has to be tightly controlled. Poly-ADPR-polymerase enzymes constitute one of the major family of NAD^+-consuming enzymes, catalysing the transfer of multiple ADP-ribose moieties to form long and branched chains of poly-ADPR. The presence of poly-ADPR was first described by Chambon and co-workers in 1963 (Chambon et al., 1963), and a few years later its structure was solved (Reeder et al., 1967; Sugimura et al., 1967). The gene encoding the enzyme responsible for poly-ADPR formation is known as a poly-ADPR polymerase (PARP), which was isolated some 20 years later, in the late 1980's (Alkhatib et al., 1987; Kurosaki et al., 1987; Uchida et al., 1993). In the meantime, another ADP-ribosylation reaction was discovered during the analysis of bacterial toxins (Gill et al., 1969; Honjo et al., 1968). While PARP enzymes catalyse poly-ADP-ribosylation of proteins, these newly discovered toxins were shown to mono-ADP-ribosylate proteins. Consequently, the presence of mammalian mono-ADP-ribosyltransferases (mARTs) was suggested, and ecto-enzymes with mART activity were discovered, although the molecular identities of postulated intracellular mARTs are only at the beginning of their elucidation (Corda and Di Girolamo, 2003; Hassa et al.,

2006; Okazaki and Moss, 1999; Seman et al., 2004). The present study is aimed at adding new and specific depths to the study of intracellular mARTs, and to investigate a new ADP-ribosylation mechanism that is catalysed by the fungal toxin brefeldin A (BFA). The two main aspects analysed in the present thesis can be summarised as follows:

1. Study of the BFA-dependent ADP-ribosylation reaction of CtBP1/BARS and its effects on CtBP1/BARS functions;
2. Study of intracellular mono-ADP-ribosylation, with specific interest focussed on PARP12 as a mono-ADP-ribosyltransferase.

Thus, in the next sections I will give an overview on the ADP-ribosylation reactions catalysed by toxins, and on the different eukaryotic NAD^+-consuming enzymes (mARTs, ADP-ribosyl cyclases, Sirtuins and PARPs). The description of PARP enzymes is covered in more details, since a part of my PhD project focused on PARP12. The last part of the introduction is dedicated to the description of a specific case of ADP-ribosylation (the BFA-dependent ADP-ribosylation of CtBP1/BARS) and of the cellular functions of the target of this reaction, CtBP1/BARS.

1.2 ADP-ribosylation by toxins

Bacterial pathogens invade and then damage their host through the actions of their toxins.

ADP-ribosylation was the first covalent modification shown for a bacterial toxin, in which diphtheria toxin (DTX) transfers the ADPR moiety of NAD^+ to the R-group of a post-translationally modified histidine of elongation factor-2 (EF-2) (Collier, 1975). Since then, several toxins have been identified as catalysing ADP-ribosylation of host target proteins. The ADP-ribosylating

toxins (ADPRTs) form a large family of deleterious and potentially lethal toxins. Examples of these toxins can be found in a diverse range of bacterial pathogens, and they are the main active agents in many diseases, including cholera, whooping cough and diphtheria (Krueger and Barbieri, 1995).

Table 1.1 provides a representative list of the members of the ADP-ribosylating toxins. Each of these toxins has a unique property, including the host protein that is targeted for ADP-ribosylation, the amino acid that is modified, and the outcome of ADP-ribosylation on the modified protein. The majority of the modified targets are key regulators of cellular functions, and as the modification interferes with their activity, this leads to dysregulation of key cellular processes, and eventually to cell death (Krueger and Barbieri, 1995).

The structural organisation of toxins and the targets they modify are described in the next section (1.2.1). Particular emphasis is then given to the exotoxin ExoS from *Pseudomonas aeruginosa*, because it targets some of the Rabs (small GTPases that control intracellular trafficking), proteins that I have also covered in this study.

1.2.1 Structural organisation of ADPRTs

The bacterial ADPRT family can be split into four groups on the basis of their domain organisation and the nature of their targets. In describing the toxin structure, it is commonly accepted to refer to the A and B domains. The **A** domain encodes the catalytic domain, and the **B** domain comprises a translocation (**T**) domain that facilitates translocation of the **A** domain into the cytoplasm of the host cells, and a receptor binding (**R**) domain that binds the toxin to host cell-surface receptors (Figure 1.2). The A and B domains can be structured as a single protein (**AB**), a complex of non-covalently bound

Table 1.1: Representative ADP-ribosyltransferase toxins

The bacterial ADPRTs. Note that each ADPRT has a unique property, including its targets, the amino acid residue modified, and the outcome of ADP-ribosylation on the modified protein.

Toxin	Target (residue)	Physiological response
Diphtheria toxin, Pseudomonas ETA	EF-2 (diphatamide, His*)	Inhibition of protein synthesis
Cholera toxin, *E. coli* LT	$G_{\alpha s}$ (Arg)	Inhibition of GTPase activity of G_s
Pertussis toxin	$G_{\alpha i}$ (Cys)	Uncoupled Gi protein-mediated signal transduction
C. botulinum C2, iota toxin	Actin (Arg)	Prevention of actin polymerisation

ETA: exotoxin A; LT: heat labile enterotoxin; $G_{\alpha s}$: α subunit of stimulatory heterotrimeric G-protein $G_{\alpha i}$: α subunit of inhibitory heterotrimeric G-protein. His*: posttranslationally modified histidine.

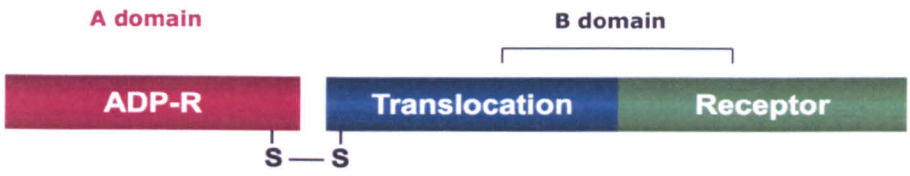

Figure 1.2: Schematic representation of bacterial toxin structure

The bacterial toxin structure can be schematically represented as the A and B domains. The A domain encodes the catalytic domain; the B domain comprises a translocation domain that facilitates translocation of the A domain into the cytoplasm of the host cells. The receptor-binding domain binds the toxin to the host cell-surface receptors. The structure shown is of diphtheria toxin.

proteins (**A5B**), or as two different proteins that encode the **A** and **B** domains (**A-B**). In this last case (**A-B**), the two proteins are independently synthesised and secreted from the bacterium, and they can associate only when the **B** domain binds to the surface receptors of sensitive cells (Deng and Barbieri, 2008b).

The most well known toxins, cholera toxin (CTX), produced by *Vibrio cholerae*, pertussis toxin (PTX), produced by *Bordetella pertussi,* and *Escherichia coli* heat-labile enterotoxin (LTX) are members of the A5B family, which targets small regulatory G-proteins (see table 1.1). Here, the enzymatically active A subunit is situated on a scaffold made of a pentamer of B subunits (Deng and Barbieri, 2008b; Gill, 1976; Streatfield et al., 1992; Zhang et al., 1995).

The second group of toxins comprises DTX and *Pseudomonas* exotoxin A (ExoA), whih can ADP-ribosylate a diphthamide residue on EF-2 (see table 1.1). The structure here can be schematised as AB toxins; both toxins are large multidomain proteins with receptor binding, transmembrane targeting, and protease-resistant catalytic domains (Allured et al., 1986; Collier, 1975).

The third group of toxins comprises the actin-targeting AB binary toxins. Unlike the more common A5B binary toxins, these are composed of two domains: an active catalytic domain and a cell-binding domain. This group includes a wide range of clostridial toxins including C2 toxin from *Clostridium botulinum*, *Clostridium perfringens* Iota toxin (see table 1.1), *Clostridium spiroforme* toxin, *Clostridium difficile* toxin and the vegetative insecticidal protein (VIP2) from *Bacillus cereus* (Aktories et al., 2011; Krueger and Barbieri, 1995).

The final group of toxins are the small single domain C3 exoenzymes, which are proteins with molecular mass of 20-25 kDa, that comprise an **A** domain but lack either a **T** or **R** domain. In this case, the bacterial secretion systems deliver **A**-domain-containing toxins from the cytoplasm of the bacterium to the intracellular environment of the host cell, thus allowing for the absence of both the T and R domains. Some examples here are represented by C3bot from *C. botulinum*, and toxins from *Clostridium limosum*, *B. cereus* and *Staphylococcus aureus* (Krueger and Barbieri, 1995).

1.2.2 Cellular properties of ADPRTs

The bacterial ADPRTs are all thought to have important roles in bacterial pathogenesis, through acting as key virulence factors in many diseases. The effects caused by the ADPRTs all rely on ADP-ribosylation of key regulatory proteins in host cells, which leads to impairment of cell signalling. The A5B proteins, including PTX, LTX and CTX, all ADP-ribosylate a subset of heterotrimeric GTP-binding proteins. For all three of these toxins, the A catalytic domain sits on a 'doughnut-shaped' pentamer of binding domains that comprise the cell binding and translocation apparatus (Sixma et al., 1991; Stein et al., 1994; Zhang et al., 1995). In the bacterial cell, this hetero-hexamer is assembled in the bacterium before being transported across the membrane via the type II secretion apparatus (Sandkvist et al., 2000). Once secreted, the B-pentamer recognises GM1 ganglioside on the host cell surface, through which it induces its endocytosis and translocation into the cytosol. For the toxin to become active, however, the catalytic domain must undergo proteolytic cleavage of the disulphide linked A1-A2 domain (Kassis et al., 1982). This also results in the A1 domain being released from the A2-B5 complex. Even at this

stage, these toxins are not fully functional, because they also require activation by host-cell proteins to become fully active. In the case of CTX, these ADP-ribosylation activation factors (ARFs) come from the host. ARFs are small GTPases that bind CTX in their GTP-bound state. Disease results from both CTX and LTX co-opting molecular machineries of the host cell: the toxins enter by endocytosis of the toxin-receptor complexes, move to the Golgi cisternae or to the endoplasmic reticulum (ER) via retrograde transport, and finally translocate to the site of their action on the inner surface of the plasma membrane (Lencer et al., 1999). Both CTX and LTX target $G_{s\alpha}$, the α subunit of the stimulatory G-protein of the adenylyl cyclase system. ADP-ribosylation of this subunit causes the G-protein to be maintained in its activated GTP-bound state, and leads to massive up-regulation of adenylyl cyclase, and the subsequent increase in the amount of cytosolic cyclic AMP (cAMP). This eventually leads to a major loss of fluid and ions from the intestinal cells that are affected, and gives rise to the severe diarrhoea and fluid loss that are associated with both cholera and enterotoxigenic *E. coli* pathogenesis (Gill and Richardson 1980).

PTX is produced by *Bordetella pertussis*, the major causative agent of whooping cough. PTX ADP-ribosylates an exposed cysteine residue on several small heteromeric G proteins (such as $G_{i\alpha}$ and $G_{t\alpha}$). Unlike CTX, PTX-catalysed mono-ADP-ribosylation occurs when G_{α} is associated with the βγ-dimer, thus generating a modified G protein that cannot transduce signals (Collier, 1975; Krueger and Barbieri, 1995). This results in the uncoupling of the G-proteins from their effectors, and in an unregulated increase in adenylyl cyclase activity, and the consequent increase in cAMP.

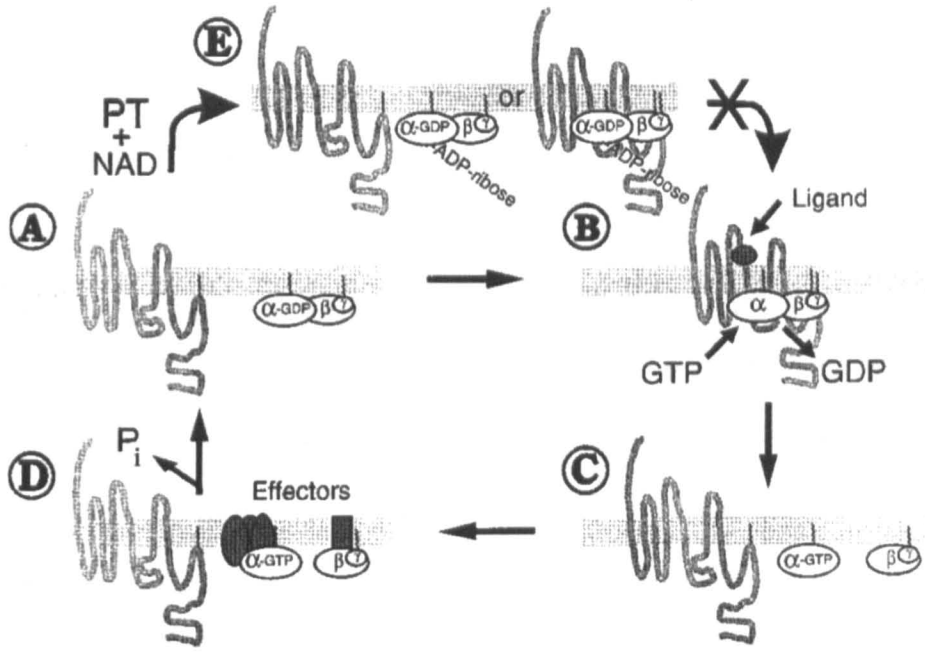

Figure 1.3: Uncoupling of G-protein-coupled receptors from G proteins by PTX-catalysed ADP-ribosylation of Gα.

The cycle for G-protein activation by ligand binding to G-protein-coupled receptors. Receptors (line traversing the plasma membrane) are composed of seven transmembrane strands. G proteins are localised to the cytosolic face of the plasma membrane through fatty acid acylation, as indicated. (A) In the absence of ligand for the receptor, there is no association between the receptor and G protein, which is in its inactive GDP-bound state. (B) In the presence of ligand, the G protein associates with the receptor and GTP is exchanged for GDP, thereby activating the G protein. (C) The α subunit containing bound GTP dissociates from the βγ dimer, and each can influence the appropriate effector systems. (D) The α subunit has an intrinsic GTPase activity. Upon hydrolysis of GTP to GDP, the α subunit is inactivated. (E) Two models for the physiological effect of ADP-ribosylation of G proteins by PTX that conform to the experimental data: the ADP-ribosylated G protein associates with the receptor, but the interaction is not functional (right); or the ADP-ribosylated G protein no longer interacts with the receptor (left). From Krueger and Barbieri (1995).

DTX is an example of a eukaryotic EF-2 (eEF-2) ribosylating toxin (Moynihan and Pappenheimer, 1981). It is secreted by *Corynebacterium diphtheriae* as a single protein, encompassing the three A-T-R domains. DTX binds to the heparin binding epidermal growth factor-like growth factor precursor (HB-EGF), and it is cleaved on the cell surface by furin or furin-like proteases, to produce a di-chain protein that is linked by a disulphide bond. Receptor binding triggers the entry of DTX into the lumen of a developing endosome by receptor-mediated endocytosis. Upon acidification, the **T** domain facilitates the translocation of the **A** domain across the endosomal membrane into the host-cell cytoplasm, where the **A** domain catalyses ADP-ribosylation of eEF-2 on an exposed histidine that is modified by the addition of a diphthamide side-group. The ADP-ribosylation interrupts the function of eEF-2 in the host cell, which in turn interfers with protein synthesis, and results in profound physiological changes and ultimately cell death (Krueger and Barbieri, 1995).

A further well-known target of ADP-ribosylation by toxins is actin. Iota toxin, from *Clostridium perfringens*, and VIP2 from *Bacillus cereus* are both actin ADPRTs, and each of these can ADP-ribosylate actin at an exposed arginine, Arg177. This ADP-ribosylation prevents actin polymerisation by capping the exposed ends of the actin filaments, which leads to cell rounding and eventual cell death, as the actin cytoskeleton breaks down (Aktories and Wegner, 1989). This class of actin modifying binary toxin also includes *C. botulinum* C2 toxin, *C. spiroforme* toxin and *C. difficile* toxin components cdtA and cdtB. The toxins do not bind cells as complete A-B units. Instead proteolytically activated B monomers bind to cell-surface receptors as homo-

heptamers. These homo-heptamers then bind the A domains and are taken into the cell via endocytosis. Once inside the acidic endosomes, the low pH activates the translocation function of the B domain heptamers, and they translocate the catalytic A domains across the endosomal membrane into the cytoplasm, where they can act to ADP-ribosylate actin and bring about cell death (Barth et al., 2004).

The C3 exoenzymes are characterised by C3bot from *C. botulinum*, and also includes representatives from *Clostridium limosum* (C3lim), *B. cereus* (C3cer) and *S. aureus* (C3EDIN, C3Stau2). This family of ADPRTs selectively ADP-ribosylates the small GTPases RhoA, B and C at an exposed arginine residue (Arg41). This prevents Rho moving into its active GTP-bound state and leads to a loss of control in the downstream pathways controlled by the Rho GTPases, thus resulting in loss of control of the cell cytoskeleton and eventual cell death (Wilde and Aktories, 2001). Although these effects are seen *in vitro*, the roles of C3bot and its related ADPRTs in pathogenesis are not yet known, as they lack any cell translocation or binding domains.

- Pseudomonas aeruginosa ExoS and ExoT exotoxins

P. aeruginosa is an opportunistic human pathogen that is associated with multi-drug-resistant nosocomial infections (Obritsch et al., 2005).

P. aeruginosa produces ExoA that, similarly to DTX, ADP-ribosylates EF-2, and it also produces the Type III cytotoxins ExoS, ExoT, ExoU and ExoY, which create an environment that favours bacterial survival and dissemination. These exotoxins are delivered across the bacterial cell membrane and cell wall into a mammalian cell through a secretion apparatus

that is composed of 20-30 proteins. Among the above-mentioned Type III cytotoxins, only ExoS and ExoT function as mARTs. They are bi-functional toxins that comprise a Rho GTPase activating protein (RhoGAP) domain and an ART domain (Deng and Barbieri, 2008b).

ExoS- and ExoT-RhoGAPs inactivate small Rho GTPases, including RhoA, Rac1, and Cdc42, which disrupts the host-cell cytoskeleton (Deng and Barbieri, 2008b). While the RhoGAP activity is similar for both of these, ExoS and ExoT are still distinct, in that they ADP-ribosylate unique host substrates (Barbieri and Sun, 2004).

ExoT was originally thought to be an inactive precursor of ExoS, but later studies implicated a role for the ART domain in eliciting cell rounding. Indeed, ExoT was determined to ADP-ribosylate CT10-regulator of kinase (Crk) (Sun and Barbieri, 2003). Crk proteins are SH2-SH3-domain-containing adaptor proteins that are components of the integrin signaling pathway leading to Rac1 and Rap1 activation, required for the integrin-mediated phagocytosis and formation of focal adhesions. Mass spectroscopic analysis identified Arg20 as the site of ADP-ribosylation of Crk by ExoT. Arg20 is a conserved residue located within the SH2 domain that is required for interactions with upstream signaling molecules such as paxillin and p130cas. ADP-ribosylated Crk-I failed to bind p130cas or paxillin. This indicates that ADP-ribosylation inhibited the direct interaction of Crk with these focal adhesion proteins, thus leading to cell rounding (Deng et al., 2005).

In contrast to the restricted group of substrates of ExoT, ExoS ADP-ribosylates numerous substrates. Several small monomeric GTPases have been identified as cellular targets of ExoS (Coburn et al., 1989). ExoS was shown to

ADP-ribosylate Ras at Arg41, which is adjacent to the switch region of the GTPase (Ganesan et al., 1998), and subsequent studies showed that ADP-ribosylation inhibited guanine nucleotide exchange factor (GEF)-catalysed nucleotide exchange, which uncoupled Ras signal transduction (Ganesan et al., 1998).

Other targets of ExoS include the Ezrin/Radixin/Moesin (ERM) family proteins (Maresso et al., 2004), which are regulators of the actin network. The Rab proteins are also targets of ExoS. Rab GTPases have essential roles in host-cell vesicle trafficking, including endocytosis, receptor recycling, vesicle maturation and trafficking to the Golgi complex and lysosomes (van der Bliek, 2005). It has been demonstrated that ExoS localises to Rab-positive vesicles and that it ADP-ribosylates Rab5, Rab7, Rab8 and Rab11, both *in vitro* and *in vivo* (Fraylick et al., 2002).

The effects and mechanism of the ADP-ribosylating activity of ExoS were investigated by Barbieri and co-workers. These authors demonstrated that ExoS ADP-ribosylation influences the intracellular trafficking of the EGF receptor (EGFR), as well fluid phase endocytosis, through inhibition of Rab5 activity (Deng and Barbieri, 2008a).

It is well recognized that the binding of EGF to the extracellular domain of EGFR leads to the activation of EGFR as well as to the internalisation of the EGF-EGFR complex via the canonical clathrin-mediated endocytic pathway, through early and late endosomes, for degradation in lysosomes (Ceresa, 2006). Endocytic trafficking of the EGFR is necessary for the correct temporal and spatial regulation of EGF signalling. Several G proteins have been implicated in EGFR endocytic trafficking. While dynamin drives EGFR

endocytosis, Rab5 mediates entry of the EGFR into early endosomes, Rab7 is required for degradation of the EGF-EGFR complex by the lysosomes, and Rab11 facilitates EGFR recycling to the plasma membrane (Ceresa, 2006).

In cells treated with ExoS, upon EGF activation, the EGFR still internalises to clathrin-coated vesicles, but it does not mature to the Rab5-positive early endosomes (Deng and Barbieri, 2008a). The observation that a constitutively active Rab5 protein can reverse ExoS inhibition of EGF-activated EGFR trafficking out of clathrin-coated vesicles suggests that ADP-ribosylation catalysed by ExoS inhibits Rab5 activity in cells. The uncoupling of Rab signalling might enable *P. aeruginosa* to evade trafficking to perinuclear vacuoles, while endowing *P. aeruginosa* with the capacity for intracellular replication.

1.3 Eukaryotic NAD^+-consuming enzymes

NAD^+ was identified a century ago as a cofactor and coenzyme, and it has attracted attention for its versatile function in relation to energy metabolism (Houtkooper et al., 2010).

NAD^+-consuming ecto-enzymes are primarily represented by the CD38/CD157 system and by the family of ecto-mARTs. In contrast, the PARPs and sirtuins operate within the cell. Currently, 22 human genes encoding proteins with an ART activity are known, and these can be divided in ecto-mARTs and PARPs. Recently, a unified nomenclature referring to this family of proteins as ARTs was proposed, sub-dividing the ARTs according to structural criteria of their catalytic domains, into ART DTX-like (ARTD) and ART CTX-like (ARTC) proteins (Hottiger et al., 2010). Table 1.2 shows the new nomenclature, in comparison with the old one, and the postulated/demonstrated enzymatic activity for each member of the PARP family.

In the following sections I will describe each of these NAD^+-consuming enzyme families, starting from ADP-ribosylcyclases, going through mART, and sirtuins. Particular emphasis is then given to the PARP family members. In this regard, I will refer to the different enzymes using the old nomenclature.

Table 1.2: Nomenclature and enzymatic activity of PARP family members

Comparison of the PARP catalytic core motifs and described/ postulated enzymatic activities of the PARP family members. The new proposed nomenclature is also given. Asterisks indicate that experimental evidence has demonstrated the mART activity. Light purple, pART; green, mART; light blue, inactive enzymes. Even though PARP3 shows structural features similar to the classical PARPs, it has been demonstrated to function as a mART (Loseva *et al.*, 2010). Note that only PARPs 3, 10 and 14 have been demonstrated to function as mARTs. For all of the other members, mART activity has only been postulated.

Protein name	New nomenclature	Gene symbol	Catalytic core motif	ADP-ribosylation activity
PARP1	ARTD1	*PARP1*	HYE	Poly
PARP2	ARTD2	*PARP2*	HYE	Poly
PARP3	ARTD3	*PARP3*	HYE	Mono *
PARP4 (vPARP)	ARTD4	*PARP4*	HYE	Poly
PARP5a (TNKS1)	ARTD5	*TNKS*	HYE	Poly
PARP5b (TNKS2)	ARTD6	*TNKS2*	HYE	Poly
PARP6	ARTD17	*PARP6*	HYI	Mono
PARP7	ARTD14	*TiPARP*	HYI	Mono
PARP8	ARTD16	*PARP8*	HYI	Mono
PARP9 (BAL1)	ARTD9	*PARP9*	QYT	Inactive
PARP10	ART10	*PARP10*	HYI	Mono *
PARP11	ARTD11	*PARP11*	HYI	Mono
PARP12 (ZC3HDC1)	ARTD12	*PARP12*	HYI	Mono
PARP13 (ZC3HAV1/ZAP)	ARTD13	*ZC3HAV1*	YYV	Inactive
PARP14 (BAL2)	ARTD8	*PARP8*	HYL	Mono *
PARP15 (BAL3)	ARTD7	*PARP15*	HYL	Mono
PARP16	ARTD15	*PARP16*	HYY	Mono

1.3.1 The ADP-ribosylcyclase CD38/CD157 family

ADP-ribosylcyclase (ADPRC) from A. californica was the first enzyme shown to have this cyclase function (Lee and Aarhus, 1991). Based on sequence homology (States et al., 1992), two human antigens, CD38 and CD157, were shown to also have the cyclase activity (Hirata et al., 1994; Howard et al., 1993). The following sections describe the current knowledge concerning the structures and enzymatic functions of both CD38 and CD157.

1.3.1.1 CD38 structure

Human CD38 is a type II surface glycoprotein that is characterised by a large extracellular domain (257 amino acids), a single transmembrane domain (23 amino acids), and a short cytoplasmic tail (20 amino acids) (Alessio et al., 1990). Within the human immune system, CD38 is expressed by immature haematopoietic cells, down-regulated by mature lymphocytes and re-expressed at high levels by activated T and B cells and dendritic and natural killer cells. It represents the main mammalian member of the ADPRC family of enzymes and it appears to be ubiquitous in eukaryotic cells (Malavasi et al., 2008).

The protein encoded by the CD38 gene has a molecular weight of 45 kDa. The overall structure of the CD38 molecule is 'L' shaped, and it can be divided into two separate domains: the NH_2-terminal domain (residues 45-118 and 144-200) and the COOH-terminal domain (residues 119-143 and 201-300), which are connected by a hinge region that is composed of three peptide chains. A disulphide bond that is unique to CD38 (Cys-119–Cys-201), plus five other pairs of disulphide bonds that are conserved in ADPRC family members, further stabilise the relative conformations of the two domains by linking peptides 118-119 with 200-201 (Liu et al., 2005) (Figure 1.4).

As well as the membrane form of CD38, a soluble form was identified in cell-culture supernatants of activated T lymphocytes, in several tumour cell lines, and *in vivo* under normal and pathological conditions (Funaro et al., 1996).

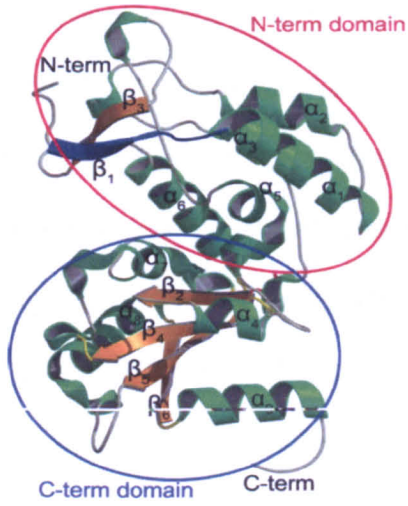

Figure 1.4: Crystal structure of CD38

The 'L' shaped structure of CD38 is divided into two separate domains. The C-terminal domain consists of four β-sheets surrounded by two long (α8 and α9) and two short (α4 and α7) α-helices. The N-terminal domain is formed by a bundle of α-helices and two β-strands. These two domains are connected by a hinge region that is composed of three peptides. From Malavasi *et al.* (2008).

1.3.1.2 CD157 structure

Human CD157 is a glycosylated single chain of 42-45 kDa that is anchored to the membrane via a glycosylphosphatidylinositol (GPI) tail (Itoh et al., 1994). Similar to CD38, the CD157 molecule is divided into two domains, known as the N-domain and the C-domain, which are connected by a hinge region of three peptides. All 10 cysteine residues that are conserved among the cyclase family form disulphide bonds, as seen in the structure of the *Aplysia* cyclase (Yamamoto-Katayama et al., 2002). Each subunit of the CD157 dimer contains a substrate-binding cleft, which is covered mainly by hydrophobic and acidic residues, and which is important for its catalytic function. The three key residues, Trp-77, Trp-140 and Glu-178, are invariant among the sequences of CD157, CD38 and the *Aplysia* cyclase, which share a common substrate-recognition mode and catalytic scheme (Yamamoto-Katayama et al., 2002) (Figure 1.5).

1.3.1.3 Enzymatic activities controlled by CD38

The identification of sequence similarity between the human lymphocyte antigen CD38 and the *Aplysia* ADPRC (States et al., 1992) marked the beginning of long-term investigations into the enzymatic properties of CD38 and into its role in human physiology and pathology.

CD38 is a multifunctional ecto-enzyme that is involved in the catabolism of NAD^+ and $NADP^+$, the two main substrates of CD38 thus far identified. This reaction leads to the generation of potent intracellular $Ca2^+$-mobillising compounds: cADPR, nicotinic acid adenine dinucleotide phosphate (NAADP) and ADPR.

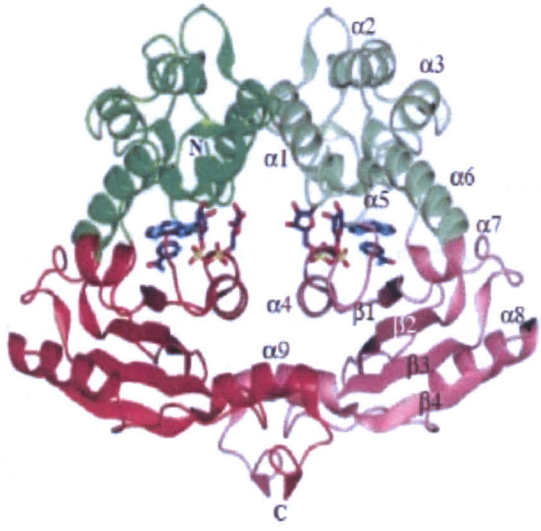

Figure 1.5: Crystal structure of CD157 complexed with etheno-NAD

CD157 forms a homodimer of two symmetrical subunits. Each subunit is divided into two domains, termed the N domain (green-light green) and the C domain (red-light red), which are connected by a hinge region of three peptide chains. Each subunit of the CD157 dimer contains a substrate-binding cleft, formed by the N and C domains. This large cleft is surrounded by α4, α5, α6, α7, and β1, and is mainly covered by hydrophobic and acidic residues. Adapted from Yamamoto-Katayama *et al.* (2002).

The enzymatic properties of CD38 were formally demonstrated after analysing a purified recombinant soluble form of CD38 (sCD38). When added to NAD^+, sCD38 catalysed the formation and hydrolysis of cADPR (Howard et al., 1993). Similar results were obtained using solubilised human erythrocyte membranes: the three ecto-enzyme activities, i.e., NADase, ADPRC, and cADPR hydrolase, could be purified to homogeneity using an anti-CD38 monoclonal antibody (Zocchi et al., 1993). These results were also confirmed in human T-cell models, where the NAD-hydrolysing enzymatic activity was shown to correlate with the amount of CD38 on the cell surface. Moreover, CD38 immunoprecipitated from thymocytes behaved as an authentic NADase enzyme, by transforming NAD^+ stoichiometrically into nicotinamide and ADPR (Gelman et al., 1993). As above-mentioned, the human cyclase family of enzymes has *A. californica* as its founding member. Even if the human version of ADPRC retains high homology with its Aplysian ancestor, its functional activities have evolved significantly. Indeed, while the *Aplysia* enzyme functions mainly as a cyclase, the human CD38 is mainly a NAD^+ glycohydrolase that leads to the generation of ADPR and nicotinamide as products, accounting for >90% of all NAD^+ase activity in humans (Liu et al., 2009). The cyclase function is present, but its activity is approximately 100-fold lower than that of the hydrolase. The structural determinants critical for the catalytic characteristics of ADPRC and CD38 were described by Liu and co-workers, by comparing the crystal structures of the complexes of ADPRC and CD38 bound with various catalytically revealing substrates and products (Liu et al., 2009). The results identify residues Phe-174 in the cyclase and Thr-221 in CD38 as the main determinants for the cyclase and hydrolysis activities

of these enzymes. Indeed, a point mutation of Phe-174 to glycine can turn ADPRC from a cyclase towards a NADase. The equivalent residue in CD38, Thr-221, is shown not to favour the cyclising folding of the substrate, which results in NADase being the dominant activity.

Being the major NADase enzyme in cells, CD38 has an important role in controlling NAD^+ levels, both in the extracellular and intracellular space (Aksoy, White et al. 2006). This last aspect was examined by the Chini group. These authors postulated that CD38 is the major NADase in mammalian cells and that it regulates intracellular NAD^+ levels (Aksoy, White et al. 2006), modulating the activity of the sirtuins, which are NAD^+-dependent deacetylases that are implicated in ageing, cell protection, and energy metabolism in mammalian cells (see section 1.3.3). This regulation occurs inside the nucleus and is mediated by CD38 expressed by the inner nuclear membrane (Aksoy et al., 2006).

A separate enzymatic activity that has been attributed to CD38 involves catalytic exchange of the nicotinamide group of $NADP^+$ with nicotinic acid (NA). The product is nicotinic acid adenine dinucleotide phosphate (NAADP), a potent Ca^{2+}-mobilising metabolite (Aarhus et al., 1995). This activity occurs selectively at an acidic pH; the acidic dependence of NAADP metabolism, coupled with its biological function in targeting the acidic Ca^{2+} stores in cells, suggests that NAADP serves as a specific Ca^{2+} messenger for the acidic organelles of the endocytic pathway in cells (Santella, 2005). Moreover, it has also been shown that NAADP can release Ca^{2+} from the ER (Gerasimenko et al., 2006). Thus, in addition to inositol 1,4,5-trisphosphate, internal Ca^{2+} stores

can be mobilised by at least two other molecules, cADPR and NAADP, which target separate Ca^{2+} stores and are bound by distinct receptors.

1.3.1.4 Enzymatic activities controlled by CD157

Similar to the *Aplysia* enzyme and to CD38, soluble CD157 incubated with NAD^+ produces cADPR, and subsequently ADPR, which indicates that CD157 has both ADPRC and cADPR hydrolase activities. However, the catalytic efficiency of CD157 is several-hundred-fold lower than that of CD38 (Ortolan et al., 2002).

1.3.1.5 Receptor activities of CD38/CD157

The most radical change in the evolutionary path of CD38 was the acquisition of a membrane anchor, which made it possible to interact laterally and frontally with molecules other than its substrate. Indeed, CD38 forms supra-molecular complexes that generally include other receptors, adhesion molecules and structural proteins (Malavasi et al., 2008). The receptor aspect of CD38/CD157 has been reviewed in details by Malavasi and co-workers (Malavasi et al., 2008; Vaisitti et al., 2011). I will not describe this aspect, since it does not fall within the main topic of the introduction to my thesis (1.3.1), which has the aim to describe the NAD^+-linked functions of the different enzyme families.

1.3.2 The mammalian ecto-ADP-ribosyltransferases

After the discovery of the bacterial ARTs, similar enzymatic activities were sought in eukaryotic cells. However, the enzymes responsible for these activities eluded molecular cloning until the groups of Moss and Shimoyama succeeded in purifying and sequencing proteins with ADP-ribosylating

activities from rabbit skeletal muscle and chicken bone-marrow cells (Tsuchiya et al., 1991; Zolkiewska et al., 1992). These findings constituted the starting point for further characterisation of other enzymes of this type (Koch-Nolte and Haag, 1997).

The knowledge acquired to date allows us to group the mammalian ecto-mARTs into a single family of structurally and functionally related genes. This family comprises five members, ART1-5. They are all ecto-enzymes, which are anchored to the outer leaflet of the plasma membrane via a GPI tail, with the exception of ART5, which is secreted into the extracellular space (Okazaki and Moss, 1998). Among these five ARTs, only ART1, ART2 and ART5 show enzymatic activity, whereas ART3 and ART4 appear to have lost their catalytic function (Glowacki et al., 2002). In humans, the presence of a *art2* pseudogene that carries three premature stop signals limits the number of ART enzymes to four. Conversely, the duplication of the *art2* gene in mouse increases the number of enzymes to six (Glowacki et al., 2002).

This family of enzymes shares very limited amino-acid sequence identity, with 20% to 30% seen among the ART paralogue members within any species. The exception here is mouse ART2.1 and ART2.2, where their sequence identity (85%) indicates recent evolutionary duplication of the mouse *art2* gene (Braren et al., 1998).

The ART2 enzymes have also been cloned from rat, and in this case the two isoforms are alternative splicing variants of the two alleles known as ART2.a and ART2.b (Bortell et al., 1999). These two allelic variants show sequence variation of only 10 amino acids, which is associated with a change in the enzymatic activity between ART2.a and ART2.b; indeed, while both

isoforms can catalyse the hydrolysis of NAD^+ to ADPR and nicotinamide, only ART2.b can undergo auto-ADP-ribosylation (Haag et al., 1995).

As the human and mouse genome sequences have been completely determined, all of the recognisable members of these ARTs have been identified for these two species, with an amino acid sequence identity between orthologues ranging from 75% to 85%. As an example, the deduced amino-acid sequence of mouse ART1, which was the first cloned and characterised mammalian arginine-specific ART, is 77% and 73% identical to human and rabbit ART1, respectively (Braren et al., 1998; Okazaki and Moss, 1998)

As expected by the sequence similarity, there are common structural features that characterise the family of mammalian ecto-ARTs (Domenighini et al., 1994; Domenighini and Rappuoli, 1996). The catalytic domain of these enzymes is completely coded for by a single exon in all of the ARTs, and it contains a conserved glutamate residue that has been demonstrated to be crucial for catalytic activity, as demonstrated by site-specific mutagenesis for the ART1 and ART2 murine and rat isoforms (Hara et al., 1996; Takada et al., 1995). In addition, mutational analysis performed on the ART1 from rabbit show that besides the classical glutamate, the neighbouring glutamic residue (E238) has an important role for ADPR transfer (Hara et al., 1996; Takada et al., 1995). Indeed, in several of the ARTs, the replacement of this second glutamate abolishes the ability of the transferases to use arginine as acceptor, thus further supporting the hypothesis that this region is involved in substrate recognition (Han and Tainer, 2002). According to the structural model proposed by Rappuoli and colleagues (Domenighini and Rappuoli, 1996), the catalytic domain is composed of 70-100 amino acids and consists of three

regions. Region 1 is near the N-terminal portion of the protein and is characterised either by a conserved histidine (as in DTX, ART3 and the PARPs) or by a conserved arginine (as in PTX, CTX, the LTX and the other ARTs). Region 2 is characterised either by hydrophobic amino acids that are involved in NAD^+ binding or by a serine-x-serine motif (where x represents threonine, serine or alanine). Region 3 is highly acidic and is characterised by the conserved glutamate residue. The arginine-serine-glutamate-x-glutamate motif (R-S-E-Q-E; which spans regions 1–2–3, respectively) is present in CTX and in ART1, ART2 and ART5, and it is typical of the arginine-specific ARTs. This motif is missing in ART3 and ART4 (Koch-Nolte et al., 1997). Through a comparative analysis of crystallographic structures, Han and Tainer (Han and Tainer, 2002) extended the significance of the region 3 sequences by identifying an ADP-ribosylating turn-turn (ARTT) motif that they have implicated in substrate recognition. Consistent with the relevance of the ARTT motif, it has been shown that the auto-ADP-ribosylation of ART2.b is abolished by mutations of its R204, which is part of the ARTT motif. Similarly, if the Y204 of ART2.a is mutated to an arginine (Y204R), it is possible to promote ART2.a auto-ADP-ribosylation (Stevens et al., 2003).

The other common structural features of the ARTs include an α-helix-rich N-terminal region, which represents a signal sequence for extracellular proteins, and a C-terminal region folded into β-sheets, which is characteristic of GPI-anchored membrane proteins (Bazan and Koch-Nolte, 1997). As mammalian (human and mouse) ART5 does not contain this hydrophobic C-terminal signal sequence, it is a secreted protein (Glowacki et al., 2001).

Finally, there are four cysteines involved in disulphide bridge formation that are conserved among all of the ART isoforms.

The identification of this class of enzymes gave new impetus to studies of the physiological significance of the ADP-ribosylation reaction. Thus, in the next section, I report the current knowledge concerning the specific targets that are known to be modified by ecto-ARTs, and how the modifications affect their substrate functions.

1.3.2.1 Ecto-ART substrates as functions of their distribution

Although substantial progress has been made with regard to the molecular characterisation of ARTs, identification of their physiological target proteins has been difficult. In the identification of the substrates, and thus their functions, it is important to remember that ecto-ART-encoding genes show tissue-specific expression. Northern blotting and RT-PCR with human and animal tissues have revealed relatively broad distributions of ART3 and ART4, and rather specific expression of ART1 in heart and skeletal muscle in both species. ART5 is mainly expressed in testis, while ART2, which is absent in man, has been detected in mouse peripheral and rat lymphoid tissues (Seman et al., 2004).

In addition to these different distributions, the patterns of ART expression in some cases are related to cell differentiation and/or activation states. In human polymorphonuclear neutrophils, for example, translocation of ART1 to the cell surface depends on the presence of activating ligands, such as interleukin (IL)-8 or platelet-activating factor (Kefalas et al., 1999). Similarly, the rate of ART3-transcription is increased upon exposure of human monocytes

to lipopolysaccharide, which also induces expression of ART4 mRNA (Grahnert et al., 2002). Another typical example is ART2 expression on murine T cells. ART2 is expressed only on a small subpopulation of mature thymocytes, and thus appears to be developmentally regulated (Koch-Nolte et al., 1999). Moreover, whereas ecto-ART expression increases with human polymorphonuclear-leukocyte or monocyte activation, ART2 is shed from the membrane upon T-cell activation (Kahl et al., 2000).

The following sections describe the known substrates modified by ecto-ARTs in relation to their expression.

ART1

ART1 was identified as the first mammalian ART after its purification from skeletal muscle and cDNA cloning from rabbit (Zolkiewska et al., 1992), human skeletal muscle (Okazaki et al., 1994) and mouse lymphoma cells (Okazaki et al., 1996). In search of proteins that can be ADP-ribosylated by ART1, α7-integrin was identified as a key protein (Zolkiewska and Moss, 1997). α7-Integrin is expressed specifically in skeletal and cardiac muscle, and it forms a dimer with β1-integrin, and binds to laminin, an extra-cellular matrix (ECM) protein. ADP-ribosylation enhances the interaction between α7/β1-integrin and its ligand, laminin (Zolkiewska and Moss, 1997). This effect might represent a mechanism of up-regulation of α7/β1-integrin function in situations where more efficient interactions are required, such as muscle injuries or diseases (Zolkiewska, 2005). Interestingly in mouse skeletal muscle cells, the expression of ART1 correlates with the transition from non-differentiated

mononucleated myoblasts to multinucleated non-replicating myotubes (Zolkiewska and Moss, 1993).

Another well-known substrate for ART1 is the human defensin HPN-1 (Paone et al., 2002). Defensins are small cationic arginine-rich peptides (2 kDa to 6 kDa) that act as protein mediators of innate immunity and are produced by inflammatory cells, such as neutrophils, and epithelial cells lining the airways. As components of adaptive immunity, HPN1-3 can also be produced by human natural killer cells and T and B lymphocytes stimulated with cytokines. Defensins induce cytokine production, and modulate cell proliferation (Ganz, 2003).

In vitro studies performed by Paone and colleagues demonstrated that ART1 specifically modifies a synthetic HNP-1 on Arg14, with a secondary site on Arg24. The reaction is almost specific for ART1, since other arginine-specific ARTs show minor, if any, activity towards this HNP-1 (Paone et al., 2006). In its ADP-ribosylated form, the peptide reduces both its antimicrobial and cytotoxic activities, while enhancing its promotion of release IL-8 from epithelial cells. Conversely, the chemotactic activities evaluated for the recruitment of T lymphocytes are not affected by ADP-ribosylation. The concept here is that once modified, HNP-1 acquires properties that result in the recruitment of neutrophils (by the release of IL-8) and in the modulation of its own antimicrobial and cytotoxic activities.

Importantly, high concentrations of HNP-1 are likely to be present in sites of inflammation and these can inhibit the transferase activity of ART1 and thus the formation of reduced modified HNP-1. This might represent a regulatory mechanism. The same inhibitory effect has been demonstrated for

ART5 activity, although it does not modify HNP-1 (Paone et al., 2006). Additional substrates of ART1 have been identified in various cell lines over-expressing ART1, as demonstrated for the basic fibroblast growth factor (FGF)-2 in ART1-transfected rat adenocarcinoma cells. FGF-2 binds its specific extracellular receptor (FGFR), as well as heparin, with high affinity. It can thus be sequestered by the heparan sulphates on the cell surface and in the ECM. Heparin inhibits the ADP-ribosylation reaction, implying that the heparin binding of FGF-2 and its ADP-ribosylation are mutually exclusive reactions. Furthermore, the ADP-ribosylated site of FGF-2 is in its receptor-binding domain, and so it is possible that ADP-ribosylation modulates the binding of FGF-2 to its receptor and to heparin, thus regulating its availability to the cell (Jones and Baird, 1997).

ART1 can also ADP-ribosylate another growth factor, i.e. the specific BB isoform of platelet-derived growth factor (PDGF-BB), as demonstrated in ART1-transfected Chinese hamster lung fibroblasts. Here, the role of ADP-ribosylation is to inhibit PDGF-BB stimulation of mitogenic and chemotactic responses in human pulmonary smooth muscle cells, as well to reduce PDGF binding to its receptors as demonstrated in competition-binding assays (Saxty et al., 2001). Similar to the effects of ADP-ribosylation of FGF-2, in this case also ADP-ribosylation has an inhibitory effect on PDGF-BB, thus negatively regulating its signalling at the cell surface.

ART2

ART2 is expressed in immune system cells, such as resting T cells and natural killer cells, where it should have an immunomodulatory activity. Indeed, in different animal models, autoimmune disorders, such as juvenile diabetes and

systemic lupus, have been found to coincide with defects in the structure and function of ART2 (Koch-Nolte et al., 1995). In rat, susceptibility and resistance to diabetes correlate with the absence and presence, respectively, of ART2-expressing T cells (Fowell and Mason, 1993). Nolte and co-workers (Seman et al., 2003) uncovered an intriguing function of ART2: activation of the P2X7 purinoceptor as a consequence of ADP-ribosylation. P2X7 is a member of the P2X family of ATP-gated ion channels, and it is widely expressed in several types of blood cells. The presence of ATP at millimolar concentration activates this purinoreceptor, thus inducing the formation of large membrane pores that trigger calcium fluxes and phosphatidylserine exposure, typical features of the apoptotic process (Di Virgilio et al., 2001).

Similar to ATP, micromolar concentrations of NAD^+ have the same effects, through ADP-ribosylation catalysed by ART2 (Seman et al., 2003). These data provide an excellent explanation for the rapid apoptosis induced by extracellular NAD (NAD-induced cell death) in naive T cells (Scheuplein et al., 2003). The molecular mechanism that explains how ADP-ribosylation can activate the channel is still not clear. However, it might be that ADPR functions as a ligand for the adenosine-binding site on the P2X7 receptor, or could activate P2X7 by an allosteric conformational change, independent of the ligand-binding site. Identification of the ADP-ribosylated arginine residues will help to solve this question.

The regulation of the P2X7 channel constitutes an interesting signalling pathway that is regulated by ADP-ribosylation. As mentioned above, ART2 is not present in humans and so far is not known if such a mechanism is catalysed by another enzyme. Trying to answer this question constitutes an interesting

point of investigation. Nevertheless, a common role for ART1 and ART2 can still be defined, that of the regulation of the immune response.

ART3, ART4 and ART5

The biological roles of ART3, ART4 and ART5 remain almost completely obscure. Looking at their sequences, they show conspicuous substitutions of key residues that line the catalytic site. It is therefore conceivable that ART3 and ART4 have acquired novel target specificities or that they have lost ART enzyme activity, as has happened for some members of the PARP family (Koch-Nolte et al., 2008) (explained in section 1.3.4).

1.3.3 Sirtuins

Sirtuins comprise an ancient family of NAD^+-dependent protein deacetylases that have been evolutionarily conserved from bacteria to eukaryotes (Michan and Sinclair, 2007). The founding member of the sirtuin family, yeast Sir2 (silent information regulator 2) was originally isolated in a screening for silencing factors, and later shown to regulate the lifespan in lower organisms (Kennedy et al., 1995; Rine et al., 1979). Subsequent analysis revealed that Sir2 functioned biochemically as a HDAC, in a unique reaction that required the energetic intermediate NAD^+ as a co-factor (Imai et al., 2000). The requirement of NAD^+ as part of their enzymatic action suggested a mechanistic link between sirtuin activity and intracellular energetics. Based on these observations, there have been efforts to understand if there is a similar role for sirtuins in mammals; here indeed sirtuins have been connected to an ever widening circle of activities, which encompasses cellular stress resistance, genomic stability, tumorigenesis, and energy metabolism (Finkel et al., 2009).

In the next sections, I will mainly describe the enzymatic features of the mammalian enzymes and their localisation, while giving a brief report on some of the pathways in which they are involved as mART. Since the sirtuins are not specifically part of my study and to date are best recognised as deacetylases more than ARTs, I will not describe their roles as deacetylase.

1.3.3.1 Enzymatic mechanism

Mammals have seven sirtuins, SIRT1-7, which are characterised by their highly conserved central NAD^+-binding and catalytic domain, termed the sirtuin core domain (Haigis and Guarente, 2006). Although sirtuin sequences are relatively conserved, their N and C termini differ, and they are likely to have highly divergent biological functions owing to (*a*) different enzymatic activities, (*b*) unique binding partners and substrates, and (*c*) distinct subcellular localisation and expression pattern (reviewed in section 1.3.3.2).

The predominant reaction catalysed by the sirtuins is NAD^+-dependent lysine deacetylation (Figure 1.6), via a unique enzymatic mechanism that requires NAD^+ cleavage for each reaction cycle (Landry et al., 2000; Tanner et al., 2000). Unlike other HDACs that hydrolyse acetyl-lysine residues, sirtuin activity is intimately tied to the metabolic state of the cell. The mechanistic basis for deacetylation by sirtuins is both elegant and peculiar. The deacetylation reaction begins with amide cleavage of NAD^+ and formation of nicotinamide and a covalent ADPR peptide-imidate intermediate. The intermediate is resolved to form *O*-acetyl-ADPR (AADPR), and the deacetylated substrate is released (Sauve et al., 2001). Although some details remain to be resolved, it is thought that peptide binding facilitates an allosteric change in sirtuin structure that enables the reaction of NAD^+ with a nucleophile

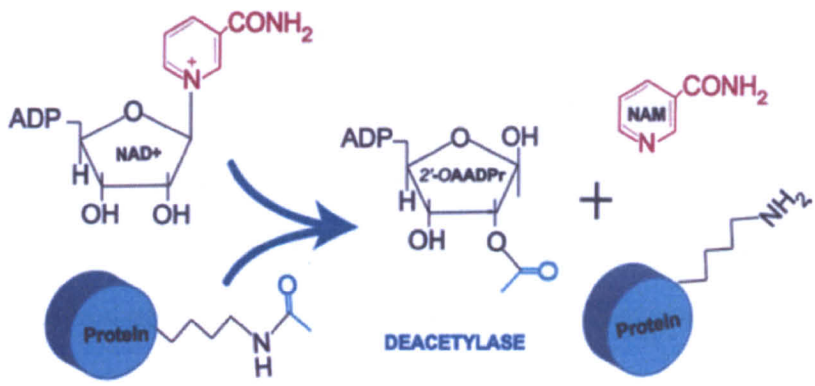

Figure 1.6: Deacetylation reaction catalysed by the sirtuins

The sirtuins are NAD^+-dependent deacetylases that regulate a wide array of proteins that are involved in metabolism and cell survival. The ε-acetyl lysine residues of the target protein serve as substrates for sirtuin deacetylation, which generates 2′-OAADPr as a by-product. 2'-OAADPr: 2'-O-acetyl ADP-ribose; NAM, nicotinamide. From Michan and Sinclair (2007).

from the sirtuin to generate the enzyme-stabilised ADPR intermediate (Sauve et al., 2006). Deacetylase activity is not the only activity associated to the sirtuins, even if the most prominent. An mART activity has been clearly associated to SIRT4, while for SIRT6 the mART activity is still under debate.

Regarding SIRT4, it has been demonstrated that it ADP-ribosylates the glutamate dehydrogenase GDH. This event leads to down-regulation of mitochondrial glutamate dehydrogenase (GDH) in pancreatic β-cells, thereby down-regulating insulin secretion in response to amino acids (Haigis et al., 2006) and, thus, regulating glucose homeostasis (Haigis et al., 2006) .

SIRT6 represents an interesting case. Recently, Denu and co-workers (Pan et al., 2011) reported the first quantitative assessment of SIRT6 activity, providing direct evidence that *O*AADPR is formed as a product of the deacetylase reaction; importantly, the rate of nicotinamide cleavage is similar to the rate of *O*AADPR formation, suggesting that SIRT6 functions as a NAD^+-dependent deacetylase rather than as an ART.

However, a general consensus on a clear role for SIRT6 is still lacking. Indeed, recently it has been demonstrated that under stress conditions, SIRT6-catalysed mono-ADP-ribosylation promotes DNA repair by activating PARP1. In this case, the poly-ADP-ribosylation activity of PARP1 is stimulated by its ADP-ribosylation on lysine 521 that is catalysed by SIRT6. This enhances DSB repair by both homologous recombination (HR) and non-homologous end-joining (NHEJ), and thus suggests a new role for SIRT6 in DNA repair, by integrating the DNA repair and stress signalling pathways (Mao et al., 2011).

1.3.3.2 Subcellular localisation

The seven mammalian sirtuins are found in numerous compartments within the cell (Figure 1.7). SIRT1, SIRT6, and SIRT7 are found predominantly in the nucleus; SIRT3, SIRT4 and SIRT5 reside in the mitochondria; and SIRT2 is primarily cytoplasmic. Their localisation can be dictated by their sequences as well by cell status (Michishita et al., 2005).

Each sirtuin contains primary amino-acid signal sequences that contribute to their intracellular localisation. For example, the nuclear localisation of SIRT1, SIRT6, and SIRT7 is largely attributed to their nuclear localisation signals. In addition to having two nuclear localisation signal regions, SIRT1 contains two nuclear export signals (Tanno et al., 2007). Thus, the exposure of nuclear localisation signals *versus* nuclear export signals might dictate the nuclear *versus* cytosolic localisation of SIRT1, respectively.

SIRT3, SIRT4 and SIRT5 contain N-terminal mitochondrial targeting sequences, and they are widely believed to localise to the matrix of the mitochondria (Michishita et al., 2005). However, studies have not conclusively ruled out localisation for these proteins to other compartments. The localisation of SIRT3 has been controversial (Hallows et al., 2008). Initial reports found that overexpressed SIRT3 was localised exclusively to the mitochondria (Schwer et al., 2002). However, subsequent studies using a Sirt3 antibody that recognises the endogenous protein demonstrated that SIRT3 localises to the nucleus and that it can translocate from the nucleus to the mitochondria during cell stress (Scher et al., 2007). These authors demonstrated that the human protein goes to the nucleus, where it functions as a histone deacetylase, and that here it can be cleaved at the N-terminus (region required for the nuclear

localisation); only this processed protein travels to the mitochondria, where it can target other substrates (Jin et al., 2009; Scher et al., 2007). For example, SIRT3 deacetylates and activates acetyl-CoA synthetase 2 in mitochondria, both *in vitro* and *in vivo*, thus directly modulating the activity of a metabolic enzyme (Schwer et al., 2006). Strictly associated with this aspect is the idea that the different distributions of the sirtuins among multiple compartments is a dynamic process, which depends on tissue/ cell type and physiological conditions.

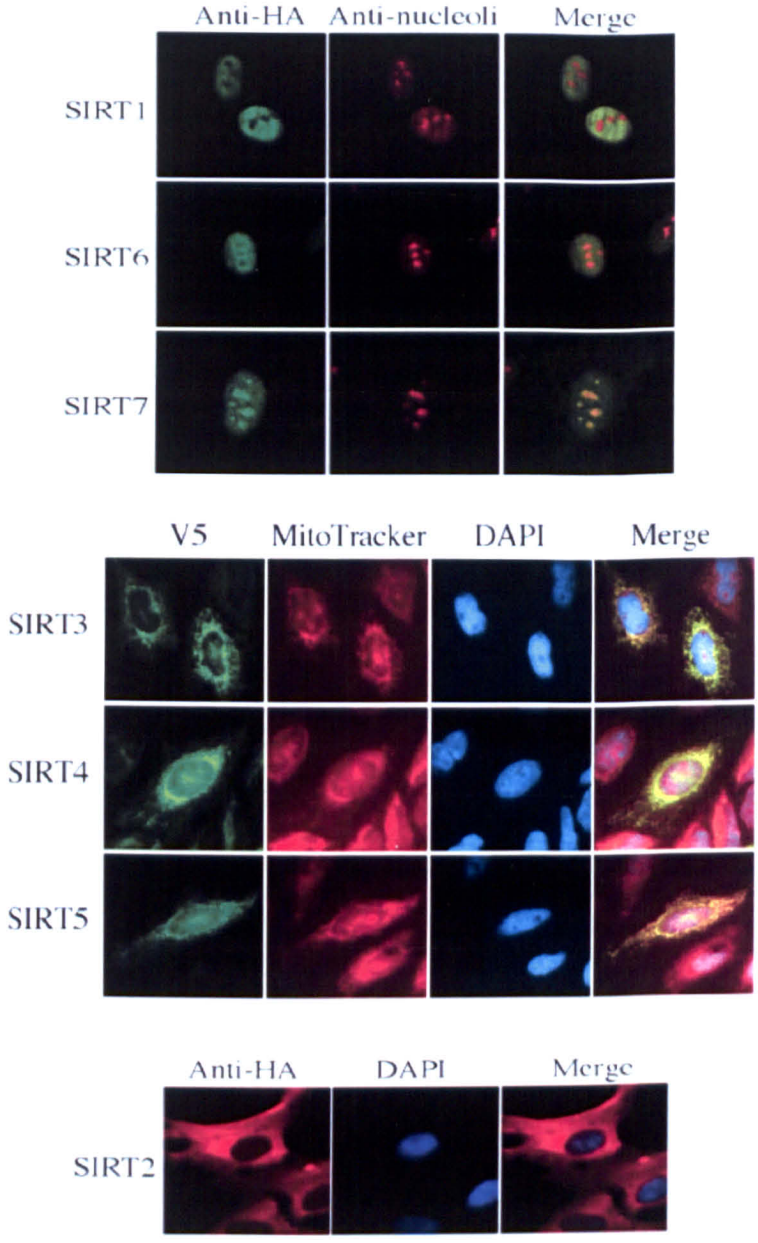

Figure 1.7: sub-cellular localisation of sirtuins

Mammalian sirtuins show different sub-cellular localisations. SIRT1, SIRT6 and SIRT7 are predominately in the nucleus. In the nucleus a large fraction of SIRT1 is associated with euchromatin, whereas SIRT6 associates with heterochromatin and SIRT7 is found in the nucleolus. The sirtuin that resides most prominently in the cytoplasm is SIRT2. SIRT3, SIRT4 and SIRT5 have been described as mitochondrial sirtuins.

Adapted from Michishita *et al.*, 2005. Mol Biol Cell, 16: 4623-4635.

1.3.4 The PARP-superfamily of ADP-ribosylating enzymes

As mentioned in section 1.1, NAD^+/NADH is among the most versatile of biomolecules, as it can be used not only as a coenzyme for a large number of oxidoreduction reactions, but in its oxidised version, it can also serve as substrate for different ADP-ribosylation reactions, the main theme of my thesis. So far, I have described how NAD^+ can be used by toxins to modify host targets, by ADP-ribosyl cyclases to generate second messengers that modulate calcium homeostasis, by ecto-mARTs to modulate protein functions, and in the deacetylation reaction catalysed by the sirtuins.

The PARPs are major players in the consumption of NAD^+. They are an ancient family of enzymes that are encoded in humans by a set of 18 different genes. Sequence and structure analysis of the PARPs has demonstrated that while PARP1-PARP6 show a conserved HYE triad in the catalytic domain, the other 11 members have the glutamic residue that is indispensable for polymerase activity replaced, by different residues (I-L-Y) (Otto et al., 2005). Moreover, two members of the family (PARP9 and PARP13) also show changes in the first histidine residue of the triad that is involved in NAD^+ binding, and for this reason they have been classified as inactive enzymes (Otto et al., 2005). Together, these features suggest that the PARP family is not homogenous regarding its catalytic activity, and indeed, the new members have been indicated to function as mARTs, with experimental evidence for PARP10 (Kleine et al., 2008) and PARP14 (Goenka et al., 2007) now available (see Table 1.2).

In the following sections, I describe the current understanding of the roles of the different PARPs, starting with PARP1, the founding member of the

family. Figure 1.8 shows the domain organisation for all the different PARPs, organized into subgroups based on the presence of specific domains.

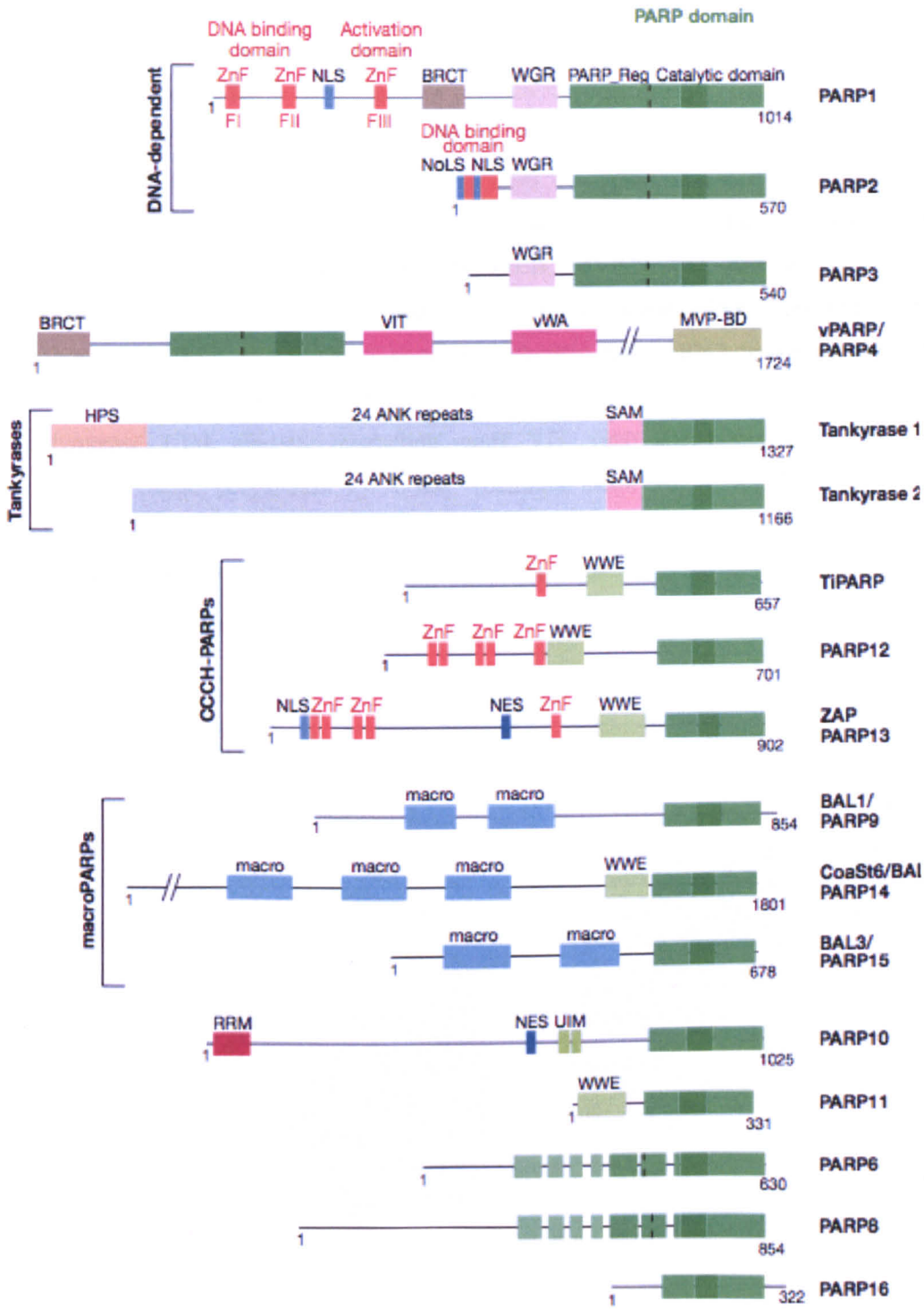
PARP domain
DNA binding domain
Activation domain
DNA-dependent
ZnF
ZnF
NLS
ZnF
BRCT
WGR
PARP_Reg
Catalytic domain
FI
FII
FIII
1014
PARP1
DNA binding domain
NoLS
NLS
WGR
570
PARP2
WGR
540
PARP3
BRCT
VIT
vWA
MVP-BD
1724
vPARP/ PARP4
Tankyrases
HPS
24 ANK repeats
SAM
1327
Tankyrase 1
24 ANK repeats
SAM
1166
Tankyrase 2
CCCH-PARPs
ZnF
WWE
657
TiPARP
ZnF
ZnF
ZnF
WWE
701
PARP12
NLS
ZnF
ZnF
NES
ZnF
WWE
902
ZAP PARP13
macroPARPs
macro
macro
854
BAL1/ PARP9
macro
macro
macro
WWE
1801
CoaSt6/BAI PARP14
macro
macro
678
BAL3/ PARP15
RRM
NES
UIM
1025
PARP10
WWE
331
PARP11
630
PARP6
854
PARP8
322
PARP16

Figure 1.8: The PARP superfamily

The domain architecture of the human PARP family members. Within each putative PARP domain, the region that is homologous to residues 859-908 of PARP1 (the PARP signature) is indicated by the darker green. BRCT, SAM, UIM, MVP-BD, VWA and ANK are protein-interaction modules. ANK, ankyrin; BRCT, BRCA1-carboxy-terminus; HPS, homopolymeric runs of His, Pro and Ser; macro, the macro domain that is involved in ADP-ribose and poly(ADP-ribose) binding; MVP-BD, MVP-binding domain; NES, nuclear export signal; N(o)LS, nuclear (nucleolar) localisation signal; PARP, poly(ADP-ribose) polymerase; PARP_Reg, putative regulatory domain; RRM, RNA-binding motif; SAM, sterile α-motif; TiPARP, 2,3,7,8-tetrachlorodibenzo-p-dioxin-inducible poly(ADP-ribose) polymerase; UIM, ubiquitin-interacting motif; VIT, vault inter-α-trypsin; vPARP, vault poly(ADP-ribose) polymerase, vWA, von Willebrand factor type A; WGR, conserved W, G and R residues; WWE, conserved W, W and E residues; ZnF, DNA or RNA binding zinc fingers (except PARP1 ZnFIII, which coordinates DNA-dependent enzyme activation). From Hakmè *et al.* (2008).

1.3.4.1 PARP1

PARP1 structure

PARP1 was identified almost five decades ago by Chambon, Weill and Mandel (Chambon et al., 1963), which gave rise to an interesting and intriguing field of research. PARP1 is a highly conserved and abundant nuclear protein, which is catalytically active as a dimer and is the major acceptor protein of poly-ADPR in intact cells, via the so-called auto-modification reaction (D'Amours et al., 1999). PARP1 has a modular structure that comprises multiple independently folded domains (Figure 1.8). The major functional units of PARP1 are an amino-terminal DNA-binding domain (DBD), a central auto-modification domain (AMD), and a carboxy-terminal catalytic domain (CD), which can be further broken down into modules that have specific functions (Figure 1.8). The DBD contains two zinc fingers (FI/Zn1 and FII/Zn2) that mediate binding to DNA, a newly discovered third zinc finger domain (FIII/Zn3) that is responsible for DNA-dependent enzyme activation (Langelier et al., 2010; Langelier et al., 2008), a nuclear localisation signal (NLS), and a caspase-3 cleavage site (Hakme et al., 2008; Schreiber et al., 2006). In the central AMD, specific glutamate and lysine residues serve as acceptors of ADPR moieties, thereby allowing the enzyme to ADP-ribosylate itself (Tao et al., 2009). Interestingly, this domain also comprises a BRCA1 carboxy-terminal (BRCT) repeat motif, and a protein-protein interaction domain found in other members of the DNA-damage response pathway (Schreiber et al., 2006). Finally, the CD domain, which is the most conserved domain across the PARP family, contains a PARP signature motif, which binds NAD^+, as well as a 'WGR' motif, which is named after the most conserved amino-acid sequence in the motif (Trp, Gly,

Arg) and which has an unknown function. Together, the structural and functional domains of PARP1 confer the activities required for the broad range of functions of PARP1 in the nucleus (Schreiber et al., 2006).

At steady state, PARP1 has a very low basal enzymatic activity that increases up to 500-fold after DNA damage (Alvarez-Gonzalez and Althaus, 1989). However, its auto-modification can also be triggered by alternative activation mechanisms that are independent of DNA strand breakage. Indeed, PARP1 can recognise distortions in the DNA helical backbone, such as DNA hairpins, cruciforms and stably unpaired regions (Lonskaya et al., 2005). Following its activation, PARP1 modifies many nuclear proteins, including histones, DNA repair enzymes, transcription factors, and even itself. It is this diversity of modified substrates that accounts for the vast array of functions in which PARP1 is involved, an issue covered in the next section.

PARP1 function

PARP1 contributes in many unique ways to the molecular biology of nuclear processes, with key roles in DNA damage signalling pathways, chromatin modification and transcriptional regulation (Krishnakumar and Kraus, 2010a).

In the next section, I provide an overview on the different functions in which PARP1 is involved.

PARP1 in DNA damage and cell death

The earliest functions ascribed to PARP1 were related to DNA repair and the maintenance of genomic integrity (D'Amours et al., 1999). As mentioned above, PARP1 binds to and is activated by DNA damage, leading to an

immediate (15 s to 30 s after damage) and dramatic PARP1-dependent poly-ADP-ribosylation response, which targets a variety of nuclear proteins (Alvarez-Gonzalez and Althaus, 1989). Owing to the size and large negative charge of poly-ADPR, its addition to proteins such as histones, topoisomerase I and DNA protein kinase (DNA-PK) interferes with their functions (D'Amours et al., 1999). However, the bulk of poly-ADPR is attached to PARP1 itself. Notably, this polymer can recruit hundreds of other proteins, typified by XRCC1, a scaffolding protein of the DNA base excision repair (BER) machinery (El-Khamisy et al., 2003; Masson et al., 1998). Some of these proteins bind directly to poly-ADPR through specific domains (see paragraph 1.4), while others are indirectly recruited because they interact with poly-ADPR-binding proteins. At the same time, formation of poly-ADPR reduces the affinity of PARP1 and histones for DNA, providing a mechanism for removing PARP1 from damaged DNA and for the local modulation of chromatin compaction (Poirier et al., 1982; Timinszky et al., 2009). Indeed, *in vitro* studies have demonstrated that removal of PARP1 allows the access of repair proteins and suppresses further poly-ADPR synthesis (Satoh and Lindahl, 1992). ADPR hydrolases and poly-ADPR-glycohydrolases (PARG) remove the poly-ADPR, which contributes to the switching off of the signal (Oka et al., 2006).

As well as its role in the BER pathway, growing evidence suggests that PARP1 is also involved in alternative DSB repair pathways, by both homologous recombination and non-homologous end joining. DSBs are routinely repaired via the NHEJ pathway, which involves the coordinated action of DNA-PK and the XRCC4-DNA ligase IV complex. In addition to this

'classical mechanism', the BER components PARP1, XRCC1 and DNA ligase III can also repair DSBs, which provides a back-up pathway for the classical NHEJ mechanism (Audebert et al., 2004; Audebert et al., 2008; Audebert et al., 2006). Moreover, it has been shown that poly-ADPR synthesis is required to recruit two important components of the homologous recombination system, namely mitotic recombination 11 and ataxia telengiectasia-mutated (ATM), which suggests that PARP1 has an additional role in this process (Haince et al., 2007; Haince et al., 2008). Consistent with the involvement of PARP1 in all of these DNA-damage responses, $Parp1^{-/-}$ mice are more sensitive to DNA-damaging agents, such as alkylating agents and ionising radiation (Shall and de Murcia, 2000).

Although poly-ADPR has a half-life of seconds to minutes, the consequences of poly-ADPR metabolism on cellular homeostasis can persist long after PARP1 and the hydrolases have acted. Polymer synthesis consumes substantial amounts of NAD^+ and poly-ADPR cleavage generates large amounts of AMP, leading to the activation of the bioenergetic sensor AMP-activated protein kinase (AMPK), which can induce an authophagic state (Huang et al., 2009). Moreover, long and branched polymers can directly trigger specific cell death, known as parthanatos. Parthanatos specifically indicates a type of cell death triggered by PAR (indeed this word refers to PAR, poly-ADP-ribose, and thanatos, the greek personifition of death and mortality) (Andrabi et al., 2006; David et al., 2009). Thus, the various consequences of PARP1 activation reflect the collective effects of poly-ADPR synthesis on PARP1 substrates, binding of various proteins to poly-ADPR,

changes in cellular NAD^+ (and ATP) levels during poly-ADPR synthesis and changes in AMP levels through poly-ADPR degradation.

In summary, DNA-damage-dependent poly-ADPR production has three main purposes:

- first, poly-ADP-ribosylated histones and/or PARP1 itself cause relaxation of chromatin, which increases the access of other proteins to the site of the DNA lesions;
- second, it mediates the fast recruitment of SSBs/BER factors (such as XRCC1 and DNA ligase III) to the sites of lesions;
- third, it signals the extent of damage, so that the cell can response appropriately, according to the damage (DNA repair or cell death).

Based on the important roles of PARP1 in the maintenance of genomic stability and regulation of cell death, several clinical studies are using PARP1 inhibitors to treat cancers that are associated with defects in DNA repair machines. These studies are based on the concept that PARP1 is a potential synthetic lethal therapeutic target for the treatment of cancers that carry specific DNA-repair defects. An example here is the familial form of breast cancer, which is caused by an inherited defect and subsequent loss of heterozygosity in one of the BRCA1 or BRAC2 alleles, both of which have important roles in the repair of DNA DSBs by homologous recombination (Venkitaraman, 2002). Of interest, Fong and colleagues (Fong et al., 2009) conduced a phase I clinical trial using an oral PARP1 inhibitor, oloparib, and showed that it has few side effects and has antitumour activity in cancer associated to BRCA1 or BRCA2 mutations. Spontaneously occurring SSBs cannot be repaired in the absence of PARP1 activity, which in this case is

achieved by chemical inhibition of PARP1, and which results in the collapse of replication forks. BRCA proficient cells can repair these profound lesions via homologous recombination, while in BRCA-deficient cells these lesions are either repaired by error-prone pathways, leading to further genetic instability, or are directly lethal to cells (Helleday et al., 2005).

Defects in homologous-recombination repair can also be caused by loss of function of proteins other than BRCA1 and BRCA2, including ATM and the checkpoint kinases CHK1 and CHK2. Such defects in homologous-recombination repair may be relatively common in some sporadic cancers, including breast cancer and ovarian cancer, making this therapeutic strategy more widely useful as an anticancer treatment (Peng and Lin, 2011).

PARP1 and transcriptional regulation

- Regulation of chromatin structure

Although historically PARP1 has been mainly related to DNA damage, later studies revealed its important role in transcriptional regulation (Kraus and Lis, 2003). It is now evident that PARP1 carries out this role by participating to different processes, such as modulation of chromatin structure, regulation of transcription factors, and regulation of methylation pattern (Kraus, 2008).

PARP1 disruption of chromatin through the modification of histones was one of the first functional effects identified for PARP1 (Poirier et al., 1982). Under steady-state conditions, PARP1 is associated with chromatin, where it binds core histone proteins (H2A, H2B, H3 and H4) in the nucleosome. Atomic force microscopy shows that this binding promotes the

compaction of nucleosomes into higher order structures that are refractory to transcription (Wacker et al., 2007). As soon as PARP1 is activated, the highly charged poly-ADPR reduces the affinity of PARP1 for its associated proteins, which leads to a loosening of the chromatin structure and restoration of transcription (Kim et al., 2004; Wacker et al., 2007). At first glance, this would appear to be at odds with genomic studies that demonstrate that PARP1 is associated to actively transcribed genes (Krishnakumar et al., 2008), which would suggest that it has a role in promoting the formation of chromatin structures that are permissive to transcription. It is therefore important to consider the specific NAD^+ concentration: in the absence of NAD^+ (non-physiological conditions) PARP1 favours a closed chromatin structure, whereas at physiological nuclear NAD^+ concentrations, PARP1 does the opposite, acting both on PARP1 itself and on chromatin-associated factors. Indeed, in this regard, PARP1 and histone H1, a nucleosome binding protein that is associated to gene repression (Happel and Doenecke, 2009), show reciprocal patterns of chromatin binding at many RNA polymerase II transcribed promoters (Krishnakumar et al., 2008). Recently, Krishnakumar and co-workers (Krishnakumar and Kraus, 2010b) demonstrated that PARP1 establishes a permissive chromatin environment at the promoters of its regulated genes by preventing demethylation of histone H3, through ADP-ribosylation of the specific histone H3 demethylase KDM5B, while promoting the exclusion of histone H1. The permissive chromatin environment is required for the efficient loading of the polymerase II transcription machinery and subsequent transcription. Moreover, the authors showed that while the histone H3 demethylation is necessary to reduce gene expression, it is not sufficient,

and that the PARP1 protein must be physically removed from the promoter to allow histone H1 binding and subsequent changes in chromatin structure. In this mechanism, PARP1 catalytic activity is only required for the regulation of KDM5B activity, while it is dispensable for displacing histone H1.

Furthermore, during oestrogen-induced transcription of the *TFF1* gene, PARP1 not only promotes the removal of histone H1, but also recruits HMGB1, thus enhancing transcription (Ju et al., 2006). Along the same line of evidence, PARP1 can also modify another repressive chromatin-associated protein, known as DEK, thus promoting its release from chromatin (Gamble and Fisher, 2007).

Moreover, as well as its modulation of chromatin structure through regulation of its composition, PARP1 can regulate transcription by functioning as a classical co-regulator and regulating the methylation state of DNA.

- PARP1 as co-regulator

In a 'co-regulator' mode, PARP1 can be recruited to target promoters as a functional endpoint of signalling pathways, to regulate components of the transcription complex assembled at the promoter. In some cases, the enzymatic activity of PARP1 is required (e.g., with HES1 and Elk1) (Cohen-Armon et al., 2007; Ju et al., 2004), while in others it is not (e.g., NF-kB and RAR) (Hassa et al., 2001; Pavri et al., 2005). When acting as a co-regulator during signal-regulated transcriptional responses, PARP1 can function as a promoter-specific exchange factor that promotes the release of inhibitory factors and the recruitment of stimulatory factors.

In the context of NF-kB-dependent gene activation, for example,

PARP1 can physically interact with the co-activator complex Mediator and the histone acetyl transferase (HAT) p300, as well as with HDAC1-3. Acetylation of several lysine residues in PARP1 by p300/CBP results in an enhanced interaction with p50 (a subunit of Nf-kB) and subsequent activation of NF-kB-dependent gene expression in response to inflammatory stimuli, which suggests stimulus-dependent induction of PARP1-dependent NF-kB activation in concert with further transcriptional co-activators (Hassa et al., 2005).

Interplay between PARP1 and Mediator was also observed when studying the essential factors for retinoic acid receptor (RAR)-mediated transcription from the RARß2 promoter (Pavri et al., 2005). PARP1 occupies RAR-responsive promoters continuously, along with the Mediator complex and other factors, as confirmed by ChIP experiments. After ligand-dependent induction of gene expression, PARP1 is indispensable for converting Mediator from its inactive state (Cdk8+) to its active state (Cdk8-), through the release of the repressing Cdk8 module (Pavri et al., 2005). Interestingly, PARP1 directly binds Cdk8 via its N-terminal region, and the interaction is weakened after TNFα stimulation, which precedes acetylation of PARP1 and the subsequent NF-kB activation (Hassa et al., 2005). A similar situation was observed in neural differentiating stem cells: PARP1 is a component of the groucho/TLE co-repressor complex that mediates the release of this complex upon PDGF stimulation and after PDGF-triggered activation of calcium/calmodulin dependent protein kinase II, which allows for the recruitment of co-activators and subsequent promoter activation (Ju et al., 2004). The PARP1 catalytic activity is essential for this function, and several components of the groucho/TLE complex, including TLE1, the DNA topoisomerase TopoIIß and

Nucleolin, are ADP-ribosylated by PARP1 (Ju et al., 2004). These authors extended their model by a further study that provided evidence that the signal-dependent activation of transcription requires the transient formation of dsDNA breaks by TopoIIß and concomitant PARP1 activation, with the latter inducing a nucleosome-specific exchange of histone H1 against the high-mobility group (HMG) B protein and local changes in chromatin structure (Ju and Rosenfeld, 2006).

- PARP1 and DNA methylation

Studies over the past decade have begun to link PARP1-dependent poly-ADP-ribosylation to DNA methylation, a stable epigenetic mark that can be passed to daughter cells upon cell division and is associated with the repression of gene expression (Caiafa and Zampieri, 2005). One of the ways in which PARP1 affects DNA methylation is by regulating the expression and activity of the DNA methyltransferase Dnmt1 (Zampieri et al., 2009; Zlatanova and Caiafa, 2009). PARP1 binds to the promoter of the Dnmt1 gene and protects it from DNA-methylation-induced silencing in a poly-ADPR-dependent manner (Zampieri et al., 2009). In this regard, overexpression of poly-ADPR-glycohydrolase (PARG), an enzyme that degrades poly-ADPR, leads to aberrant methylation of a CpG island in the promoter of the Dnmt1 gene in mouse fibroblasts, which in turn inhibits Dnmt1 transcription. The loss of Dnmt1 expression leads to widespread passive hypomethylation of genomic DNA (Zampieri et al., 2009).

In addition, PARP1 has been shown to interact with Dnmt1 in a complex that contains poly-ADPR (Reale et al., 2005). The non-covalent

binding of poly-ADPR polymers by Dnmt1 within the complex inhibits the Dnmt1 DNA methyltransferase activity, probably through a steric inhibitory mechanism (Reale et al., 2005). Interestingly, the effects of PARP1 on DNA methylation are modulated by the protein CTCF, which might promote PARP1 auto-modification, and thus CTCF poly-ADP-ribosylation and accumulation of poly-ADPR polymers, which ultimately inhibits Dnmt1 DNA methyltransferase activity (Guastafierro et al., 2008). Future studies will be required to determine the extent to which PARP1 has a role in the dynamic regulation of DNA methylation under different physiological and pathological states.

1.3.4.2 PARP2

PARP2 was discovered in the late 1990s and it is the only other known PARP that contributes to the formation of ADPR polymers in response to DNA damage. This enzyme bears the strongest similarity to PARP1; nevertheless, the N-terminal DNA-binding domain is very different to PARP1 and consists of only 64 amino acids. PARP2 has high homology (62%) with the C-terminus of PARP1, which bears the catalytic domain (Ame et al., 1999). As expected, its catalytic properties strongly resemble those of PARP1, with the synthesis of long ADPR polymers being dependent on the binding to and activation by nicked DNA (Ame et al., 1999). However, the differences in their DBD might account for differential substrate recognition: for instance, PARP2 cannot modify histones, which are instead the prototypical PARP1 substrates (Messner et al., 2010; Nguewa et al., 2005).

PARP2 shares many functions with PARP1 in DNA repair processes: it interacts with the same components of the BER pathway, its enzymatic activity is required for efficient BER of DNA lesions, it can hetero-dimerise with PARP1 within the same regions, being responsible for its homo-dimerisation, and PARP1 and PARP2 can poly-ADP-ribosylate each other in a trans-ADP-ribosylation reaction (Nguewa et al., 2005). In addition, $Parp2^{-/-}$ mice are hypersensitive to DNA-damaging agents, similar to $Parp1^{-/-}$ mice, and the double mutant $Parp1^{-/-}$ $Parp2^{-/-}$ mice are embryonic lethal, demonstrating their essential roles in early embryogenesis and underlining their at least partial functional redundancy in maintaining genome integrity (Menissier de Murcia et al., 2003). Further similarities between PARP2 and PARP1 include their roles in the maintenance of telomere integrity through binding to telomeric-repeat binding factor 2 (TRF2) (Dantzer et al., 2004; Gomez et al., 2006). Additionally, the cleavage of PARP2 and PARP1 during caspase-dependent apoptosis, mediated by caspase-8 and caspase-3, respectively (Benchoua et al., 2002; Kaufmann et al., 1993), and their localisation to centromeres, where they interact with centromeric proteins and poly-ADP-ribosylate them after DNA damage, thus modulating the compact chromatin structure of the centromeres (Saxena et al., 2002).

1.3.4.3 PARP3

PARP3 was initially discovered in an expressed sequence tag (EST) library screening using the catalytic domain of human PARP1 (Johansson, 1999). The human PARP3 gene has two splicing variants, which gives rise to two proteins that differ by seven amino acids at the N-terminus. The full-length protein is a core component of the centrosome, and it resides preferentially in the daughter

centriole throughout the cell cycle; the shorter splice variant accumulates within the nucleus (Augustin et al., 2003). As for PARP1 and PARP2, PARP3 can undergo auto-ADP-ribosylation and can activate PARP1 in the absence of DNA damage (Loseva et al., 2010). Overexpression of PARP3 or its N-terminal domain interferes with the G1/S phase of cell-cycle progression, without inducing centrosomal amplification (Augustin et al., 2003). Moreover, it has been demonstrated that PARP3 associates with the polycomb group proteins that are involved in transcriptional silencing and with DNA repair networks, including SSB/BER and NHEJ, thus suggesting a role for PARP3 in the maintenance of genomic integrity (Rouleau et al., 2007). In this study of Rouleau *et al.* (2007), PARP3 was identified as part of the DNA repair protein complexes by a proteomic approach, which revealed an association with PARP1 and the DNA ligases III and IV. Thus, PARP3 might be involved in the maintenance of transcriptional repression and might be linked to the DNA repair machinery.

A recent study by Dantzer and co-workers (Boehler et al., 2011) provided evidence for a synergistic role of PARP3 and PARP1 in cellular responses to DSBs, with PARP3 acting to accelerate the repair response. Additionally, these authors identify PARP3 as a key component of a protein complex containing NuMa and tankyrase1; in this complex, PARP3 stimulates NuMa ADP-ribosylation by tankyrase1, which facilitates the formation and maintenance of the mitotic spindle and genomic integrity. Both of these findings open promising prospects for targeting PARP3 in cancer therapy.

1.3.4.4 PARP4

PARP4 (also known as vault-PARP) was originally identified as a component of the mammalian ribonucleoprotein (RNP) complexes known as vaults (Kickhoefer et al., 1999) and shown to share 28% identity with the catalytic domain of PARP1; as for PARP1, the PARP4 catalytic domain can undergo auto-modification. Additionally, it can modify one of the major components of vaults, the major vault protein (MVP), and it has been shown that ADP-ribosylation is retained into the vault complexes (Kickhoefer et al., 1999). However, further studies demonstrated that even though ADP-ribosylation at vault complexes leads to a more stable association between PARP4 and MVP, PARP4 incorporation in this structure was not dependent on PARP4 catalytic activity: indeed, PARP4 association to vaults depends only on the PARP4 C-terminal domain, which lacks the catalytic activity (Zheng et al., 2005).

Besides this structural role, PARP4 has been found at other cellular locations, such as the nucleus and mitotic spindle, which indicates that it might have multiple roles *in vivo* (Kickhoefer et al., 1999). Interestingly, PARP4 interacts with telomerase-associated protein 1 (TEP1), suggesting that PARP4 and TEP1 might have roles in both cytoplasmic and nuclear RNP complexes. However, an analysis of Parp4$^{-/-}$ mice revealed that these mice are viable and fertile without any apparent defects in telomere length or function, or in the structure of the vault particles (Liu et al., 2004), and indicated that PARP4 is therefore dispensable for the function of vaults as well as for maintaining telomere function. The only phenotype observed so far for Parp4$^{-/-}$ mice is an increased susceptibility to carcinogen-induced colon tumorigenesis (Raval-Fernandes et al., 2005).

1.3.4.5 PARP5a and PARP5b (Tankyrase 1 and 2)

PARP5a and PARP5b, also known as tankyrase1 and tankyrase2 (hereafter indicated as PARP5a and PARP5b), are two closely related members of the PARP superfamily and were identified as components of a telomeric complex (Kaminker et al., 2001; Smith and de Lange, 1999). They share 85% identity and differ in the N-terminal HPS domain, which is missing in PARP5b (see figure 1.8). They can form homo- and hetero(oligo)mers through their sterile-alpha motif domains (Hsiao and Smith, 2008). Their functions have mainly been connected to telomeres, although additional roles in mitosis and vesicular trafficking have been proposed (Hsiao and Smith, 2008)

PARP5a was identified in a yeast two-hybrid screen as an interaction partner for telomeric repeat binding factor 1 (TRF1), with binding to TRF1 being mediated through its ankyrin repeats (Smith et al., 1998). PARP5a can auto-modify itself, as well as poly-ADP-ribosylate TRF1, with which it co-localises at telomeric DNA (Smith et al., 1998). A careful analysis of the PARP5a ADP-ribosylation capacity revealed that PARP5a can synthesise poly-ADPR with an average chain length of 20 units, but lacks the ability to form branched polymers, as has been described for PARP1 and PARP2 (Rippmann et al., 2002). In addition to its telomeric localisation, PARP5a shows multiple subcellular localisation, related to the cell-cycle; at mitosis, PARP5a is located around the pericentriolar matrix of mitotic centrosomes, while during interphase I is on the cytoplasmic side of the nuclear envelope and partially in the Golgi complex (Chi and Lodish, 2000; Smith and de Lange, 1999).

The role for PARP5a in telomere elongation is associated with ADP-ribosylation of TRF1; indeed, once modified, TRF1 is released from telomeres,

allowing access of telomerase to the telomeres (Cook et al., 2002; Smith and de Lange, 2000). This release might be regulated by a second TRF1-interacting factor, TIN2 (Ye and de Lange, 2004). In contrast to this model, a mutant PARP5a that cannot ADP-ribosylate TRF1 appeared to be sufficient to loosen the telomeric heterochromatin and to promote telomere elongation (Muramatsu et al., 2008).

As well as its function in telomere elongation, the catalytic activity of PARP5a has a fundamental role in mitosis (Chang et al., 2005; Dynek and Smith, 2004). Of note, poly-ADPR has been shown to be required for spindle assembly (Chang et al., 2004), and knockdown of PARP5a results in pre-anaphase mitotic arrest. Taking these findings together, they support the idea that PARP5a activity is necessary for correct spindle formation. Accordingly, the spindle protein NuMA was demonstrated to be a substrate for PARP5a-mediated poly-ADP-ribosylation during mitosis, which results in the regulation of some NuMa functions. These authors demonstrated that even the knockdown of PARP5a does not cause displacement of NuMa from the spindle poles, it migh have a role in ensuring the correct spindle number. Knockdown of NuMA completely abolished the localisation of PARP5a to the spindles during mitosis, indicating an essential role for NuMA in the recruitment of PARP5a (Chang et al., 2005).

As mentioned above, a fraction of PARP5a is also associated with the Golgi complex. Here, PARP5a interacts with the insulin-responsive amino peptidase that probably recruits it to GLUT4 storage vesicles in adipocytes (Chi and Lodish, 2000). Later studies demonstrated that the catalytic activity of

PARP5a is required to regulate GLUT4 storage-vesicle trafficking (Yeh et al., 2007).

The gene encoding PARP5b, at that time designated as the *TNKL* gene, was cloned in 2001 (Kuimov et al., 2001). Almost simultaneously, the PARP5b protein was identified as an interaction partner of the adaptor protein Grb14, and both proteins were shown to be enriched in a subcellular fraction containing Golgi vesicles and endosomes (Lyons et al., 2001). Similar to PARP5a, PARP5b interacts with and can modify TRF1, which indicates a potentially redundant role for PARP5a and PARP5b in telomere regulation (Cook et al., 2002). Considering the high homology of PARP5a and PARP5b, these observations were not surprising. Indeed, the discovery of a tankyrase-binding motif in several of the interaction partners shared between both tankyrases, and their reciprocal ability to associate and to co-localise (Sbodio and Chi, 2002), suggested a high redundancy in terms of physiological function, a situation resembling the close connection between PARP1 and PARP2.

1.3.4.6 The 11 members of mono-ADP-ribosyltransferases of the PARP family

The following sections focus on the current knowledge of the 11 putative mARTs of the PARP family. As mentioned in section 1.3.4, sequence alignment analysis performed by Koch-Nolte and co-workers identify two main groups of PARPs: one containing six *bona-fide* PARPs (PARP1-PARP6) and a second group composed of the other 11 members, which are believed to function as mono-ADP-ribosyl-transferases (Table 1.2). These 11 members are characterised by a conserved catalytic domain (the PARP domain) that is

associated - in a Lego-like fashion - with a broad spectrum of known protein domains (see Figure 1.8). These different domains allow a further division of the PARP super-family into subgroups that share specific domains. I will use this criterion to describe the 11 members.

The Macro PARPs: PARP9, PARP14 and PARP15

PARP9 (also known as BAL1), PARP14 (also known as BAL2/CoaSt6) and PARP15 (also known as BAL3) belong to the subfamily of macro-PARPs, which link 1–3 macro domains to a PARP domain.

The gene encoding PARP9 was originally identified as the *BAL1* (B-aggressive lymphoma 1) gene in a screen for risk-related genes in diffuse large B-cell lymphoma (DLBCL) and mapped to chromosome 3q21 (Aguiar et al., 2000). It encodes a nuclear protein of 88 kDa with an N-terminal duplicated macro domain, a protein motif that is involved in the detection of different forms of ADPR and in transcriptional repression (discussed in section 1.4). The overexpression of PARP9 in B-cell lymphoma cells stimulated their migration in transwell assays, which indicated a tumour-promoting role for PARP9 in malignant B cells (Aguiar et al., 2000). Interestingly, PARP9 interacts with the ubiquitin E3 ligase Deltex-3 (Takeyama et al., 2003). Deltex-3 regulates the subcellular localization of PARP9, and PARP9 overexpression in DLBCL cell lines resulted in an increase in the expression of multiple interferon-stimulated genes, suggesting an important role for PARP9 in inflammatory processes (Juszczynski et al., 2006). Although PARP9 contains a C-terminal PARP domain, it lacks catalytic activity due to the absence of the conserved residues that are essential for catalysis, although it can repress transcription in general

via its macro domains, as assessed by reporter gene assays (Aguiar et al., 2005).

A database search identified two genes related to BAL1, which consequently were named BAL2 and BAL3. Both of these genes were mapped to chromosome 3q21, arranged in tandem with the previously identified BAL1. The encoded proteins, PARP14 and PARP15, like PARP9, have N-terminal macro domains and a C-terminal PARP domain, but in contrast to PARP9, the C-terminal regions of both PARP14 and PARP15 are subject to auto-ADP-ribosylation, which indicates an intact catalytic activity (Aguiar et al., 2005). PARP15 was reported to have a transcriptionally repressive function, which is not as pronounced as for PARP9, but which is also mediated by its macro domains. Since its PARP domain alone slightly stimulated transcription, it was suggested that the intrinsic PARP activity of PARP15 might counteract the repressive effect of the macro domains (Aguiar et al., 2005).

PARP14 was identified in a yeast two-hybrid screen as an interaction partner of STAT6, and so it was named collaborator of STAT6 (CoaSt6) (Goenka and Boothby, 2006). In spite of its three macro domains, and in contrast to the repressive effect of the related PARP9 and PARP15 proteins, PARP14 was described as having a potentiating effect on the IL-4-induced transcriptional activation by STAT6 that is mediated mainly by its macro domains. Importantly, PARP14 appears to be a specific co-activator for STAT6-mediated transcription, since it did not stimulate the interferon-γ-induced gene expression by STAT1 (Goenka and Boothby, 2006). These authors proposed a model in which PARP14 ADP-ribosylates p100, a STAT6 co-activator, which enhances the interaction of STAT6 with the basal

transcription machinery, thereby mediating a stimulatory effect on STAT6-driven gene expression (Goenka et al., 2007). More recently, the same group described the molecular mechanism responsible for this effect, defining PARP14 as a transcriptional switch for STAT6-dependent gene activation. In particular, these authors demonstrated that under non-stimulating conditions (i.e., in the absence of IL4), PARP14 recruits HDAC2 and HDAC3 to IL-4-responsive promoters, thus blocking transcription. Upon IL-4 stimulation, Stat6 is activated and binds to its promoter element, inducing PARP14 enzymatic activity, so that it can modify itself on the N terminus and HDAC2 and HDAC3 in the complex. This results in the dissociation of PARP14 and the HDACs from the promoter, while allowing access to coactivators, such as HATs like CBP/p300, to activate transcription (Mehrotra et al., 2011).

PARP10

PARP10 has a unique domain composition among the PARP family members, combining potential DNA/RNA binding motifs and ubiquitin-interacting motifs with the catalytic PARP domain (see Figure 1.8). PARP10 can ADP-ribosylates itself as well as core histones (Chou et al., 2006).

PARP10 was initially identified as an interaction partner of the oncoprotein MYC (Yu et al., 2005). It was reported to localise preferentially in the cytoplasm and to shuttle between the cytoplasm and the nucleus through its functional nuclear-export sequence (NES). Importantly, PARP10 can impair the c-MYC/H-RAS-driven transformation of rat embryo fibroblasts in a dose-dependent manner, a feature that is abrogated in a PARP10 mutant carrying a

non-functional NES, but is not dependent on the PARP10 catalytic activity (Yu et al., 2005).

Subsequent work by Lusher and co-workers (Kleine et al., 2008) clearly defined the catalytic activity of PARP10 in more detail, and found that PARP10 functions as a mART, thereby defining a new class of intracellular mARTs. Interestingly, they proposed the mechanism of substrate-assisted catalysis for the automodification. According to this model, PARP10 uses a substrate glutamate and possibly an aspartate for catalysis, thus allowing for the absence of the glutamic residue found in the 'classical' PARPs.

However, a physiological role for PARP10 has not been elucidated yet.

CCCH-PARPs: PARP7-PARP12 and PARP13

The CCCH-type PARP subfamily contains three members (PARP7, PARP12 and PARP13) that share a similar domain organization, comprising PARP catalytic domain, a WWE domain (protein-protein interaction domain) and $CX_8CX_5CX_3$-like zinc fingers. These zinc finger domains are known to recognise RNA and thus are different from PARP1 zinc finger domain involved in DNA recognition.

PARP7

PARP7 was identified as a gene that is up-regulated by treatment of mouse hepatoma cells with 2,3,7,8-tetrachlorodibenzo-*p*-dioxin (TCDD), a prototype substance from the class of dioxins that cause pleiotropic harmful effects in mammalian species through modulation of gene expression. PARP7 is broadly expressed in murine tissues and is likely to have enzymatic ADP-ribosylation

ability, although it was not been determined whether it undergoes auto-ADP-ribosylation (Ma et al., 2001).

To date, there is no available information about a role for PARP7.

PARP12

Figure 1.9 shows the structure of PARP12, which includes five zinc-finger domains, two WWE domains, and a catalytic domain at its C-terminus. The function of PARP12 is still not known, and indeed, the study of PARP12 and its cellular function constitute a part of my PhD project.

PARP13

PARP13 is also known as ZAP (zinc-finger CCCH-type antiviral protein 1) and it was identified during a search for genes that prevent viral infection. Its antiviral property has been linked to its specific binding and degradation of viral mRNAs in the cytoplasm (Gao et al., 2002), with this binding shown to be mediated by the four CCCH zinc finger motifs in ZAP (Guo et al., 2007). Degradation of viral mRNAs involves recruitment of the RNA processing exosome through an interaction of ZAP and the exosome component hRrp46p (Guo et al., 2007). Interestingly, expression of the murine *ZAP* gene is induced by interferon-γ and interferon-ß stimulation, and its protein product inhibits Sindbis virus replication, thereby linking the ZAP protein to interferon-mediated antiviral activities (Zhang et al., 2007). The human ZAP gene can be expressed as two alternatively spliced isoforms. While the short isoform ZAP(S) does not code for a PARP domain, the longer isoform ZAP(L) encodes a protein containing a C-terminal PARP domain in addition to the CCCH zinc

finger motifs, the TiPARP homology domain and a WWE domain (Kerns et al., 2008).

According to analysis by Koch-Nolte and co-workers (Otto et al., 2005), PARP13 is enzymatically inactive, as it lacks the important residues for NAD^+ binding, and therefore its anti-viral functions cannot be associated with an intrinsic ADP-ribosylation activity. Further studies are required to cast more light upon this aspect.

To date, there are no available data on PARP6, PARP8, PARP11 and PARP16, which remain to be fully characterised. The structure of these PARPs is shown in Figure 1.8.

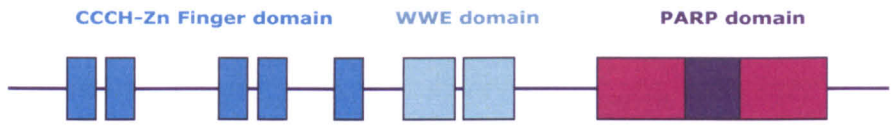

Figure 1.9: Domain architecture of human PARP12

PARP12 belongs to the CCCH-Zinc Finger PARPs. It has five Zn-finger domains, as found in proteins involved in RNA binding, two WWW domains (named after three of its conserved residues), which are predicted to mediate protein-protein interactions, and a PARP catalytic domain. The darker colour in the PARP domain indicates the homologous residues to PARP1.

1.4 How to read ADP-ribosylation: the ADP-ribose binding modules

In the previous sections, I indicated the different functions in which ADP-ribosylation is involved, ranging from the action of bacterial toxins to a role for ADP-ribosylation in DNA repair, maintenance of genomic stability, and regulation of mitosis. Despite these important roles of ADP-ribosylation, progress in understanding how these PTMs are 'read' by other proteins has been made only recently. Work by three different groups (Ahel et al., 2009; Gottschalk et al., 2009; Timinszky et al., 2009) have provided insights into the actions of an ADPR interaction domain, known as the macro-domain, in the process of DNA repair.

The first macro domain to be described was that of Af1521, a protein from the thermophilic organism *Archaeoglobus fulgidus*, which was shown to bind ADPR with high affinity (K_D in the range of 120 nM) (Karras et al., 2005). The crystal structure of Af1521 bound to ADPR provided a clear explanation for this high affinity, showing that ADPR is bound in an L-shaped cleft on the protein surface, with the adenine moiety residing in a deep hydrophobic pocket, where the distal ribose can form several H-bonds that are not present in the ADP-bound structure of Af1521 (Karras et al., 2005).

The three research groups mentioned above demonstrated that macro domains interact with poly-ADPR in living cells. To show this, the authors use a laser-microirradiation procedure to introduce DNA breaks at discrete locations and to stimulate PARP1 activity. The local synthesis of poly-ADPR was recognised by fluorescently tagged macrodomains from different proteins overexpressed in the cell system (Timinszky et al., 2009). Among the proteins recruited to the site of damage, there were the histone variant macroH2A1.1

and the oncoprotein ALC1 (amplified in liver cancer 1), a member of the SWF2 ATPase superfamily of remodelling proteins, both of which are involved in the alteration of chromatin structure. Furthermore, ALC1 interacts with other DNA repair proteins, including XRCC1, and these interactions are also dependent on poly-ADPR formation (Ahel et al., 2009). Thus, macro domains can be used by proteins 'to read the message encoded by ADPR'. According to databases, only 10 human proteins containing macro domains have been reported. This low number suggests that other domains that bind ADPR will exist. Nature has invented other 'tools' to recognise ADPR, and so far at least two additional motifs have been identified.

Indeed, in addition to macro domains, several groups have defined poly-ADPR-interacting proteins and derived potential consensus sequences for proteins with this capacity; the most refined of these is an eight amino acid motif, which is found in many proteins linked to DNA repair and chromatin regulation (Gagne et al., 2008). Accordingly, the first indication for an ADPR binding motif was published in the late 1990's by Malanga *et al.*, which showed that three regions within the tumour suppressor protein p53 can bind poly-ADPR, either free or attached on PARP1, through strong non-covalent interactions, thus interfering with p53 binding to DNA (Malanga et al., 1998). The following studies led to the discovery of a poly-ADPR-binding motif that is composed of a cluster that is rich in basic amino acids and a pattern of hydrophobic amino acids interspersed with basic residues (Pleschke et al., 2000). However, it is not certain whether the binding of poly-ADPR is indeed a specific feature of the proteins with the 'eight amino acid motif', or whether the preponderance of basic residues reflects their general affinity for the ADPR

polymer. Another characterised motif is the poly-ADPR-binding zinc finger (PBZ), which is also associated with DNA repair proteins (Ahel et al., 2008).

In summary, three different protein motifs have been identified that specify interaction with ADPR (Figure 1.10). The functional differences among these three motifs are unclear, and require further studies.

1.5 A specific case: ADP-ribosylation and CtBP1/BARS

The predominant topic of this thesis is my study of ADP-ribosylation. As explained in the previous sections, this post-translational modification is 'used' by toxins and cellular enzymes to modulate cell functions. I explored both aspects of these modifications. In particular, on the one side, my project was focused on the study of the ADP-ribosylation reaction that is dependent on the toxin brefeldin A (BFA), to understand how it affects C-terminal binding protein 1 (CtBP1) functions, as described in Chapter 3. On the other side, I analysed intracellular ADP-ribosylation, with particular focus on the enzyme PARP12, as described in Chapter 4.

Thus, after this general introduction to ADP-ribosylation, I will now introduce the current knowledge on BFA-dependent ADP-ribosylation and the target of this modification: CtBP1, or BFA-dependent ADP-ribosylated substrate (CtBP1/BARS). This introduction will be instrumental to the understanding of the results I describe in Chapter 3.

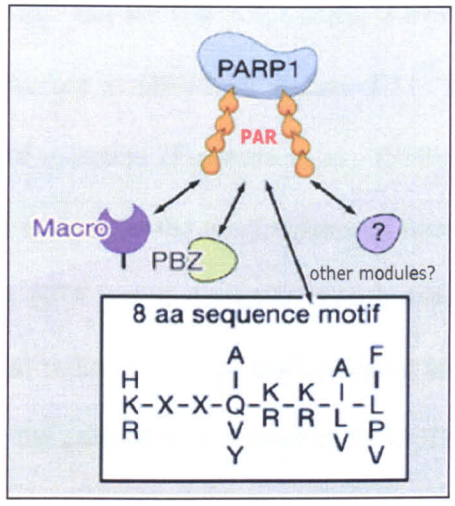

Figure 1.10: ADP-ribose binding modules

Summary of the three poly-ADP-ribose-binding domains that have been described. Additional domains might exist that can read the modifications. See text for details. PAR, poly-ADP-ribose; PBZ, poly-ADP-ribose- binding zinc finger.

Adapted from Kleine *et al.* (2009).

1.5.1 Brefeldin A

BFA is a macrocyclic lactone that is synthesised from palmitate by a variety of fungi, and its structure is shown in Figure 1.11. BFA induces a rapid and reversible block of secretion (Fujiwara et al., 1988), and for this reason it has been widely used to analyse the mechanisms of membrane transport. The best known effects of BFA are a dramatic morphological reorganisation of the Golgi complex and redistribution of both resident and cargo proteins from the Golgi complex to the endoplasmic reticulum (ER) (Doms et al., 1989; Fujiwara et al., 1988; Lippincott-Schwartz et al., 1989; Sciaky et al., 1997). However, BFA also affects the morphology and function of the endosomal/ lysosomal compartments (Lippincott-Schwartz et al., 1991). The redistribution of the Golgi proteins induced by BFA is very rapid, occurring in a few minutes, and it is completely reversible (Doms et al., 1989). The effects of BFA are caused, at least in part, by the release of a set of proteins from the Golgi complex, which includes two major non-clathrin coat proteins, ß-COP, a component of the cytosolic protein complex coatomer, and ADP-ribosylation factor (ARF; a small Ras-like GTPase) (Donaldson et al., 1991; Donaldson et al., 1990). As with the other small GTPases in the cell, the regulatory activity of ARF is through its continuous switching between its GTP-bound and GDP-bound forms. In its GTP-bound state, ARF is active and membrane bound, and it mediates the assembly of the coats on membranes. In its GDP-bound state, ARF is inactive, and dissociates from membranes, and thus these membrane coats are disassembled. The activity of ARF is in turn regulated by two factors that determine the rate of guanine nucleotide exchange (guanine nucleotide exchange factors; GEFs) and the rate of hydrolysis of GTP

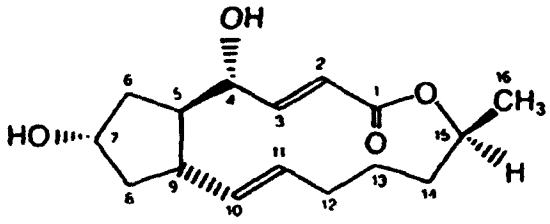

Figure 1.11: Structure of brefeldin A

BFA is a macrolide antibiotic that is produced by fungal organisms such as Eupenicillium brefeldianum. It is a potent inhibitor of membrane trafficking and vesicular transport. It induces disassembly of the Golgi complex and retrograde transport of Golgi proteins back to the endoplasmic reticulum, thereby blocking transport and secretion.

(GTPase activating proteins; GAPs) (Barlowe, 2000; Donaldson and Jackson, 2000). All of the GEFs share a conserved 200-amino-acid domain, known as the Sec7 domain, which catalyses the GTP/GDP exchange on ARF (Peyroche et al., 1999).

As demonstrated by Payroche and co-workers, BFA acts as an uncompetitive inhibitor for the ARF GEF; thus, rather than binding to the Sec7 domain of the GEF for ARF, BFA binds to the transient ternary complex formed by ARF, GDP and the Sec7 domain, and it stabilises this complex. Therefore, BFA forms a stable abortive complex with ARF and its exchange factor, which will also remove exchange factor molecules from exchange reactions with other ARF molecules, i.e. BFA makes endogenous ARF-GDP behave as a 'dominant negative' (Peyroche et al., 1999).

BFA has also been described as a toxin that can affect the ADP-ribosylation of endogenous eukaryotic proteins (De Matteis et al., 1994): GAPDH and a protein of 50 kDa, that in his context was named as BARS (BFA-ADP-ribosylated substrate). This BARS was later identified as a member of CtBP family: CtBP1-S (short-form) (Spano et al., 1999). To date, this BFA-dependent ADP-ribosylation mechanism has not yet been fully characterized, and indeed, it constitutes a part of my findings.

A more detailed description of the CtBP protein family is reported in the next sections.

1.5.2 The CtBP family

The CtBP family of proteins are modulators of several essential cellular processes. Invertebrate and plant genomes contain only a single copy of the

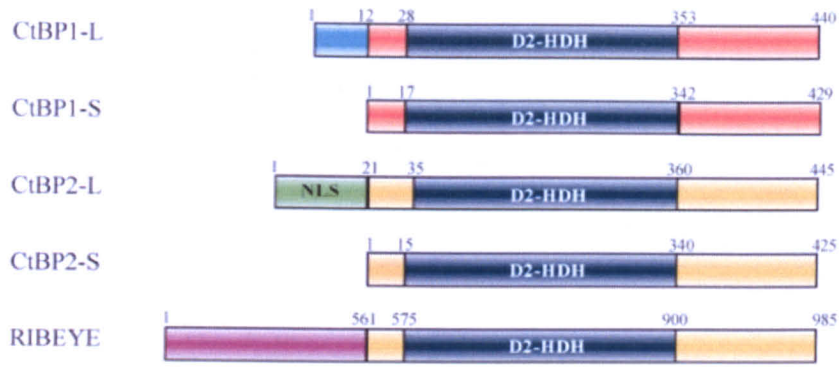

NLS: Nuclear localization signal
D2-HDH: D-isomer specific 2-hydroxy acid dehydrogenases

Figure 1.12: The CtBP family proteins

Schematic representation of the sequences of the CtBP family of proteins. CtBP1-L and CtBP1-S/BARS are the alternative splice variants of the CtBP1 gene; CtBP2-L, CtBP2-S and Ribeye are alternative splice variants of the CtBP2 gene. The region conserved in all of the CtBPs is shown in dark blue; this includes a dehydrogenase homology region (D2-HDH) that has a weak but significant similarity to the D-stereoisomer-specific 2-hydroxyacid NAD-dependent dehydrogenases (Nardini *et al.*, 2003). CtBP2-L is the only isoform of the CtBPs that has a nuclear localisation signal (NLS, green) (Verger *et al.*, 2006).

CtBP gene (Folkers et al., 2002; Nibu et al., 1998), which code for different isoforms as a result of its RNA processing (Mani-Telang and Arnosti, 2007). In contrast, vertebrates have two CtBP-encoding genes, *CtBP1* and *CtBP2*. As a result of alternative RNA splicing, the *CtBP1* gene gives rise to two protein isoforms: CtBP1-L (long) and CtBP1-S (short) (Chinnadurai, 2003; Corda et al., 2006), which differ only in their first 11 N-terminal amino acids (Figure 1.12). CtBP1-L was identified as a protein that binds the C-terminal region of the adenovirus E1A oncoprotein (Boyd et al., 1993; Schaeper et al., 1995), which contains the PLDLS amino acid sequence and subsequently characterised as a transcriptional co-repressor in *Drosophila* (dCtBP) (Nibu et al., 1998). Later, the short isoform of CtBP1 was first identified as a substrate of the ADP-ribosylation induced by the fungal toxin BFA, and hence it was named as BARS (De Matteis et al., 1994). Soon after, BARS was shown to be a member of CtBP family, and to have important roles in membrane fission (Weigert et al., 1999). However, the observation that CtBP1-L behaves similarly to CtBP1-S/BARS in different intracellular transport assays (Corda et al., 2006; Liberali et al., 2008) indicates that their functions are very likely to overlap, also because most of the tools used in different assays do not discriminate between these two isoforms (Valente et al., 2005). Moreover, since the identity between the two CtBP1 isoforms is very high and the role of the 11 amino acids at the N-terminus of CtBP1-L has not been characterised, I will refer to both proteins collectively as CtBP1/BARS.

The *CtBP2* gene codes for three protein isoforms: CtBP2-L (Katsanis and Fisher, 1998) and CtBP2-S (Verger et al., 2006), which share 80% identity with the CtBP1 isoforms, and RIBEYE (Schmitz et al., 2000). CtBP2-S lacks

the N-terminal nuclear localisation signal (NLS) of CtBP2-L (Verger et al., 2006). RIBEYE has a different organisation, as it contains a large N-terminal domain that is otherwise unrelated to the CtBPs. This is linked to a form of CtBP2 that is devoid of the 20 N-terminal amino acids (Schmitz et al., 2000). Therefore, CtBP2-L is the only CtBP isoform that contains a NLS (Figure 1.12).

The major splice variants of both CtBP1 and CtBP2 (i.e. CtBP1-L and CtBP2-L) function as transcriptional co-repressors, while CtBP1-S/BARS and RIBEYE have cytosolic functions, controlling different aspects: CtBP1/BARS has a role in membrane fissioning events, while RYBEYE has a role in synaptic function (Corda et al., 2006).

The two different functions of CtBP1/BARS are tightly regulated by post-translational modifications as well by the presence of co-factors, and these mechanisms are strictly related to its structure. In the following sections, I will describe the structure of CtBP1/BARS, and thence its regulation, and finally the functions in which it is involved (the co-repressor functions and the fissioning functions). As to date there is no direct evidence that CtBP1 and CtBP2 have different functions in the nucleus, for the description of the co-repressor activity I will refer to both of these proteins as CtBP.

1.5.2.1 CtBP1/BARS structure

To delineate the structural basis of the transcriptional co-repressor and/or fissioning activities shown by CtBP1/BARS, the truncated form of the rat protein (devoid of the 80, mostly hydrophobic, C-terminal residues) was crystallised with NAD(H) (Nardini et al., 2003). Its structure is very similar to those of the D-stereoisomer-specific-2-hydroxyacid NAD-dehydrogenases

(Kumar et al., 2002), with which CtBP1/BARS shares <20% sequence identity (Nardini et al., 2003). The CtBP1/BARS:NAD(H) binary complex forms an elongated homodimer in which each CtBP1/BARS monomer consists of two compact domains that are separated by a deep cleft. In accordance with the literature on enzymes with similar structures (Kumar et al., 2002), the two domains are referred as the nucleotide-binding domain (NBD; residues 113-308) and the substrate-binding domain (SBD; residues 1-112 and 309- 350). NBD contains all of the residues for NAD^+ binding, while SBD contains the binding cleft for the PxDLS sequence (Nardini et al., 2003). The central core of the dimer is built around two NBDs, whereas the two SBDs are at opposite poles of the assembled dimer (Figure 1.13).

Structural modelling and binding studies have shown that CtBP1/BARS can bind NAD(H) and long-chain acyl-CoAs through the same site. This structural analysis suggested that NAD(H) binding promotes a 'closed conformation/ dimerisation' of CtBP1/BARS, whereas acyl-CoA binding induces an 'open conformation/ monomerisation' (Nardini et al., 2003; Nardini et al., 2009). This mechanism might represent a functional molecular switch between the transcriptional activity and fissioning activity of the CtBP1/BARS proteins. Indeed, the activity of CtBP1/BARS in transcription and in membrane fissioning is regulated in different ways, and one of these is through the presence of different co-factors.

The description of the various mechanisms mediating the functional switch of the CtBPs is reported in the next section.

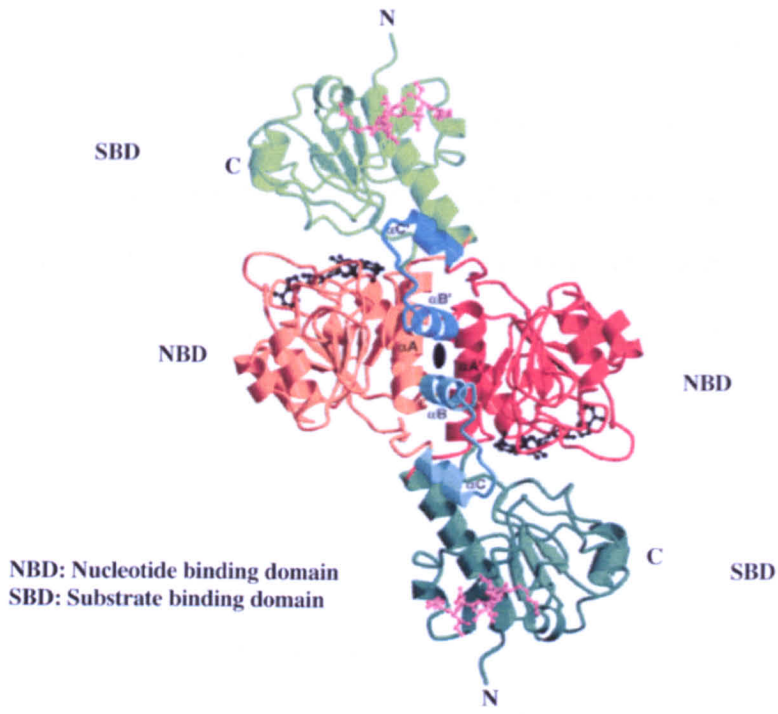

Figure 1.13: The structure of CtBP1-S/BARS

Ribbon diagram of a truncated form of CtBP1-S/BARS (lacking the C-terminal segment; t-CtBP1-S/BARS) as a dimer bound in its interdomain cleft to NAD(H) (shown in black). Light/dark green, substrate binding domain (SBD); orange/red, nucleotide binding domain (NBD). The light/dark colouring illustrates the individual CtBP1-S/BARS molecules.

From Nardini *et al.* (2003).

1.5.2.2 Mechanisms of the CtBP1/BARS functional switch

Proteins that show switches between two roles are often connected to changes in intracellular localisation, oligomerisation state, binding to different ligands and/or proteins, or post-translational modifications (Jeffery, 2004). CtBP also shows similar behaviour, as it appears to shuttle between the nucleus and the cytoplasm, and it is probably the regulation of this movement that controls the functions of this protein (Figure 1.14). This regulation is assured by post-translational modifications, as well by co-factor binding and protein-protein interactions, an issue analysed in the next sections.

CtBP1/BARS regulation by co-factors

As mentioned above, structural and biochemical analyses indicate that CtBP1/BARS binds both acyl-CoAs and NAD(H) in the same pocket (Nardini et al., 2003) and that this event can induce a structural change that appears connected to the change in CtBP1/BARS functions. Accordingly, it has been suggested that the CtBP1 conformational changes upon NAD(H) binding are propagated to the N-terminus, and that this event promotes binding to PxDLS-containing proteins. Therefore, NAD(H) stabilises the dimer, and the interaction with PxDLS-containing proteins is increased. At the same time, the effect of NAD(H) is also to decrease the interaction between some non-PxDLS-containing proteins and the CtBP1/BARS (Mirnezami et al., 2003). Therefore, it has been suggested that the structural changes induced by elevated levels of NADH have opposing effects on the interactions of PxDLS-containing and non-PxDLS-containing proteins with CtBP1/BARS (Mirnezami et al., 2003). These results suggest that NAD(H) can

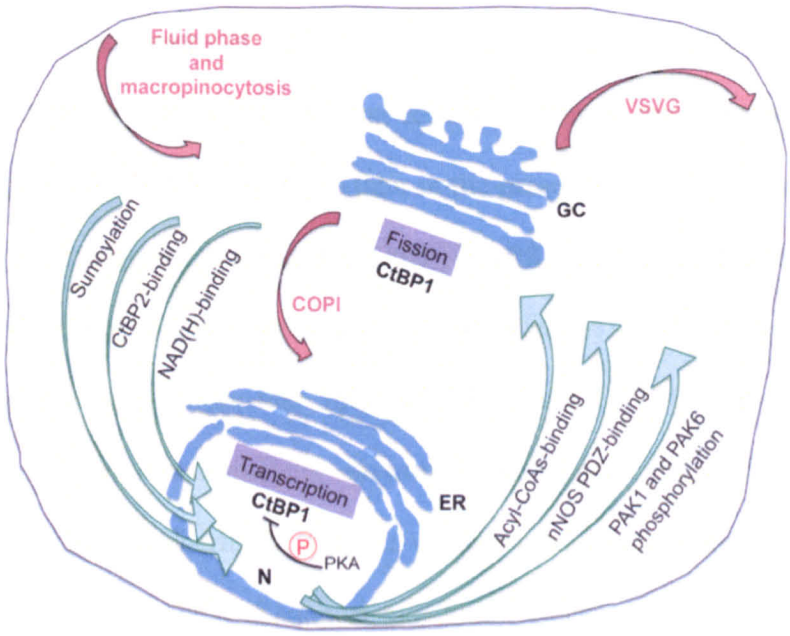

Figure 1.14: Regulation of the nuclear/ cytoplasmic activities of CtBP1

CtBP1 is a multitasking protein that is involved in several cellular functions that depend on its cellular localisation. In the nucleus, where SUMOylated CtBP1 is found, CtBP1 can act as a transcriptional corepressor. Here, CtBP1 can form oligomers and regulate the assembly of multiprotein complexes that are involved in the regulation of transcription. The oligomerisation of CtBP1 is also stabilised by NAD(H) binding, which in turn enhances the CtBP1-mediated repression of some genes (e.g. E-cadherin). With its nuclear localisation signal, CtBP2 binding by CtBP1 can direct CtBP1 to the nucleus as well, implying that a mechanism for nuclear localisation of CtBP1 might depend on its heterodimerisation with CtBP2. In the nucleus, CtBP1 is also phosphorylated by PKA. This phosphorylation results in dimerisation of CtBP1, reducing its corepressor function. In the cytoplasm, where CtBP1 that has been phosphorylated by PAK1 is found, CtBP1 can act in membrane fission and is involved in several dynamin- independent membrane- fissioning steps: fragmentation of the Golgi complex (GC) membranes during mitosis; transport of the cargo reporter VSVG from the TGN to the basolateral plasma membrane in epithelial cells; fluid-phase endocytosis; macropinocytosis and COPI-vesicle-mediated retrograde transport of the KDEL receptor. Like PAK1, PAK6 phosphorylates CtBP1, which inhibits its dimerisation and thus blocks its corepressor activities. AcylCoA binding is required for CtBP1-dependent membrane fissioning, while nNOS binding to the CtBP1 PDZ domain can regulate the cytosolic CtBP1 localisation. ER, endoplasmic reticulum; N, nucleus; P, phosphorylation.

modulate protein-protein interactions through its regulation of the oligomerisation state of CtBP1. Interestingly, the interactions between CtBP1/BARS and PxDLS-containing cellular repressors appear to be enhanced in the presence of NAD(H) more than in the presence of NAD^+ (Zhang et al., 2002), thus suggesting a role for CtBP1/BARS as a sensor linking cellular metabolic status to transcriptional regulation (Fjeld et al., 2003). Accordingly, experimental conditions that increase the NAD(H)/NAD^+ ratio, such as hypoxia or hypoxia-mimicking environments, enhance the CtBP1-mediated repression of E-cadherin as a result of increased interactions with cellular repressors such as ZEB (Zhang et al., 2002). Consistent with results on E-cadherin repression, hypoxia has been reported to increase tumour-cell migration due to decreased E-cadherin expression (Zhang et al., 2006).

From the opposite site, NAD(H) binding to CtBP1/BARS inhibits its membrane fission function (Yang et al., 2005). Indeed, the role for CtBP1/BARS in COPI-coated vesicle formation requires its interaction with ARFGAP1, which is in turn oppositely regulated by acyl-CoAs and NAD(H). Acyl-CoAs, the other co-factors in the regulation of CtBP/BARS function, favours the interactions between CtBP1/BARS and ARFGAP1, which promotes membrane fissioning, while NAD(H) inhibits this interaction, and thus negatively modulates the CtBP1/BARS activity during the fissioning of COPI vesicles (Yang et al., 2005). Structural and biochemical analyses indicate that CtBP1/BARS binds acyl-CoAs in the same pocket where NAD(H) is bound, with an affinity in the low μM range, and both NAD(H) and NAD^+ are competitors of this binding (Nardini et al., 2003). Additionally, CtBP1/BARS-dependent membrane fission is inhibited more potently in the presence of

NADH than in the presence of NAD^+ (Victor Hsu, personal communication), and similar to what has been proposed for the co-repressor activity, this effect would link the metabolic status of the cell not only to transcriptional regulation, but also to membrane trafficking.

CtBP1/BARS regulation by protein-protein interactions

The cytoplasmic and nuclear localisation of CtBP1/BARS can also be regulated by its interactions with other proteins, including CtBP2 and neuronal nitric-oxide synthase (nNOS). It has been shown that CtBP1 and CtBP2 can homodimerise and heterodimerise, and indeed they can be co-purified in the same transcriptional co-repressor complex (Shi et al., 2003). As indicated above, CtBP2 has a unique first coding exon (absent in CtBP1-S/BARS) that contains a NLS (Figure 1.12). However, CtBP2 not only localises to the nucleus, but it can also shuttle between the nucleus and the cytoplasm. Interestingly, expression of CtBP2 can direct CtBP1/BARS to the nucleus: this implies that the mechanism for nuclear localisation of CtBP1 might depend on its heterodimerisation with CtBP2 (Verger et al., 2006).

Conversely, CtBP1/BARS can also interact with nNOS, through the PDZ domain of nNOS. Interestingly, when CtBP1/BARS and nNOS are co-overexpressed in epithelial cells, their distributions are mainly cytosolic. These data suggest a function for nNOS as a regulator of the nuclear/ cytosolic localisation of CtBP1/BARS (Riefler and Firestein, 2001).

CtBP1/BARS regulation by post-translational modifications

The shuttling of CtBP1 between the nucleus and the cytoplasm is also controlled by post-translational modifications (Figure 1.14), namely phosphorylation and sumoylation. CtBP can be phopshorylated by p21-

activated kinase 1 (PAK1), an ubiquitous kinase that is involved in several cellular functions, including signalling, regulation of cytoskeletal dynamics, and membrane trafficking. PAK1 phosphorylates CtBP1-L at Ser158 and CtBP1-S/BARS at Ser147 (Barnes et al., 2003; Liberali et al., 2008).

PAK1-mediated CtBP1/BARS phosphorylation can trigger the change in the CtBP1 cellular localisation, from the nucleus to the cytoplasm. A phospho-mimetic CtBP1/BARS mutant localises mostly to the cytosol, whereas a phospho-depleted mutant localises predominantly to the nucleus (Barnes et al., 2003; Liberali et al., 2008). Moreover, phosphorylation blocks CtBP1/BARS co-repressor activity (Barnes et al., 2003). Molecular dynamics simulation studies have suggested that PAK1-dependent phosphorylation on the serine 147 could change the oligomerisation status of CtBP1/BARS, shifting it towards the monomeric state (Liberali et al., 2008). In addition to PAK1, PAK6 can also phosphorylate CtBP1-L at Ser100 (Ser89 on CtBP1-S/BARS). As with PAK1-dependent phosphorylation, this phosphorylation is predicted to sterically interfere with CtBP1/BARS dimerisation, blocking the co-repressor activities (Dammer and Sewer, 2008). The phosphorylation of CtBP1/BARS by PAK1 might provide a mechanistic link between the two activities of CtBP1/BARS: PAK1 switches CtBP1/BARS on for membrane fissioning, and at the same time it turns it off as a co-repressor. Indeed, the findings of Liberali and co-workers suggested the following model for membrane fission driven by CtBP1/BARS: membrane-associated CtBP1/BARS is phosphorylated by PAK1, and through this phosphorylation, the stability of the dimeric conformation is reduced in favour of the monomeric state. The same dimer-monomer shift is believed to be induced by binding to

CtBP1/BARS of the acyl-CoA co-factor, which is involved in fissioning of COPI-coated vesicles (Nardini et al., 2003; Yang et al., 2005). Thus, PAK1-dependent phosphorylation and acyl-CoA binding potentially act synergistically to promote the monomeric form of CtBP1/BARS. These monomers might facilitate fissioning by either binding new protein partners in the forming fission complex, or by exposing hydrophobic residues that can then participate directly in the final destabilisation (Liberali et al., 2008).

The other modification is the SUMOylation of CtBP. This is essential for the localisation of CtBP1 in the nucleus and for its co-repressor activity (Lin et al., 2003). CtBP1-L/BARS is SUMOylated at a single Lys residue, Lys428 (Lys418 in CtBP1-S/BARS); indeed mutation of Lys428 into Arg (K428R) shifts CtBP1-L from the nucleus to the cytoplasm, while it has little effect on its interaction with PxDLS-containing proteins. Consistent with a change in localisation, this K428R mutation abolishes CtBP1 repression of E-cadherin expression. Notably, the PDZ domain of nNOS inhibits SUMOylation of the CtBP1s, which correlates with the known inhibitory effects of nNOS on nuclear accumulation of the CtBP1s (Lin et al., 2003). This study identifies SUMOylation as a regulatory mechanism underlying CtBP1/BARS-dependent transcriptional repression.

1.5.2.3 The dual role of CtBP

CtBP as a co-repressor

A large number of specific DNA-binding transcriptional repressors mediate their activity through the recruitment of CtBP. An exception is the case of the *C. elegans* homologue that binds directly to promoter regions via its N-terminal

domain (Liew et al., 2007). The various DNA-binding repressors recruit CtBP through motifs related to the CtBP-binding sequence motif (PLDLS) that was originally identified in the adenovirus E1A protein, which is generally referred to as the PxDLS motif (Schaeper et al., 1995). In addition to the PxDLS motif, certain transcription factors use a different domain to interact with CtBP, the RRT motif (Quinlan et al., 2006a). Importantly, most of the known RRT-motif-containing proteins also contain PxDLS motifs, and thus it is possible that the RRT motif has a role in stabilising PxDLS-mediated interactions (Quinlan et al., 2006a; Quinlan et al., 2006b).

Structural analyses have shown that CtBPs can oligomerise (Kumar et al., 2002; Nardini et al., 2003; Nardini et al., 2006) and that this is crucial for their co-repressor activity (Kumar et al., 2002; Shi et al., 2003). Thus, each CtBP oligomer contains multiple PxDLS-binding and RRT-binding motifs, which would allow CtBP to bridge two (or more) PxDLS-motif-containing partners. However, a number of CtBP partners, including some histone-modifying enzymes, do not have PxDLS motifs and probably bind to a different surface of CtBP (Shi et al., 2003). An example here is the neuronal repressor NRSF/REST, which does not contain any of these motifs, but which still binds CtBP to repress transcription of neuronal genes (Garriga-Canut et al., 2006).

Thus, as a general scheme, it can be envisaged that CtBP functions in the assembly of a multi-protein repressor complexes involved in the modulation of gene expression. Indeed, an analysis of a CtBP1/BARS nuclear protein complex purified by tandem affinity purification combined to mass spectrometry has revealed the presence of various histone-modifying

enzymatic constituents as well as DNA-binding transcription factors (Shi et al., 2003), such as ZEB1/2, RREB-1 and Znf217, all of which are implicated in direct binding to promoter elements. All of these DNA-binding factors appear to directly interact with CtBP through the PxDLS motif (ZEB1/2 and RREB-1) or through PxDLS/RRT motifs (Znf217). Additionally, the complex contained enzymes involved in the modulation of chromatin structure, such as HDAC1/2, histone lysine methyl transferases (HMTases G9a and GLP) and histone lysine-specific demethylase (LSD1). The class I HDACs do not have apparent CtBP-binding motifs and have been reported to bind indirectly to CtBP through the presence of other co-repressors, including CoREST. In contrast to class I HDACs, class II HDACs are directly recruited through the PxDLS motif (Zhang et al., 2001). The involvement of HDACs, however, is not the only route of action of CtBP; indeed, CtBP in vertebrates can also function in an HDAC-independent manner, depending on the different promoter contexts. In this regard, different studies have identified several factors of the RNA polymerase II transcription machinery as potential PxDLS-motif-containing proteins. These include various bromodomain-containing HAT coactivators, such as p300/CBP, GCN5 and P/CAF, as well as TAFII and TAFII-250. Kim and co-workers (Kim et al., 2005) demonstrated that CtBP1/BARS directly associates to p300 by binding the PxDLS motif found in the p300 bromodomain. P300 is a member of the HAT family of transcriptional coactivators, and it is required for gene activation through its acetylation of histones in the promoter regions of target genes. The authors demonstrated that the binding of CtBP1/BARS to p300 leads to repression of p300-mediated general transactivation, since CtBP1 competes with the binding of p300 to

acetylated histones (the PxDLS motif is found in the bromodomain of p300, a domain that is important for the binding to acetylated histones), thus impairing transcription.

Additionally, the SUMO moiety attached to CtBP might serve as a potential binding site for class II HDACs (Hay, 2005). Sumoylation might also regulate interactions between CtBP and its interacting proteins. For example, it has been demonstrated that ZEB1/2 are SUMOylated near the PxDLS motif, thus interfering with CtBP binding. Thus, SUMOylation might serve as a mechanism in the regulation of the subunit composition of the CtBP repression complex.

CtBP in oncogenesis

A comprehensive gene expression profiling study using CtBP-null mouse embryo fibroblasts (MEFs) and CtBP1-rescued MEFs revealed co-repression of several epithelial genes and pro-apoptotic genes by CtBP, including *PERP* (p53-effector related to pmp-22), *p21*, *BAX* and *NOXA* (Grooteclaes et al., 2003). Additionally, *PTEN*, a phosphatase and a negative regulator of the survival kinase Akt, was also identified as a CtBP repression target. Consistent with these results, the CtBP-null MEFs were found to be hypersensitive to anoikis (a form of apoptosis mediated by the loss of contact from the ECM) and apoptotic stimuli, such as Fas ligand and UV. These results show that by repressing expression of epithelial cell adhesion molecules (such as E-cadherin, desmoglein-2 and plakoglobin) and pro-apoptotic genes, CtBP contributes to epithelial-to-mesenchymal transition (EMT). This represents a step that contributes to the malignant property of tumour cells, due to the loss of intercellular adhesion in tumours, acquisition of motile and invasive

phenotypes, and resistance to apoptosis. The role of CtBP in EMT may be particularly critical in cancers that overexpress Zeb1 (e.g., breast, colon, and endometrial). Indeed, Zeb1 overexpression with concomitant E-cadherin repression has been reported in several human cancers. Studies with colon carcinomas have revealed that high levels of Zeb1 and CtBP were correlated with low levels of E-cadherin (Pena et al., 2006).

CtBP-mediated transcriptional repression of E-cadherin appears to be regulated by the hypoxic environment seen in solid tumours with poor vascularisation and high metabolic activity. According to the regulation of CtBP by co-factors, it has been shown that hypoxic conditions, by increasing free NADH levels (Zhang et al., 2002), enhance recruitment of CtBP to the E-cadherin promoter; this leads to enhanced motility of tumour cells (Zhang et al., 2006). Cell motility can be reduced by siRNA-mediated depletion of CtBP, which suggests that this effect is independent of HIF-1 or other E-cadherin repressors. CtBP also modulates the expression and activities of the Ink4 family tumour suppressors. The Ink4 region codes for three different cell-cycle inhibitors, p16Ink4a, Ink4a/Arf and p15Ink4b. Rocco and colleagues (Mroz et al., 2008) have reported that expression of E1A in primary human fibroblasts and keratinocytes resulted in a substantial increase in p16Ink4a expression. The effect of E1A on p16Ink4a expression was lost in cells that expressed a mutant of E1A that lacked the CtBP-binding motif, or in cells depleted of CtBP, suggesting that interactions of E1A with CtBP were responsible for this activity.

Moreover, three different groups have reported on strong interactions between CtBP and another tumour suppressor, adenomatous polyposis coli

(APC) (Hamada and Bienz, 2004; Nadauld et al., 2006; Sierra et al., 2006). One of these reports (Nadauld et al., 2006) provided compelling evidence that APC can function as a platform for proteasome-dependent degradation of CtBP1, in addition to regulating the stability of ß-catenin. This view was supported by the observation that adenomas from patients with familial adenomatous polyposis contained high levels of CtBP1 compared to healthy samples. Furthermore, reintroduction of APC in colon carcinoma cell lines also resulted in degradation of CtBP1. These results received strong support from a zebrafish model harbouring a mutant form of APC and expressing high levels of CtBP1 (whereas CtBP1 mRNA levels remained unchanged). These data are consistent with a model in which APC targets both ß-catenin and CtBP1 simultaneously, to inhibit expression of Wnt target genes and to relieve repression of CtBP target genes that are involved in intestinal cell differentiation.

CtBP1/BARS in membrane fission

The study of CtBP1/BARS in membrane fission *in vivo* have revealed that this protein is an essential component of dynamin-independent trafficking steps. Indeed CtBP1/BARS has been shown to have a role in different fissioning steps of various trafficking processes: transport from the Golgi complex to the basolateral membrane in epithelial cells (Bonazzi et al., 2005), (Valente *et al.*, *in press*), fluid phase endocytosis, retrograde transport of the KDEL receptor to the endoplasmic reticulum by COPI-coated vesicles (Yang et al., 2005) and macropinocytosis (Liberali et al., 2008). These transport events do not require dynamin, and indeed several dynamin-dependent transport processes, like apical transport to the plasma membrane and receptor-mediated endocytosis,

do not require CtBP1/BARS. This indicates that dynamin and CtBP1/BARS drive non-overlapping fissioning machineries. Moreover, CtBP1/BARS fissioning also regulates Golgi fragmentation during mitosis (Colanzi et al., 2007; Hidalgo Carcedo et al., 2004). A brief description for each processe is provided as follows.

Post-Golgi carrier formation

During the trafficking of cargo from the *trans*-Golgi network (TGN) to the basolateral plasma membrane, large pleiomorphic tubular carriers elongate out of the Golgi complex along microtubules, before detaching and moving to the plasma membrane. When CtBP1/BARS function is inhibited, these tubules do not detach from the Golgi complex, but continue to elongate out and retract back into the Golgi complex. Thus, under these conditions, the fissioning step of post-Golgi carrier formation is inhibited (Bonazzi et al., 2005). Recently, the function of the fissioning protein CtBP1/BARS in post-Golgi carrier formation has been elucidated (Valente et al., *in press*). Using CtBP1/BARS as bait in affinity purification approaches, followed by mass spectrometry, Valente and co-workers described a protein complex that contains both budding and fissioning molecules already known to have crucial roles in carrier formation, as well as novel players, such as the adaptor protein 14-3-3γ. The authors demonstrated that 14-3-3γ dimers bridge the fission-inducing protein CtBP1/BARS and ARF- activated PI4KIIIβ (the probable initiator of the transport process). This complex is stabilised by reversible phosphorylation, which is mediated by two of the other CtBP1/BARS complex components identified: protein kinase D and p21-activated kinase (PAK) kinases, which

phosphorylate Ser294 in PI4KIIIβ and Ser147 in CtBP1/BARS, respectively, thus enabling carrier fission. Disrupting this complex inhibits fissioning of elongating carrier precursors, indicating that the complex couples budding with fission. The regulated assembly of this complex provides new insights into the mechanisms of action of CtBP1/BARS and the molecular organisation required for the formation of large pleiomorphic carriers.

COPI-coated vesicle formation

COPI-coated vesicles mediate retrograde transport of the KDEL-receptor from the Golgi complex to the ER. When CtBP1/BARS function is inhibited, COPI-coated vesicles bud, but do not detach from the Golgi cisternae *in vivo* and from Golgi membranes *in vitro* (Yang et al., 2005). This role of CtBP1/BARS requires its interaction with ARFGAP1, which is in turn regulated oppositely by acyl-CoAs and NAD(H).

Fluid-phase-endocytosis

This is the least-well-characterized CtBP1/BARS-dependent fissioning event. Constitutive fluid-phase endocytosis monitored by dextran uptake is inhibited by CtBP1/BARS impairment (Bonazzi et al., 2005).

Macropinocytosis

This form of endocytosis (bulk uptake of fluid and solid cargo) results in the formation of large endocytic vesicles, called macropinosomes, which originate from actin ruffles at the plasma membrane. This ruffling is followed by invagination of the plasma membrane and formation of the macropinocytic

cup, which then undergoes fissioning of its junction with the plasma membrane (Swanson and Watts, 1995). Inhibition of CtBP1/BARS, e.g., by injection or expression of a dominant-negative mutant, did not affect macropinocytic cup formation, which formed normally, but this did inhibit the membrane fission that was required for macropinosome closure, again underlining the specific CtBP1-S/BARS role in membrane fissioning (Liberali et al., 2008).

Golgi fragmentation during mitosis

During the G2-mitosis transition, the Golgi ribbon is first fragmented into isolated stacks of cisternae, and then further fragmented into tubulo-vesicular elements. These elements are separated into the two main pools that constitute the new Golgi complexes in the daughter cells. CtBP1/BARS is necessary for the first stage of this fragmentation. Inhibition of CtBP1/BARS by microinjection of a blocking antibody results in inhibition of mitotic Golgi partitioning and arrest of the cell cycle at the G2 stage (Colanzi et al., 2007; Hidalgo Carcedo et al., 2004).

1.6 My findings

In the previous sections I have described what ADP-ribosylation is and its 'use' by toxins and by cellular enzymes, for the modulation of cell functions. I have explored both of these aspects (as described in Chapters 3 and 4). In particular, on the one hand, my project was focused on the study of the BFA-dependent ADP-ribosylation reaction, to understand how this affects CtBP1 functions, thus describing a novel mechanism in CtBP1/BARS regulation; on the other hand, I have analysed intracellular ADP-ribosylation, focusing on the enzyme PARP12. My results demonstrate that PARP12 is a novel mART, and through the identification of its substrates, this suggests new roles for ADP-ribosylation in the regulation of cellular functions.

CHAPTER 2: Materials and Methods

2.1 Materials

DL-dithiothreitol (DTT), bovine serum albumin (BSA), saponin, Tris-[hydroxymethyl]-aminomethane (Tris), ethylene glycolbis(beta-aminoethylether)-N,N,N',N'-tetraacetic acid (EGTA), ethylenediaminetetraacetic acid (EDTA), H_2PO_4, Na_2HPO_4, KH_2PO_4, sucrose, brefeldin A (BFA), reduced L-glutathione, Igepal, and sodium deoxycholate were all from Sigma-Aldrich (WI, USA). NaCl, HCl, NaOH, KOH, dimethylsulphoxide (DMSO), acetone, ethanol, methanol, chloroform, xylene cyanol, and bromophenol blue were all from Carlo Erba (Italy). 4-(2-Hydroxy-ethyl)-piperazine-1-ethane-sulfonic acid (HEPES), glycerol, KCl, $HgCl_2$, and $MgCl_2$ were all from Merck (Germany). C-mercaptoethanol was from Fluka-Analytical (Switzerland). Mowiol was from Calbiochem (CA, USA). Paraformaldehyde (16% in H_2O) was from Electron Microscopy Sciences (PA, USA). The sources of the other materials used will be specified for each procedure.

2.2. Solutions

Phosphate-buffered saline (PBS): 1.5 mM KH_2PO_4, 8 mM Na_2HPO_4, 2.7 mM KCl, 137 mM NaCl, pH 7.4.

Paraformaldehyde (16%, v/v) was diluted in PBS, pH 7.4, to the appropriate concentrations (as indicated), and stored at 4 °C.

The blocking solution for immunofluorescence experiments was prepared as follows: 0.5% (w/v) BSA, 50 mM NH_4Cl in PBS, pH 7.4. Saponin was added to the preparation to 0.05% (w/v). Aliquots of this blocking solution were stored at –20 °C.

2.3 Subcloning and mutation of DNA

2.3.1 Materials

Restriction enzymes were from New England Biolabs (USA), T4 DNA ligase and DNA molecular size standards were from Gibco/BRL (NY, USA), oligonucleotides and Pfu Turbo DNA Polymerase were from Stratagene (CA, USA); pcDNA3.1/myc-His vector was from Invitrogen (Carlsbad, CA, USA), untagged full-length PARP12 cDNA cloned into pCMV6-XL5 was from Origene (Rockville, MD, USA). Sequencing was performed by BMR Genomics (Italy).

'QIAquick PCR Purification kits', 'QIAprep Spin Miniprep kits', 'QIAGEN Plasmid Maxi kits' were from Qiagen (CA, USA). Tryptone peptone, yeast extract, and agar were from Difco, Becton Dickinson (MD, USA).

2.3.2 Solutions and media

Lysogeny broth (LB): 1% (w/v) tryptone peptone, 0.5% (w/v) yeast extract, 1% (w/v) NaCl; autoclaved 15 min at 121 °C.

LB-agar: LB plus 1.5% (w/v) agar: autoclaved 15 min at 121 °C.

TE (Tris/EDTA) buffer: 10 mM Tris-HCl, 1 mM EDTA, pH 8.

TAE (Tris/acetic acid/EDTA) buffer (50×, 1.0 l): 242 g TRIZMA base, 57.1 ml glacial acetic acid, 100 ml 500 mM EDTA.

2.3.3 DNA agarose gels

Agarose gels were prepared by dissolving agarose (Bio-Rad Laboratories, UK) in TAE buffer and heating in a microwave oven. Ethidium bromide was added (to 0.5 μg/ml), and the gels were poured and run on an agarose gel apparatus from Bio-Rad Laboratories (UK). DNA standards (0.5 μg) were loaded and used as the reference for approximate estimations of the amounts of DNA in the samples.

2.3.4 DNA constructs

GFP-tagged Rab1A was kindly provided by Prof. Bruno Goud, Curie Institute (Paris, France).

The pYFP-CtBP1/BARS and its point mutant pYFP-CtBP1/BARS (H304A) vectors were provided by Claudia Cericola, in the Laboratory of Daniela Corda (previously of the Departemnt of Cell Biology and Oncology [DCBO], Consorzio Mario Negri Sud [CMNS], Santa Maria Imbaro, Italy). Untagged full-length PARP12 cDNA cloned into the pCMV6-XL5 vector was purchased from Origene (Rockville, MD, USA).

Myc-His-tagged PARP12 was generated by subcloning PARP12 cDNA from the pCMV6-XL5 vector into a C-terminal tagged pcDNA3.1/myc-His vector.

The primers used for the PCR reactions were:

forward primer: 5′- GTACGTAAGCTTATGGCCCAGGCCGGCGTCGT - 3′

reverse primer: 5′- GTACGTCTCGAGCTGTCGGCTGCTGAACAGGG - 3′

PCR reactions were performed as follows: 1 min at 95 °C, followed by 30 cycles of 95 °C for 30 s, 65 °C for 60 s, 72 °C for 180 s, and a final extension

at 72 °C for 10 min. The PCR product was purified using a PCR purification kit, digested with HindIII/XhoI restriction enzymes and subcloned (as described in sections 2.3.5, 2.3.6) in the HindIII/XhoI linearised pcDNA3.1/myc-His vector and processed for automatic sequencing.

The His-Myc PARP12 vector was used to generate the PARP12 mutants (see section 2.3.7).

His-tagged PARP12 and GST-tagged PARP12 were generated using Gateway technology (see sections 2.4.2, 2.4.3).

2.3.5 PCR amplification of DNA inserts

To amplify specific regions of DNA inserts, PCR was performed by incubating 10 ng DNA plasmid as a template in 50 µl 20 mM Tris-HCl, pH 8.8, 10 mM KCl, 2 mM $MgSO_4$, 10 mM $(NH_4)SO_4$, 0.1% Triton X-100, 0.1 mg/ml nuclease-free BSA, 200 nM each oligonucleotide, 200 µM each dNTP, 2.5 U Pfu Turbo DNA Polymerase. The PCR reaction mixtures were subjected to 25-30 temperature cycles in a programmable thermal cycler (MJ Research Inc., Massachussets, USA). The melting, annealing and elongation temperatures were adjusted according to the features of the templates and primers. To facilitate the subsequent subcloning of the PCR products, the forward and the reverse primers were provided with restriction sites at their 5' ends.

2.3.6 Restriction and ligation

DNA (vectors and inserts) was cut with 5 U/µg of the appropriate restriction enzymes in the buffer supplied with each enzyme. After restriction, the reaction mixture was loaded onto 1.0% (w/v) agarose gels; the bands of interest were cut from the gels with a sterile scalpel, and the DNA was extracted from these gel samples with the Qiaex II extraction kit (Qiagen, CA, USA),

according to the manufacturer instructions. The DNA was eluted in water. To ligate the vector and the insert, ~100 ng of the vector and an ~3-fold molar amount of the insert were incubated with 1 U T4 DNA ligase in T4-DNA-ligase buffer (Gibco/BRL, UK), for 1-3 h at room temperature (RT).

2.3.7 DNA mutagenesis

The DNA (10 ng myc-His tagged PARP12) was amplified by PCR using 2.5 U Pfu Turbo DNA Polymerase and 150 ng of the two synthetic oligonucleotide primers containing the desired mutations, as follows: 1 min at 95 °C, followed by 14 cycles of 95 °C for 30 s, 55 °C for 1 min, 68 °C for 16 min, and a final extension at 65 °C for 15 min. The melting, annealing, and elongation temperatures were adjusted according to the features of the template and the primers. After the reactions, DpnI endonuclease was added to the mixture for 1 h at 37 °C, to digest the parental non-mutated DNA template. The products were checked on agarose gels and the mutations were verified by DNA sequencing (BMR Genomics, CRIBI, Padova, Italy).

The primers used to generate each mutation are listed below. For each mutation, the forward (fw) and reverse (rev) primer names and sequences are reported in Table 2.1.

Table 2.1: Primers used for PARP12 mutagenesis.

Stock concentrations is 100 μM.

Oligo name	Oligo sequence
P12-H564A-fw	CGAGCGGCAGCTGTTCGCCGGCACCAGCGCCATTTTT
P12-H564A-rev	AAAAATGGCGCTGGTGCCGGCGAACAGCTGCCGCTCG
P12-H564Q-fw	CGAGCGGCAGCTGTTCCAAGGCACCAGCGCCATTTTT
P12-H564Q-rev	AAAAATGGCGCTGGTGCCTTGGAACAGCTGCCGCTCG
P12-I660A-fw	GAACAGTGTGTCCGACCCCTCCGCCTTTGTGATCTTTGAGAAA
P12-I660A-rev	TTTCTCAAAGATCACAAAGGCGGAGGGGTCGGACACACTGTTC

2.3.8 Transformation of bacteria

The DNA plasmid of interest (10 ng of uncut plasmid, or half of a ligation reaction) was added to competent bacteria. After gentle mixing, the cells were left on ice for 30 min, and then heat shocked for 45 s at 42 °C. After the addition of 800 µl LB, the bacteria were incubated under continuous shaking (200 rpm) at 37 °C for 60 min. The bacteria were plated onto LB agar containing the appropriate selective antibiotic, and incubated overnight (O/N), at 37 °C. The next day, isolated bacterial colonies were picked and used to inoculate 2 ml LB containing the appropriate antibiotic. The culture was incubated O/N at 37 °C. Sterile glycerol (300 µl) was added to 700 µl of the bacterial culture, which was then stored at -80 °C.

Unless otherwise specified, the preparation of heat-shock transformation-competent bacteria was carried out by Michele Santoro and Giuseppe Di Tullio (previously of DCBO, CMNS, Italy).

2.3.9 Small-scale preparation of plasmid DNA (minipreps)

The clones obtained after the transformation of the ligation reaction were usually screened using minipreps and subsequent restriction analysis. Isolated bacterial colonies were picked and inoculated into 5 ml LB containing the appropriate antibiotic. After O/N growth at 37 °C under continuous shaking (200 rpm), 700 µl of the cultures was mixed with 300 µl 50% (v/v) sterile glycerol and stored at -80 °C; the rest of each culture was chilled on ice and centrifuged 10 min at 4,000× *g*. The DNA was extracted using 'QIAprep Spin Miniprep kits' (Qiagen, CA, USA), according to the manufacturer instructions, and analysed by restriction analysis and separation on agarose gels.

2.3.10 Large-scale preparation of plasmid DNA (maxipreps)

A small amount of the bacteria transformed with the plasmid of interest was scraped from the glycerol stock, inoculated into 2 ml LB containing the appropriate selective antibiotic, and grown at 37 °C under continuous shaking (200 rpm) for 4-6 h. This pre-culture was used to inoculate 250 ml LB containing the selective antibiotic. After an O/N incubation, the bacteria were collected by centrifugation at 6,000 rpm in a JA14 rotor (4,000× *g*) for 10 min at 4 °C and processed according to the maxi-plasmid purification protocol of 'Qiagen Plasmid Maxi kits'. The DNA obtained was resuspended in water, checked on agarose gel, quantified, and stored at -20 °C.

2.4 Gateway cloning

The Gateway technology is a universal cloning method based on the site-specific recombination properties of bacteriophage lambda. It allows for the rapid and efficient movement of DNA sequences into multiple vector systems. First, the desired target DNA is amplified by PCR using primers containing four nucleotides (CACC) that base pair with the overhang sequence (GTGG) of each pENTR TOPO vector. Second, the overhang in the pENTR vector invades the 5' end of the PCR product, anneals to the added bases, and stabilises the PCR product in the correct orientation. Finally, this entry vector can be used to recombine into the destination vector of interest depending on the intended use.

Gateway cloning was performed according to the manufacturer instructions. However, the main steps are described in the next sections.

2.4.1 Materials

The pENTR vector (pENTR™/SD/D-TOPO) was kindly provided by Michele Sallese, DCBO, CMNS, Italy. The pDEST vectors were purchased from Invitrogen (Carlsbad, CA, USA). The following pDEST vectors were used: pDEST26 (cat. no.11809-019), pDEST15 (cat. no. 11802-014), and pDEST10 (cat. no. 11806-015). One Shot TOP10 and DH10Bac Chemically Competent *E. coli*, LR Clonase II enzyme mix, Cellfectin II transfection reagent were from Invitrogen (Carlsbad, CA, USA). Gentamicin solution was from Gibco. Tetracycline, kanamycin and X-Gal (5-bromo-4chloro-3-indolyl-D-galactoside) were from Fluka-Analytical (Switzerland).

2.4.2 Generation of pENTR PARP12

The primers used to obtain PARP12 blunt-end PCR products are listed below:

Forward: CACCGCCCAGGCCGGCGTCGT

Reverse: TCACTGTCGGCTGCTGAACAG

For PCR amplification, *Pfu* polymerase from Stratagene (CA, USA) was used. The PCR reaction was performed as follows: 1 min at 95 °C, followed by 30 cycles of 95 °C for 30 s, 55 °C for 1 min, 72 °C for 3 min, and a final extension at 72 °C for 10 min. The PCR product was analysed by agarose gel electrophoresis. The TOPO cloning reaction (to allow the insertion of the PCR product into the pENTR vector) was performed for 5 min at RT, according to the manufacturer instructions, using a 1:1 molar ratio of PCR product: TOPO vector. Here, 2 µl of TOPO cloning reaction mix were used to transform One Shot TOP10 chemically competent *E. coli*. To analyse the transformants, six colonies were picked, and plasmid DNA was purified and used for PCR analysis. PCR reactions were performed using the M13 forward primer 5'-

GTAAAACGACGGCCAG-3' (which hybridises onto pENTR vector) and a PARP12 specific reverse primer (sequence as reported above), as follows: 1 min at 95 °C, followed by 30 cycles of 95 °C for 30 s, 55 °C for 1 min, 72 °C for 3 min, and a final extension at 72 °C for 10 min. The PCR products were visualised by agarose gel electrophoresis. Additionally, the plasmid DNA was sequenced. The correct clone was used to make a glycerol stock.

2.4.3 Generation of pDEST PARP12 vectors

The destination vectors used during this study were: pDEST26 (for mammalian expression of recombinant His-tagged PARP12), pDEST10 (for expression of recombinant His-tagged PARP12 with the Baculovirus expression system), pDEST15 (for expression of recombinant GST-tagged PARP12 in *E. coli*).

The recombination reactions were carried out using the amount of reagents as recommended (100 ng PARP12 recombinant pENTR and 1 µl pDEST vectors, corresponding to 150 ng) diluted in TE buffer (Tris HCl 10 mM, pH 8, 1 mM EDTA) and using 2 µl LR Clonase II enzyme mix. The reaction was carried out for 1 h at 25 °C. Then 1 µl proteinase K solution was added to each reaction, with incubation for 10 min at 37 °C. Then 1 µl of each reaction mix was used to transform DH5α competent cells. Five colonies were picked, plasmid DNA was purified and analysed by PCR, using a PARP12 forward primer and a T7 reverse 5′- TAATACGACTCACTATAGGG- 3′ (that hybridises on pDEST vectors). The PCR reactions were performed as reported above. In the case of GST-PARP12, plasmid DNA was then used to transform BL21-DE3 cells for the production and purification of the protein.

2.5 Bac-to-Bac Baculovirus Expression System

The Bac-to-Bac Baculovirus Expression System facilitates rapid and efficient generation of recombinant baculoviruses (Ciccarone et al., 1998). This method takes advantage of the site-specific transposition properties of the Tn7 transposon to simplify and enhance the process of generating recombinant bacmid DNA.

In the pDEST10 vector used in this study, the expression of the gene of interest (His-PARP12) is controlled by the *Autographa californica* multiple nuclear polyhedrosis virus (AcMNPV) polyhedrin (PH) promoter, for high-level expression in insect cells. This expression cassette is flanked by the left and right arms of Tn7, and also contains a gentamicin resistance gene and an SV40 polyadenylation signal, to form a mini Tn7.

The second major component of the system is the DH10Bac *E. coli* strain that is used as the host for the vector of interest. DH10Bac cells contain a baculovirus shuttle vector (bacmid) with a mini-attTn7 target site and a helper plasmid. Once the vector containing the gene of interest (PARP12 recombinant pDEST10, in this specific case) is transformed into DH10Bac cells, transposition occurs between the mini-Tn7 element on the pDEST10 vector and the mini-attTn7 target site on the bacmid, to generate a recombinant bacmid. This transposition reaction occurs in the presence of transposition proteins supplied by the helper plasmid. Once the transposition reaction has been performed, it is possible to isolate the high molecular weight recombinant bacmid DNA and transfect the bacmid DNA into insect cells to generate a recombinant baculovirus that can be used for preliminary expression experiments.

2.5.1 Generation of the His-PARP12 recombinant bacmid

To generate the His-PARP12 bacmid, 1-2 ng plasmid DNA obtained from the selected His-PARP12 pDEST10 clone was used to transform 100 µl MAX efficiency DH10Bac chemically competent *E. coli*. The transformation conditions were similar to the conditions described in section 2.3.8, with the cells left at 37 °C for 4 h to allow the recombination to take place. Then 100 µl of three 10-fold serial dilutions of the cells were plated on LB agar containing 50 µg/ml kanamycin, 7 µg/ml gentamicin, 10 µg/ml tetracycline, 100 µg/ml X-gal and 40 µg/ml IPTG. The plates were incubated for 48 h at 37 °C. White colonies were picked for the analysis. Insertions of the mini-Tn7 into the mini-*att*Tn7 attachment site on the bacmid disrupt the expression of the LacZα peptide, so colonies containing the recombinant bacmid are white.

To check for the recombination, 100 ng of recombinant bacmid DNA were analysed by PCR using pUC/M13 forward and reverse primers (that hybridise to sites flanking the mini-attTn7 site). A schematic representation is reported in Figure 2.1. The PCR reaction was performed as follows: 3 min at 95 °C, followed by 30 cycles of 94 °C for 45 s, 55 °C for 45 s, 72 °C for 5 min, and a final extension at 72 °C for 7 min, as indicated by the Bac-to-Bac manufacturer instructures. The selected clone of the recombinant DH10Bac *E. coli* was used to prepare glycerol stocks. The bacmid DNA was also stored at -20 °C. The bacmid DNA purification was performed using PureLink HiPure Plasmid Maxiprep kits from Invitrogen (Carlsbad, CA, USA).

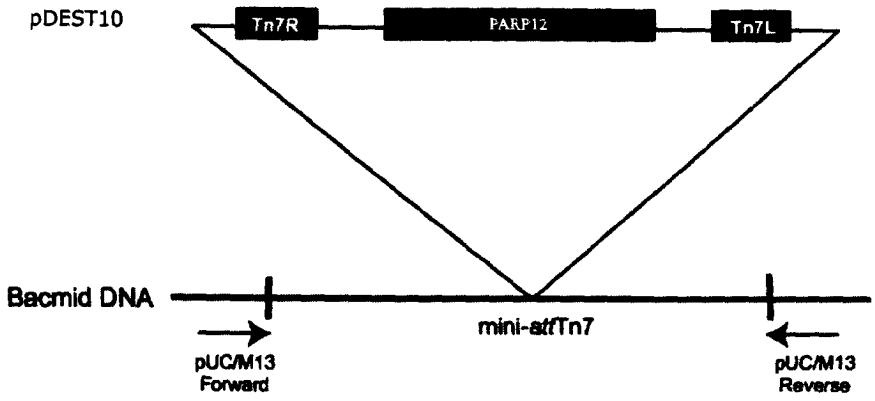

Figure 2.1: PCR analysis of the recombinant BAC plasmid

Schematic representation of PCR analysis of the recombinant BAC plasmid. pUC/M13 forward and reverse primers hybridise to sites flanking the mini-attTn7 site of the BAC plasmid, thus allowing the amplification of the region of interest.

Oligo name: pUC/M13 Forward

Sequence: 5'- CCCAGTCACGACGTTGTAAAACG-3'

Oligo name: pUC/M13 Reverse

Sequence: 5'-AGCGGATAACAATTTCACACAGG-3'

Modified from the Bac-to-Bac manual, Invitrogen.

2.5.2 Transfection of Sf9 insect cells to generate His-PARP12 Baculovirus

Recombinant bacmid DNA was used to transfect Sf9 insect cells using a Cellfectin II reagent, according to the manufacturer instructions. Briefly, 8 $\times 10^5$ Sf9 insect cells were plated for each well of a 6-well format, in 2 ml unsupplemented Grace's insect medium (without antibiotics and serum). The cells were left to attach for 15 min at RT and then transfected with 1 μg baculovirus DNA, previously mixed with 8 μl Cellfectin. After 5 h at 27 °C, the transfection mixture was removed and complete growth medium was added. The cells were incubated at 27 °C until signs of infection appeared (as described in the manual). After 6 days, the media (containing the virus) was recovered and stored at 4 °C. This media represented the P1 viral stock. The P1 viral stock was used to subsequently infect Sf9 insect cells to generate a P2 viral stock. The P2 viral stock was used at a 1:30 dilution to infect Sf9 cells for His-PARP12 production. Here, 96 h was chosen as the optimal time for the expression of His-PARP12. An aliquote of each viral stock was stored at -80 °C. Figure 2.2 shows the PARP12 expression levels after 72 h, 96 h and 6 days post transfection. The growth conditions for the Sf9 insect cell are described in section 2.8.2.

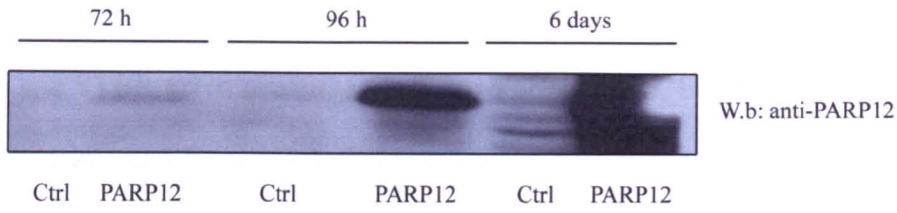

Figure 2.2: His-PARP12 expression in PARP12 baculovirus infected Sf9 insect cells

Sf9 insect cells were infected with PARP12 recombinant baculovirus and incubated at 27 °C for the indicated times. The cells were then lysed and the expression of His-PARP12 was monitored by western blotting using an anti-PARP12 antibody. Non-infected Sf9 cells represent control of the procedure (ctrl). PARP12 expression was started after 72 h incubation. 96 h were chosen as the optimal time for protein production. Even the protein was still present after 6 days post-infection, degradation products were visible and thus this time was not considered as appropriate for protein production.

2.6 Real-time qRT-PCR

2.6.1 Materials

Plates and SYBR green mixture were from Roche (Basel, Switzerland). RNA extraction kits and QuantiTect Reverse Transcription kits were from Qiagen (CA, USA). Primers used for the real-time RT-PCR were from Sigma-Aldrich (WI, USA).

2.6.2 RNA extraction and the RT-PCR reaction

Total RNA was isolated from control and $CD38^{+/+}$ HeLa cells using RNAeasy Qiagen (CA, USA) kits, according to the manufacturer instructions. The quality of the RNA was checked on agarose gel.

For each experiment, 1 μg total RNA was converted to cDNA using QuantiTect Reverse Transcription kits (Qiagen, CA, USA), according to the manufacturer instructions. The procedure comprised two main steps: elimination of genomic DNA, and reverse transcription. Briefly, the purified RNA samples were incubated in gDNA Wipeout Buffer at 42 °C for 2 min, to effectively remove contaminating genomic DNA. After this step, the RNA sample was used for reverse transcription using a master mix prepared from Quantiscript Reverse Transcriptase, Quantiscript RT Buffer, and RT Primer Mix. The entire reaction was performed at 42 °C and then inactivated at 95 °C.

2.6.3 Preparation of samples for real-time qRT-PCR analysis

Here, 20 μl of a mix containing 100 ng cDNA, 200 nM of each primer and SYBR Green master mix (Roche, Basel, Switzerland) were used for real-time PCR. Real-time PCR measurements were performed using a Light Cycler 480 Real-Time PCR System (Roche, Basel, Switzerland). Each sample was

measured in duplicate and the data were analysed using the $\Delta\Delta C_T$ method (2^{-DDCT}) for comparing relative expression results. Resting cells were considered the reference sample, and *Homo sapiens* hypoxanthine phosphoribosyltransferase 1 (HPRT1) served as the house-keeping gene. Statistical analysis were performed using a GraphPad Prism Software. The list of primers used is given in Table 2.2.

Table 2.2: Primers used for real-time qRT-PCR

Name	Sequence (5'-3')	Company	Stock conc. (μM)
HPRT1 forward	tgctgacctgctggattaca	Sigma-Aldrich	100
HPRT1 reverse	cctgaccaaggaaagcaaag	Sigma-Aldrich	100
E-cadherin forward	cgacccaacccaagaatcta	Sigma-Aldrich	100
E-cadherin reverse	gctggctcaagtcaaagtcc	Sigma-Aldrich	100
Bax forward	ggggacgaactggacagtaa	Sigma-Aldrich	100
Bax reverse	ctgtaatcccagctccttgg	Sigma-Aldrich	100
p21 forward	gacaccactggagggtgact	Sigma-Aldrich	100
p21 reverse	ggcgtttggagtggtagaaa	Sigma-Aldrich	100
Noxa forward	agctggaagtcgagtgtgct	Sigma-Aldrich	100
Noxa reverse	ttcctgagcagaagagtttgg	Sigma-Aldrich	100

2.7 Luciferase assay

2.7.1 Materials

The Dual-Luciferase Reporter 1000 assay system was purchased from Promega (Madison, WI, USA). Plates were from Roche (Basel, Switzerland). The pGL2 vector containing the firefly luciferase gene under the control of the E-cadherin promoter was kindly provided by Eric Fearon, Division of Medical Genetics (University of Michigan, USA). pLA/S 5Kb-WT vector containing the firefly luciferase gene under the control of the Bcl6 promoter was kindly provided by Dr. Riccardo Dalla-Favera, Institute for Cancer Genetics (Columbia University). These vectors are referred to as reporter I. The control vector containing the Renilla luciferase gene (referred reporter II) was kindly provided by Dr. Fulvio Chiacchiera, CMNS.

2.7.2 Procedure

Control and $CD38^{+/+}$ HeLa cells (60,000) were plated for each well of a 24-well format and co-transfected with 500 ng Reporter I and 10 ng Reporter II using the *Trans*IT-LT1 transfection Reagent (according to the method described in section 2.8.3). After 12 h, the cells were stimulated with 40 μg/ml BFA in DMEM in the presence of exogenously added 5 mM NAD^+. After 12 h treatment, the cells were lysed using 100 μl of freshly prepared Passive Lysis Buffer (PLB) of the Dual-Luciferase Reporter assay system, according to the manufacturer instructions. Then 20 μl PLB cell lysate was used to measure the luciferase activity. To measure the firefly luciferase activity, 100 μl of Luciferase Assay Reagent II (LARII) was added to each sample to generate a stabilised luminescent signal. After quantifying the firefly luminescence, the

Renilla luciferase reaction was initiated by adding 100 µl Stop & Glo Reagent to the same sample. The Stop & Glo Reagent also produces a stabilised signal from the Renilla luciferase, which decays slowly over the course of the measurement. The luminescence measurements were performed using a plate-reading luminometer in Dr. Antonio Moschetta's Laboratory (CMNS), with the help of Dr. Giuseppe Lo Sasso. The values obtained were analysed as ratios between RepI/RepII*10000. Statistical analyses were performed using GraphPad Prism Software.

2.8 Work with eukaryotic cell lines

2.8.1 Materials

HeLa cells and Sf9 insect cells were purchased from the European Collection of Cell Culture (ECACC). $CD38^{+/+}$ and control HeLa cells were kindly provided by Prof. Antonio De Flora (Advanced Biotechnology Centre, University of Genoa, Italy). Dulbecco's Modified Eagle's Medium (DMEM), Minimum Essential Medium (MEM), foetal bovine serum (FBS), penicillin, streptomycin, trypsin-EDTA, L-glutamine and MEM Non-Essential Amino Acids Solution were all from Gibco/BRL (NY, USA). Grace's Insect medium (supplemented and unsupplemented) was from Invitrogen (Carlsbad, CA, USA). All of the plastic cell culture materials were from Corning (NY, USA). Filters 0.2 µm were from Amicon (MA, USA).

2.8.2 Cell-growth conditions

Control and $CD38^{+/+}$ HeLa cells were grown in DMEM supplemented with 2 mM L-glutamine, 50 U/ml penicillin and 50 µg/ml streptomycin, and 10% (v/v) FBS. HeLa cells were grown in MEM supplemented with 2 mM L-

glutamine, 50 U/ml penicillin and 50 μg/ml streptomycin, 10% (v/v) FBS and 100 μM MEM Non-Essential Amino Acids Solution containing glycine, L-alanine, L-asparagine, L-aspartic acid, L-glutamic acid, L-proline and L-serine. Sf9 insect cells were grown in Grace's Insect medium supplemented with 2 mM L-glutamine, 50 U/ml penicillin and 50 μg/ml streptomycin, 10% (v/v) FBS. Complete growth media were prepared by diluting stock solutions in MEM, DMEM or Grace's medium, and filtering the resulting media through 0.2 μm filters.

Cells were grown in flasks under a controlled atmosphere in the presence of 95% air/ 5% CO_2 at 37 °C, until they reached 90% confluence. For propagation, the medium was removed, the cells were washed with sterile PBS, and 0.25% (v/v) trypsin solution was added for 2 min to 5 min. The medium was then added back to block the protease action of the trypsin, and the cells were collected in a plastic tube. After centrifugation for 5 min at 300× *g*, the cell pellet was resuspended in fresh medium. Sf9 insect cells were grown in flasks at 27 °C, in absence of 5% CO_2. For propagation, cells were resuspended in old medium by dislodging the cells by pipetting, centrifuged at 500× *g* for 5 min and resuspended in fresh complete growth medium.

2.8.3 DNA transient transfection

2.8.3.1 Materials

DNA constructs used for transient transfection are reporetd in section 2.3.4. *Trans*IT-LT1-Reagent was from Mirus Bio LLC (Madison, WI, USA). OptiMEM was from from Invitrogen/Gibco (Carlsbad, CA, USA).

2.8.3.2 *Trans*IT-LT1-Reagent-based cell transfection

HeLa cells were plated onto glass coverslips in 24-well plates or in 10-cm petri dishes in complete culture medium in the absence of antibiotics at a concentration suitable to have 50% to 70% confluence for transfection. The day after, a transfection mixture was prepared by diluting the *Trans*IT-LT1 Reagent in OptiMEM medium and incubated it at RT for 5 min. The cDNA (0.5 μg for a 24-well format, or 6 μg for a 10-cm petri dish) was then added to the transfection mixture, which was then gently shaken, and kept at RT for another 20 min, to allow the DNA-*Trans*IT-LT1 Reagent complex to form. The cells were then incubated prior to the assays with the transfection mixture for 24 h at 37 °C, in complete medium without antibiotics, as reported for each experiment. For control and $CD38^{+/+}$ HeLa cells, 2×10^6 cells were plated in a 10-cm petri-dish, and soon after, the transfection mixtures (prepared as described above) were directly added to the cells. The cells were then incubated for 24 h at 37 °C, in complete medium without antibiotics.

2.8.4 siRNA transfection

2.8.4.1 Materials

SiRNAs were from Dharmacon (CO, USA): ON-TARGET plus SMARTpool L-013740-00-0020, Human PARP12, NM_022750, 20 nmol (stock 20 μM); non-targeting siRNA pool, D-001206-13-20 (siRNAs; stock 20 μM). OptiMEM culture medium and Lipofectamine 2000 were from Invitrogen/Gibco (Carlsbad, CA, USA). Rab1A specific siRNAs were kindly provided by Dr. Rossella Venditti, of the Dr. De Matteis Laboratory, TIGEM, Naples, Italy.

2.8.4.2 Procedure

HeLa cells were plated onto glass coverslips in 24-well plates in normal culture medium (in the absence of antibiotics) at a concentration suitable to have 30% confluence for transfection (for HeLa cells, 20,000 cells were usually plated the day before transfection). One day later, a transfection mixture was prepared by diluting the siRNA smart pool in OptiMEM medium, and Lipofectamine 2000 with the same medium in a separate tube, according to the manufacturer instructions. The tubes were gently shaken and incubated for 5 min at RT; after this, the diluted siRNAs smart pool was mixed with the diluted Lipofectamine 2000 and incubated further for 20 min at RT, to allow the siRNAs-Lipofectamine complex to form. The transfection mixture thus included the specific concentration of siRNA sequences or the non-targeting siRNA was added to the cells in complete medium without antibiotics, with an incubation for an additional 72 h prior to assay. For the PARP12 knock-down experiments, 100 nM PARP12 specific siRNA was transfected for 72 h. For Rab1A knock-down experiments, 50 nM specific siRNA were transfected for 72 h. The efficiency of interference was assessed by Western blotting.

2.9 Cell-cycle synchronisation of HeLa cells

HeLa cells were grown on fibronectin-coated glass coverslips. Once they were attached to the coverslips, they were incubated in growth medium plus 9 μM RO-3306, a CdK1 inhibitor (from Calbiochem, CA, USA), for 20 h, to accumulate the cells in G_2 phase. Then the cells were immediately fixed (in G_2 phase) or washed in complete growth medium and incubated in complete growth medium for 1 h (causing the cells to accumulate in M phase) (Vassilev et al., 2006). For accumulation of cells in G_0 phase, they were maintained in

starvation medium (MEM without serum) for 24 h. At the end of each experimental condition, the cells were fixed and stained with Hoechst to visualise DNA organisation, and with anti-phosphorylated-histone H3 antibodies as a marker for the cell-cycle phase.

2.10 Immunofluorescence procedures

2.10.1. Materials

The Alexa 488- and Alexa 546-conjugated donkey anti-rabbit, anti-mouse and anti-goat antibodies were from Molecular Probes (OR, USA).

2.10.2 Sample preparation

Cells were fixed in 4% paraformaldehyde for 10 min at RT, washed three times in PBS, and incubated for 40 min at RT in blocking solution with saponin. The cells were subsequently incubated with the specified antibodies diluted in blocking solution (see Table 2.3 for the antibodies and the dilutions used) for 2 h at RT or O/N at 4 °C. After incubation with the primary antibody, the cells were washed three times in PBS and incubated with a fluorescent-probe-conjugated secondary antibody directed against the constant region of the primary IgG molecule, for 45 min at RT. Commonly, Alexa 488- or Alexa 546-conjugated anti-rabbit, anti-mouse or anti-goat donkey antibodies were used at a dilution of 1:400 in blocking solution. After immuno-staining, the cells were washed three times in PBS and twice in sterile water, to remove salts. The coverslips were then mounted on glass microscope slides (Carlo Erba, Italy) with Mowiol (20 mg mowiol dissolved in 80 ml PBS, stirred O/N and centrifuged for 30 min at 12,000× *g*).

Table 2.3: Antibodies used in immunofluorescence experiments.

Antibody target	Dilution	Animal source	Company/ source
Giantin	1:500	Mouse, monoclonal	Dr H. P. Hauri (University of Basel, Switzerland)
PARP12	1:100	Goat, polyclonal	Abcam
Phospho S10 histone H3	1:100	Rabbit, polyclonal	Upstate

2.11 Expression and purification of recombinant proteins from *E. coli*

2.11.1 Materials

Ampicillin, chloramphenicol and serine protease inhibitor Pefabloc (4-(2-aminoethyl)benzenesulfonyl fluoride hydrochloride, AEBSF) were from Fluka Analytical (Switzerland). Lysozyme, isopropyl-C-D-1 thiogalactopyranoside (IPTG), imidazole, reduced glutathione, sodium borate and triethanolamine were from Sigma-Aldrich (WI, USA). Triton X-100 was from Bio-Rad Laboratories (UK). All of the other enzymes used were from Roche (Basel, Switzerland). Dimethylpimelidate (DMP) was from Pierce (IL, USA). Glutathione Sepharose 4B matrix and glutathione were from Amersham Pharmacia Biotech (NJ, USA).

2.11.2 Expression and purification of GST-tagged proteins

(These procedures were carried out entirely by Claudia Cericola, in the Corda Laboratory, DCBO, CMNS)

GST-E1A, GST-14-3-3γ and GST-PAK1 were purified as previously described for recombinant GST-BARS (Valente et al., 2005). The following procedures led to 4-5 mg of these recombinant GST-tagged proteins. The bacteria transformed with the empty vector, pGEX4T1, were usually processed in parallel, which led to the production of about 10 mg GST. A small amount of the bacteria were scraped from the glycerol stocks, inoculated into 2 ml LB containing 60 μg/ml ampicillin, and grown at 37 °C under continuous shaking (200 rpm) for 6-8 h. Two ml of these cultures were inoculated into 100 ml of the same medium and grown O/N under the same conditions. These cultures

were then diluted 1:20 in 1.0 l of the same medium, and the optical density at 600 nm (OD_{600}) was monitored until it reached 0.4. The bacteria were then induced with the addition of 0.1 mM IPTG for 2 h, at 37 °C. After this, the cultures were chilled on ice and centrifuged at 6,000 rpm in a JA10 rotor (4,000× *g*) for 10 min at 4 °C. After discarding the supernatant, the pellets were resuspended in 50 ml GST lysis buffer containing a protease inhibitor cocktail, and lysozyme and Triton X-100 were added to final concentrations of 1 mg/ml and 1% (w/v), respectively. The suspensions were incubated with gentle agitation at 4 °C for 30 min, sonicated on ice 8 times for 15 s, and centrifuged at 18,000 rpm in a JA20 rotor (20,000× *g*) for 20 min at 4 °C. The supernatants were recovered and added to 2 ml glutathione Sepharose 4B matrix (Amersham Pharmacia Biotech, NJ, USA) that had been previously equilibrated in GST lysis buffer. The suspension was incubated with gentle agitation at 4 °C for 30 min and then centrifuged at 700× *g* for 5 min, to sediment the matrix. Each matrix was washed 5 times with 50 ml PBS (centrifuging as above). After washing, each matrix was packed into a 10 ml chromatography column (Bio-Rad Laboratories, UK), drained, and the bottom cap of the column was replaced. The protein was eluted by adding 2 ml GST elution buffer, incubating for 10 min at room temperature, removing the bottom cap, and collecting the eluate. The elution and collection steps were repeated at least 5 times. The protein usually peaked in the first or second fraction. The fractions containing the greater amounts of protein (at least 0.2 mg/ml) were pooled, dialysed twice against 1,000× volumes of PBS, and stored in aliquots at -80 °C.

2.11.3 Expression and purification of His-tagged proteins

(These procedures were carried out entirely by Claudia Cericola, in the Corda Laboratory, DCBO, CMNS).

His-CtBP1/BARS was purified as described previously (Valente et al., 2005). The following procedure led to about 2 mg of recombinant His-tagged proteins. A small amount of bacteria were scraped from the glycerol stocks, inoculated into 5 ml LB containing 60 μg/ml ampicillin and 10 μg/ml chloramphenicol, and grown O/N at 37 °C under continuous shaking (200 rpm). The cultures were then diluted 1:20 in 80 ml of the same medium, and the OD_{600} was monitored until it reached 0.6. The bacteria were then induced with the addition of IPTG to 0.4 mM for 2 h, at 37 °C. After this, the cultures were chilled on ice and centrifuged at 8,000 rpm in a JA14 rotor (5,000× *g*) for 10 min at 4 °C. After discarding the supernatants, the pellets were resuspended in 4 ml His lysis buffer containing a protease inhibitor cocktail, and frozen by immersion in liquid nitrogen. The lysates were stored at -80 °C O/N, or for up to a few days. Each suspension was thawed by transferring it to a 4 °C waterbath, protease inhibitor cocktail was added again, and lysozyme was added to a final concentration of 1 mg/ml. Each lysate was incubated with gentle agitation at 4 °C for 30 min and sonicated on ice 8 times for 15 s. Then $MgCl_2$ (to 10 mM) and DNAse I (to 10 μg/ml) were added, and each lysate was incubated for 15 min on ice, and then centrifuged at 18,000 rpm in a JA20 rotor (20,000× *g*) for 20 min at 4 °C. Each supernatant was recovered and added to 0.5 ml Ni-NTA beads (Qiagen, CA, USA) that had been previously equilibrated in His lysis buffer. Each suspension was incubated with gentle agitation at 4 °C for 1 h, and then packed into a 10 ml chromatography column

(Bio-Rad Laboratories, UK). The columns were washed 5 times with 10 ml His wash buffer, and the protein was eluted by adding aliquots of 0.5 ml His elution buffer, with each eluate collected in a clean tube. The elution and collection steps were repeated at least 5 times. The protein usually peaked in the first fraction. The fractions containing the greater amounts of protein (at least 0.2 mg/ml) were pooled, dialysed twice against 1,000× volume of PBS, and stored in aliquots at -80 °C.

2.11.4 Preparation of cross linked GST-tagged macro-domain resins

2.11.4.1 Materials

Vectors coding for full-length Af1521 wild-type and its G42E mutant macro domains were provided by Dr. Andreas Ladurner (EMBL, Heidelberg) and sub-cloned into the pGEX4T1 vector by Dr. Annalisa Stilla, in the Corda and Di Girolamo Laboratories, DCBO, CMNS.

STE buffer: 150 mM NaCl, 20 mM Tris HCl, pH 8, 1 mM EDTA.

Washing buffer: PBS, 1 mM EDTA, 1 mM DTT, 0.5 mM pefabloc.

2.11.4.2 Procedure

A small amount of BL21-DE3 cells was scraped from the glycerol stocks, inoculated into 50 ml LB containing 100 μg/ml ampicillin, and grown O/N at 37 °C under continuous shaking (200 rpm). The cultures were then diluted 1:10 in 500 ml of the same medium, and the OD_{600} was monitored until it reached 0.6. The bacteria were then induced with the addition of 0.2 mM IPTG for 3.5 h at 20 °C. After this, the cultures were chilled on ice and centrifuged at 6,000 rpm in a JA14 rotor (5,000× *g*) for 10 min at 4 °C. After discarding the supernatants, the pellets were resuspended in 4 ml STE buffer containing

protease inhibitor cocktail, 1 mM DTT and 0.5 mg/ml lysozyme, and incubated with gentle shaking for 30 min on ice; after this step, suspensions were frozen by immersion in liquid nitrogen and stored at -80 °C O/N, or for up to a few days. Each suspension was thawed by transferring it to a 20 °C waterbath, and 1% (w/v) Triton X-100, protease inhibitor cocktail and 1 mM DTT were added. Lysates were incubated with gentle agitation at 4 °C for 20 min and sonicated on ice 3 times for 30 s. The lysates were clarified by centrifuging at 15,000 rpm in a JA20 rotor (20,000× *g*) for 15 min at 4 °C. Ten µl of lysates were saved as inputs to monitor the purification procedure. Each supernatant was recovered and incubated with 0.5 ml glutathione sepharose matrix, (previously equilibrated in washing buffer) for 1-2 h on a rotating wheel at 4 °C. Each suspension was then washed 6 times with 12 ml washing buffer. Ten µl of each suspension were saved to monitor the cross-linking procedure. The resin was then treated with the cross-linker DMP, as follows. First, the resin was washed twice with 10 ml 0.2 M sodium borate, pH 8.6, and centrifuged at 1,000× *g* for 5 min at RT. All of the further centrifugation steps were performed under the same conditions. After, the suspensions were incubated with 600 µl of 0.2 M tris-ethanolamine, pH 8.3, added with 20 mM of the cross-linker DMP, on a rocker for 30 min at RT. Ten µl of the suspension was removed, for monitoring of the efficiency of cross-linking. At the end of this incubation, the suspension was centrifuged, and the supernatant removed. The reaction was stopped by washing the beads once with 14 ml 0.2 M ethanolamine, pH 8.2, and then incubating in the same buffer (10 ml) for 1 h at RT on a rocker. At the end of this incubation, 10 µl were removed (as above), and after centrifugation and removal of the buffer, the beads were washed three times in PBS, three times

with 20 mM GSH, in 20 mM Tris HCl, pH 8, once again in PBS, and finally with 100 mM glycine, pH 2.5, to remove material not covalently bound to the resin. Finally, the cross- linked matrices were washed twice with PBS and stored in PBS with 0.02% (w/v) sodium azide at 4 °C. The efficiency of cross-linking was monitored by boiling samples removed at each step (before adding DMP, after incubation with DMP, after washing with PBS) in SDS sample buffer, running on a 10% SDS-PAGE gel, and revealing of the protein by silver staining. Before use for the pull-down assay, the resins were monitored using NarE as a positive control, a toxin from *Neisseria meningitidis* that shows auto-ADP-ribosyltransferase activity (Koehler et al., 2011). The ADP-ribosylation reaction was carried out as follows: 3 µg purified NarE were incubated for 1 h at 37 °C in ADP-ribosylation buffer (50 mM Tris-HCl, pH 7.4, 500 µM $MgCl_2$, 4 mM DTT, 100 µM total NAD^+, 5 µCi [^{32}P]-NAD^+). At the end of incubation, equal amounts of the reaction mixture were diluted in 450 µl RIPA buffer and incubated with 15 µl resin cross-linked with the wild-type or mutated GST-macro-domain, at 4 °C. After an O/N incubation, the samples were centrifuged for 5 min at 500× *g*, washed tree times in RIPA buffer, analysed on a 12% SDS-PAGE, and transferred onto nitrocellulose. The amount of [^{32}P]-ADP-ribose incorporeted was visualised by autoradiography. Figure 2.3 shows the ADP-ribosylated NarE bound to the GST-macro-domain cross-linked resins. These resins were used for the macro-domain pull-down assay for the identification of PARP12 substrates (as described in Chapter 4). The purification of His-NarE was carried out by Claudia Cericola, DCBO, CMNS, as described by Koehler C. *et al.* (2011).

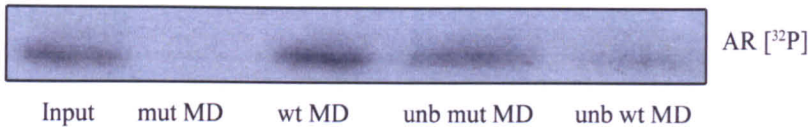

Figure 2.3: wild type GST-macro domain cross-linked to resin can recognise ADP-ribosylated NarE

GST-macro-domain cross-linked resins were tested using ADP-ribosylated NarE. After the ADP-ribosylation reaction of NarE toxin, GST-tagged mutated and wild-type macro domains (mut MD, wt MD) cross-linked to resins were incubated with ADP-ribosylated NarE. After an O/N incubation, the protein bound to resins, input and unbound materials (unb) were analysed on 12% SDS-PAGE, and transferred onto nitrocellulose. The amount of [^{32}P]-ADP-ribose incorporeted was visualysed by auto-radiography (AR).

Note that ADP-ribosylated NarE is recognised by wild-type macro-domain cross-linked resin and not by the mutated macro-domain. ADP-ribosylated NarE is present in the unbound material from mut MD and only as a small fraction in the unbound material from wt MD.

2.12 General biochemical procedures

2.12.1 Materials

Sodium dodecyl sulphate (SDS), glycine, TRIZMA base, Ponceau red, polyoxyethylenesorbitan monolaurate (Tween-20), ammonium persulphate (APS), N,N,N',N'-tetramethylethylenediamine (TEMED) and the acrylamide stock solution at 40% (w/v) acrylamide:bis-acrylamide (37.5:1) were from Sigma-Aldrich (WI, USA). Acetic acid was from Carlo Erba (Italy). Secondary antibodies conjugated with horse-radish peroxidase (HRP) and directed against mouse or rabbit IgGs were from Calbiochem (CA, USA). The ECL reagents were from Amersham Pharmacia Biotech (NJ, USA). GelCode Blue Stain Reagent was from Pierce (IL, USA).

2.12.2 Solutions

- Running buffer: 25 mM TRIZMA base, 200 mM glycine, 0.1% (w/v) SDS.
- SDS sample buffer: 62.5 mM Tris-HCl, pH 6.8, 2% (w/v) SDS, 10% (v/v) glycerol, 5% (v/v) C-mercaptoethanol and 0.1% (w/v) bromophenol blue.
- Transfer buffer: 25 mM TRIZMA base, 200 mM glycine, 20% (v/v) methanol.
- TBS: 150 mM NaCl, 20 mM Tris-HCl, pH 7.5.
- TTBS (TBS plus Tween 20): TBS + 0.05% (w/v) Tween 20
- Blocking solution for Western blotting: 1% (w/v) BSA in TTBS.

2.12.3 Sodium dodecyl sulphate-polyacrylamide gel electrophoresis (SDS-PAGE)

2.12.3.1 Assembly of polyacrylamide gels

Two 16 cm × 18 cm plates were used for standard gels. The plates were assembled to form a chamber using two 1.5 mm plastic spacers aligned along the lateral edges of the plates. The plates were then fixed using two clamps and mounted onto a plastic base which sealed the bottom. All of the materials were from Hoefer Scientific Instruments (Germany). The 'running' polyacrylamide gel was prepared by mixing H_2O, 40% (w/v) acrylamide:bisacrylamide solution, 1.5 M Tris-HCl, pH 8.8, 10% (w/v) SDS, to have the selected concentration of acrylamide in 375 mM Tris-HCl, 0.1% (w/v) SDS. Then, 0.06% (w/v) APS and 0.06% (v/v) TEMED were added; the solution was mixed and poured into the gap between the plates, leaving ~5 cm for the stacking gel. Soon after pouring, the gel was covered with a layer of H_2O and left at RT for ~1 h. The H_2O layer was then removed (by aspiration). The 'stacking' polyacrylamide gel was prepared by mixing H_2O, 40% (w/v) acrylamide: bisacrylamide solution, 500 mM Tris-HCl, pH 6.8, 10% (w/v) SDS, to have 4% (w/v) acrylamide, at a final concentration of 125 mM Tris-HCl, 0.1% (w/v) SDS. Then, 0.1% (w/v) APS and 0.07% (v/v) TEMED were added, and the solution was mixed and poured onto the 'running' gel. Immediately, a 10-well comb was inserted between the glass sheets and the apparatus was left for 1 h at RT.

2.12.3.2. Evaluation of protein concentrations

Protein concentrations were evaluated using a commercially available protein assay kit (Bio-Rad Laboratories, UK). This assay is based on the colour change

of Coomassie brilliant blue G-250 dye in response to various protein concentrations. 1-5 µl of samples were diluted in 800 ml H_2O and mixed with 200 ml reagent. After 5 min, a blue colour developed, the adsorbance of which (wave-length, OD 595 nm) was measured using a spectrophotometer. The protein concentrations were obtained by extrapolation from standard curves using known concentrations of BSA.

2.12.3.3. Sample preparation and running

Samples were prepared by adding SDS sample buffer, incubating at 100 °C for 5-10 min in a multi-block heater (Lab-Line, IL, USA), cooling to RT, briefly centrifuging and finally loading onto the gel. One well was loaded with 5 µl Rainbow recombinant protein molecular weight markers (Amersham Pharmacia Biotech, NJ, USA) or with 5 µg Low Molecular Weight Standards (Bio-Rad Laboratories, UK). The gel was then transferred into the electrophoresis apparatus (Hoefer Scientific Instruments, NJ, USA), and the electrophoresis was carried out under a constant current of 8 mA (for O/N runs) or 40 mA (for ~ 4-h runs).

2.12.3.4 Gel staining with GelCode Blue Stain Reagent

The GelCode Blue Stain Reagent uses the colloidal properties of the Coomassie G-250 dye for protein staining on polyacrylamide gels. After electrophoresis, the gels were placed in a clean tray and rinsed 3 × 5 min with 200 ml ultrapure water and for 30 min with 50% (v/v) methanol and 7% (v/v) acetic acid solution, with gentle shaking. After this step, 50 ml of GelCode Blue Stain Reagent were added for a 16 × 20 cm gel and incubated at room temperature for 3-4 h with gently shaking, to allow protein band development. To destain gels, the Stain Reagent was replaced with ultrapure water and the

water was changed several times over 1-2 h. The gel was then left in water at 4 °C before LC-MS/MS analysis.

2.12.4 Western blotting

2.12.4.1. Protein transfer onto nitrocellulose

The polyacrylamide gels were soaked for 15 min in transfer buffer, placed on a sheet of 3MM paper (Whatman, NJ, USA) and covered with a nitrocellulose filter (Schleicher & Schuell, Germany). The filter was covered with a second sheet of 3MM paper, to form a 'sandwich', which was subsequently assembled into the blotting apparatus (Hoefer Scientific Instruments, NJ, USA). The protein transfer was carried out at 400 mA for 5 h or at 125 mA for 16 h. At the end of the run, the sandwich was disassembled, and the nitrocellulose filter was soaked in 0.2% (w/v) Ponceau red (Sigma-Aldrich, WI, USA) and 5% (v/v) acetic acid for ca. 5 min, to appropriately visualise the protein bands, and then rinsed with 5% acetic acid to remove excess unbound dye.

2.12.4.2. Probing the nitrocellulose with specific antibodies

The nitrocellulose filters were cut into strips with a razor blade. The strips containing the proteins of interest were incubated in the blocking solution for Western blotting plus 1% (w/v) BSA or 5% (w/v) milk powder for 1 h at RT, and then with the primary antibody diluted to its working concentration in the blocking solution for Western blotting (see Table 2.3 for the antibodies used in the Western blotting experiments). After a 2-4 h incubation at RT, or an O/N incubation at 4 °C, the antibody was removed and the strips were washed twice in TTBS, for 10 min each. The strips were next incubated for 1 h with the appropriate HRP-conjugated secondary antibody diluted in the blocking

solution for Western blotting (anti-rabbit: 1:10,000; anti-mouse: 1:5,000) and washed twice in TTBS, for 10 min each, and once in TBS for 5 min. After washing, the strips were incubated with the ECL reagents, according to the manufacturer instructions, and protein signals were detect by autoradiography using Kodak film.

Table 2.4: Antibodies used in immunoprecipitation and Western blotting experiments

Antibody target	Dilution	Animal source	Company/ source
BFA	1:500	Rabbit, polyclonal	Kindly provided by Prof. Ignazio Sandoval, University of Madrid
Biotin	1:10000	Rabbit, polyclonal	Bethyl Laboratory, Inc.
CtBP1/BARS (BC3)	1:100	Mouse, monoclonal	Piccini D. (IFOM-IEO, Milan)
CtBP1/BARS ($p50_2$)	1.5 µg/mg total lysate	Rabbit, polyclonal	Our laboratory (Corda D., IBP, Naples)
GAPDH	1:80000	Mouse, monoclonal	Sigma-Aldrich
GFP	1:1000	Rabbit, polyclonal	Abcam
GFP (for I.P.)	1.0 µg/mg total lysate	Mouse, monoclonal	Abcam
GST	1:10000	Rabbit, polyclonal	Di Tullio G. and Santoro M. (De Matteis Laboratory)
Myc (for I.P.)	1.0 µg/mg total lysate	Mouse, monoclonal	Invitrogen
PARP12	1:2000	Rabbit, polyclonal	Sigma-Prestige Antibodies
Rab1A	1:1000	Rabbit, polyclonal	Santa Cruz Biotechnology, Inc.

2.13 Immunoprecipitation experiments

2.13.1 Preparation of cell lysates

2.13.1.1 Lysis buffers

1% Triton lysis buffer: 50 mM Tris HCl, pH 7.4, 150 mM NaCl, 5 mM $MgCl_2$, 1 mM DTT, 5 mM EGTA, 1% (w/v) Triton X-100, supplemented with protease inhibitor cocktail (Complete Mini EDTA-free, Roche, Basel, Switzerland) RIPA Buffer: 100 mM Tris pH 7.4, 150 mM NaCl, 0.1% SDS, 1% (w/v) Igepal, 0.1% (w/v) sodium deoxycholate, supplemented with protease inhibitor cocktail (Complete Mini EDTA-free, Roche, Basel, Switzerland).

2.13.1.2 Procedure

Cells maintained in the appropriate growth medium were washed three times with ice-cold PBS and directly scraped in the specific lysis buffer on ice. Cell lysates were kept on a turning wheel for 30 min at 4 °C. The lysates were then clarified by centrifugation at 13,000× *g* for 10 min. The supernatants obtained from the centrifugation were recovered and the protein concentrations evaluated according to the method described in section 2.10.3.2.

2.13.2 CtBP1/BARS immunoprecipitation procedure

$CD38^{+/+}$ HeLa cells (12×10^6) plated in six 10-cm petri dishes were transiently transfected with cDNAs coding for YFP-CtBP1/BARS WT or its point mutant H304A (6 μg cDNA were used for each petri) using *Trans*IT-LT1 (see section 2.8.3). Twenty-four hours after transfection, three 10-cm petri dishes for each condition (WT and H304A mutant) were treated with BFA (80 μg/ml) or vehicle alone as a control (DMSO), in DMEM for 4 h at 37°C. After 4 h, the

media were removed and the cells were washed three times in ice-cold PBS. All of the following steps were performed on ice and using ice-cold solutions. Cells were lysed using 1% Triton lysis buffer (see section 2.11.1) and 3 mg of total lysates for each condition were incubated with 5 μg of an anti-CtBP1/BARS antibody. After an O/N incubation, 25 μl Protein-A Sepharose beads (Amersham) were added, with an incubation for an additional 1 h at 4 °C. The suspensions were then centrifuged for 5 min at 500× *g*, and the supernatants were recovered. The matrices were washed 4 times, each time by adding 1 ml lysis buffer and two times with lysis buffer without Triton X-100, inverting the tubes several times and centrifuging as before. The bound proteins were eluted by boiling the samples for 10 min in 80 μl SDS sample buffer. The immunoprecipitated proteins were separated on 10% SDS-PAGE gels and transferred onto nitrocellulose. Western blotting with anti-BFA antibodies was performed to reveal the ADP-ribosylated CtBP1/BARS.

2.13.3 Myc-tagged PARP12 immunoprecipitation procedure

HeLa cells (8×10^6) were plated in four 10-cm petri dishes and transiently transfected with cDNAs coding for Myc-tagged PARP12 or the Myc empty vector (6 μg cDNA were used for each petri) using TransIT-LT1 (see section 2.8.3). Twenty-four hours after transfection, the growth media were removed and the cells were washed three times in ice-cold PBS. All of the following steps were performed on ice and using ice-cold solutions. The cells were lysed using RIPA buffer (see section 2.11.1.1), and 4 mg total lysates for each condition were incubated with 4 μg of an anti-Myc antibody (for dilution see Table 2.4). After 3 h incubation at 4 °C on a rotating wheel, 25 μl Protein-G Sepharose beads (Amersham) previously equilibrated in RIPA buffer were

added, with an incubation for an additional 1 h at 4 °C. The suspensions were then centrifuged for 5 min at 500× *g*, and the supernatants recovered (referred to as the unbound materials). The matrices were washed 4 times, each time by adding 1 ml lysis buffer with ice-cold RIPA buffer and two times with the same buffer without detergents, inverting the tubes several times and centrifuging as before. The bound proteins were eluted by boiling the samples for 10 min in 80 µl SDS sample buffer. The immunoprecipitated proteins and 30 µg of the input and unbound materails were separated on 12% SDS-PAGE gels and transferred onto nitrocellulose. Western blotting was performed to reveal the immunoprecipitated proteins.

2.14 Preparation of total membrane fractions

Confluent HeLa cells (3 $\times 10^6$ cells for each 10-cm petri dish) were washed three times with ice-cold PBS, and mechanically detached in 800 µl HEPES buffer (20 mM HEPES pH 7.4, 1 mM EDTA, 250 mM sucrose) using a cell scraper. The cells were recovered and then sonicated on ice three times for 15 s; unbroken cells were removed by centrifugation at 500× *g* for 5 min. The resultant supernatants were ultra-centrifuged for 1 h at 100,000× *g*; with the supernatants representing the cytosolic fraction and the pellets the total membrane fraction. The total membrane fractions were then resuspended in 20 mM HEPES, pH 7.4, containing 1 mM EDTA and protease inhibitors, and stored at -80 °C. A few microliters were lysed in 1 M NaOH and the protein concentration was evaluated by the method described in section 2.10.3.2.

2.15 Macro-domain-based pull-down assay

For MS analysis, the pull-down assay was performed using solubilised total membranes (previously ADP-ribosylated as described in section 2.18), while for routine experiments, the protein amounts used were lower (as described later). Total membrane fractions were prepared as described above, starting from 30 10-cm petri dishes with cells that had not been transfected or had been transiently transfected with untagged PARP12. Eight mg total membranes were ADP-ribosylated for 8 h, as described in section 2.18, washed once with PBS to remove unbound NAD^+, and then recovered by centrifugation at 100,000× *g* for 60 min at 4 °C. The pellet was solubilised in 4.5 ml RIPA buffer (100 mM Tris HCl, pH 7.5, 150 mM NaCl, 1% Igepal, 0.1% deoxycholate, 0.1% SDS, and protease inhibitors), under constant rotation for 30 min at 4 °C. The mixtures were clarified by centrifugation at 13,000× *g* for 10 min at 4 °C. The supernatants were incubated with 100 µl 10 µg/µl GST cross-linked mutated macro-domain resin for 8 h at 4 °C, on a rotating wheel. After the incubation, the mixtures were centrifuged at 500× *g* for 5 min to recover the proteins bound to the mutated macro domain, and the supernatants were incubated for a further 8 h with the same amount of GST cross-linked wild-type macro-domain resin. The resins were previously equilibrated with RIPA buffer. After 8 h incubation, the samples were centrifuged at 500× *g* for 5 min. Both of the resins were then washed 8 times with RIPA buffer and another 8 times in the same buffer without detergents. Each time, the samples were centrifuged at 500× *g* for 5 min. At the end of the washing steps, the resins were resuspended in 100 µl SDS sample buffer, boiled and analysed by 10% SDS/PAGE. The gels were then stained with GelCode Blue Stain Reagent (as described in

section 2.11.3.4). The bands were analysed by LC-MS/MS, which was performed by Dr. Maria Monti, CEINGE Institute, Naples, Italy.

For routine experiments, 2 mg total lysates was used, and incubated with 25 µl GST-macro-domain cross-linked resins. The samples were processed as described above, analysed by SDS-PAGE, and transferred onto nitrocellulose for Western blotting.

2.16 BAC purification

(The BAC purification was carried out entirely by Claudia Cericola, in the Corda Laboratory, DCBO, CMNS. This method is described by Colanzi A. *et al.* (manuscript in preparation).

2.16.1 BAC synthesis

Salt-washed rat brain membranes (1.5 mg/ml), BFA (80 µg/ml), NAD^+ (5 mM) were incubated under agitation in metabolite buffer (20 mM Tris, pH 7.0, 50 mM NaCl), for 2 h at 37 °C. At the end of the incubation, the sample was centrifuged at 18,000 rpm in a JA 20.1 Beckman rotor, for 45 min. The pellet (representing the total membrane fraction) was discarded.

The supernatant was recovered and filtered using an Amicon pressure apparatus (10,000 molecular-weight cut-off). The filtrate was extracted twice in two volumes of MeOH/ $CHCl_3$ (1:2), and the aqueous phase was collected and lyophilised.

2.16.2 HPLC methods

Large scale BAC purification. The lyophilised BAC preparation was resuspended in 1 ml buffer A (10 mM KH_2PO_4, 2.5 mM TBA) and purified using a Kontron HPLC Pump 420, equipped with a Reodine injector (2 ml

loop), with an ACS UV-Vis detector (model 750/11/AZ) set at 254 nm; the chromatograms were recorded using a Shimadzu C-R60 CHOMATOPAC integrator. The peaks were resolved using a semi-preparative C18 reverse phase column (Viosfer, 10 μm, 25x250 mm) equilibrated with 2.5 ml/min buffer A and eluted with a non-linear gradient of buffer B (40% buffer A, 60% methanol), as: time 0, 0% buffer B; time 20 min, 50% buffer B; time 30 min, 100% buffer B; time 35 min, 100% buffer B; time 40 min, 0% buffer. The eluate was collected in 2.5 ml fractions that were then analysed in ADP-ribosylation assays (as described in section 2.15.2). The fraction containing the activity was supplemented with sucrose (final concentration, 10 mM), lyophilised, resuspended in 1 ml 20 mM HEPES (pH 7.2), and further purified using the same C18 reverse-phase column. The column was equilibrated with water and eluted with a gradient of buffer C (80% methanol) (time 0, buffer C 0%; time 60 min, buffer C 100%). All the % values used here refer to v/v. Using this procedure, it was possible to purify to homogeneity the molecule that eluted at 26 min, with this fraction supplemented with 10 mM sucrose, lyophilised, and resuspended in 20 mM Hepes, pH 7.2 (final BAC concentration, 100 μM). The BAC solution was then aliquoted and stored at -20 °C for up to several months.

2.17 GST pull-down assays

2.17.1. Solutions

GST incubation buffer: 20 mM Tris, pH 8.0, 100 mM KCl, 1 mM EDTA, 0.2% (w/v) Triton X-100 and protease inhibitor cocktail (Complete Mini EDTA-free, Roche, Basel, Switzerland).

GST elution buffer: 100 mM Tris, pH 8.0, 20 mM reduced glutathione, 5 mM DTT.

2.17.2 CtBP1/BARS ADP-ribosylation using purified BAC

Twenty μg His-CtBP1/BARS were incubated for 3 h at 37 °C with 8 μl HPLC-purified BAC (120 μM) or with 8 μl buffer alone (20 mM Tris, 10 mM sucrose), to allow binding of BAC to the His-CtBP1/BARS. The reaction mixture was then stopped on ice, split in four samples, and used for the GST pull-down assays (see next section).

2.17.3 Procedure

All of the following steps were performed on ice or at 4 °C using ice-cold solutions, unless otherwise indicated. Equimolar amounts of GST-PAK1 (120 kDa, corresponding to 11 μg), GST-14-3-3γ (55 kDa, corresponding to 5.5 μg), GST-E1A or GST (30 kDa, corresponding to 2.5 μg) were incubated with 5 μg His-CtBP1/BARS or CtBP1/BARS bound to BAC (50 kDa), in GST incubation buffer for 2 h with gentle agitation. After this step, 25 μl glutathione sepharose 4B matrix (previously equilibated in GST incubation buffer) was added to each sample, which were then further incubated for 1 h at 4 °C. The suspensions were then centrifuged at 500× *g* for 5 min, to sediment the matrix. The matrix was washed 6 times with GST incubation buffer (centrifuging as above). The interacting proteins were eluted by adding GST elution buffer, incubating for 10 min at 4 °C, centrifuging as before, and collecting the supernatants in tubes. The eluted fractions were examined by SDS-PAGE and Western blotting. The experimental procedure is schematised in Figure 2.4.

GST Pull-down assay

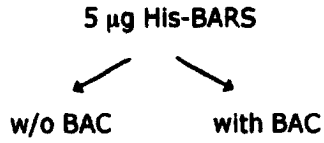

- incubation for 3 h at 37 °C;
- incubation with GST, GST-E1A, GST-14/3/3γ or GST-PAK1 for 3 h at 37 °C (buffer: 20 mM Tris HCl, 1 mM EDTA, 0,2% Triton, 100 mM KCl);
- incubation with glutathione resin for 1h at 4 °C;
- 6 washes in the same buffer;
- elution with 100 mM Tris HCl, pH 8, 20 mM glutathione, 5 mM DTT.

Figure 2.4: GST *in vitro* pull-down assay

Schematic representation on the GST pull-down assay. For a detailed description see text.

2.18 ADP-ribosylation assay

2.18.1 Materials

β-NAD^+, 3-aminobenzamide (3-AB), PJ-34 hydrochloride hydrate, vitamin-K1, and meta-iodobenzylguanidine (MIBG) were from Sigma-Aldrich (WI, USA). [^{32}P]-β-NAD^+ was from PerkinElmer. 3-AB was dissolved in DMSO, MIBG was dissolved in methanol, PJ-34 was dissolved in water. Biotinylated-NAD^+ was from Trevigen. Biotin was from Sigma-Aldrich (WI, USA).

2.18.2 Procedure

The ADP-ribosyltransferase activity was measured by following the incorporation of [^{32}P]-ADP-ribose into membrane proteins. Samples were incubated in 50 µl ADP-ribosylation buffer (50 mM Tris-HCl pH 7.4, 4 mM DTT, 500 µM $MgCl_2$, 50 µM total NAD^+) at 25 °C for 30 min (standard conditions), unless otherwise specified. 500 ng of His-PARP12 from total membrane fraction of Sf9 insect cells were routinely used. His-PARP12 concentration was determined by comparing the PARP12 band intensity with the intensities of known concentrations of a His-tagged protein. Alternatively, 50 µg of total membrane fractions from HeLa were usually used in ADP-ribosylation assays, unless otherwise specified.

For chemical treatments or experiments with ADP-ribosylation inhibitors, the assays were performed as described above in presence of the specific compounds. Control experiments (0 µM) were performed with the highest concentrations of solvent used for the compounds. The reactions were stopped by the addition of SDS sample buffer; the samples were subjected to SDS-PAGE and transferred onto nitrocellulose. For the quantification of the

incorporated label, an Instant Imager was used or the radioactive bands were cut out and their activities were measured by Cerenkov counting. For the determination of kinetic parameters, ADP-ribosylation reactions were performed with a fixed amount of [^{32}P]-NAD$^+$ and increasing concentrations of total NAD$^+$ for 30 min at 25°C. Reactions were stopped by the addition of 500 µl BSA (100 µg/ml) and 530 µl ice-cold TCA; the precipitated material was washed twice with diethyl ether, once with acetone, air-dried and measured by Cerenkov counting. Data were analysed by Lineweaver-Burk plot.

For the ADP-ribosylation experiments using biotinylated NAD$^+$, the ADP-ribosylation assays were performed as described above, with the ADP-ribosylation mixtures contained 10 µM biotinylated NAD$^+$ (or biotin alone, as control) and 40 µM unlabelled NAD$^+$. For these experiments, 200 µg of total membranes from HeLa cells were used. The reactions were carried out at 25 °C. After 1 h, the membranes were solubilised with RIPA buffer, and the solubilised proteins were incubated with 30 µl streptavidin resin (previously equilibrated in RIPA buffer) at 4 °C. After an O/N incubation, the samples were centrifuged for 5 min at 500× *g*, washed three times in RIPA buffer and another three times with the same buffer without detergents. The resins were then resuspended in 80 µl SDS sample buffer and analysed by SDS-PAGE and Western blotting (using an anti-biotin antibody), to visualise the ADP-ribosylated proteins.

2.19 Analysis of ADP-ribosylation reaction products

2.19.1 Materials

Phosphodiesterase I was from USB Corp. (Cleveland, OH, USA). Acrylamide:bis-acrylamide (19:1) and urea were from Sigma-Aldrich (WI, USA). Trichloroacetic acid was from Carlo Erba (Italy).

2.19.2 Procedure

Analysis of the ADP-ribose polymer length was carried out as described by (Panzeter and Althaus, 1990; Shah et al., 1995). Briefly, after the ADP-ribosylation assay (as described in section 2.18), the proteins were TCA precipitated, washed twice with diethyl ether and acetone, and [^{32}P]-labeled reaction products were detached from proteins by incubating at 60°C for 3 h with 10 mM Tris, 1 mM EDTA, pH 12. At the end of incubation, the samples were mixed with 1/3 vol of 4x loading buffer [25 mM NaCl, 4 mM EDTA, pH 7,5, 0.02% (w/v) xylene cyanol 0.02% (w/v) bromophenol blue], to which an equal volume of 100% urea has been added. After pre-electrophoresis for 1 h at 300 V, samples were loaded onto a 20% (w/v) polyacrylamide gel. Electrophoresis at 300 V was carried out until the bromophenol blue dye had migrated over about three-quarters of the entire gel length. The gel was then exposed to X-ray film at -80 °C.

2.20 Analysis of ADP-ribosylated residue

The ADP-ribosylation reaction was performed as described in section 2.18, using His-PARP12 from baculovirus-infected Sf9 insect cells. At the end of the incubation, the samples were treated with 1 M NaOH or 1 mM $HgCl_2$ for 2 h at 25 °C. Control samples were treated with 1 M NaCl. Alternatively, the

reactions were performed in the presence of the different MIBG concentrations (5 μM, 50 μM, 500 μM); as controls, the reaction was performed in the presence of the maximum concentration of MIBG solvent. The reactions were stopped by the addition of SDS sample buffer, and then the protein separated by SDS-PAGE and transferred onto nitrocellulose. The radioactivity incorporated was analysed using an Instant Imager (from PerkinElmer).

For identification of the ADP-ribosylated residue by MS, the total membrane fraction from His-PARP12 baculovirus infected Sf9 insect cells was used in the ADP-ribosylation assay in the absence of radiolabel NAD^+ (see section 2.18). After a 3 h incubation at 25 °C, the membranes were TCA precipitated, washed with diethyl ether and acetone, and then resuspended in phosphodiesterase-I-containing buffer. The phosphodiesterase reaction was carried out at 37 °C. After 2 h incubation, the reactions were stopped by the addition of SDS sample buffer and processed for MS for the identification of the residue, as run by Angela Amoresano, at the CEINGE Institute (Naples, Italy). Briefly, the samples were loaded onto 8% SDS-PAGE. The gels were then washed several times with water to remove the SDS, and then stained with colloidal Coomassie and destained with repeated washes in water. The band corresponding to PARP12 was excised from gel and processed for the MS analysis.

RESULTS

Preface

Chapters 3 and 4 are dedicated to the description of the results that I obtained during my PhD project. In the first chapter dedicated to the description of results (Chapter 3-Results I), I describe the novel BFA-dependent ADP-ribosylation mechanism of CtBP1/BARS (Results I), while in the second part (Chapter 4-Results II), I deal with the characterisation of PARP12 as a new mono-ADP-ribosytransferase and the identification of its potential substrates, with particular emphasis on Rab1A (Results II).

Note that throughout these Results sections I use the generic term of CtBP1/BARS to refer collectively to CtBP1-L and CtBP1-S/BARS.

CHAPTER 3. Results I

A novel ADP-ribosylation mechanism regulates CtBP1/BARS function

3.1 Introduction

CtBP1/BARS is a multitasking protein that is involved in several cellular functions that depend on its cellular localisation. CtBP1/BARS is regulated by two different post-translational modifications and protein interactions that affect its localisation and functions. In section 1.5.2.2, I described how phosphorylation of CtBP1/BARS by PAK1 induces its translocation from the nucleus to the cytoplasm, along with inhibition of its transcriptional activity. Sumoylation of CtBP1/BARS has the opposite effects. BFA-induced ADP-ribosylation represents another post-translational modification that might regulate these CtBP1/BARS activities.

Previous studies in our laboratory have demonstrated that BFA-dependent ADP-ribosylation of CtBP1/BARS is a non-classical reaction that comprises two distinct steps (Figure 3.1). The first step is the synthesis of a BFA-ADP-ribose conjugate (hereafter referred as BAC), which is catalysed by a membrane-bound enzyme that starts from NAD^+. This NAD-derivative, BAC, can be purified by HPLC. The second step is the covalent binding of BAC into the CtBP1/BARS NAD^+-binding pocket. Through mass-spectrometry analysis and mutagenesis experiments, it has been shown that the entire BAC binds covalently to CtBP1/BARS through histidine 304 of CtBP1/BARS (Figure 3.2).

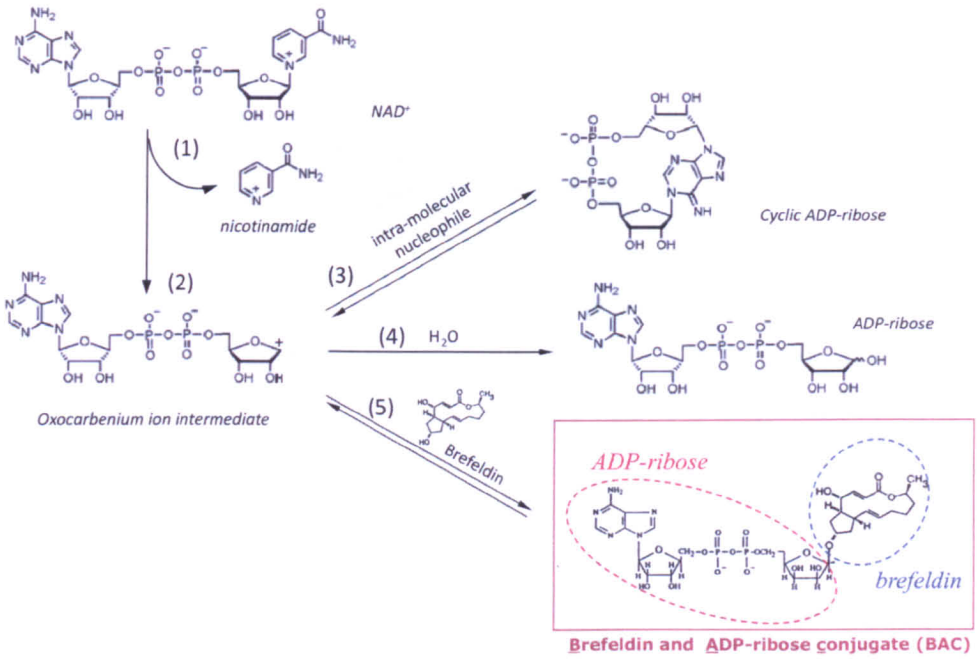

Figure 3.1: Molecular mechanism of BAC synthesis

The ADP-ribosyl cyclases convert NAD^+ to cyclic ADP-ribose and/or ADP-ribose through cleavage of the nicotinamide-ribose bond (1) and formation of an enzyme-stabilised ADP-ribosyl oxocarbenium ion intermediate (2). This intermediate is a good nucleophile acceptor that can react with the intra-molecular adenine (3) or water (4), to give cyclic ADP-ribose or ADP-ribose, respectively. Since BFA has two hydroxyl groups, it can act as a nucleophile and form a conjugate with the oxocarbenium ion intermediate (5), thus leading to the formation of the BFA and ADP-ribose conjugate (BAC).

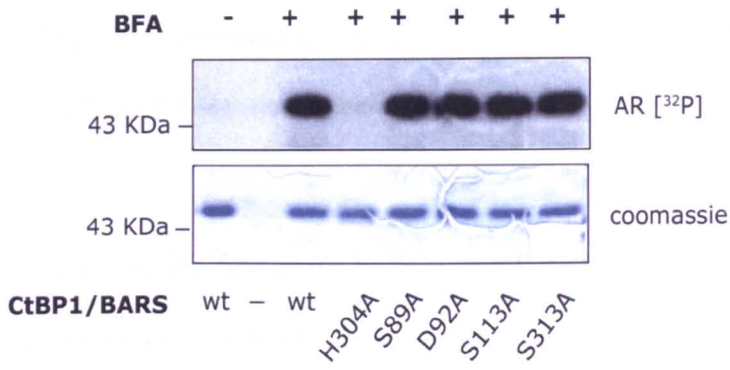

Figure 3.2: BAC binding occurs on histidine 304 of CtBP1/BARS

Histidine 304 as the residue involved in BAC binding was identified by mass spectrometry. To confirm the involvement of this amino-acid residue in the formation of the covalent bond between BAC and CtBP1/BARS, different point mutants of the CtBP1/BARS protein were generated and tested in *in vitro* ADP-ribosylation assays, using recombinant His-CtBP1/BARS proteins and brain total membranes as the enzyme source. Only the mutant protein in which histidine 304 was replaced by alanine (H304A) did not show BAC binding. Mutation of the other residues shown did not affect BAC binding.

In this context, my study was aimed at:

1. Identification of the enzyme that catalyses the first step of this reaction (section 3.2);

2. Providing an understanding of how this post-translational modification affects CtBP1/BARS functions (section 3.3).

I analysed the first point by evaluating the involvement of the ADP-ribosyl cyclase CD38 in this BFA-dependent mono-ADP-ribosylation, both *in vitro* and in intact cells, showing that CD38 can indeed support this reaction. Subsequently, I analysed the effects of this modification on CtBP1/BARS activities, i.e. its fissioning activity and its co-repressor activity. The experiments described demonstrate that BFA-dependent mono-ADP-ribosylation is important in modulating CtBP1/BARS functions.

3.2 The enzyme involved in the BFA-dependent mono-ADP-ribosylation of CtBP1/BARS

3.2.1 CD38 can catalyse the BFA-ADP-ribose conjugate synthesis both in vitro and in intact cells

An important point in the search for the enzyme that catalyses the BFA-dependent ADP-ribosylation reaction came from the HPLC analysis of the purified NAD^+-metabolite BAC synthesised *in vitro*, which showed that its synthesis is supported by NAD^+, $NADP^+$ and cyclic-ADP-ribose, but not by ADP-ribose (Colanzi, A. *et al.*, manuscript in preparation). These data are

consistent with the involvement of an ADP-ribosyl cyclase in the synthesis of this NAD derivative.

To test the hypothesis that BAC is synthesised by an ADP-ribosyl cyclase, I focused on the mammalian membrane-bound ADP-ribosyl cyclase CD38. To this end, I performed *in vitro* ADP-ribosylation assays (according to the method described in section 2.18) using total membranes prepared both from control HeLa cells, which do not express CD38, and from CD38 stably transfected HeLa cells (kindly provided by Prof. Antonio De Flora, University of Genoa, Italy). The total membrane fractions were incubated with recombinant His-CtBP1/BARS in [^{32}P]-NAD$^+$-containing ADP-ribosylation buffer for 2 h at 37 °C, in the absence and presence of 80 μg/ml BFA. At the end of the incubation, the samples were analysed by SDS-PAGE and autoradiography. As shown in Figure 3.3, only the total membrane fraction obtained from CD38$^{+/+}$ HeLa cells supported ADP-ribosylation of CtBP1/BARS. This thus demonstrated that CD38, the main mammalian ADP-ribosyl cyclase, is the enzyme responsible for the synthesis of the NAD-derivative BAC in this cell model.

To further analyse this result, I also examined the features of BAC formation and its binding to CtBP1/BARS in intact living cells. Here, CD38$^{+/+}$ HeLa cells were transfected with YFP-CtBP1/BARS or its point mutant on the histidine 304, H304A (the CtBP1/BARS residue involved in BAC binding). After 24 h, the cells were incubated at 37 °C for 4 h in the absence and presence of 80 μg/ml BFA and with 5 mM NAD$^+$ added to the growth medium. At the end of the incubation, the cells were lysed, then YFP-CtBP1/BARS was immunoprecipitated with an anti-CtBP1/BARS antibody, and the various

samples were subjected to SDS-PAGE and immunoblotting with antibodies against BFA. Strikingly, the over-expressed YFP-CtBP1/BARS protein in the $CD38^{+/+}$ Hela cells showed binding to BAC. As a control, the YFP-CtBP1/BARS H340A point mutant (the residue for the ADP-ribosylation) was not modified (Figure 3.4). No signal was detected in the absence of BFA.

In the experiments described above, I added 5 mM NAD^+ to the growth medium that results in a hugely increased production of BAC by CD38. This concentration is not physiological, since the extracellular NAD^+ concentration is in the nanomolar range. For this reason, I performed the same experiments also in the absence of exogenously added NAD^+. Control HeLa cells (which do not express CD38) and CD38 stably transfected HeLa cells were transiently transfected with YFP-CtBP1/BARS. After 24 h, the cells were incubated for 1 h and 4 h in the presence and absence of 80 μg/ml BFA and without and with 5 mM NAD^+ in the medium. At the end of the incubation, the cells were lysed, then YFP-CtBP1/BARS was immunoprecipitated, and the various samples were subjected to SDS-PAGE and immunoblotting with antibodies against BFA. Again, the YFP-CtBP1/BARS expressed in $CD38^{+/+}$ Hela cells incubated with BFA and NAD^+ for 1 h or 4 h showed BAC binding. Importantly, the fraction of modified protein was substantial, albeit lower, also in cells incubated with BFA without the addition of NAD^+ to the medium (Figure 3.5). Moreover, the modification is completely reversible, indicating that an enzyme that can remove BAC should also exist.

Altogether, these results show that CD38 can catalyse the formation of the NAD^+ metabolite, BAC, also in intact cells and under physiological NAD^+ conditions.

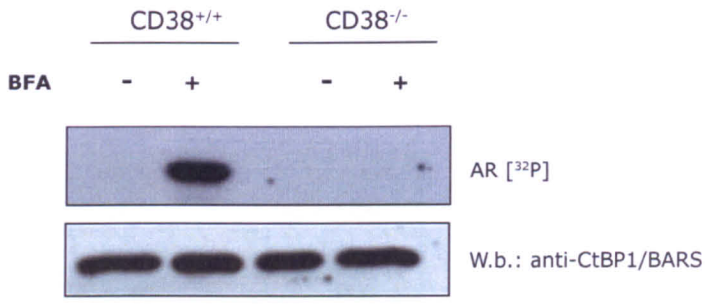

Figure 3.3: CD38 can support BAC synthesis in *in vitro* ADP-ribosylation assays

In vitro ADP-ribosylation assay. Ten µg total membrane fractions from control ($CD38^{-/-}$) and $CD38^{+/+}$ HeLa cells were incubated for 2 h at 37 °C with 0.5 µg recombinant His-CtBP1/BARS and 30 µM total NAD^+ (labelled with 5 µCi [^{32}P]-NAD^+), in the absence and presence of BFA (80 µg/ml). At the end of the incubation, the samples were analysed by SDS-PAGE and transferred onto nitrocellulose. Autoradiography (AR [^{32}P]) shows the modified CtBP1/BARS; CtBP1/BARS total levels were been analysed by Western blotting (W.b).

Note that BAC binding was observed only in presence of CD38 and BFA, which indicates that CD38 can catalyse the formation of BAC.

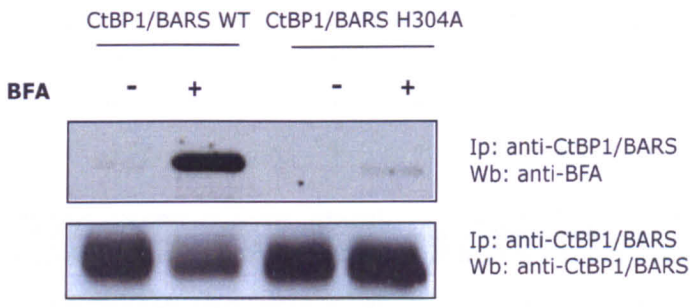

Figure 3.4: CD38 can support BAC synthesis in intact cells

$CD38^{+/+}$ HeLa cells were transfected with YFP-CtBP1/BARS wild-type (WT) and its point mutant on histidine 304 (H304A). After 24 h, the cells were treated with 80 μg/ml BFA for 4 h at 37 °C, in the presence of 5 mM extracellular NAD^{+}. YFP-CtBP1/BARS was immunoprecipitated from the total lysates using an anti-CtBP1/BARS antibody, and the ADP-ribosylated protein was revealed using an anti-BFA antibody. Total CtBP1/BARS levels are shown in the bottom panel.

BAC binding also occurs in intact cells, and no binding is observed when the H304A CtBP1/BARS mutant is over-expressed.

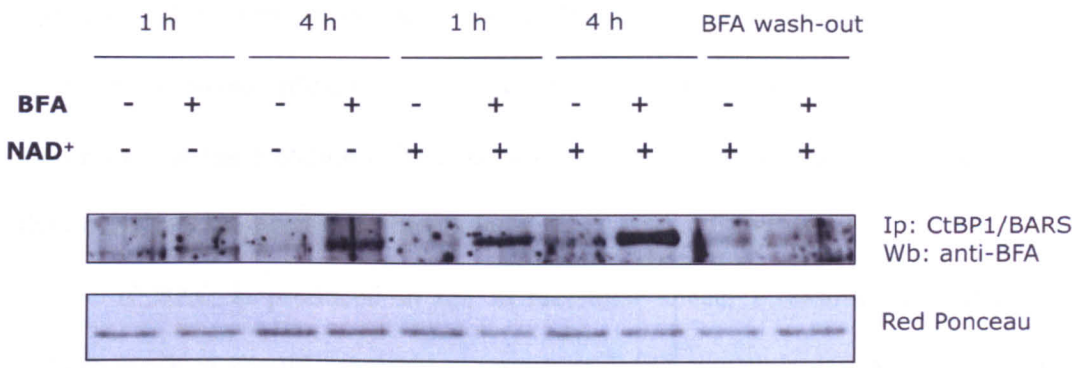

Figure 3.5: BAC is also formed in the absence of exogenously added NAD^+

$CD38^{+/+}$ HeLa cells were transfected with YFP-CtBP1/BARS. After 24 h, the cells were treated with 80 µg/ml BFA for 4 h at 37 °C, in the presence or absence of exogenously added 5 mM NAD^+. BFA wash-out was performed in BFA-free complete medium for a further 3 h. YFP-CtBP1/BARS was immunoprecipitated from total lysates using an anti-CtBP1/BARS antibody, and the ADP-ribosylated protein was revealed using an anti-BFA antibody. Total CtBP1/BARS levels are shown in the bottom panel.

BAC binding occurs also in the absence of exogenously added NAD^+, and it becomes evident after 4 h of BFA treatment. The lack of BAC binding after BFA wash-out suggests that the reaction is completely reversible.

3.2.2 CD38 acts as a transporter for the entrance of the metabolite BAC

As described in the Introduction (section 1.3.1.1), CD38 is an ectoenzyme, with its catalytic domain facing the extracellular space, whereas CtBP1/BARS is an intracellular protein. This 'topological paradox' can be explained assuming that the metabolite BAC is produced in the extracellular space, and then it reaches its substrate intracellularly.

If BAC is produced in the extracellular space, I reasoned that the culture medium should represent a source of BAC, and thus can be used to induce the *in vitro* ADP-ribosylation of recombinant CtBP1/BARS (the second step of the reaction described in Figure 3.1). To demonstrate this point, I stimulated control and $CD38^{+/+}$ HeLa cells with BFA in the presence of exogenously added NAD^+, for 4 h at 37 °C. After the incubation, I collected the different media to perform the second step of the BFA-dependent ADP-ribosylation reaction. Figure 3.6 shows that CtBP1/BARS immuno-reacts with the specific BFA antibody only when the supernatant of $CD38^{+/+}$ HeLa cells was used, thus demonstrating that it is produced in the extracellular space, according to the initial hypothesis. Moreover, it is clear that BAC binding is specific, since no labelling is present when using the supernatant of control HeLa cells stimulated with BFA.

To clarify whether CD38 also has a role in the intracellular transport of the metabolite BAC I performed the following experiment. $CD38^{+/+}$ and control Hela cells were transfected with YFP-CtBP1/BARS. After 24 h, the cells were stimulated for 4 h without and with 80 μg/ml BFA, in the presence of 5 mM NAD^+ added to the growth medium. To compensate for the absence of CD38 in the control HeLa cells, and thus for the production of BAC, I added

recombinant CD38 to the growth medium of one sample of the control Hela cells. At the end of the incubation, the cells were lysed, then YFP-CtBP1/BARS was immunoprecipitated with an anti-CtBP1/BARS antibody, and the various samples were subjected to SDS-PAGE and immunoblotting with antibodies against BFA. To check for the correct formation of BAC, I also saved all of the supernatants and I used them to induce the ADP-ribosylation of recombinant His-CtBP1/BARS in an *in vitro* assays. According to the previous results, Figure 3.7A shows that in intact cells, YFP-CtBP1/BARS is ADP-ribosylated only in $CD38^{+/+}$ HeLa cells stimulated with BFA, and so not in control HeLa cells. Importantly, despite the presence of recombinant CD38 in the medium, YFP-CtBP1/BARS was not modified in intact control HeLa cells stimulated with BFA (Figure 3.7A), while the supernatant of this sample (containing BAC produced by the added recombinant CD38), still ADP-ribosylated recombinant His-CtBP1/BARS *in vitro* (Figure 3.7B).

These data suggest that not only is CD38 involved in the production of the metabolite BAC, but it can have a role in the translocation of BAC itself into the cytoplasm, where CtBP1/BARS is located.

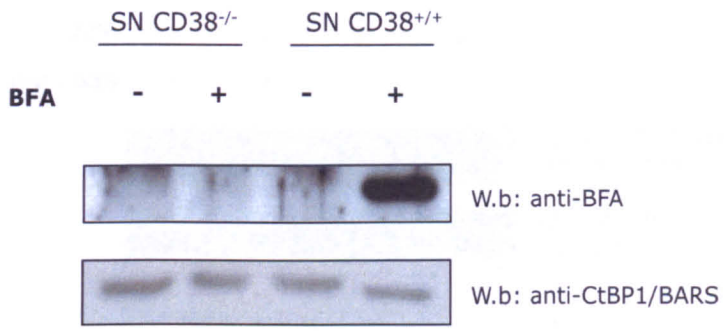

Figure 3.6: BAC is produced by CD38 in the extracellular space

Control ($CD38^{-/-}$) and $CD38^{+/+}$ HeLa cells were treated with BFA (80 µg/ml) at 37 °C. After 4 h treatment, the supernatants (SN) were recovered and incubated with recombinant His-CtBP1/BARS for 2 h at 37 °C. The samples were analysed by SDS-PAGE and transferred onto nitrocellulose. The modified CtBP1/BARS was analysed using an anti-BFA antibody. Total levels of CtBP1/BARS are shown in the bottom panel.

CtBP1/BARS shows BAC binding only when incubated with the supernatant of BFA-treated $CD38^{+/+}$ HeLa cells.

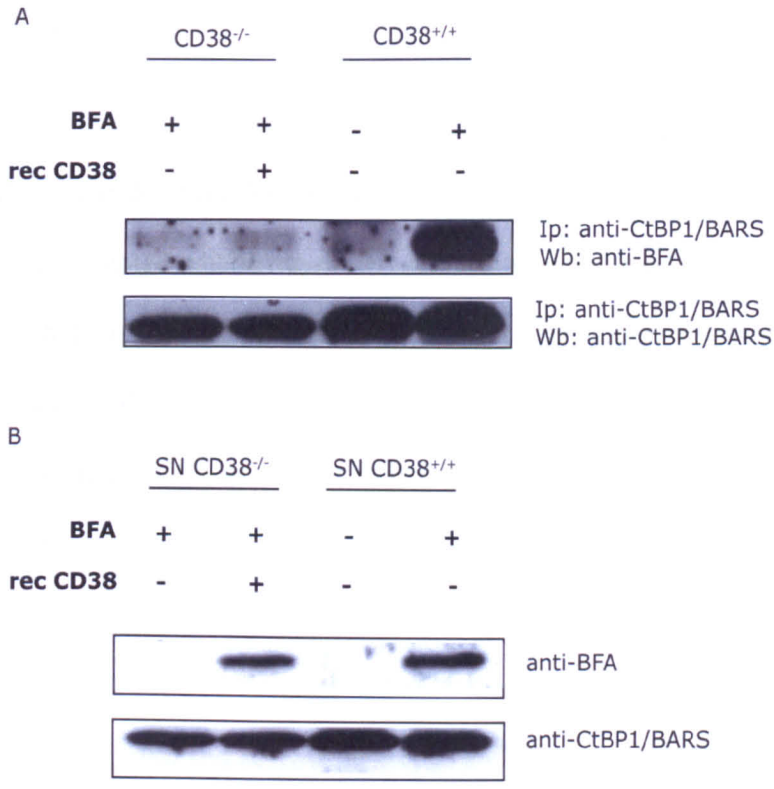

Figure 3.7: CD38 is required for BAC entrance into the intracellular space

Control ($CD38^{-/-}$) and $CD38^{+/+}$ HeLa cells were transiently transfected with YFP-CtBP1/BARS. After 24 h of over-expression, the cells were treated for 4 h with BFA (80 µg /ml) at 37 °C. To compensate for the absence of CD38, the recombinant CD38 enzyme (rec CD38) was added to the extracellular medium for the treatment time. All of the supernatants (SN) were saved and used to check for the presence of BAC. (A) At the end of the incubation, the cells were lysed and CtBP1/BARS was immunoprecipitated. The samples were resolved on SDS-PAGE and transferred onto nitrocellulose. Modified CtBP1/BARS was analysed using an anti-BFA antibody. Total levels of CtBP1/BARS are shown in the bottom panel. (B) Recombinant His-CtBP1/BARS was incubated with the supernatants (SN) for 2 h at 37 °C, to induce BAC binding *in-vitro*. An anti-BFA antibody was used to check for modified CtBP1/BARS. BAC produced by both recombinant CD38 and by the membrane fraction of $CD38^{+/+}$ HeLa cells can bind to recombinant His-CtBP1/BARS. Note that despite the presence of BAC produced by the recombinant CD38 (B), intracellular CtBP1/BARS was not modified in control HeLa cells (A), indicating that BAC did not reach the intracellular space due to the absence of CD38.

3.3 BFA-dependent ADP-ribosylation of CtBP1/BARS modulates its functions

3.3.1 BAC modulates the binding of CtBP1/BARS with its interactors

Next, I investigated whether the ADP-ribosylation mediated by BFA can affect CtBP1/BARS functions. Previous studies in our laboratory have demonstrated that, indeed, BFA-induced ADP-ribosylation of CtBP1/BARS inhibits its fissiogenic activity (Spano et al., 1999; Weigert et al., 1999). As reported in Chapter 1 (see section 1.5.2.3), the fissioning protein CtBP1/BARS is an essential component of Golgi complex fragmentation during mitosis. This process can be followed by using an assay that reconstitutes the fragmentation process in permeabilised normal rat kidney (NRK) cells incubated with mitotic cytosol. The mitotic cytosol induces the break-up of the Golgi ribbon into tubulovesicular clusters, which then disperse throughout the cell, similar to the Golgi clusters that are characteristic of prometaphase in intact cells (Warren et al., 1995).

The effects of BAC binding on the fissiogenic activity of CtBP1/BARS was evaluated by an analysis of Golgi complex fragmentation during mitosis (experiments performed by Prisca Liberali). These results showed that BAC addition to the mitotic cytosol in the Golgi fragmentation assay induced a strong inhibition of Golgi fragmentation. This finding was in agreement with other previous data showing that BFA-dependent ADP-ribosylation inhibits CtBP1/BARS fissiogenic activity.

Based on these data, I investigated whether once modified, CtBP1/BARS still binds to known partners involved in both co-repressor and fissioning activities. To this end, I performed *in vitro* GST-pull-down assays using recombinant His-CtBP1/BARS and some known GST-tagged interactors, i.e. the viral repressor E1A, as an interactor for the co-repression function, and 14/3/3γ and PAK1 as interactors for the fissioning activity. First, I induced CtBP1/BARS modification by incubating purified BAC and His-CtBP1/BARS (for 3 h at 37 °C), and then I incubated the modified CtBP1/BARS protein with GST-tagged interactors (as described in section 2.17). Figure 3.8 shows that BAC strongly impaired the CtBP1/BARS binding to GST-tagged 14/3/3γ and GST-tagged PAK1, which are two essential CtBP1/BARS interactors in post-Golgi trafficking (Valente, C. *et al.*, submitted manuscript) and macropinocytosis (Liberali et al., 2008), respectively. No binding was observed using GST alone as the control. The interaction with E1A, a viral repressor that contains a specific CtBP-binding motif (PLDLS), was not affected by BAC binding to CtBP1/BARS.

In addition, previous data from gel-filtration analysis of ADP-ribosylated CtBP1/BARS demonstrated that the modified CtBP1/BARS protein forms a tetramer, while the non-ADP-ribosylated CtBP1/BARS remains monomer (Colanzi *et al.*, manuscript in preparation).

Taken together, these results suggest that the covalent binding of BAC to CtBP1/BARS can 'lock' CtBP1/BARS in a closed, tetrameric conformation, which is not available for binding to proteins involved in membrane fission.

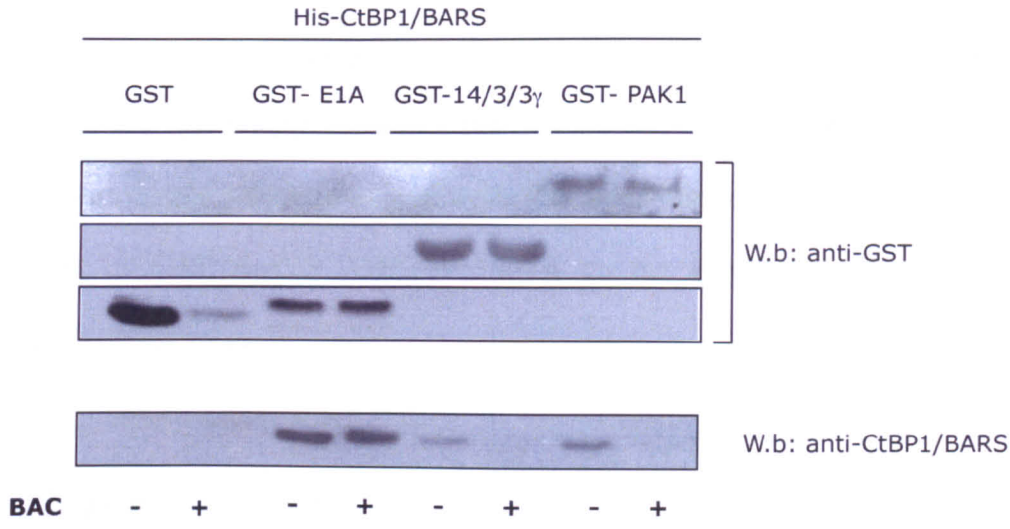

Figure 3.8: CtBP1/BARS interactions with its fission partners is affected by BAC binding

In-vitro GST pull-down assay. His-CtBP1/BARS was pre-incubated with BAC at 37 °C to induce BAC binding. After 3 h, equimolar amounts of GST, GST-E1A, GST-14/3/3γ or GST-PAK1 were added to the mixture, which was then incubated for a further 2 h at 4 °C. The GST-tagged proteins were recovered using glutathione resin, and eluted with a 20 mM glutathione-containing buffer. The samples were subjected to SDS-PAGE and immuno-blotted (W.b.) with antibodies directed against GST and CtBP1/BARS.

Note that the interaction between CtBP1/BARS and GST-14/3/3γ or GST-PAK1 is affected when BAC is bound to CtBP1/BARS (bottom panel).

According to the literature, the closed conformation of CtBP1/BARS is required for the transcriptional activity of CtBP1/BARS (Nardini et al., 2009). For this reason, even though the results from the *in vitro* pull-down assays showed that the binding between CtBP1/BARS and the viral repressor E1A was not affected, I decided to investigate this aspect further, by evaluating the effects of CtBP1/BARS ADP-ribosylation on the transcription levels of specific target genes.

3.3.2 Effects of BAC binding on CtBP transcriptional activity

As reported in the Introduction (1.5.2.2), it is known that NAD(H) promotes the dimeric/ tetrameric conformation of CtBP1/BARS and enhances the binding of CtBP1/BARS to cellular and viral transcriptional repressors; conversely, binding of palmitoyl-coenzyme A to CtBP1/BARS promotes the monomeric conformation of CtBP1/BARS and its interaction with ARF-GAP (a component of COPI-coated vesicles), thus promoting vesicle fission. In a similar manner, the CtBP1/BARS conformation is influenced by covalent binding to BAC, which locks CtBP1/BARS in a closed, dimeric/ tetrameric conformation (Colanzi *et al.*, manuscript in preparation); i.e., according to data reported in the literature, the conformation required for CtBP1/BARS to act as a transcription co-repressor.

For this reason, I tested the effects of BFA-dependent ADP-ribosylation on the expression levels of genes under the control of CtBP1/BARS. As described in Chapter 1 (section 1.5.2.3), CtBP1/BARS transcriptional co-repressor activity has been shown to have important regulatory roles in cell development and transformation, through the regulation

of the expression of adhesion molecules (such as E-cadherin) and pro-apoptotic genes (such as *P21, BAX and NOXA*). Thus, I tested the effects of BFA-induced ADP-ribosylation on the transcriptional activity of CtBP1/BARS, by making use of two different approaches, a luciferase assay and real-time RT-PCR (for methods see sections 2.6, 2.7).

The dual-luciferase reporter assay is a genetic reporter system that is widely used to study eukaryotic gene expression. Dual reporters are commonly used to improve experimental accuracy. The term 'dual reporter' refers to the simultaneous expression and measurement of two individual reporter enzymes within a single system. Typically, the 'experimental' reporter (called reporter I) is correlated with the effects of specific experimental conditions, while the activity of the co-transfected 'control' reporter (called reporter II) provides an internal control that serves as the baseline response. Normalising the activity of the experimental reporter to the activity of the internal control minimises the experimental variability caused by differences in cell viability or transfection efficiency, as well other sources of variability.

I analysed the effects of BFA administration on expression levels of the luciferase gene under the control of the E-cadherin promoter in both $CD38^{+/+}$ and control HeLa cells. These $CD38^{+/+}$ and control HeLa cells were transfected with 500 ng reporter I (RepI) and 10 ng reporter II (RepII). After 12 h, the cells were stimulated with BFA (40 μg/ml) and after a further 12 h, the cells were processed as described in section 2.7.2, to evaluate the luciferase gene expression levels.

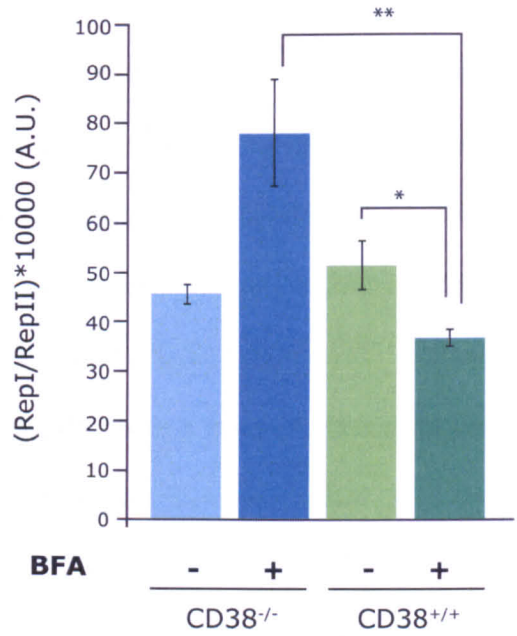

Figure 3.9: BFA treatment increases the co-repressor activity of CtBP1/BARS at the E-cadherin promoter

Luciferase assay. CtBP1/BARS-mediated transcriptional repression was monitored using an E-cadherin promoter-luciferase reporter (Reporter I). Control ($CD38^{-/-}$) and $CD38^{+/+}$ HeLa cells were transfected with 500 ng reporter I (Rep I) and 10 ng reporter II (Rep II). After 12 h, the cells were treated with BFA (40 μg/ml). After a further 12 h, the cells were lysed according to the manufacturer instructions of the Dual Luciferase assay system (Promega), and luciferase expression levels were determined using a luminometer (expressed as the RepI/RepII ratio, in arbitrary units).

BFA treatment decreased luciferase expression (29% reduction) in $CD38^{+/+}$ HeLa cells, as compared to $CD38^{+/+}$ HeLa cells not treated with BFA. This reduction is even more evident (52.8%) when the luciferase expression levels are compared to the control HeLa cells ($CD38^{-/-}$) stimulated with BFA, while no differences were seen between the two cell lines in the absence of BFA.

BFA treatment decreased luciferase expression (52.8% reduction) in $CD38^{+/+}$ HeLa cells, as compared to control ($CD38^{-/-}$) HeLa cells treated with BFA.

Data are means ± SEM of three different experiments, each performed in duplicate.

*, p= 0,0127; **, p = 0.0016.

As shown in Figure 3.9, BFA-stimulated $CD38^{+/+}$ HeLa cells showed a reduction (29%) in the luciferase expression levels, when compared to the control HeLa cells not stimulated with BFA. Interestingly, this reduction is even more evident (52.8%) when the luciferase expression levels are compared to the control HeLa cells ($CD38^{-/-}$) stimulated with BFA, while no differences were seen between the two cell lines in the absence of BFA.

Based on these first results, I additionally evaluated the effects of BFA-dependent ADP-ribosylation in a more physiological way, with an analysis of the transcription levels of the E-cadherin, Bax, p21 and Noxa mRNA, using real-time qRT-PCR. $CD38^{+/+}$ and control HeLa cells were stimulated with BFA (40 μg/ml). After 12 h, RNA was extracted and the transcription levels of the specific genes (*CDH1, BAX, NOXA* and *P21*) were analysed using real-time qRT-PCR. The results were normalised to *HPRT1* reporter gene (section 2.6.2, 2.6.3). As shown in Figure 3.11, $CD38^{+/+}$ HeLa cells display a 45% reduction in p21 transcription levels when compared to control HeLa cells stimulated with BFA, while there was no difference after BFA stimulation for Bax and Noxa mRNA levels between the two cell lines. However, an increase in the Noxa mRNA levels was observed, probably due to the toxic effects of BFA *per se*. Unfortunately, the E-cadherin mRNA levels were too low to be analysed in a reproducible manner.

Taken together, these results suggest that BAC binding to CtBP1/BARS increases its co-repressor activity, in a promoter-specific manner.

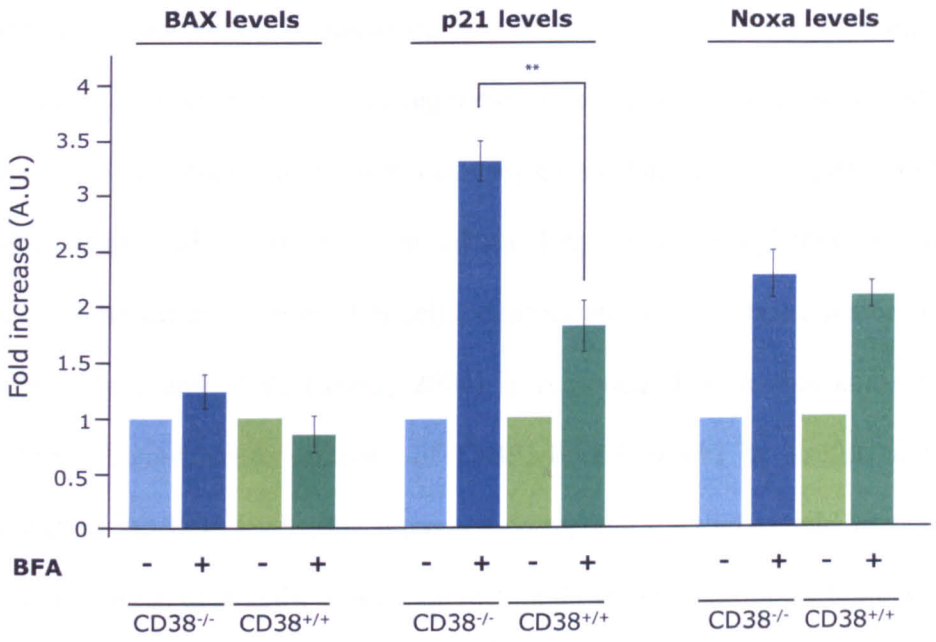

Figure 3.10: BFA treatment increases co-repressor activity of CtBP1/BARS at the p21 promoter

Control ($CD38^{-/-}$) and $CD38^{+/+}$ HeLa cells were treated with BFA for 12 h. Total RNA was extracted and processed to obtain cDNA. The mRNA levels of *BAX*, *NOXA* and *P21* genes were analysed using real-time qRT-PCR. The results were normalised to the *HPRT1* gene.

Compared to control HeLa cells ($CD38^{-/-}$), BFA treatment reduces the p21 expression levels (45% reduction), while bax and Noxa mRNA levels were not affected. The data are means of three different experiments, each performed in duplicate. **, $p = 0.0023$.

Interestingly, CtBP1/BARS also acts as a co-repressor for the *BCL6* gene (Mendez et al., 2008). Bcl6 is a transcriptional repressor that regulates B-cell differentiation at the germinal centres. It is required for the formation of germinal centres and its down-regulation is essential for B-cells to undergo further differentiation to memory cells or plasma cells (Ye et al., 1997). Bcl6 is often expressed constitutively in diffuse large B-cell lymphomas, where it blocks the differentiation of B-cells, contributing to the blastic feature of B cells (Phan and Dalla-Favera, 2004). I reasoned that in this context, an increased co-repressor activity of CtBP1/BARS would be useful. Indeed, lowering the Bcl6 levels, the increased co-repressor activity could favour the differentiation of B-cells, thus counteracting the progression of the tumour.

Based on this assumption, I asked if BFA stimulation can enhance the co-repressor activity of CtBP1/BARS at the *BCL6* promoter. HeLa cells do not express Bcl6, and for this reason I analysed the expression of the luciferase gene under the control of the *BCL6* promoter in both control and $CD38^{+/+}$ HeLa cells after BFA treatment, at different times. In contrast to the results obtained for the expression of the luciferase gene under the control of the E-cadherin promoter, BAC binding to CtBP1/BARS did not result in reduced levels of the luciferase gene under the control of the *BCL6* promoter (figure 3.11), thus ruling out the above-mentioned hypothesis.

Collectively, these effects support the idea that ADP-ribosylation can modulate the co-repressor activity of CtBP1/BARS depending on the specific promoter context. Moreover, the differential modulation observed after BFA treatment for the genes described rules out a non-specific effect due to BFA toxicity.

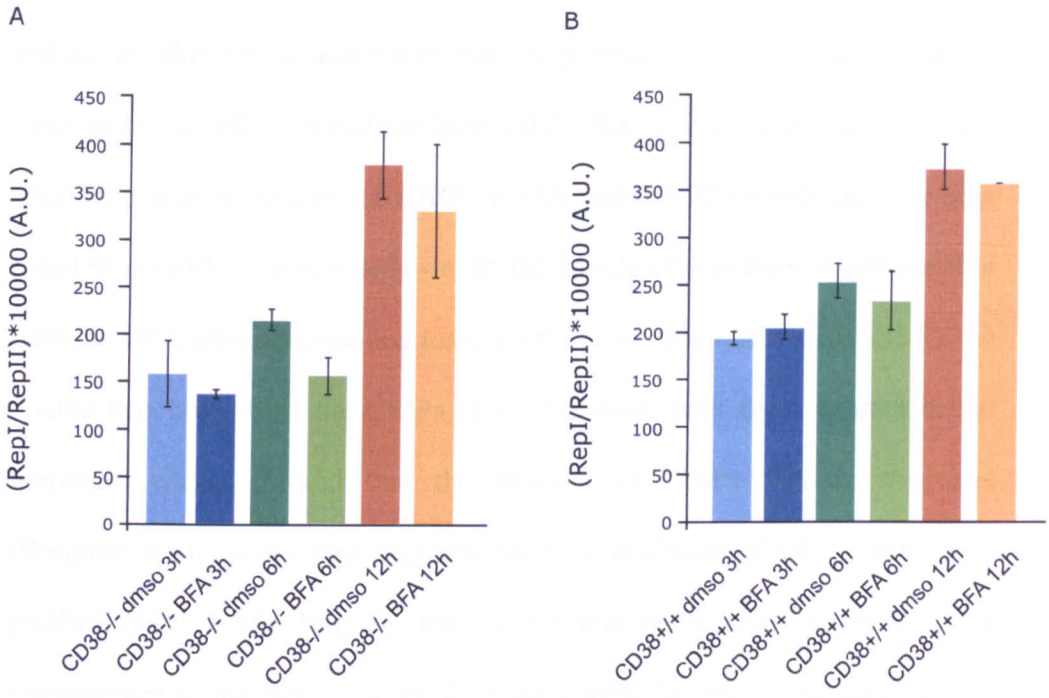

Figure 3.11: BFA treatment does not affect CtBP1/BARS co-repression activity at the *Bcl6* promoter

Luciferase assay. CtBP1-mediated transcriptional co-repression was monitored using a *BCL6* promoter-luciferase reporter (Reporter I). Control ($CD38^{-/-}$) (A) and $CD38^{+/+}$ (B) HeLa cells were transfected with 500 ng reporter I (Rep I) and 10 ng reporter II (Rep II). After 12 h, the cells were treated with BFA (40 µg/ml) for the indicated times, and then lysed according to the manufacturer instructions of the Dual Luciferase assay system (Promega). Luciferase gene expression levels were determined using a luminometer (expressed as the RepI/RepII ratio, in arbitrary units). Data are means ± SD from two single experiments.

Note that the luciferase expression levels remain unchanged after BFA treatment, for both cell lines.

To ensure that the effects of BFA stimulation on the transcription levels of the genes analysed were really due to the ADP-ribosylation of CtBPs and not to other effects associated with the presence of CD38, I performed the same assay in cells silenced for both CtBP1/BARS and CtBP2. I obtained a good reduction of both of the CtBP1/BARS and CtBP2 proteins at 48 h after transfection with the siRNAs; however, the double knock-down in combination with the BFA treatment was too toxic for the cells. The effect observed for the double knock-down of the CtBPs is in agreement with data reported in the literature, which showed that the absence of CtBPs favours apoptosis (Bergman et al., 2009). This suggests that the stimulation of cells directly with purified BAC would help to demonstrate that the effects observed are a consequence of the binding of BAC to the CtBPs. Moreover, in collaboration with Dr. Nicolosi (University of Catania, Italy), we are synthesising BFA analogues, with the aim of separating the 'ADP-ribosylating' activity of BFA from its effects on Golgi complex morphology and intracellular trafficking.

3.4 Discussion

I have shown here that the new mechanism involved in BFA-dependent ADP-ribosylation of CtBP1/BARS can be catalysed by ADP-ribosyl cyclases, such as CD38. ADP-ribosyl cyclases catalyse the conversion of NAD^+ to cyclic-ADP-ribose and/or ADP-ribose through the cleavage of the nicotinamide-ribose bond and formation of an enzyme-stabilised ADP-ribosyl oxocarbenium ion intermediate (Figure 3.1), which is a good nucleophile acceptor. This intermediate can react with water, to form ADP-ribose, or with the purinic ring of the adenine moiety of NAD^+, to form cyclic-ADP-ribose (Liu et al., 2008)

(Figure 3.1). Similarly, as it has two hydroxyl groups (positions 4 and 7; see Figure 3.1), BFA can form a conjugate with the oxocarbenium ion intermediate, which leads to the formation of BAC (Colanzi *et al.*, manuscript in preparation). Subsequently, BAC binds to CtBP1/BARS. An interesting point is that the locations of the two proteins (CD38 and CtBP1/BARS) are different, with CD38 being a type II transmembrane protein and CtBP1/BARS being an intracellular protein. Thus, I reasoned that the production of BAC should occur extracellularly, and then it should reach the cytoplasmic space, where it can bind to CtBP1/BARS. To clarify this point, I investigated a role for CD38 as a transporter for BAC. The results obtained indicate that CD38 not only supports the reaction, but can also contribute to the entrance of BAC into the intracellular space.

Here I also provided evidence that BFA-dependent CtBP1/BARS ADP-ribosylation affects CtBP1/BARS functions. The results obtained from the *in vitro* pull-down assays clearly show that there is an impairment of the binding with partners involved in the CtBP1/BARS fissioning activity, while the ability to interact with the viral repressor E1A is not affected. It is well known that CtBP1/BARS functions are tightly regulated by post-translational modifications and co-factors. In particular, sumoylation, as well as NADH, favours the nuclear functions, while phosphorylation, as well as acyl-CoA, promotes cytoplasmic localisation (see paragraph 1.5.2.2). These different activities reflect different conformational status: the co-repressor activity is associated with a closed/ dimeric conformation, while the fissioning activity is associated with the monomeric form of CtBP1/BARS. In line with these findings, data obtained in our laboratory from gel filtration experiments

(Colanzi *et al.*, manuscript in preparation), demonstrate that BAC binding to CtBP1/BARS favours the dimeric/ tetrameric conformation. Altogether, these considerations prompted me to further investigate the effects of BFA-dependent mono-ADP-ribosylation on CtBP1/BARS co-repressor activity. To this end, I analysed how the levels of CtBP1/BARS-regulated genes were changed after BFA treatment, by comparing control HeLa cells with $CD38^{+/+}$ HeLa cells. The results obtained show that the co-repressor activity of modified CtBP1/BARS is modulated, and in particular, increased, in a promoter-dependent manner. Among the genes tested (*P21*, *BAX, NOXA,* and luciferase gene under the control of the E-cadherin or *BCL6* promoters), only the expression levels of the luciferase gene under the control of the E-cadherin promoter and p21 mRNA levels were decreased after BFA treatment, while the transcriptional levels of all of the other genes were unaffected, when compared to control HeLa cells (which do not express CD38). Looking at the transcription levels of the genes above mentioned in BFA-treated samples, compared to their controls, there is an increase in mRNA levels observed for the *NOXA* gene, as well for the luciferase gene under the control of the E-cadherin promoter. The increased levels of Noxa mRNA might be connected to the toxic action of BFA, while I cannot at this stage explain the increase in the luciferase gene under the control of the E-cadherin promoter. The use of purified BAC, instead of BFA, should avoid the toxicity effects.

However, considering that the same toxic effects of BFA are present for all of the genes analysed, and considering that I only observed effects on p21 and E-cadherin-promoter regulated luciferase expression, it is reasonable to suppose that these effects are due to an enhanced co-repressor activity of

CtBP1/BARS bound to BAC, rather than to a toxic effect of BFA *per se*. Moreover, these data allow us to propose that BAC binding to CtBP1/BARS affects its co-repressor activity depending on the specific promoter context. A broader analysis of different genes will better clarify which are the specific gene subsets that are regulated by the binding of BAC to the CtBPs.

The experiments described here did not explore the molecular mechanisms underlying these effects, which remain to be fully elucidated. One possibility is that the modified CtBP1/BARS has an enhanced ability to recruit proteins that are important for the repressor activity. In this context, chromatin immuno-precipitation experiments would help to clarify this aspect.

Albeit the fact that from the experiments described in this Chapter do not directly demonstrate that the effects on the transcriptional activity of CtBP1/BARS are linked to BFA-dependent ADP-ribosylation of CtBP1/BARS, the results showing that cells that lack the enzyme catalyse this reaction suggest this is this very likely. However, different approaches (as already discussed above) will be required to definitely demonstrate this point.

CHAPTER 4. Results II

The new mono-ADP-ribosyltransferase PARP12

4.1 Introduction

As described in the Introduction (section 1.3.4), over the past 10 years, 17 mammalian genes with distant sequence homology to bacterial diphtheria toxin (DTX) have been described. The first and best characterised of these proteins is poly-ADP-ribose (ADPR) polymerase (PARP)1, the prototypical member of a family of mono- and poly-ADP-ribosyltransferases (m/pARTs). The concept that some of the PARPs can function as mARTs rather than pARTs came from an analysis across all of the PARP sequences that showed the lack of a glutamic acid residue, which is essential for elongation of poly-ADPR, in PARP7 to PARP16 (Otto et al., 2005). Since then, experimental evidence has become available indicating PARP10 and PARP14 as mARTs, with PARP10 being the 'founder member' of this sub-family (Kleine et al., 2008). All of the other members of this family remain to be fully characterised.

In this area my experiments have focused on the PARP family member PARP12. In particular, here I describe results that establish that PARP12 is a new mART and the identification of its intracellular substrates, thus providing new insights into the physiological role of PARP12. The choice of PARP12 among all of the other new PARPs (PARP7 to PARP16) was based on an

initial screening, in which the ADP-ribosylation activity of the different PARPs was tested in *in vitro* ADP-ribosylation assays using lysates from HeLa cells transiently transfected with cDNAs coding for each of the different PARPs. This first screening showed that PARP12 was among the more active of these enzymes, and that similarly to PARP10, it could ADP-ribosylate itself. Moreover, because the conserved glutamate residue in the catalytic site that is important for the polymerase activity was absent in PARP12, it was particularly important to establish if PARP12 is a possible new mART. Therefore, the first part of this Chapter describes the experimental evidence examining the catalytic properties of PARP12 (sections 4.2, 4.3), while the second part (sections 4.4-4.8) is focused on the identification of its intracellular substrates, providing a possible role for PARP12 in a cellular context.

4.2 The PARP12-mediated ADP-ribosylation reaction

4.2.1 Production of the recombinant PARP12 protein

As mentioned above, the initial screening across all of the PARP isozymes showed that the overexpressed PARP12 in HeLa cells could ADP-ribosylate itself. To further evaluate the enzymatic properties of PARP12, we sought to produce a recombinant GST-tagged full-length PARP12 in bacteria. The purification conditions were set up and performed by Claudia Cericola, a technician in our laboratory at the time. Unfortunately, the protein produced in this system was present in inclusion bodies and was mostly insoluble. Moreover, the small amounts of solubilised protein were inactive when tested in ADP-ribosylation assays. As an alternative choice, I decided to produce the recombinant PARP12 in Sf9 insect cells.

The Sf9 cell/ baculovirus expression system is widely used for high levels of protein expression, often with the purpose of purification. Importantly, proteins expressed in Sf9 cells contain most of the post-translational modifications (PTMs) known for mammalian cells. To express a protein of interest, Sf9 cells have to be infected with genetically modified baculoviruses, which can be produced using one of the several kits available. For my purposes, I used a baculovirus expression system, which uses a special *E. coli* strain that contains modified baculoviral DNA (Ciccarone et al., 1998). Recombination of the plasmid (containing the DNA of interest) with the baculovirus DNA occurs in the bacteria. The complete modified baculovirus DNA is isolated from the bacteria and used for direct transfection of Sf9 cells.

To achieve this, I first produced the His-PARP12 recombinant baculovirus, and then set up the optimal conditions to infect Sf9 insect cells (described in sections 2.4, 2.5). The His-PARP12 protein produced in this cell system was present in the total membrane fraction, where it represented the major band. Importantly, the His-PARP12 present in the total membrane fraction showed robust auto ADP-ribosylation when tested in the *in vitro* ADP-ribosylation assays.

Unfortunately the His-PARP12 protein produced by the baculovirus system is also insoluble complicating its purification. This part of the study was performed in collaboration with Giuliana Catara. Improvements in the protocol are still in progress. We have tried different solubilisation conditions, but when the protein is solubilised (mainly using denaturing conditions), it loses its catalytic activity (checked by following its auto-ADP-ribosylation activity).

One possible explanation concerning this solubilisation problem is that PARP12 forms aggregates through its WWE domains, a protein-protein interaction motif. We are still trying to solve this problem: for this reason I decided to use the total membrane fraction as an enzyme source to carry out the PARP12 biochemical characterisation.

4.2.2 PARP12 functions as a mono-ADP-ribosyltransferase

As mentioned in the introduction to this Chapter, in initial experiments, the human PARP12 overexpressed in HeLa cells could ADP-ribosylate itself and other substrates. Importantly, no mobility shift could be observed after its auto-modification, which suggested that the addition of a single ADP-ribose moiety takes place, and thus that PARP12 functions as a mART. In support of this observation, PARP12 has an important substitution in the catalytic triad; i.e. the presence of an isoleucine instead of the glutamic acid, substitution that is responsible for the lack of polymerase activity, as also shown for PARP10 (Kleine et al., 2008).

A structure-based alignment of PARP1, PARP3, PARP12 and the PARP10 model has been reported by Lusher and co-workers (Kleine et al., 2008). PARP1 has PARP activity, while PARP10 catalyses only mono-ADP-ribosylation. To identify the origins of this difference, the authors compared the PARP10 model with that of PARP1. The core secondary structure elements are retained, as are the histidine and tyrosine residues involved in NAD^+ binding, and which constitute the first two amino acids of the highly conserved "HYE" triad found throughout the PARP superfamily (Figure 4.1). However, it is clear that in PARP10 an isoleucine (I987) has replaced the catalytic

glutamate found in PARP1 (E988) (Figure 4.1). The same is the case for PARP12, where isoleucine 660 has replaced the glutamic acid of PARP1. Based on these features, I checked the role of these residues in PARP12 ADP-ribosylation activity by generating specific PARP12 mutants. I mutated the first histidine (involved in NAD^+ binding) to alanine (non-conservative mutation) or to glutamine (conservative mutation), as well as isoleucine 660 to alanine. As shown in Figure 4.2, my data demonstrate that the substitution of these important residues abolishes the PARP12 catalytic activity. Even though the expression levels of Myc-tagged PARP12 mutants were lower compared to wild-type PARP12-Myc, this difference cannot explain the abolishing of the auto-ADP-ribosylation activity. The absence of the first histidine, which is important in NAD^+ binding, is a characteristic of inactive PARPs, such as PARP9 and PARP13, and indeed the H564A PARP12 mutant and the H564Q PARP12 mutant were inactive. Of note, the absence of isoleucine 660 also impaired PARP12 catalytic activity, suggesting that this residue is involved in the catalytic mechanism. These results thus reinforce the initial hypothesis that PARP12 is a mART.

To investigate this further, I performed a series of biochemical assays that are well described in the literature as experimental tools to analyse protein ADP-ribosylation (mono-ADP-ribosylation *versus* poly-ADP-ribosylation) (Hottiger et al., 2010). In all of the experiments described in this section, the enzyme source I used was a total membrane fraction of Sf9 insect cells infected with His-PARP12 recombinant baculovirus.

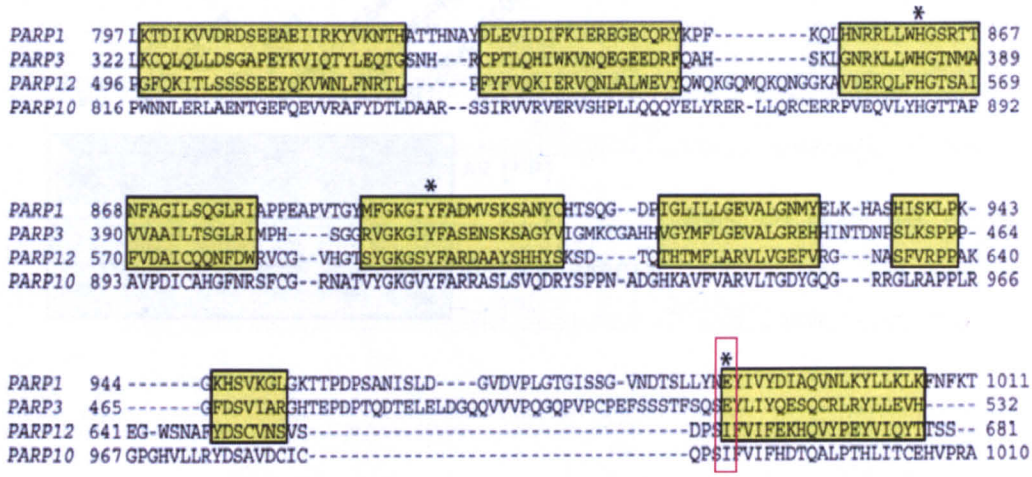

Figure 4.1: Sequence alignment of the catalytic domains of PARPs 1, 3, 10 and 12

Structure-based sequence alignment of the catalytic domains of PARPs 1, 3, 10 and 12. Yellow shading, structurally conserved regions. *, residues of the conserved "HYE" triad. Note that PARP10 and PARP12 lack the glutamic residue that is important for the polymerase activity (red box).

Modified from Kleine H. *et al.* (2008).

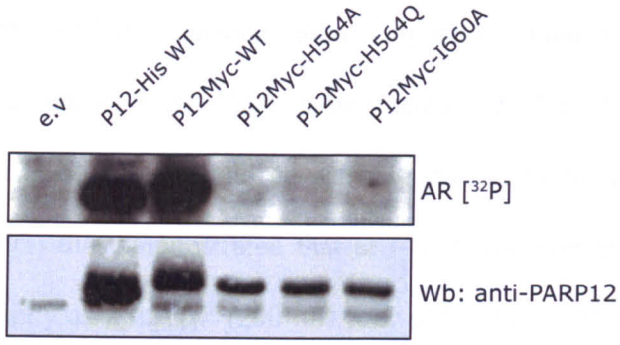

Figure 4.2: PARP12 mutants do not show auto-ADP-ribosylation activity

Total membrane fractions from HeLa cells transfected with Myc empty vector (e.v.) or cDNAs coding for His-PARP12 wild-type (P12-His WT), Myc-tagged PARP12 wild-type (P12Myc-WT) or Myc-tagged PARP12 mutants (P12Myc-H564A/P12Myc-H564Q/P12Myc-I660A), tested in the ADP-ribosylation assay performed at 37 °C for 1 h, in the presence of 30 μM total NAD^+ and 4 μCi ^{32}P-NAD^+. The reactions were stopped by adding sample buffer, and the proteins were separated by SDS-PAGE and transferred onto nitrocellulose. The incorporated label was revealed by autoradiography (AR [^{32}P]). The total amounts of PARP12 were revealed by Western blotting (Wb) using a PARP12 antibody.

First of all, I investigated whether His-PARP12 can ADP-ribosylate itself at different NAD^+ concentrations (Figure 4.3a) and reaction times (Figure 4.3b). The rationale of these experiments was based on the data reported by Mendoza-Alvarez and co-workers (Mendoza-Alvarez and Alvarez-Gonzalez, 1993) that demonstrated that at low NAD^+ concentrations, PARP1 functions mainly as a mART (200 nM to 2 μM NAD^+), while it behaves as a pART at high NAD^+ concentration (200 μM NAD). Figure 4.3 shows that, unlike PARP1, which undergoes a substantial increase in apparent molecular weight due to the formation of poly-ADP-ribose polymers (Kleine et al., 2008), PARP12 did not show any substantial changes to its mobility, even at high substrate (NAD^+) concentrations and long incubation times, indicating that the reaction was mono-ADP-ribosylation.

The ADPR chains can be detached after alkali treatment. Thus, to further characterise the PARP12-catalysed reaction, I analysed the auto-modification products after NaOH treatment, by assaying for ADP-ribose monomer release (typical of mARTs) or ADP-ribose oligomers (typical of pARTs) on a sequencing gel. As shown in Figure 4.4, ADP-ribose monomer was the only product obtained in this reaction, indicating that PARP12 functions as a mART.

The differences between mono-ADPR *versus* poly-ADPR formation is also reflected in the considerably lower V_{max} of PARP12 (Figure 4.5), as compared to PARP1 (0.5 *versus* 500 pmol/min/μg, respectively). The K_m for NAD^+ was around 30 μM for PARP12, which is lower than the K_m for PARP10 and PARP1 (roughly 50 μM).

Moreover, I also analysed the effects of some PARP1 inhibitors (PJ34 and 3-aminobenzamide [3-AB]) on PARP12 activity. The auto-ADP-ribosylation of PARP12 was inhibited by PJ34 (Figure 4.6a) and by 3-AB (Figure 4.6b), with IC_{50} values of 5 μM and 55 μM, respectively. These values are much higher than those of PARP1 (0.04 μM and 8 μM, respectively) (Loseva et al., 2010). In addition, the PARP12 activity was not affected by vitamin K1, which specifically inhibits classical mARTs (Figure 4.6c).

In summary, the experiments described here allowed me to conclude that the lack of detectable mobility shift of auto-ADP-ribosylated PARP12, the production of monomeric ADP-ribose after alkali treatment, and the kinetic parameters, demonstrate that PARP12 is a novel mART.

In addition to this, and similar to what happens for PARP10, the differential sensitivity to known PARP1 inhibitors, which distinguishes PARP12 from PARP1, and the lack of vitamin K1 inhibition, demonstrate that PARP12 belongs to a new class of mARTs.

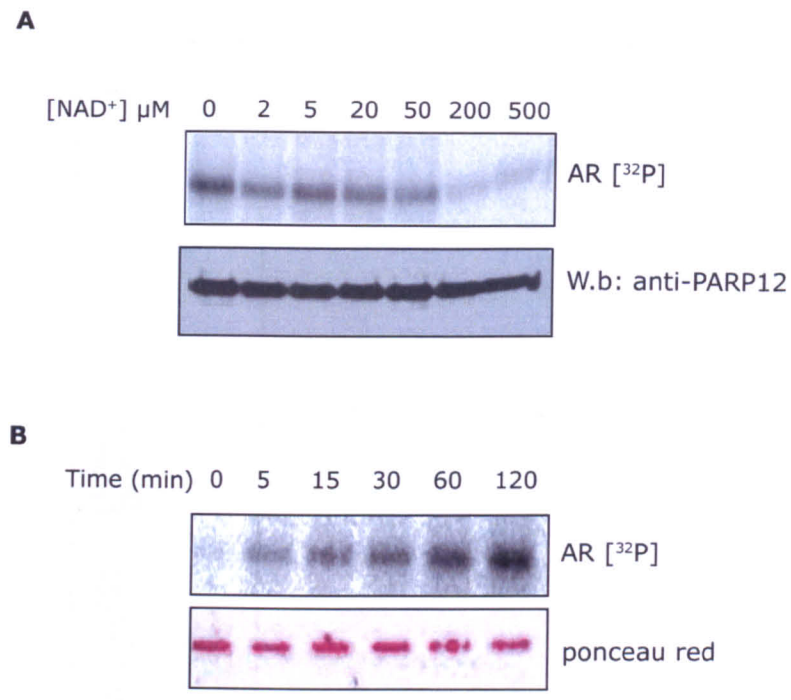

Figure 4.3: PARP12 auto-ADP-ribosylation reaction

(A) His-PARP12 from Sf9 insect cells incubated in the presence of a constant amount of [^{32}P]-NAD$^+$ and increasing concentrations of unlabelled NAD$^+$, as indicated, for 30 min at 25 °C. The reactions were stopped by adding sample buffer. The proteins were separated by SDS-PAGE and transferred onto nitrocellulose. The incorporated label was revealed by autoradiography (AR [^{32}P]). The total amount of PARP12 was revealed by Western blotting (Wb) using an anti-PARP12 antibody. (B) His-PARP12 from Sf9 insect cells incubated in the presence of a constant amount of total NAD$^+$ and [^{32}P]-NAD$^+$ at 25 °C, for the indicated times. The reactions were stopped by addition of sample buffer. The proteins were separated by SDS-PAGE and transferred onto nitrocellulose. The incorporated label was detected by autoradiography (AR [^{32}P]). The total amount of PARP12 is indicated by Ponceau red staining. The displayed experiment is representative for two independent experiments.

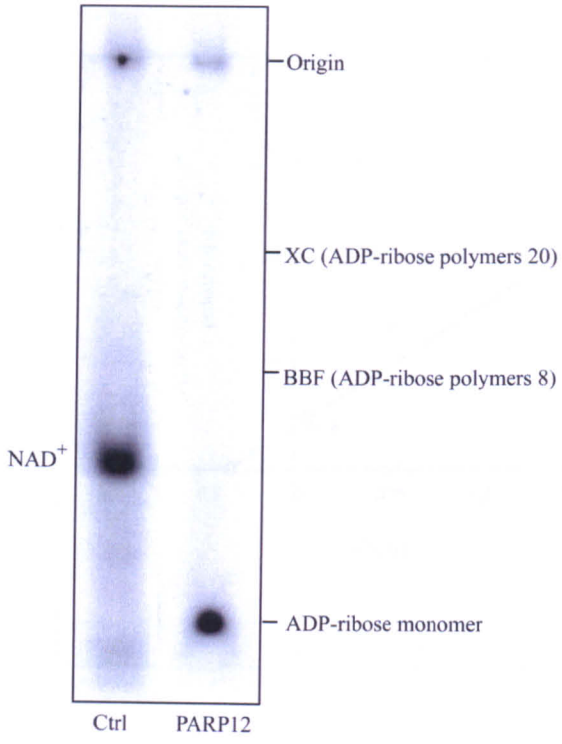

Figure 4.4: PARP12 is a mono-ADP-ribosyltransferase

His-PARP12 was auto-ADP-ribosylated under standard reaction conditions. The automodified PARP12 was TCA precipitated and then subjected to alkali treatment. The reaction products were analysed on a sequencing gel (see Methods). Marks with labels indicate the lengths of the ADP-ribose chains as determined by co-migration of bromophenol blue (BBF, 8 ADP-ribose polymers) and xylene cyanol (XC, 20 ADP-ribose polymers) (Alvarez-Gonzalez and Jacobson, 1987). The control (Ctrl) indicates the NAD^+ migration. The autoradiography analysis is shown. Note that monomeric ADP-ribose is the only product obtained after the alkali treatment.

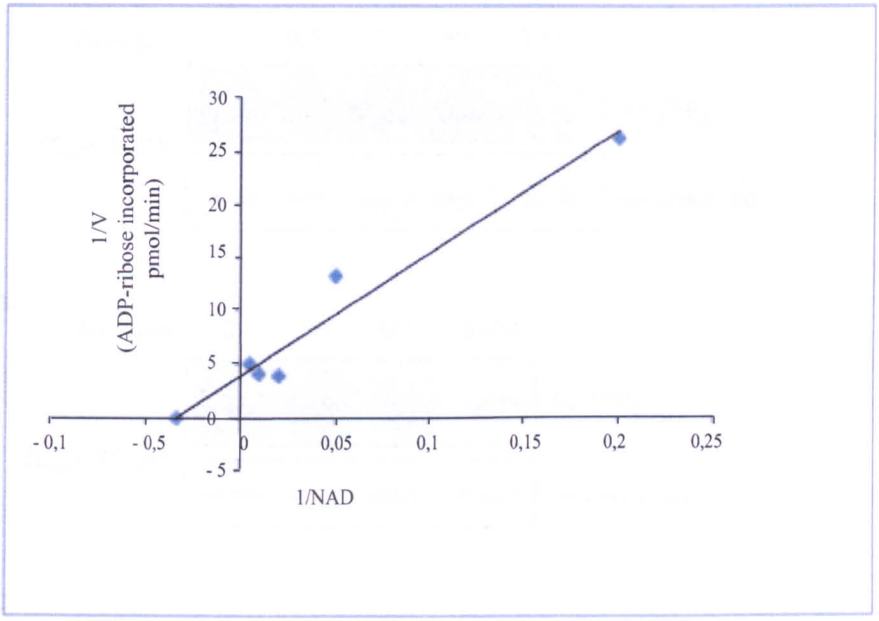

Figure 4.5: Kinetic parameters of the PARP12 auto-ADP-ribosylation reaction
PARP12 auto-modification reactions were performed with a fixed amount of [^{32}P]-NAD^+ and increasing concentrations of total NAD^+. The incorporated label was determined by TCA precipitation and Cerenkov counting, and the data were analysed using a Lineweaver-Burk plot. The kinetics shown is from the means of two independent experiments.

V_{max} = 0.5 pmol/min/μg; K_m = 30 μM

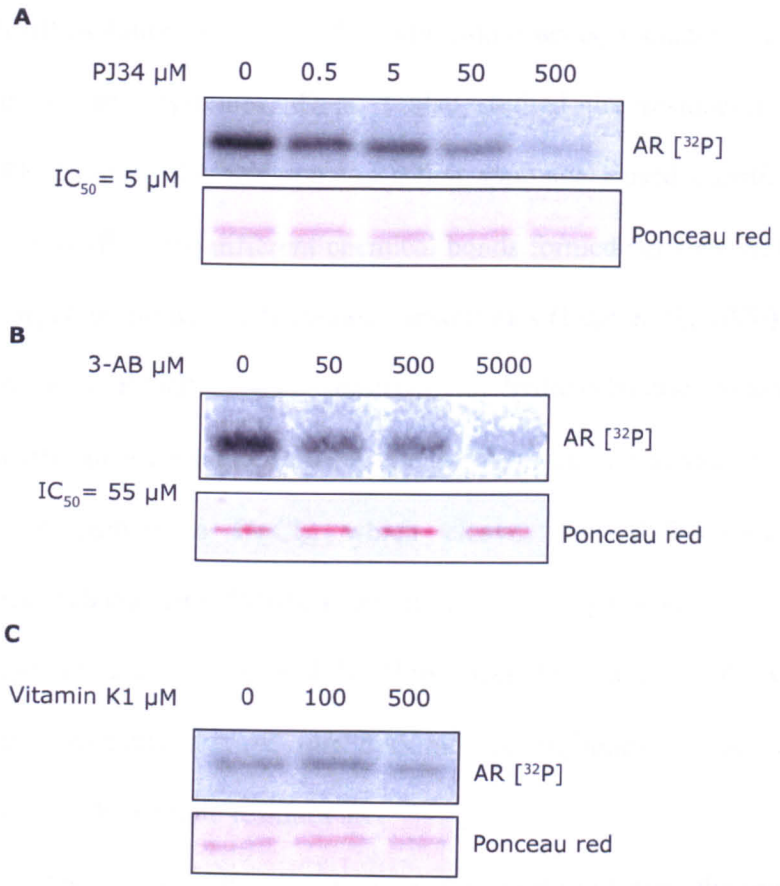

Figure 4.6: Sensitivity of PARP12 auto-ADP-ribosylation to different ADP-ribosylation inhibitors

His-PARP12 from Sf9 insect cells was subjected to the ADP-ribosylation reaction using standard conditions (50 µM total NAD^+ for 30 min at 25 °C) in the absence and presence of the indicated concentrations of different ADP-ribosylation inhibitors, as indicated. Controls (0 µM) were carried out with the highest concentrations of solvent used for the inhibitors. The IC_{50} values are indicated. All experiments were performed twice, with similar outcomes.

4.2.3 PARP12 modifies acidic residues

ADP-ribosylation occurs on different amino acids, including acidic residues, arginines and cysteines. Thus, I also studied the residue(s) modified by PARP12 during this reaction. As a first approach I used chemical treatments known to affect the different chemical bonds formed between ADP-ribose and the target amino acid with distinct sensitivities (Lupi et al., 2000). Auto-ADP-ribosylated PARP12 was sensitive to hydroxylamine treatment, which indicated an ester bond between the ADP-ribose and acidic residues. It was also insensitive to $HgCl_2$, which cleaves Cys-ADP-ribose, and *meta*-iodobenzylguanidine (MIBG), an inhibitor of arginine-specific mono-ADP-ribosyltransferases (Figure 4.7). Thus, from this first set of experiments, I could reasonably assume that cysteines or arginines are not modified by PARP12, while acidic residues are.

To further validate this point, we decided to identify the specific residue involved in this reaction by a different approach; i.e. by mass spectrometry (MS) analysis (in collaboration with Prof. Piero Pucci). MS is a versatile and indispensable tool in protein chemistry and proteomics. MS determines the mass-to-charge ratio (*m/z*) of peptide and protein ions that are generated by electrospray ionisation (ESI) or matrix-assisted laser *desorption/ ionisation* (MALDI) sources, and tandem MS (MS/MS) enables the peptides to be sequenced and PTMs to be identified and characterised. Thus, MS is ideally suited to the determination of PTMs because the covalent addition of a chemical moiety to an amino acid leads to an increase in the molecular mass of that residue, of the corresponding (tryptic) peptide, and of the intact protein. For example, the phosphorylation of a Tyr residue (163 Da) increases its mass

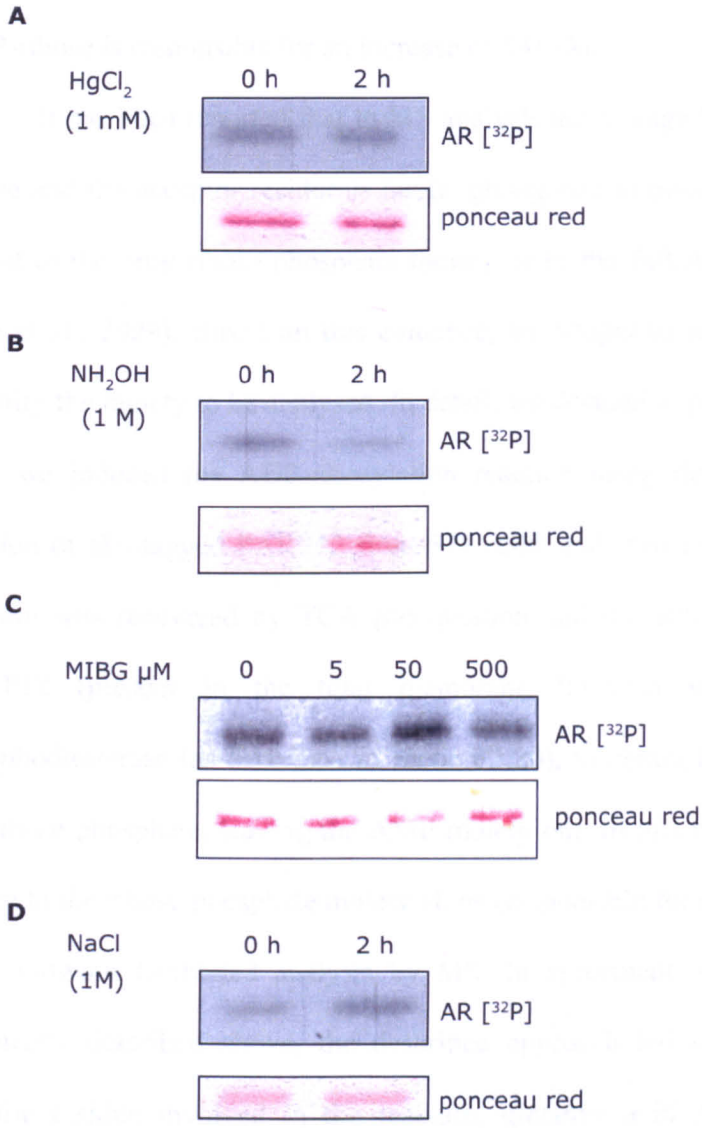

Figure 4.7: PARP12 ADP-ribosylates acidic residues

His-PARP12 was ADP-ribosylated under standard conditions and then subjected to treatment with (A) 1 mM $HgCl_2$ or (B) 1 M neutral NH_2OH for the indicated times. (C) Alternatively, the ADP-ribosylation assay was performed in presence of the indicated concentrations of meta- Iodobenzylguanidine (MIBG), an inhibitor of arginine-specific mARTs. (D) Control reactions were performed in presence of 1 M NaCl, for the indicated times. Residual radioactivity was determined by autoradiography. Total amounts of PARP12 are indicated by red Pounceau staining. Note that NH_2OH treatment reduces by 60% the ADP-ribosylation signal, while no change is observed after other chemical treatments, indicating that acidic residues are modified.

to 243 Da by the addition of an HPO_3 group (80 Da). Similarly, the addition of ADP-ribose is responsible for an increase of 541 Da.

It has been reported that in MS analysis the linkage between the ADP-ribose and the acceptor residue is labile, giving rise to mixed species that are linked to the only ribose-phosphate moiety or to the full ADP-ribose moiety (Tao et al., 2009). Based on this evidence, we sought to set up a method to simplify the moiety to be analysed. In detail, we decided to proceed as follows: first, we induced the ADP-ribosylation reaction using the total membrane fraction of His-tagged PARP12 from Sf9 cells; and then the total membrane fraction was recovered by TCA precipitation and the auto-ADP-ribosylated PARP12 (present in the total membrane fraction) was treated with phosphodiesterase (as described in section 2.20), to obtain PARP12 linked to the ribose-phosphate, leaving the AMP moiety out. In this way, PARP12 was linked to the ribose-phosphate moiety alone (responsible for an increase of 212 Da), allowing facilitated analysis by MS. In agreement with the chemical treatments described above, the described approach led us to identify the specific residue involved in the reaction, glutamic acid 39. The coverage achieved for PARP12 was 85%. Moreover, the data obtained so far indicate that Glu 39 seems to be the only residue modified, in contrast to PARP1, which has been reported to be modified on multiple sites (Tao et al., 2009). This aspect should further distinguish PARP12 from PARP1, highlighting a completely distinct enzymatic mechanism.

The preparation of the sample was carried out by Giuliana Catara, a member of our group, and the MS analysis by Angela Amoresano at CEINGE Institute, Naples.

In summary, the results described in this section clearly show that PARP12 modifies acidic residue and that the glutamic acid in position 39 seems to be the only residue modified by PARP12 during its auto-ADP-ribosylation. The construction of a specific mutant at this identified residue would thus undoubtedly confirm the modification site, and should exclude the possibility of a secondary modification sites.

The data reported here provides the basis for the design of a synthetic peptide substrate that would be useful for kinetic analyses, mechanistic investigations, substrate specificity determination, and the identification of inhibitors specific for PARP12. This last aspect is of great interest, as to date, no specific inhibitors for each individual PARP enzyme are available on the market. Thus, this area represents a future plan to develop.

4.3 Discussion I

The data presented in this chapter demonstrates that PARP12 is a novel mART. Its kinetic parameters and sensitivity towards specific PARP1 inhibitors reveal a trend similar to PARP10, a known mART, and also a different chemistry specificity compared to the poly-ADP-ribosyl polymerase PARP1. Thus, with these results, I have described a new intracellular mART that belongs to the PARP superfamily. My data are in agreement with the sequence analysis performed by Koch-Nolte and co-workers (Otto et al., 2005), from which they suggested the existence of a new family of intracellular mARTs, to which PARP12 belongs. In addition, the production of PARP12 mutants allowed me to demonstrate the importance of the HYI triad for its catalytic activity.

Moreover, these findings support the structure- and sequence-based division of the PARP family into three functionally distinct subgroups, one with poly-ADP-ribosyl polymerase activity, one with mART activity (to which PARP12 belongs) and one that is catalytically inactive, as reported by Lusher and co-workers (Kleine et al., 2008) (for summary, see Table 1.2).

Importantly, the MS analysis reported above permits the identification of the specific residue involved in the reaction, i.e. the glutamic acid in position 39. In addition to the identification of this specific residue, the data reported here show that Glu 39 can be a unique site for the modification, different from what has been shown for PARP1, which shows multiple auto-modification sites. In summary, we can consider the data described in this Chapter significant for four reasons, as follows.

First, I have described a new intracellular enzyme that can catalyse mono-ADP-ribosylation reactions, increasing the possibility of understanding how this PTM is used intracellularly with respect to its specific pathways. Secondly, I have developed a strategy to map the modification sites of the PARP12 substrates, permitting the identification of a single ADP-ribosylation site on PARP12. This represents the first verification of the acceptor amino-acid residue in PARP12, where the ADP-ribosylation takes place. Thirdly, in contrast to PARP1, the data obtained so far suggest that the auto-ADP-ribosylation of PARP12 can be limited to a single residue. Finally, using the information derived from this study, we should be able to design small peptide substrates for PARP12 that can be used as specific inhibitors, or as PARP12 substrates.

4.4 Identification of PARP12 substrates using the macro-domain pull-down assay

The first poly-ADPR molecule in mammals was identified in 1963 (Chambon et al., 1963) and PARP1, the main enzyme responsible for synthesising poly-ADPR in cells was cloned in 1987 (Alkhatib et al., 1987). At present, it is well recognised that PARP1 is the founder member of a larger family of enzymes that have distinct enzymatic activities. Nevertheless, to date the physiological consequences of ADP-ribosylation are only in part understood. In this context, an important aspect of my PhD project has been the study of the physiological role of intracellular mono-ADP-ribosylation, with a specific focus on PARP12. To link PARP12 activity to a physiological role, we decided to identify its substrates. A great limitation to the study of ADP-ribosylated proteins has been the lack of ADPR-specific antibodies that can potently recognise ADP-ribosylated proteins. In our laboratory, a new method has been described for the identification of ADP-ribosylated substrates (Dani et al., 2009). It is based on the use of a protein module, the macro domain of the protein Af1521 from *Archeoglobus fulgidus*, a domain that recognises monomeric and polymeric ADPR (Karras et al., 2005). Briefly, the method foresees the use of both a wild-type macro domain, that binds ADPR, and a mutated macro domain, where the point mutation of the glycine in position 42 to glutammic acid (G42E) is sufficient to abrogate the ADPR binding to the macro domain and thus to ADP-ribosylated proteins. The combined use of these two versions of the macro-domain together with MS analysis provides the methodology for the identification of ADP-ribosylated proteins.

The method reported above was based on the use of a His-tagged macro domain. These authors also described a slightly modified method using a GST-tagged macro domain cross-linked to Sepharose resin to minimise non-specific resin interactions with proteins. Here I have used the procedure with the GST-tagged macro domains for the identification of specific PARP12 substrates (Figure 4.8).

4.4.1 Setting up of the ADP-ribosylation conditions used for the macro-domain based pull-down assay

The use of the macro-domain-based pull-down assay represents a good, affinity based, method to enrich samples in ADP-ribosylated proteins. In addition to this strategy, to increase the amounts of ADP-ribosylated proteins, I increased the levels of ADP-ribosylation catalysed by PARP12, by performing an *in vitro* ADP-ribosylation assay before the macro-domain-based pull-down assay.

To establish the best reaction conditions to obtain high levels of ADP-ribosylation, I performed the ADP-ribosylation reaction using total membrane fractions of control and PARP12 transiently transfected HeLa cells at different NAD^+ concentrations, reaction times and temperatures. First of all, I performed the ADP-ribosylation reaction for 2 h at 37 °C using different total NAD^+ concentrations (from 500 μM up to 3.0 mM). Figure 4.9a shows that at 2 mM total NAD^+, the amount of auto-modified PARP12 was higher compared to these other NAD^+ concentrations. The efficiency of the reaction was also demonstrated by the appearance of an upper band that was recognised by the

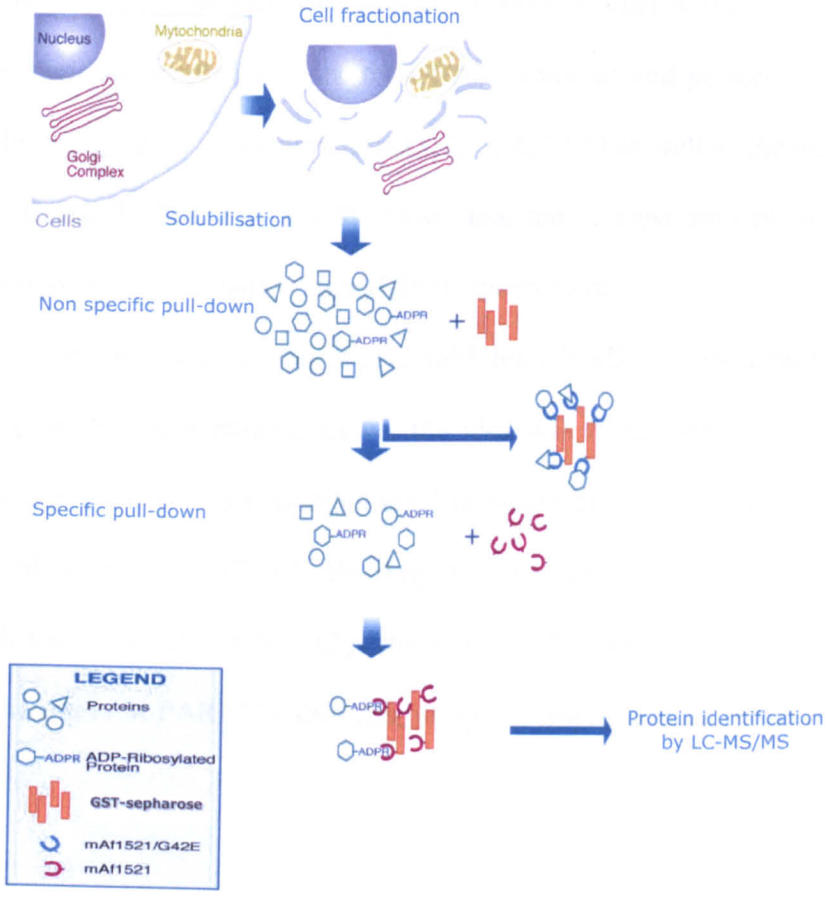

Dani et al., (2009) PNAS 106(11):4243-8

Figure 4.8: Macro-domain-based pull-down assay

Schematic representation of the macro-domain-based pull-down assay, as described by Dani N. *et al.* (2009). Solubilised proteins are incubated with the mutated macro domain (mAf1521/G42E; non-specific pull-down) and then with the wild-type macro domain (mAf1521; specific pull-down). The proteins bound to the wild-type macro domain are eluted and then analysed by LC-MS/MS.

PARP12 antibody, corresponding to the ADP-ribosylated PARP12. The intensity of this band increased with the increase in total NAD^+ concentrations. Based on this result, I kept the total NAD^+ constant and performed the assay while changing the incubation time (1, 2, 5, 8, 12 h) as well as the temperature (25 °C and 37 °C). Figure 4.9b shows that the greatest amount of modified protein was obtained using 8 h and 25 °C incubations.

It is important to note that 2 mM total NAD^+ is not a physiological condition, but as explained above, the idea was to use strong conditions to force the reaction to a maximum level to obtain an extensive modification of the substrates by PARP12. Bearing this in mind, I decided to use these conditions as described here to perform the ADP-ribosylation assay before the identification of PARP12 substrates, using the macro-domain-based pull-down assay.

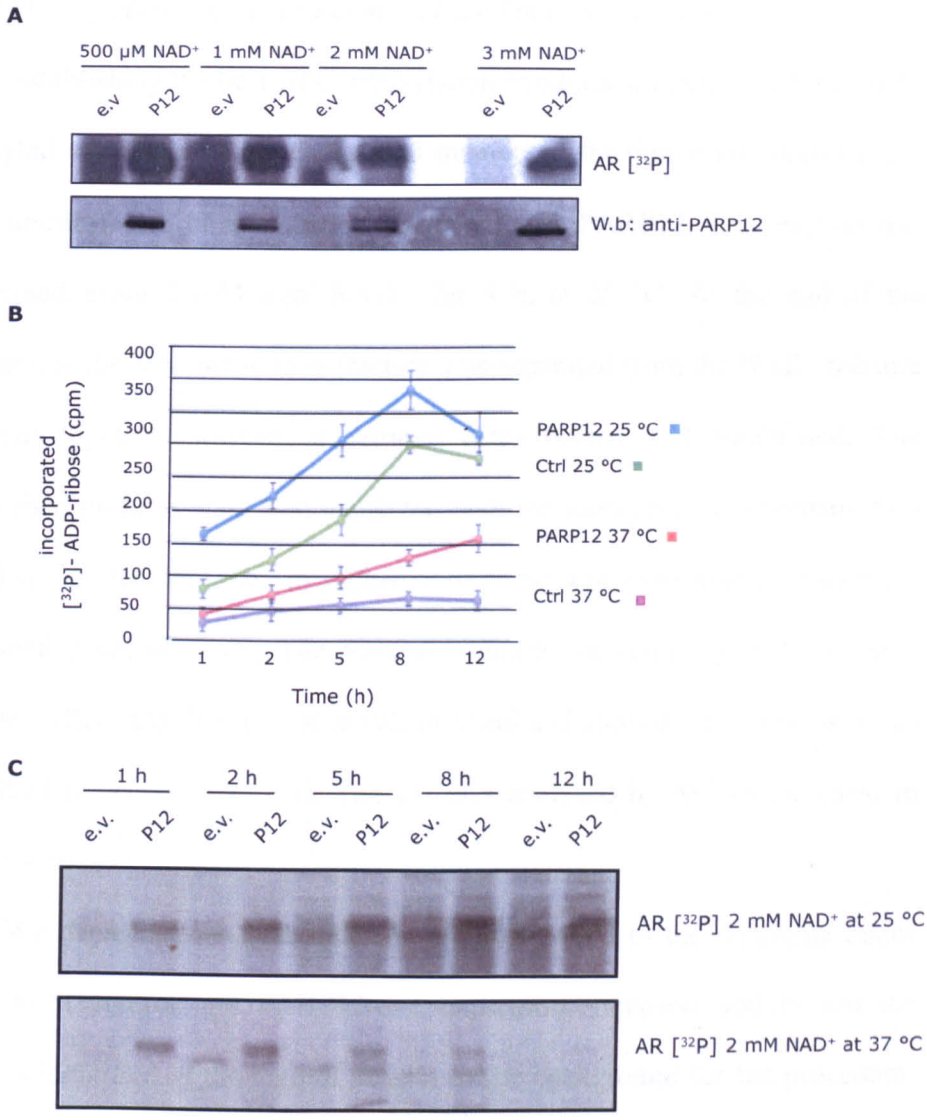

Figure 4.9: Setting-up of the ADP-ribosylation conditions

HeLa cells were transiently transfected with empty vector (e.v.) or with PARP12 (P12) cDNA. (A) Fifty µg total membrane fraction were used to perform the ADP-ribosylation assays, using 4 µCi [^{32}P]-NAD$^+$ and the indicated NAD$^+$ concentrations. The reactions were carried out for 2 h at 37 °C, and stopped by addition of sample buffer. The proteins were analysed by SDS-PAGE and transferred onto nitrocellulose. ADP-ribosylated PARP12 was followed by autoradiography (AR [^{32}P]); total levels of PARP12 were analysed by Western blotting (W.b) using an anti-PARP12 antibody. (B) Thirty µg total membrane fraction were used in the ADP-ribosylation assays, performed using 2 mM total NAD$^+$, labelled with 4 µCi [^{32}P]-NAD$^+$. The reactions were carried out at 25 °C or 37 °C, for the indicated times. The samples were processed as described above. Quantification of the ADP-ribosylated band at 80 kDa (molecular weight of PARP12) was carried out using an Instant Imager and was used to evaluate the trend of the ADP-ribosylation reaction; data are means of two independent experiments. Representative images are shown.

4.4.2 Description of the macro-domain-based pull-down assay

After establishing the best ADP-ribosylation conditions, I performed the ADP-ribosylation reaction using 8 mg total membrane fraction from control HeLa cells untransfected or transiently transfected with PARP12. The reaction was performed using 2 mM total NAD^+, for 8 h, at 25 °C. At the end of the incubation, the total membrane fraction was separated from the NAD^+ mixture by centrifugation, washed to remove extra buffer, and solubilised. The solubilised proteins were first incubated with the mutated macro domain, as a pre-clearing step, and then in sequence with the wild-type macro domain (as described in section 2.15). The proteins bound to the resins were eluted using sample buffer, and then run on acrylamide gel and stained with coomassie (as described in section 2.12.3.4). The gel was analysed by MS as indicated in Figure 4.10.

We decided to analyse only the proteins bound to the wild-type resins (from both control and PARP12-over-expressing samples) and to use the proteins identified in the control sample as the background for the procedure. In this way, we only considered those proteins that were specific for PARP12. Approaching the analysis in this way, we excluded proteins that were certainly ADP-ribosylated, but not by PARP12. Indeed, as internal control, we found glutamate dehydrogenase (GDH), a known substrate that is mono-ADP-ribosylated by SIRT4 (Haigis et al., 2006), or PARP1, a poly-ADP-ribosylated protein. Using this described approach, I found 25 specific putative substrates for PARP12. All of the identified proteins (from both control and PARP12 over-expressing HeLa cells) are reported in Table 4.1.

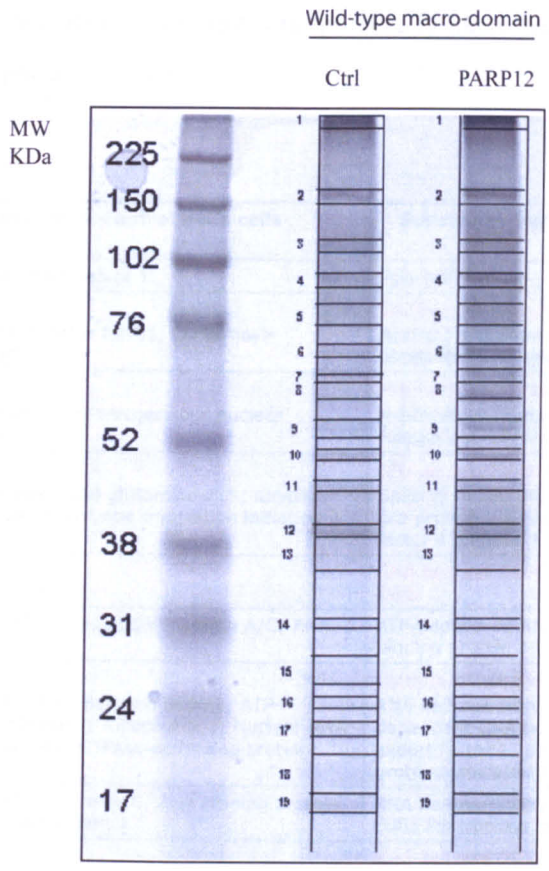

Figure 4.10: Bands analysed by MS for identification of PARP12 substrates

The solubilised proteins from the control (Ctrl) and PARP12 over-expressing HeLa cells (PARP12) were first incubated with the mutated macro-domain, as a pre-clearing step, and then in sequence with the wild-type macro-domain. The proteins bound to the resins were eluted using sample buffer, run on acrylamide gels and stained with Coomassie blue. The proteins eluted from the resin cross-linked with the wild-type macro-domain were analysed by MS, as shown by the grid drawn on the lanes. In detail, the individual protein bands were excised from the gels and subjected to in-gel trypsin digestion and MS analysis. The trypsinisation and MS analysis were performed entirely at the CEINGE Institute by Dr. Maria Monti.

Table 4.1: list of ADP-ribosylated substrates identified using the macro-domain based pull-down assay. The substrates specifically identified in PARP12 over-expressing sample are highlighted in red.

Substrates from control HeLa cells	Substrates from PARP12 overexpressing HeLa cells
Poly [ADP-ribose] polymerase 1	Poly [ADP-ribose] polymerase 1
Scaffold attachment factor B2-B1, Carbamoyl-phosphate synthase	SAFB-like, transcription modulator Scaffold attachment factor B2-B1, Carbamoyl-phosphate synthase
N-acetyltransferase 10; Heterogeneous nuclear ribonucleoprotein U	Matrin-3; Netrin receptor UNC5A N-acetyltransferase 10; Heterogeneous nuclear ribonucleoprotein U
Splicing factor, proline- and glutamine-rich; Kinesin-like protein KIF20A; Eukaryotic translation initiation factor 4 gamma 3	DNA topoisomerase 1 Splicing factor, proline- and glutamine-rich; Kinesin-like protein KIF20A; Eukaryotic translation initiation factor 4 gamma 3
	RNA helicase DDX1; DNA helicase; RNA binding protein EWS
ATP-dependent RNA helicase DDX3; Lamin A/C; RNA binding protein 14	ATP-dependent RNA helicase DDX3; Laminin A-C; RNA binding protein 14
RNA helicase DDX1; RNA helicase DDX3X; ATP-dependent DNA helicase 2; Ribophorin-1; Nuclear RNA export factor 1; p21 Ras GTPase-activating protein associated p62	Calcium-binding mitochondrial carrier protein Aralar2 RNA helicase DDX1; RNA helicase DDX3X; ATP-dependent DNA helicase 2; Ribophorin-1; Nuclear RNA export factor 1; p21 Ras GTPase-activating proteinassociated p62
RNA helicase DDX5; Laminn A/C; RNA binding protein FUS; Paraspeckle component 1	RNA helicase DDX5; Laminn A/C; RNA binding protein FUS; Paraspeckle component 1
ProteinFAM98A	RNA helicase DDX28; Heterogeneous nuclear ribonucleoprotein G ProteinFAM98A
ATP-synthase subunit alpha; glutamate dehydrogenase (GDH)	Dihydrolipoyllysine-residue succinyltransferase; RNA helicase DDX5 ATP-synthase subunit alpha; glutamate dehydrogenase (GDH)
Non-POU domain-containing octamer-BP; Polymerase delta-interacting protein 3; Heterogeneous nuclear ribonucleoprotein G; 60S ribosomal protein L4	Elongation factor 1-alpha1 Non-POU domain-containing octamer-BP; Polymerase delta-interacting protein 3; Heterogeneous nuclear ribonucleoprotein G; 60S ribosomal protein L4
Actin	Actin
hTid1	HLA class I histocompatibility antigen hTid1
Prohibitin-2; Histone H1.2 ; THO complex subunit 4	60S ribosomal protein L5; DNA-3-methyladenine glycosylase (ADPG); Heterogeneous nuclear ribonucleoproteins A2/B1-A1 Prohibitin-2; Histone H1.2 ; THO complex subunit 4
40S ribosomal protein S3;Histone H1.5	40S ribosomal protein S3;Histone H1.5
ADP/ATP translocase; 40S ribosomal protein S4	Signal recognition particle receptor subunit beta; 60S ribosomal protein L7 ADP/ATP translocase; 40S ribosomal protein S4
UPF0568 protein C14orf166; 40S ribosomal protein S8; Rab5A; Probable ribosome biogenesis protein NEP1; 60S ribosomal protein L13-L10a	GTP-binding nuclear protein Ran UPF0568 protein C14orf166; 40S ribosomal protein S8; Rab5A; Probable ribosome biogenesis protein NEP1; 60S ribosomal protein L13-L10a
Rab7A; Rab2A	Rab-14; 60S ribosomal protein L15-L9; Rab1A; Transmembrane protein 33 Rab7A; Rab2A

4.4.3 Study of the substrates identified

The first approach I used to study the substrates identified was to cluster the different proteins into subgroups based on their functions, according to the data available in the literature. This criterion allowed me to divide the substrates identified into five major subgroups, as shown in Figure 4.11. Thirteen of identified proteins are involved in RNA processing, three are DNA-binding proteins, four are members of the GTPase family, two are mitochondrial proteins and three are plasma-membrane receptors. As described in the previous section, the macro-domain module functions as the bait to fish out ADP-ribosylated proteins. It is reasonable to assume that some of the proteins identified would be interactors of ADP-ribosylated substrates rather than substrates of ADP-ribosylation. Considering this, validation experiments need to be undertaken.

One common problem in the proteomic approach is how to sort and validate all of the identified proteins. I decided to use a "hypothesis-driven approach" to start with the validation of the substrates. As a first selection criterion, I decided to choose proteins or protein families known already to be ADP-ribosylated, including by toxins. I reasoned that, indeed, toxins could use mechanisms similar to mammalian endogenous enzymes to regulate protein functions. As a proof of principle, the eukaryotic translation elongation factor-2 is the specific target of ADP-ribosylation by two lethal toxins, DTX and Pseudomonas aeruginosa exotoxin A, and it has also been demonstrated to be an endogenous mono-ADP-ribosylated protein, following interleukin-1β stimulation (Jager et al., 2011). Figure 4.11 shows that small-GTPases are among the possible substrates for PARP12.

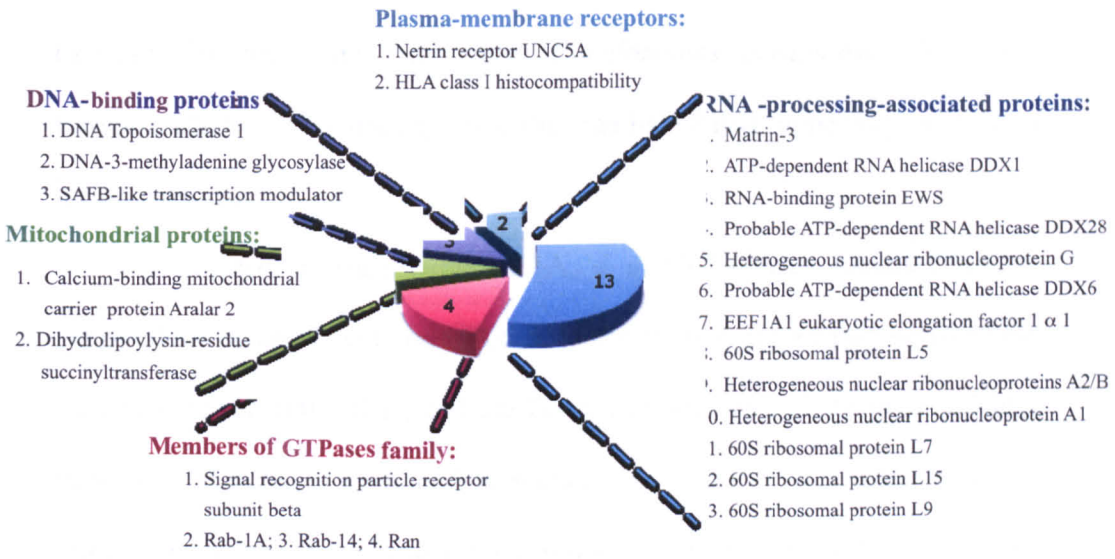

Figure 4.11: Sub-groups of ADP-ribosylated proteins

The substrates identified by MS (as indicated) were clustered into sub-groups based on their functions (as indicated), according to the data available in the literature. Five major sub-groups emerged from this analysis. Each of these is highlighted in a different colour.

Interestingly, as reported in the introduction (paragraph 1.2.2), Barbieri and co-workers showed that Rab5 and Rab4 are substrates of the ADP-ribosylation catalysed by the toxin ExoS from *Pseudomonas aeruginosa* (Deng and Barbieri, 2008a). This finding made the small-GTPases 'appealing' substrates for my analysis.

I decided to start with Rab1A, a small-GTPases localised at the intermediate compartment and involved in the control of transport between the endoplasmic reticulum (ER) and the Golgi complex, as well as in intra-Golgi transport. Of note, as described in section 4.6, PARP12 is a Golgi-localised protein. Together, the considerations reported above prompted me to select Rab1A as the first target of my analysis.

4.5 Rab1A as a PARP12 substrate: validation experiments

4.5.1 PARP12 ADP-ribosylates Rab1A

As described in section 4.4.2, to identify PARP12 substrates, I performed the ADP-ribosylation reaction using 2 mM total NAD^+ for 8 h at 25 °C, conditions that are not physiological. For this reason, I checked if the over-expressed PARP12 can modify Rab1A also in intact HeLa cells. To this end, PARP12 was over-expressed in HeLa cells and, after 18-20 h, cell lysates were used to perform the macro-domain-based pull-down assay. After a pre-clearing step to remove non-specific binding, the lysates from control HeLa cells and PARP12 over-expressing HeLa cells were incubated with the wild-type macro domain. The bound proteins were eluted with sample buffer, fractionated on SDS-PAGE gels and analysed by Western blotting, using antibodies against PARP12 and Rab1A (see section 2.15 for method). Figure 4.12 shows that

PARP12 was specifically recognised by the wild-type macro-domain; this constituted a positive internal control of the procedure. The antibody that recognised Rab1A showed that there was an enrichment in the amount of Rab1A linked to the wild-type resin when PARP12 was over-expressed (compared to control HeLa cells). One can consider the binding of Rab1A to the wild type resin observed in control HeLa cells as the amount of Rab1A modified by endogenous PARP12.

Another way I selected to confirm that PARP12 could ADP-ribosylate Rab1A was the use of biotinylated NAD^+ in *in vitro* ADP-ribosylation assays. The advantage of this tool is that it is possible to make use of the high affinity of the streptavidin resin towards biotin to recover ADP-ribosylated substrates. I performed the ADP-ribosylation reactions using total membrane fractions from control and PARP12 transiently transfected HeLa cells, using an ADP-ribosylation mixture containing biotinylated NAD^+ or, as the control, biotin alone. After the reaction, the membrane fractions were solubilised and incubated with the streptavidin resin. The bound proteins were eluted using sample buffer, separated on SDS-PAGE, and transferred onto nitrocellulose (see methods, paragraph 2.18.2).

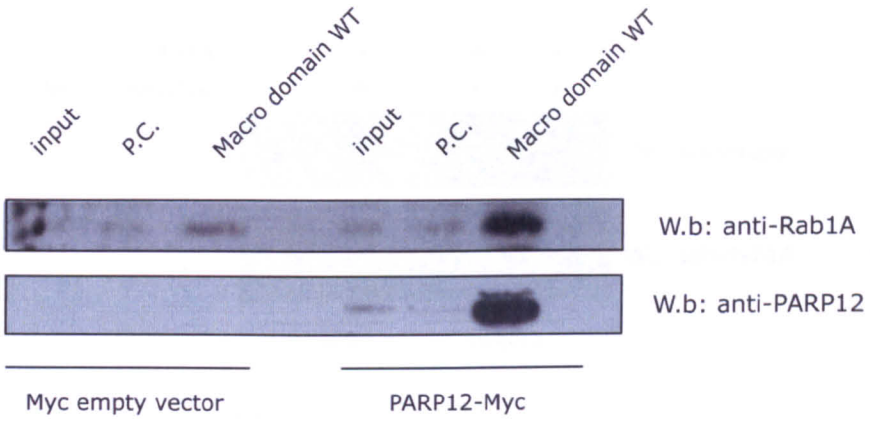

Figure 4.12: Macro domain pull-down assay in intact cells

Total lysates of HeLa cells transfected with empty vector or with Myc-tagged PARP12 were subjected to a preclearing step (P.C.) and then incubated with the wild-type macro domain (as indicated), to pull-down ADP-ribosylated proteins. The proteins were separated by SDS-PAGE and blotted onto nitrocellulose. Western blotting (W.b.) with anti-PARP12 and anti-Rab1A antibodies, as indicated. Inputs were also monitored, as indicated. Note that there was an enrichment in the amount of ADP-ribosylated Rab1A when PARP12 was over-expressed (compare macro domain WT lanes).

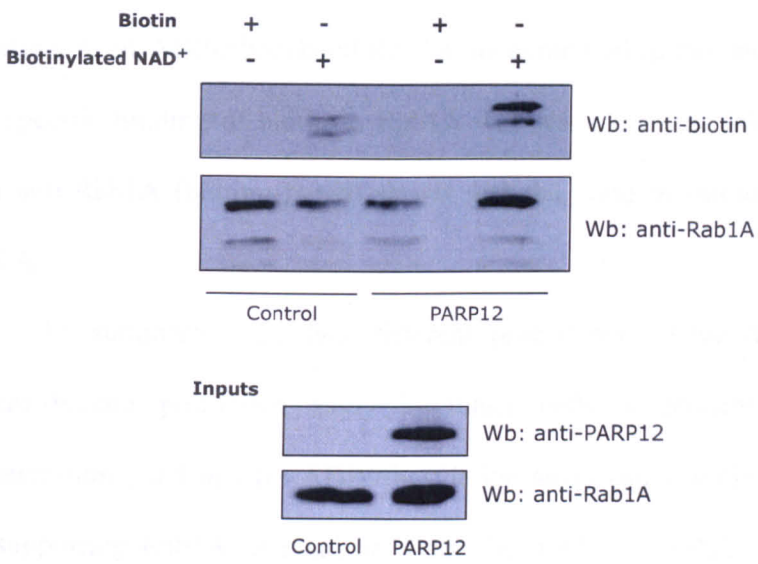

Figure 4.13: ADP-ribosylation reaction using biotinylated NAD^+

HeLa cells were transiently transfected with empty vector (Control) or PARP12 cDNA. Total membrane fractions were used to perform *in vitro* ADP-ribosylation assays, using 50 μM total NAD^+, containing 5 μM biotinylated NAD^+. The reactions were carried out for 2 h at 37 °C. The samples were analysed by SDS-PAGE and transferred onto nitrocellulose. ADP-ribosylated proteins were detected using an anti-biotin antibody. Upper panel (w.b: anti-biotin) indicates ADP-ribosylated Rab1A. Inputs were also analysed using both anti-PARP12 (to monitor the over-expression) and anti-Rab1A antibodies (bottom panels).

Note that there was an enrichment in the amount of ADP-ribosylated Rab1A when PARP12 was over-expressed (upper panel).

The modified proteins were revealed using an anti-biotin antibody. Figure 4.13 (upper panel) shows that the over-expression of PARP12 led to an increase in the amounts of ADP-ribosylated Rab1A, as compared to the control, while no non-specific binding of biotin to Rab1A was observed. The Western blotting with anti-Rab1A (bottom panel) shows that the band of interest was indeed Rab1A.

To summarise, the two different procedures I have described here (macro-domain pull-down assay in intact cells at physiological NAD^+ concentrations, and *in vitro* ADP-ribosylation assay using biotinylated NAD^+) are supporting Rab1A as a substrate for the mART PARP12, validating the data obtained through MS. However, from these experiments, it is not possible to rule-out that Rab1A might be part of a complex and that another protein of this complex is instead the direct target of PARP12. However, as also described in the next section, the strongly denaturing solubilisation conditions I used, should disrupt this putative complex, thus supporting the conclusion that Rab1A is a substrate for PARP12. Other experiments, such as an immunoprecipitation of Rab1A after *in vitro* ADP-ribosylation assays or macro-domain-based pull-down assays in cells in which the expression of PARP12 is abrogated by RNA interference should directly demonstrate that Rab1A is modified by PARP12.

4.5.2 The PARP12-Rab1A interaction

An alternative way I considered to validate Rab1A as a PARP12 substrate was to determine whether these two proteins interact. To address this question, I investigated if the over-expression of a myc-tagged PARP12 would allow the

detection of an interaction with the endogenous Rab1A. Figure 4.14 shows that under the conditions of the experiment, there was no interaction. However, it is important to note that it is not always possible to validate an interaction between two proteins, in particular if we are referring to an enzyme-substrate complex. Indeed, in this case, the interaction is transient, since by definition an enzyme has to release its substrate after the modification. However the interaction can be stabilized using cell lysates from cells that over-express PARP12 mutants and the interaction analysed by performing immune-precipitation experiments. In this case, since the mutants do not have catalytic activity, they should retain the substrates, thus allowing the interaction to be seen. The principle for this approach was proposed by Tonks and colleagues for the identification of protein phosphatase interactors (Flint et al., 1997).

Another aspect to consider is that to solubilise PARP12 strong detergents need to be used (described in section 2.13.3), hence using denaturing conditions that can interfere with the maintenance of the complex. Therefore, when the data described in the previous paragraph is considered, showing that it is not possible to follow the interaction biochemically under these experimental conditions used, support the conclusion that Rab1A is indeed a substrate, and not an interactor, of PARP12.

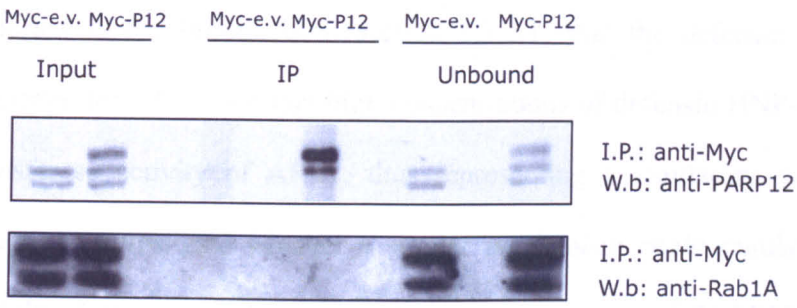

Figure 4.14: Rab1A does not co-immunoprecipitate with PARP12

HeLa cells were transiently transfected with myc empty vector (Myc-e.v.) or myc-tagged PARP12 (Myc-P12) cDNAs. The cells were lysed, and the over-expressed PARP12 was immunoprecipitated using an anti-Myc antibody. The samples were analysed by SDS-PAGE and transferred onto nitrocellulose. Immunoprecipitated PARP12 was analysed using an anti-PARP12 antibody (upper panel). Western blotting (W.b) with an anti-Rab1A antibody is shown in the bottom panel. Inputs and unbound materials were also monitored, as indicated.

Note that there is no interaction between PARP12 and Rab1A under the experimental conditions used.

4.5.3 Rab1A modulates PARP12 activity

As described in the previous section, Rab1A is ADP-ribosylated by PARP12. I reported in the Introduction (section 1.3.2.1) that the defensin HPN-1 is a substrate for ART1 and that high concentrations of defensin HNP-1 inhibit the transferase activity of ART1, thus representing a regulatory mechanism. I sought to investigate whether a similar mechanism could regulate PARP12, and thus I checked if the concomitant over-expression of PARP12 and Rab1A could affect PARP12 enzymatic activity.

To address this point, I transfected HeLa cells with cDNAs coding for GFP, PARP12, or GFP-tagged Rab1A, or co-transfected them with GFP/PARP12 and GFP-Rab1A/PARP12. The total membrane fractions from the transfected cells were used to perform *in vitro* ADP-ribosylation assays (method described in section 2.18). As shown in Figure 4.15, the concomitant over-expression of GFP-tagged Rab1A and PARP12 abrogated the ADP-ribosylation activity of PARP12, while the incubation of GFP-tagged Rab1A over-expressing total membranes together with PARP12-over-expressing total membranes did not give the same result. These data suggest that PARP12 and Rab1A should be in contact in some way or that the presence of cofactors is needed to provide an effect. For these reasons, it is possible that the simple incubation of membranes does not allow a correct environment to achieve an effect on PARP12 enzymatic activity.

I would like to point out that the results I have described here show that PARP12 catalytic activity can be modulated by Rab1A. This new finding represents the first example of regulation (in this specific case, of inhibition) of a member of the new mART family by another protein. It might be possible

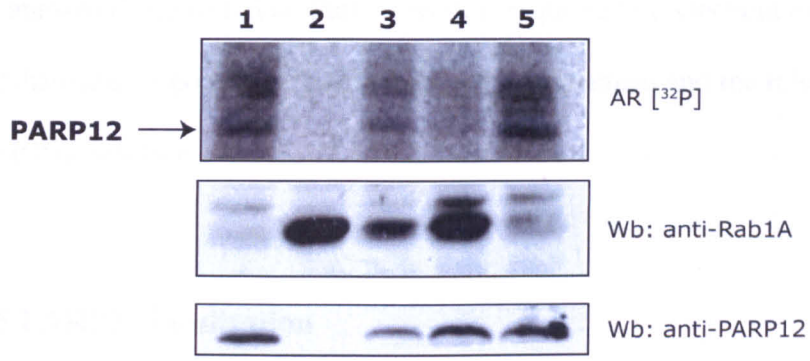

Figure 4.15: Rab1A regulates PARP12 ADP-ribosylation activity

HeLa cells were transiently transfected with cDNAs coding for GFP, PARP12, or GFP-tagged Rab1A, and co-transfected with GFP/PARP12 and GFP-Rab1A/PARP12. The total membrane fractions (TM) from the transfected cells were used to perform *in vitro* ADP-ribosylation assays. Samples were analysed by SDS-PAGE and transferred onto nitrocellulose. The ADP-ribosylated proteins were analysed by autoradiography (AR [^{32}P]). Arrow, ADP-ribosylated PARP12. PARP12 and GFP-Rab1A levels were analysed using PARP12 and Rab1A antibodies. Lane 1, TM over-expressing PARP12; lane 2, TM over-expressing GFP-Rab1A; lane 3, TM over-expressing PARP12 incubated with TM over-expressing GFP-Rab1A; lane 4, TM co-over-expressing PARP12 and GFP-Rab1A; lane 5, TM co-over-expressing PARP12 and GFP.
Note that PARP12 catalytic activity is strongly reduced by Rab1A over-expression.

that Rab1A interacts with PARP12 at the auto-modification site, thus impairing its auto-ADP-ribosylation. Further work is required to dissect out the molecular mechanisms responsible for this regulatory mechanism and the role in terms of PARP12 function.

4.6 PARP12 localisation

4.6.1 Endogenous PARP12 is localised to the Golgi complex

Sub-cellular localisation determines the environments in which proteins operate. As such, the sub-cellular localisation influences protein functions by controlling access to and availability of all types of molecular interaction partners and possibly metabolites. Accordingly, knowledge of protein localisation often has a significant role in characterising the cellular function of hypothetical and newly discovered proteins.

To understand the role of PARP12, as well as the identification of its substrates, I analysed its subcellular localisation. The cell system I used is HeLa cells, a well characterised cell model, and I investigated the localisation of endogenous PARP12 in these HeLa cells by immunofluorescence. The staining given by the PARP12 specific antibody clearly indicated that PARP12 is localised to the Golgi complex, and to some extent in the nucleus (Figure 4.16a). Here, I used a generic Golgi marker (giantin) for Golgi localisation. The staining of the antibody was specific, as confirmed by the lack of labelling after abrogation of PARP12 expression using RNA interference (Figure 4.16b).

Interestingly, the Golgi localisation seen by immunofluorescence was not as predicted, since any transmembrane domain or specific sequences of

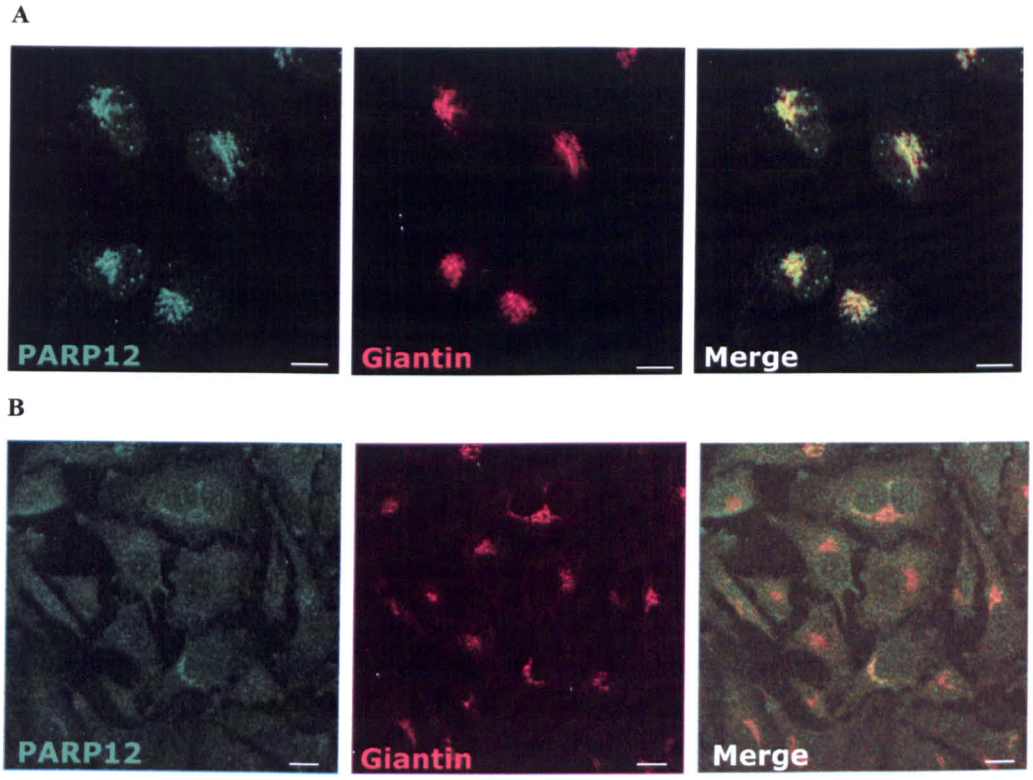

Figure 4.16: PARP12 localises to the Golgi complex

(A) Representative confocal images of non-transfected HeLa cells labelled with an anti-PARP12 antibody (green, for endogenous PARP12) and with a monoclonal anti-giantin antibody (red, Golgi marker). (B) Endogenous PARP12 expression was abrogated using a specific siRNA. The cells were labelled as above. The absence of PARP12 labelling indicates that the staining of the antibody is specific. Scale bar 10 μM.

PTMs that target proteins to membranes (such as prenylation) would be revealed by bioinformatic analysis. One possible explanation of this observation is that the presence of PARP12 on the Golgi complex is dependent on an interaction with a specific partner. Thus far, I did not evaluate this possibility, but it would be of great interest as a future extension of this study, also considering recent data that demonstrate that PARP5 (the other PARP localised at the Golgi complex) interacts with PARP12 (Leung et al., 2011).

4.6.2 PARP12 localisation during cell-cycle progression

In the previous section, I reported that PARP12 is a Golgi-localised protein and that it is also present to some extent in the nucleus. It is well known that during mitosis the Golgi ribbon undergoes extensive fragmentation through a multistage process that promotes its correct partitioning and inheritance by daughter cells (Sutterlin et al., 2002). Based on these observations, I wondered if the two different PARP12 localisations (nucleus/Golgi) might change during cell-cycle progression.

In general, I performed the immunofluorescence experiments on non-synchronised HeLa cells, and so across different phases of the cell cycle. To obtain a more homogeneous population to analyse, I performed the immunofluorescence experiments on synchronised cells (for methods, see paragraph 2.9). To achieve this, I took advantage of the use of a specific inhibitor of Cdk1 (RO-3306) that results in the accumulation of cells in the G_2 phase (Vassilev et al., 2006). This inhibition is reversible, so after inhibitor washout, cells can re-enter the cell cycle in a synchronous manner, and they reach the mitotic peak within 1 h (M phase). In addition, to accumulate cells in

the G_0 phase, the cells were starved for 24 h. To detect the different stages of the cell cycle, I used an antibody that recognises phosphorylated serine 10 of histone H3. This histone is phosphorylated by the kinase Aurora-B, a crucial event for chromosome condensation. During chromosome assembly, global phosphorylation of histone H3 occurs in a step-wise and ordered manner. In mammalian cells in G_2 phase, phosphorylation is first detected in pericentromeric heterochromatin, and as mitosis proceeds, it spreads throughout the whole of the chromosomes. This global phosphorylation of histone H3 is completed in late prophase and maintained through metaphase. Dephosphorylation of histone H3 begins in anaphase and ends at early telophase (Hans and Dimitrov, 2001), and thus it is not seen in G_1/S and quiescent cells.

Figure 4.17 shows that in cells in G_0 (no staining of phosphorylated histone H3) PARP12 was exclusively localised on the Golgi complex, without any nuclear staining. In contrast, PARP12 localisation in the nucleus varied according to cell-cycle progression. Indeed, PARP12 showed a nuclear and perinuclear staining in G_2 cells (characterised by discrete dots of phosphorylated histone H3), while it was dispersed throughout the cytosol when cells were in M-phase (when phosphorylated H3 co-localises with condensed chromosomes). I did not evaluate this observation further, but it would be interesting to further study it since one of the substrates identified for PARP12 is the small GTPase Ran, a protein that is involved in nuclear-to-cytoplasm transport and in the control of the cell cycle (Clarke and Zhang, 2008).

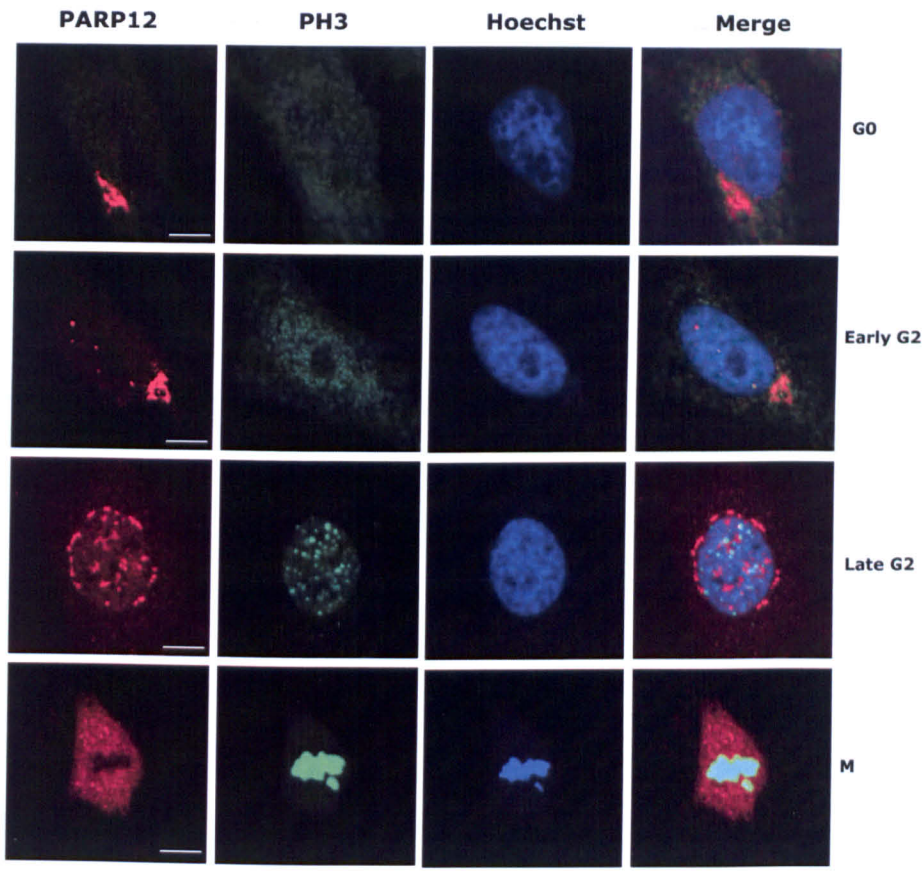

Figure 4.17: PARP12 localisation changes during cell-cycle progression

HeLa cells were synchronised in different phases of the cell cycle, fixed and labelled with the DNA-specific dye Hoechst and with an anti-phospho-histone-H3 antibody (PH3), to identify the different cell-cycle phases. An anti-PARP12 antibody was used to follow PARP12 localisation during the different phases. Representative images are shown. Scale bar 10 μM. Note that PARP12 localisation is exclusively on the Golgi complex in quiescent cells, while it starts having a nuclear localisation as cells enter the cell cycle.

4.6.3 Localisation of over-expressed PARP12

Different from the endogenous protein, over-expressed PARP12 shows a complex localisation. In particular, the protein was present as foci in the cytoplasm (Figure 4.18). Of note, I observed that PARP12 over-expression was associated with a loss of the classical Golgi-ribbon-like organisation, with the Golgi appearing fragmented. Under these conditions, PARP12 did not co-localise with the Golgi markers (Figure 4.18).

Thus, these experiments suggest that PARP12 is involved in the maintenance of the structure of the Golgi complex. Interestingly, a role for Rab1A in the control of the structure of this organelle has already been reported (Haas et al., 2007; Wilson et al., 1994), and thus it is possible to hypothesise that ADP-ribosylation of Rab1A catalysed by the over-expressed PARP12 can alter the Rab1A functions, and can lead to this fragmented phenotype. Based on these assumptions, the abrogation of Rab1A expression should have the same effects, on both the structure of the Golgi complex and on PARP12 localisation. For this reason, I decided to further investigate this aspect, by evaluating the consequences of the modulation of Rab1A expression on PARP12 localisation.

4.6.4 PARP12 localisation is affected by modulation of Rab1A expression

To determine whether the modulation of Rab1A expression affects PARP12 localisation, I first silenced Rab1A in HeLa cells and then analysed the localisation of the endogenous PARP12. As shown in Figure 4.19, Rab1A silencing strongly affected PARP12 localisation, which appeared to be displaced from the Golgi complex, which itself appeared to be fragmented. The

A

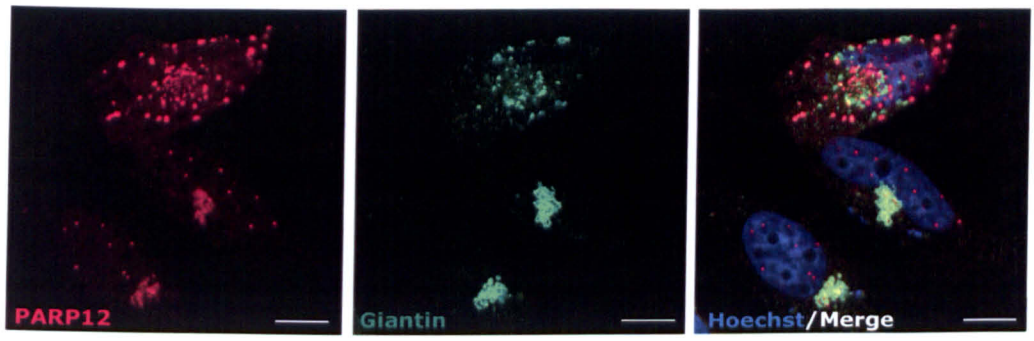

B

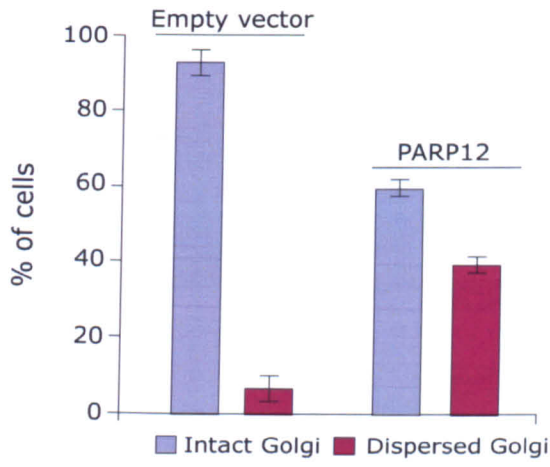

Figure 4.18: PARP12 over-expression results in fragmentation of the Golgi complex
(A) Representative confocal image of HeLa cells transiently transfected with myc-tagged PARP12, labelled with an anti-PARP12 antibody (red) and giantin antibody (green), to monitor Golgi morphology. Scale bar 10 μM. (B) The graph shows the quantification of the cells showing a fragmented Golgi, as data from three independent experiments. Note that the cells with fragmented Golgi increased by 30% when PARP12 was over-expressed.

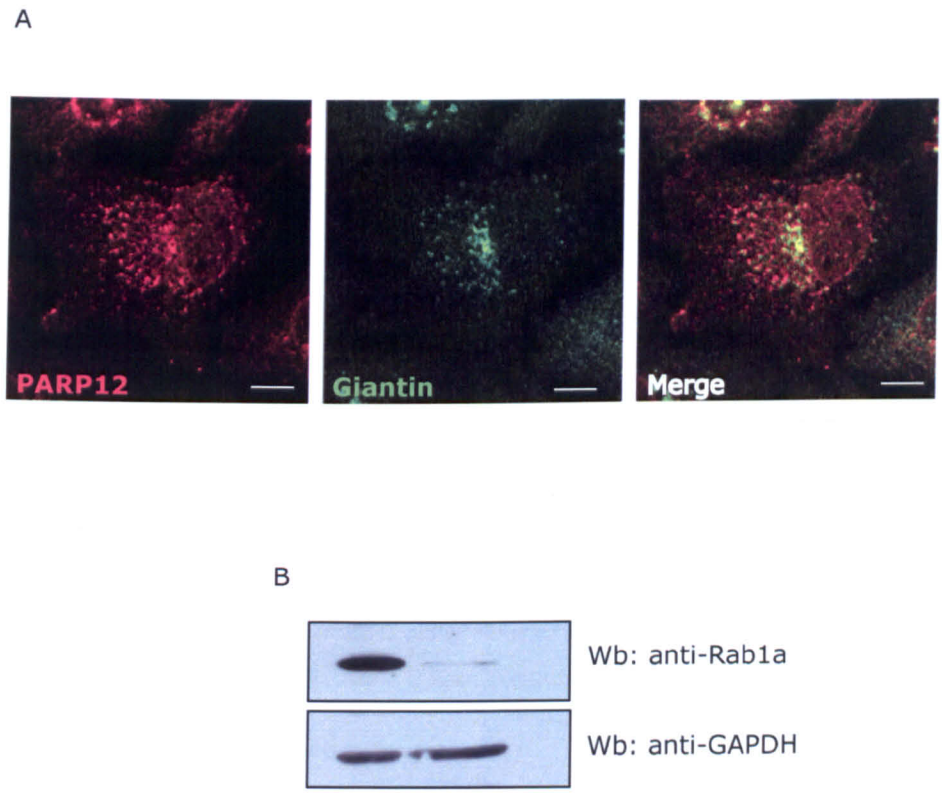

Figure 4.19: PARP12 localisation is affected when Rab1A expression is abrogated

(A) Rab1A expression in HeLa cells was abolished by using a specific siRNA. The cells were then fixed and stained with an anti-PARP12 antibody (red, endogenous PARP12) and with an anti-giantin antibody (green, Golgi marker). Representative images are shown. Scale bar 10 μM. (B) The levels of Rab1A interference were monitored by Western blotting (W.b) using an anti-Rab1A antibody, and normalised according to the GAPDH levels.

Note that in the absence of Rab1A, PARP12 is displaced from the Golgi complex, which itself appears to be fragmented.

over-expression of Rab1A, instead, did not have any effects on endogenous PARP12 localisation, which still localised to the Golgi complex (Figure 4.20).

The displacement of endogenous PARP12 from the Golgi complex after abrogation of Rab1A expression led me to suppose that Rab1A is important for PARP12 localisation, thus explaining the mis-localisation from the Golgi complex of over-expressed PARP12. For this reason, I checked if the concomitant over-expression of Rab1A-GFP and PARP12 restored the Golgi localisation of over-expressed PARP12. Figure 4.21 shows that Rab1A over-expression is not sufficient to restore the Golgi localisation of over-expressed PARP12. This suggests that other proteins are involved in ensuring the localisation of PARP12 to the Golgi complex, or that protein overexpression interferes with the localisation process.

Taken together, these data are in agreement with previous work showing that Rab1A is implicated in the maintenance of the Golgi morphology (Haas et al., 2007; Wilson et al., 1994); (Venditti Rossella, personal communication) and suggest that PARP12 localisation on the Golgi complex may be dependent on the existence of a protein complex. In this regard, recently Chang and co-workers demonstrate that PARP12 interacts with PARP5 (Leung et al., 2011), the other PARP localised at the Golgi complex. Thus, one can speculate that the Golgi localisation of PARP12 is relying on a protein complex; when the equilibrium of this complex is altered (by PARP12 over-expression), PARP12 does not localise on the Golgi complex. Interestingly, as described in the next section, a role for ADP-ribosylation seems to be required for the correct Golgi localisation of PARP12, thus suggesting that PARP5 could indeed play a role in this.

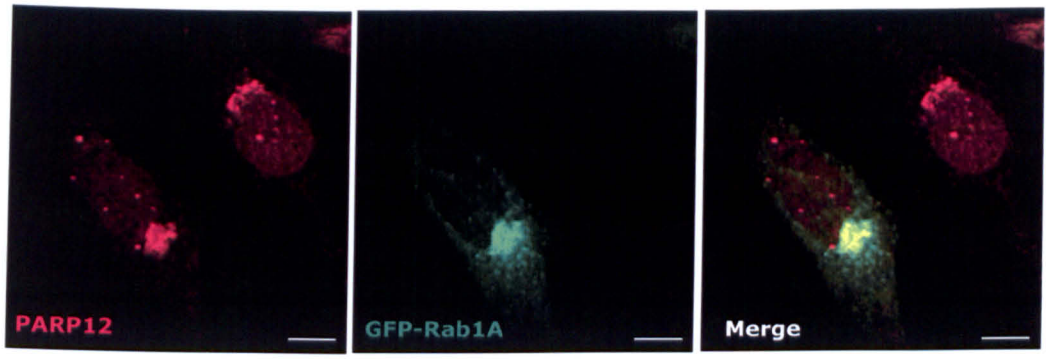

Figure 4.20: Rab1a over-expression does not affect endogenous PARP12 localisation
Representative images of HeLa cells transiently transfected with GFP-tagged Rab1A and stained with an anti-PARP12 antibody (red, endogenous PARP12). Scale bar 10 μM. Note that Rab1A over-expression does not affect the endogenous PARP12 localisation.

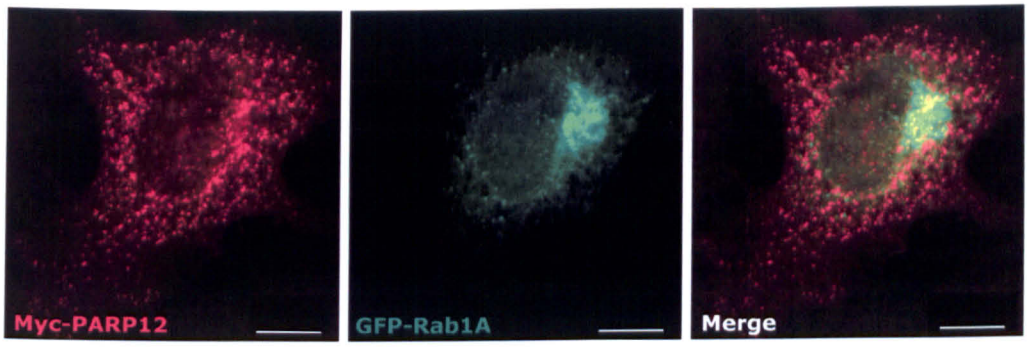

Figure 4.21: Concomitant over-expression of Rab1A and PARP12

Representative images of HeLa cells co-transfected with GFP-tagged Rab1A and myc-tagged PARP12, stained with an anti-myc antibody. Note that the concomitant overexpression of Rab1A does not restore the Golgi localisation of over-expressed PARP12 (see text for details). Scale bar 10 μM.

1.7 PARP12 has a role in the re-formation of the Golgi structure after BFA wash-out

It is well known that BFA causes a rapid dispersal of Golgi membranes and a redistribution of Golgi-resident enzymes to isolated vesicles and to the ER. This process is completely reversible, and the Golgi reassembles within 1 h of addition of BFA-free medium (Lippincott-Schwartz et al., 1989). Considering that PARP12 might have a role in the maintenance of the Golgi morphology, I investigated whether PARP12 might also have a role in the reassembly of the Golgi structure after BFA was washed out. To this end, I evaluated the re-formation of the Golgi structure in cells in which the expression of PARP12 was abolished using a specific PARP12-directed siRNA, compared to cells transfected with a non-targeting siRNA. The complete disassembly of the Golgi structure was achieved by treating the cells with 2.5 μg/ml BFA for 30 min at 37 °C, and its re-formation was achieved by the removal of the BFA, followed by incubation of complete BFA-free medium (Fujiwara et al., 1988; Lippincott-Schwartz et al., 1989). Figure 4.22 clearly demonstrates that while recovery of the Golgi structure was complete in control cells, the cells lacking PARP12 showed a defect in the re-formation of the Golgi 'ribbon'. To understand if this effect is connected to the enzymatic activity of PARP12 and not to a structural role of the protein *per se*, I analysed the Golgi reassembly in the presence of PJ34, a known inhibitor of ADP-ribosylation. PJ34 is best known as a PARP1 inhibitor, but, as reported in section 4.2.2, at micromolar concentrations it also inhibits PARP12 activity (IC_{50} for PARP1, 0.04 μM; IC_{50} for PARP12, 5 μM).

A

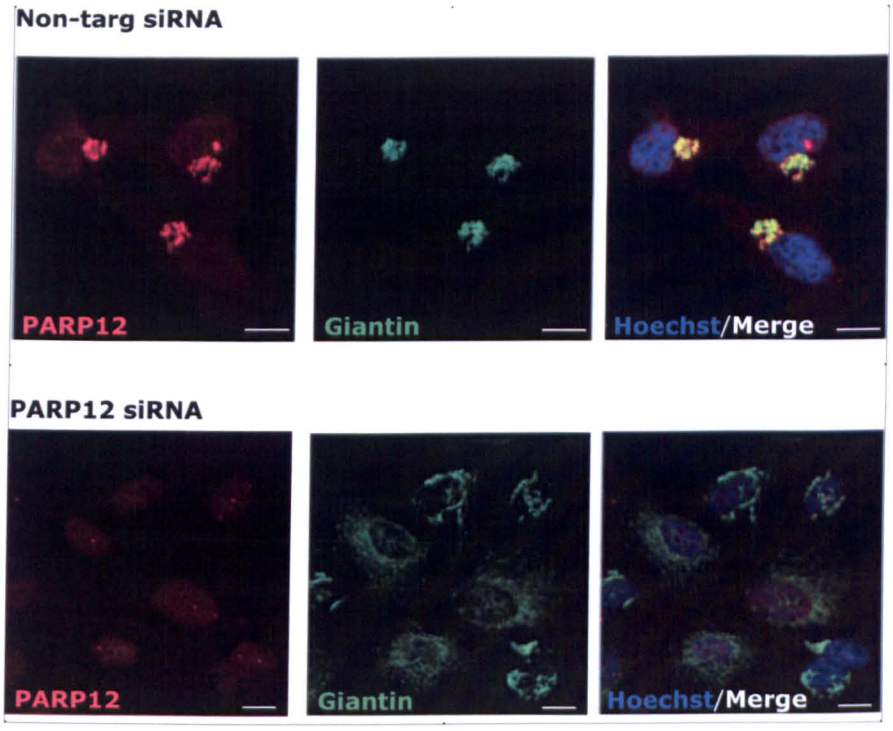

B

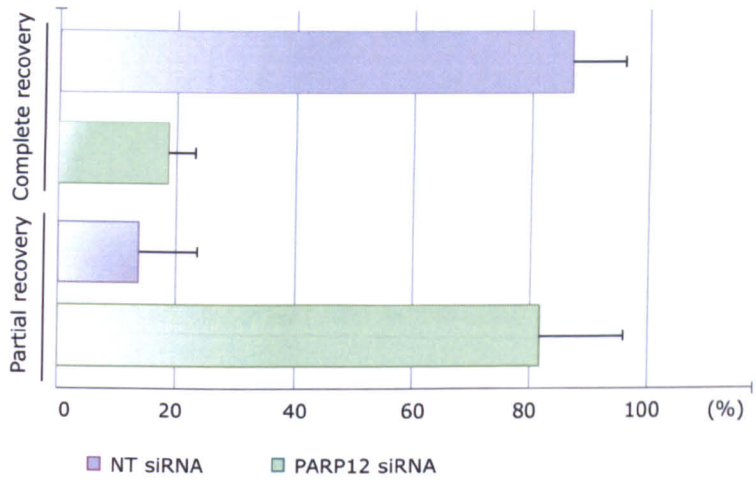

Figure 4.22: Abrogation of PARP12 expression by RNA interference affects the re-formation of the Golgi complex upon BFA wash-out

HeLa cells were transfected with a non-targeting or an anti-PARP12 siRNA. After 72 h, the cells were treated with 2.5 μg/ml BFA for 30 min at 37 °C and then incubated for 90 min at 37 °C in complete BFA-free media to allow re-formation of the Golgi complex. The cells were then fixed and labelled with the DNA-specific dye Hoechst, an anti-PARP12 antibody (to check for the interference), and with an anti-giantin antibody (to monitor for Golgi complex reassembly). Scale bar 10 μM. (A) Representative images are shown. (B) The graph indicates the percentage of cells showing a partial or complete recovery of the Golgi complex structure after BFA wash-out. The data are means ± standard deviations, from two different experiments.

Based on these data, after the complete disassembly of the Golgi complex with BFA, I allowed the reformation of the Golgi structure in BFA-free medium in presence of 1 μM PJ34 (a concentration that inhibits PARP1) and 100 μM PJ34. While the PARP1-inhibitory concentration of PJ34 did not affect the re-formation of the Golgi complex (Figure 4.23a), the higher concentration caused a defect in the recovery of the Golgi structure (Figure 4.23b), as observed in cells silenced for PARP12. As a control, the incubation of cells with only 100 μM PJ34 did not affect Golgi morphology (Figure 4.23c). Surprisingly, inhibition of ADP-ribosylation by PJ34 treatment causes an alteration in endogenous PARP12 localisation, and the apperance in cytoplasmic structures.

Together, these data thus suggest a role for PARP12 catalysed ADP-ribosylation in the control of Golgi complex reassembly. However, it is not possible to exclude other effects of the inhibitor PJ34 on other PARPs, such as PARP5, at this stage. In this context, the development of a specific PARP12 inhibitor would be of great value.

In addition, an important and unexpected finding that emerges from these data is the requirement of ADP-ribosylation to maintain PARP12 localisation on the Golgi complex. This finding could support the recent data by Chang and co-workers, demonstrating that PARP12 is part of a complex formed by PARP5, PARP13 and PARP15. Thus the idea is that this complex, and possibly ADP-ribosylation, is required for PARP12 localisation (as also mentioned in the previous section).

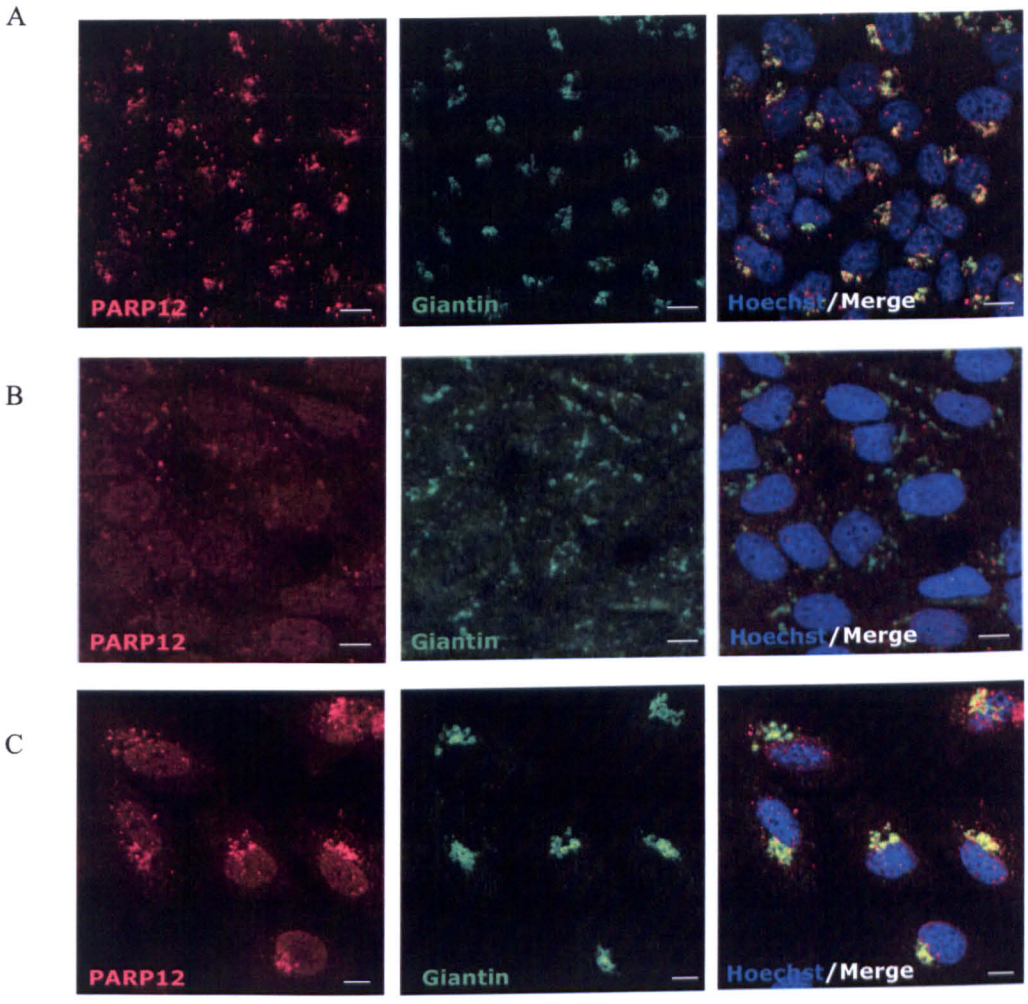
A
PARP12
Giantin
Hoechst/Merge
B
PARP12
Giantin
Hoechst/Merge
C
PARP12
Giantin
Hoechst/Merge

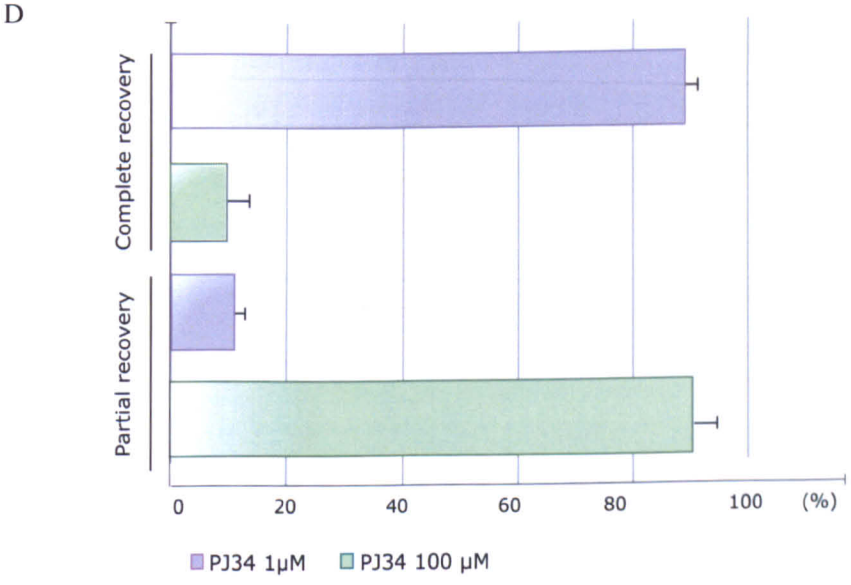
D
Complete recovery
Partial recovery
0
20
40
60
80
100
(%)
PJ34 1μM
PJ34 100 μM

Figure 4.23: Golgi structure re-formation after BFA wash-out is affected when ADP-ribosylation is inhibited by PJ34

HeLa cells were treated with 2.5 μg/ml BFA for 30 min at 37 °C and then incubated for 90 min at 37 °C in complete BFA-free media in the presence of 1 μM (A) or 100 μM PJ34 (B), to allow Golgi complex re-formation. As the control, cells not treated with BFA were incubated with 100 μM PJ34 for 90 min (C). The cells were then fixed and labelled with the DNA-specific dye Hoechst, with an anti-PARP12 antibody and with an anti-giantin antibody (to monitor for Golgi complex re-assembly). (D) The graph indicates the percentage of cells showing a partial or complete recovery of the Golgi complex structure after BFA wash-out. The data are means ± standard deviations, from two different experiments. Scale bar 10 μM.

Note that the presence of 100 μM PJ34 alters Golgi complex re-formation (B), while the re-formation process is normal at lower concentrations of PJ34 (1 μM) (A).

4.8 Discussion II

In this Results chapter, I have provided evidence that PARP12 is a Golgi-localised mART and that it can modify Rab1A. Rab1A was identified using the macro-domain-based pull-down assay, and then validated through other approaches. This method also allows me to identify 24 other new putative PARP12 substrates that still need to be validated. Among these, one of particular interest is the small GTPase Ran. Here I have also provided evidence that PARP12 localisation can vary according to the cell cycle, and as Ran has a well-known role in regulation of the cell cycle (Clarke and Zhang, 2008) this observation is particulary intrigueing.

The choice of Rab1A as the first target to analyse was based on a "hypothesis driven approach": Rabs are indeed known substrates of ADP-ribosylation by toxins (Deng and Barbieri, 2008a), and thus I reasoned that similar mechanisms might be used by mammalian cells to regulate their functions. Moreover, this idea was further supported by the subcellular localisation of these two proteins, both of which were present on the Golgi complex, where Rab1A controls ER-to-Golgi and intra-Golgi transport. Through the different experiments I have reported here, I found that as also demonstrated for Rab1A, PARP12 appears to be important in guaranteeing the correct structure of the Golgi complex. This conclusion arises from the following observations:

1. PARP12 over-expression causes Golgi disassembly (Figure 4.18b);
2. Abolishing Rab1A expression causes Golgi disassembly (Figure 4.19);

3. Over-expressed PARP12 is not localised to the Golgi complex (Figure 4.18a);

4. Endogenous PARP12 is not localised to the Golgi after abolishing Rab1A expression (Figure 4.19).

A possible explanation for this effect is that ADP-ribosylation impairs Rab1A functions, thus leading to Golgi fragmentation. On the other hand, the mis-localisation of PARP12 after its over-expression can be explained by the need of a protein-complex (maybe containing PARP5, the other Golgi-localised PARP, and Rab1A) that should recruit PARP12; when PARP12 is over-expressed, the endogenous levels of proteins forming the complex are not enough to recruit all the over-expressed PARP12, that thus displaces from the Golgi complex. Similarly, abrogation of Rab1A expression causes a displacement of endogenous PARP12 from the Golgi complex. Moreover, the finding that ADP-ribosylation inhibition by PJ34 treatment affects endogenous PARP12 localisation indicates that ADP-ribosylation events are required to tether PARP12 to the Golgi complex.

I also reported here that abolishment of PARP12 expression, as well as inhibition of ADP-ribosylation, are connected to a defect in Golgi complex re-formation after BFA has been washed out. This supports the idea that PARP12 catalysed ADP-ribosylation is required for the Golgi complex re-formation process.

My findings pinpoint to further research to understand these new aspects of the Golgi morphology that appear to be regulated by mono-ADP-ribosylation.

CHAPTER 5: final discussion

Although the mono-ADP-ribosylation has been known for some time mainly as the mechanism of action of some bacterial toxins, this post-translational modification (PTM) is now emerging as an important mechanism also used by mammalian cells to control a vast array of cellular processes (Hottiger et al., 2011). Here I have provided new evidence of how this PTM can be used to regulate protein function, by describing the new ADP-ribosylation mechanism of BFA-dependent ADP-ribosylation of CtBP1/BARS, and the new intracellular function of mono-ADP-ribosylation that is catalysed by the mono-ART PARP12.

5.1 BFA-dependent ADP-ribosylation of CtBP1/BARS regulates its functions

CtBP1/BARS is a dual-function protein that is involved in two widely diverse biological processes, namely intracellular membrane trafficking and gene transcription. After its discovery as a BFA target, CtBP1/BARS was demonstrated to be an essential component of the machinery controlling Golgi tubule fission (De Matteis et al., 1994; Spano et al., 1999; Weigert et al., 1999).

Membrane fission is an essential event for the cell. Indeed, it is used in intracellular membrane trafficking for the transport of proteins and lipids from donor to acceptor membranes. Following the initial generation of membranous carriers through a process of membrane budding and fission, they are

transported to their acceptor membranes, with which they undergo fusion (Wilson et al., 2010). Membrane fission also has an important role during cell division, when the Golgi complex undergoes extensive fragmentation. This process is thought to facilitate the equal partitioning of Golgi membranes between the two daughter cells (Sutterlin et al., 2002). By promoting Golgi tubule fission, CtBP1/BARS is an essential component of both these aspects, and is indeed involved in the control of intracellular transport (Bonazzi et al., 2005) (Valente C. *et al.*, submitted) as well as mitotic fragmentation of the Golgi complex (Colanzi et al., 2007; Hidalgo Carcedo et al., 2004).

In addition to these important roles, CtBP1/BARS has been shown to be a member of the CtBP family, as it has very high amino acid sequence identity with mammalian CtBP1 and CtBP2, and it is indeed a splice variant of CtBP1 (Spano et al., 1999).

CtBP1 and CtBP2 are transcriptional corepressors that repress gene expression by interacting with DNA-binding transcription factors and recruiting histone methyltransferases, histone deacetylases, polycomb group proteins, and other chromatin remodeling proteins to targeted promoters (Chinnadurai, 2007). The targets of repression of CtBP include epithelial and proapoptotic genes, which is consistent with its known roles in promoting cell survival and migration (Chinnadurai, 2009).

CtBP1/BARS can control these two entirely different cellular functions through a change in its intracellular localisation (cytoplasmic/nuclear), an event that is mediated through the binding to different proteins as well as through different PTMs. A further level of regulation is the CtBP1/BARS binding with cofactors, namely NAD(H), and acyl-CoAs. Here, NAD(H) stabilises the

dimeric conformation of CtBPs, and thus the co-repressor function, and acyl-CoAs promote the monomeric conformation, and thus the fissioning role (Corda et al., 2006).

The description of this new BFA-dependent ADP-ribosylation reaction adds a further level of regulation to this dual functional protein, thus contributing to the unravelling of the main mechanisms by which the CtBP functions can be interchanged. Previous findings from our laboratory showed that BFA-dependent ADP-ribosylation could inhibit CtBP1/BARS fissiogenic activity, but the mechanism was unknown (Weigert et al., 1999).

The data described in Chapter 3 demonstrated that this mechanism involves ADP-ribosyl cyclases, such as CD38, for the formation of an ADP-ribosylated adduct, BAC (figures 3.3, 3.4), which covalently binds to the CtBP1/BARS Rossman fold (similarly to NAD(H)/AcylCoA) (Colanzi *et al.*, manuscript in preparation). Importantly, BAC binding inhibits the CtBP1/BARS interactions with its protein partners that are involved in the membrane fissioning functions, such as 14-3-3γ and PAK1 (Figure 3.9). In addition, BAC binding to CtBP1/BARS can shift CtBP1/BARS conformation from monomer to dimer/tetramer (Colanzi *et al.*, in preparation), thus favouring the conformation required for its co-repressor activity, while inhibiting its fissiogenic function.

In the nucleus, the CtBP dimers regulate the formation of protein complexes that are involved in the inhibition of transcription, by binding to the Pro-X-Asp-Leu-Ser (PXDLS) motifs in DNA-binding proteins and by regulating the expression of epithelial genes, such as keratin-8 and E-cadherin, and apoptosis genes such as Bik, Noxa, Puma and PERP. Additionally, the

CtBPs target multiple growth inhibitory tumour suppressors for repression, including PTEN, p16INK4a and p15INK4b, thus promoting cell survival (Chinnadurai, 2009). Indeed, data obtained from mouse embryo fibroblasts (MEFs) derived from CtBP1- and CtBP2-knock-out mice show that these cells have up-regulated epithelial and pro-apoptotic genes (Grooteclaes et al., 2003).

My data demonstrate that the co-repressor activity of CtBP1/BARS can be regulated – and in this specific case increased - in a promoter-dependent context. Indeed, among the genes analysed (*BAX, NOXA, P21, E-cadherin* and *BCL6*), I found that BAC binding to CtBP1/BARS modulates CtBP1/BARS co-repression function at the E-cadherin and p21 promoters (Figures 3.10, 3.11). It is possible that this event (BAC binding) could enhance the CtBP1/BARS interactions with specific repressors, or affect its interactions with other chromatin-regulating enzymes (such as the HDACs). Even if the molecular mechanism associated to its increased co-repressor activity has not been addressed in the present study and further work is required to elucidate this point, from the results obtained during my project, a new mechanism for the regulation of CtBP co-repressor activity emerged: BAC binding to CtBP1/BARS stabilises a dimeric/tetrameric conformation of CtBPs, that cannot function in fissioning processes (because of a lack of binding with its fissioning partners), while it enhances the co-repressor function of CtBP1/BARS. Figure 5.1 shows the proposed working model.

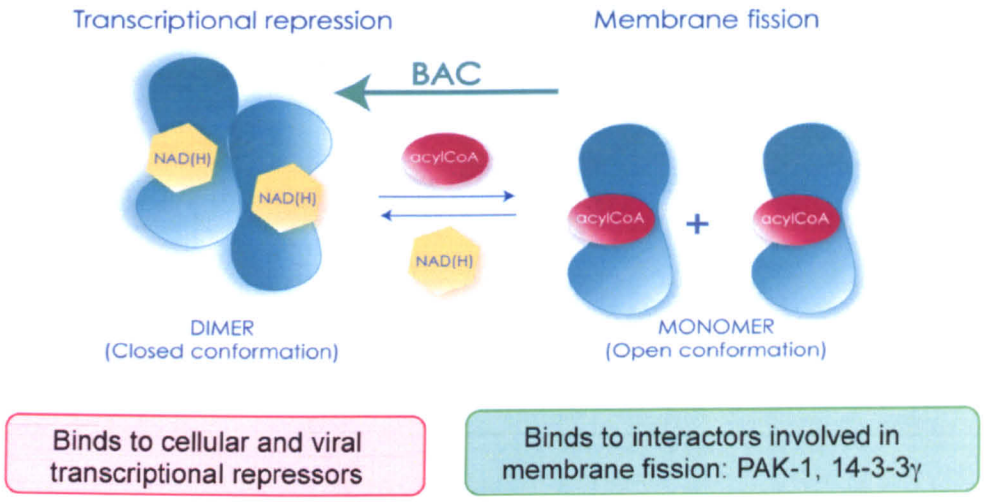

Figure 5.1: working model. BAC increases CtBP co-repressor activity

CtBP proteins can be regulated by cofactors. NAD(H) promotes a dimeric conformation, active in transcriptional co-repression. AcylCoA favours a monomeric conformation, required for membrane fission.

Similarly to NAD(H), BAC binding to CtBP favours the dimeric conformation. This change in the oligomerisation status is associated to a promoter-dependent increased co-repressor activity.

As mentioned above, I tested a small subset of all the genes that might be regulated by CtBP1, and therefore a wider analysis of the CtBP target genes could help in our understanding whether and how other genes are affected by BAC binding to CtBP1/BARS.

The CtBPs are among the very few transcription factors that harbour an intrinsic enzymatic functional domain, which thus represents a 'druggable' target. A growing body of evidence suggests that CtBP has a role in human cancer through the promotion of multiple pro-oncogenic activities, including epithelial to mesenchymal transition (EMT), cell migration/invasion, and cell survival. Loss of function of the CtBPs leads to enhanced expression of epithelial phenotype-related proteins, such as E-cadherin, occludin and keratin-8, and this counteracts EMT and tumour malignancy (Chinnadurai, 2009).

Consideration of the numerous pro-oncogenic properties of CtBP suggest it is a potential therapeutic target in cancer. Therefore, the possibility of regulating CtBP co-repressor activity using small molecules is of undisputed value. Even if the analysis of the genes tested does not support the use of BAC as a tool to counteract the pro-oncogenic properties of CtBPs, a wider analysis of different genes could help in better understanding whether the effects of BAC binding can be exploited as a pharmacological tool.

The requirement for the presence of CD38 to allow BAC to enter the intracellular space (figure 3.7) restricts the range of the possible use of BAC. However, this aspect can still be considered positive, as some tumours, such as diffuse large B-cell lymphomas, express high levels of CD38 (Malavasi et al., 2011); thus BAC could selectively target these kind of tumours.

Importantly, a striking result that emerges from my data is the reversibility of BAC binding to CtBP1/BARS. It is important to highlight that BAC binding to CtBP1/BARS occurs through the BFA molecule, and thus an intracellular enzyme that can catalyse the removal of BFA should exist. These data lead us to think that, indeed, a molecule similar to BAC is also present in cells. Moreover, it is likely that the toxins exploit mechanisms similar to endogenous ones in their modulation of protein functions. So, based on the existence of an endogenous enzyme that can remove BAC from CtBP1/BARS, it will be very interesting to investigate whether similar endogenous mechanisms can regulate CtBP functions. It is thus tempting to speculate that an endogenous 'BAC-like' molecule will represents a further mechanisms that is highly specific for the regulation of the different CtBP functions.

5.2 The mono-ADP-ribosyltransferase PARP12 is involved in the control of the structure of the Golgi complex

ADP-ribosylation is an ubiquitous protein modification that controls many cellular processes, including transcription, DNA repair and bacterial toxicity. Mono-ADP-ribosylation is only recently emerging as an important post-translational modification that is used by mammalian cells to control a vast array of cellular processes (Hottiger et al., 2011). While more evidence exists regarding the roles of poly-ADP-ribosylation in different cellular processes, our present knowledge of mono-ADP-ribosylation catalysed by the new members of the PARP family is less advanced, and thus their characterisation will help in our understanding of their roles.

Here I have provided evidence that PARP12 is a mono-ART. Similar to PARP10, PARP12 lacks the polymerase activity, while showing robust mono-ART activity. In agreement with the sequence alignment data reported by Lusher and co-workers (Kleine et al., 2008), I have shown here that the residues of the catalytic triad of PARP12 are indeed indispensable for its ADP-ribosylation activity, thus demonstrating that PARP12 is an additional member of the new sub-family of mono-ARTs.

More importantly, my data provide the initial evidence for a previously uncharacterised function that can be ascribed to mono-ADP-ribosylation: a role in the control of the morphology of the Golgi complex. The identification of PARP12 substrates, as well as the analysis of PARP12 sub-cellular localisation, has been instrumental for gaining of insights into a function for PARP12. Indeed, I have shown here that PARP12 is a new Golgi localised

protein (Figure 4.18). Interestingly, the Golgi complex has been demonstrated to be an important compartment for NAD^+ synthesis (Dolle et al., 2010), and thus this NAD^+ pool can be used to catalyse the ADP-ribosylation reaction also at the level of this organelle. In line with these findings, I have shown that, indeed, Rab1A, can be ADP-ribosylated by PARP12.

The Rab proteins are key players in the control of crucial steps in vesicular transport (Stenmark, 2009). A role for these proteins has been reported in vesicle budding (e.g., Rab9 functions in the recycling of mannose-6-phosphate receptors from late endosomes to the trans-Golgi network), in vesicle motility (as in the case of Rab11), and also in vesicle fusion (as reported for Rab5) (Carroll et al., 2001; Hales et al., 2002; McLauchlan et al., 1998).

Rab1 is involved in the regulation of the earliest stages of protein trafficking through the secretory pathway: from the ER to the Golgi complex (Allan et al., 2000; Moyer et al., 2001; Tisdale et al., 1992). Protein transport between the ER and the Golgi complex occurs via an intermediate compartment (IC), which is also known as vesicular tubular clusters (VTCs), the ER-Golgi intermediate compartment (ERGIC), or simply the IC. Carrier exit from the ER is initiated at specific domains in the ER network known as ER exit sites (ERES), via COPII-coated transport carriers. These COPII vesicular carriers deliver cargos from the ERES to the stationary ERGIC clusters, and then COPI-coated vesicles bud from this compartment to deliver material to the *cis*-Golgi compartment. COPI vesicles are also responsible for retrograde transport to the ER from the ERGIC and the Golgi complex (Lorente-Rodriguez and Barlowe, 2011). Rab1 is involved in both COPI

(Alvarez et al., 2003; Monetta et al., 2007) and COPII-mediated events (Allan et al., 2000; Moyer et al., 2001). When active and bound to GTP, Rab proteins recruit effectors, which function in downstream events that lead to membrane fusion. In particular, the activated membrane-bound Rab1 recruits the tethering protein p115, and possibly other golgins, thus coordinating fusion events (Allan et al., 2000). Besides this fundamental role, Rab1 has also been shown to be required for the maintenance of Golgi complex morphology. In particular, it has been reported that microinjection of inactive Rab1A mutants (i.e. in the GDP-bound form) as well over-expression of a Rab1-GAP protein, result in fragmentation of the Golgi complex (Haas et al., 2007; Wilson et al., 1994).

Data reported here show that the over-expression of PARP12 leads to a loss of the classical ribbon-like organisation of the Golgi complex and PARP12 localisation in cytoplasmic foci (Figure 4.18). Strikingly, as well as PARP12 over-expression, abrogation of Rab1A expression causes Golgi fragmentation and displacement of PARP12 from the Golgi complex, from where it instead appears in cytoplasmic structures (Figure 4.19). Thus, an intriguing possibility is that PARP12 over-expression causes Golgi fragmentation through the ADP-ribosylation of Rab1A.

Although the Rab GTPases mainly function as regulatory switches that spatio-temporally coordinate the recruitment of various regulators of membrane trafficking, their outputs also impinge on other regulatory circuits, such as phosphorylation (Stenmark, 2009). These post-translational modifications might alter either the function of the Rab GTPase itself or that of its interacting partners, thereby adding another layer of control to their activities. In this way, phosphoregulation of Rab functions contributes to the

dramatic changes in membrane trafficking that occur during, for example, mitosis. Rab1 is indeed phosphorylated by Cdk1, which might contribute to the inhibition of vesicle tethering and fusion (Preisinger et al., 2005). This event leads to persistent budding of COPI vesicles without fusion, thus generating a disassembly of the Golgi (Lowe et al., 1998a).

Considering that Rab1A is one of the substrates I found for PARP12, my data suggest the existence of a new link between ADP-ribosylation and Rab1A functions. It is tempting to speculate that ADP-ribosylated Rab1A might mimic the same effects as inactive Rab1A (i.e. in the GDP-bound state) or can impair Rab1A interaction with specific partners that are important for its functions, thus explaining the fragmentation of the Golgi complex after PARP12 over-expression. Moreover, I have also reported that Rab1A over-expression inhibits PARP12 catalytic activity, suggesting that these two proteins are able to regulate each other. One possible explanation is that Rab1A can interact with PARP12 at its catalytic site, thus blocking its enzymatic function. However, data obtained so far cannot explain this finding at the molecular level, and remains to be explored.

A crucial point that still needs further analysis is that the over-expressed PARP12 localises in cytoplasmic foci and not on the Golgi complex, as is seen for the endogenous protein. My data show that as with over-expression, the Golgi localisation of PARP12 is also lost after Rab1A interference and after the use of the PJ34 ADP-ribosylation inhibitor (Figures 4.19, 4.23). Based on these data, it can be assumed that PARP12 localisation on the Golgi complex is reliant on ADP-ribose formation (even produced by other PARPs), while the fragmentation effect on the Golgi structure is dependent on Rab1A ADP-

ribosylation by PARP12. This would explain the fragmentation of the Golgi structure after PARP12 over-expression (due to Rab1A ADP-ribosylation, and thus possibly its inactivation), an effect that is comparable to Rab1A interference.

Regarding PARP12 localisation, recently Chang P. and co-workers (Leung et al., 2011) demonstrated that PARP5, the other PARP that is located to the Golgi complex, interacts with PARP12. My data show that inhibition of ADP-ribosylation by the ADP-ribosylation PJ34 inhibitor causes a displacement of PARP12 from the Golgi complex, thus suggesting that ADP-ribosylation is required to target PARP12 at this organelle. Based on this evidence, it will be interesting to determine whether PARP12 localisation at the Golgi complex is dependent on the ADP-ribosylation catalysed by PARP5.

Leung, A. K. *et al.* also reported data on PARP12 localisation after over-expression. Similarly to my findings, they showed the over-expressed PARP12 localisation as cytoplasmic foci, that they identify as stress granules using specific markers, such as the eukaryotic initiation factor eIF3. Here, PARP12 is part of a complex of PARPs, which includes PARP5, PARP13 and PARP15. The authors proposed that the accessibility of Argonaute/miRNA complex to its target mRNA is affected by an increased ADP-ribosylation of multiple proteins that bind to the target, resulting in the relief of miRNA silencing. The production of pADPR is dependent on this 'PARP complex' activity. However, they had no comment regarding endogenous PARP12.

Thus, an interesting aspect to be investigated is how these foci are formed, performing live-cell imaging to follow the over-expression of PARP12 with time. It is possible that PARP12 is a multi-functional protein, that

harbours different roles according to its localisation and the cellular conditions. However, it cannot be excluded that the PARP12 localisation in stress granules is a consequence of its over-expression. If this is the case, it is possible that the endogenous levels of PARP5, and potentially the basal levels of ADP ribosylation, are not sufficient to recruit over-expressed PARP12, thus displacing it from the Golgi complex.

In addition, my data also indicate a clear role for PARP12 and for ADP-ribosylation in the re-formation of the Golgi complex. Interestingly, I observed a defect in Golgi reassembly after BFA was washed out both after abrogation of PARP12 expression by RNA interference and after treatment with the ADP-ribosylation inhibitor PJ34. These results suggest a role for PARP12, and thus for ADP-ribosylation, during Golgi complex re-formation. This new finding could have interesting implications in the study of Golgi biogenesis during different cellular events, such as the cell cycle. During mitosis, COPI vesicles continue to form (Xiang et al., 2007), but the vesicles cannot fuse with their target membranes because of the disruption of vesicle tethering complex (Lowe et al., 1998b; Misteli and Warren, 1994; Nakamura et al., 1997). For example, phosphorylation of GM130 by Cdk1 in early mitosis prevents p115 from binding, thereby blocking vesicle tethering and subsequent fusion (Levine et al., 1996; Lowe et al., 1998b). My data show that the removal of PARP12 expression, as well as the inhibition of ADP-ribosylation, causes a defect in Golgi re-formation after BFA was washed out (Figure 4.23).

It is tempting to speculate that PARP12-catalysed ADP-ribosylation might contribute to the regulation of tethering/fusion events. When this situation is altered (by PARP12 siRNA, or by PJ34 treatment), this regulatory

mechanism is lost, thus leading to an imbalance between the tethering and fusion processes. However, structural studies are needed to understand the specific step(s) controlled by ADP-ribosylation, and the molecular mechanism through which this effect is achieved.

In addition, it will be also interesting to investigate whether anterograde transport (event in which Rab1A is involved) is impaired by PARP12 catalysed ADP-ribosylation activity. A possible explanation is that if ADP-ribosylation regulates Rab1A functions, this trafficking step should be affected. However, future studies are needed to determine this.

In conclusion, my work has highlighted a possible regulatory role of mono-ADP-ribosylation at the level of the Golgi complex. Seen from a more general perspective, the substrates identified for PARP12 suggest that this enzyme, and thus the mono-ADP-ribosylation catalysed by PARP12, might be involved in multiple cellular functions, ranging from regulation of small-GTPases to the control of RNA. Consistent with my findings, the recent findings of Chang P. and co-workers (Leung et al., 2011) indeed demonstrate a role of ADP-ribosylation associated to RNA control. The study of the substrates identified for PARP12 might thus add other important contributions to the understanding of the role of mono-ADP-ribosylation in cells.

References

- Aarhus, R., R.M. Graeff, D.M. Dickey, T.F. Walseth, and H.C. Lee. 1995. ADP-ribosyl cyclase and CD38 catalyze the synthesis of a calcium-mobilizing metabolite from NADP. *J Biol Chem.* 270:30327-30333.
- Aguiar, R.C., K. Takeyama, C. He, K. Kreinbrink, and M.A. Shipp. 2005. B-aggressive lymphoma family proteins have unique domains that modulate transcription and exhibit poly(ADP-ribose) polymerase activity. *J Biol Chem.* 280:33756-33765.
- Aguiar, R.C., Y. Yakushijin, S. Kharbanda, R. Salgia, J.A. Fletcher, and M.A. Shipp. 2000. BAL is a novel risk-related gene in diffuse large B-cell lymphomas that enhances cellular migration. *Blood.* 96:4328-4334.
- Ahel, D., Z. Horejsi, N. Wiechens, S.E. Polo, E. Garcia-Wilson, I. Ahel, H. Flynn, M. Skehel, S.C. West, S.P. Jackson, T. Owen-Hughes, and S.J. Boulton. 2009. Poly(ADP-ribose)-dependent regulation of DNA repair by the chromatin remodeling enzyme ALC1. *Science.* 325:1240-1243.
- Ahel, I., D. Ahel, T. Matsusaka, A.J. Clark, J. Pines, S.J. Boulton, and S.C. West. 2008. Poly(ADP-ribose)-binding zinc finger motifs in DNA repair/checkpoint proteins. *Nature.* 451:81-85.
- Aksoy, P., C. Escande, T.A. White, M. Thompson, S. Soares, J.C. Benech, and E.N. Chini. 2006. Regulation of SIRT 1 mediated NAD dependent deacetylation: a novel role for the multifunctional enzyme CD38. *Biochem Biophys Res Commun.* 349:353-359.
- Aktories, K., A.E. Lang, C. Schwan, and H.G. Mannherz. 2011. Actin as target for modification by bacterial protein toxins. *FEBS J.*

- Aktories, K., and A. Wegner. 1989. ADP-ribosylation of actin by clostridial toxins. *J Cell Biol.* 109:1385-1387.
- Alessio, M., S. Roggero, A. Funaro, L.B. De Monte, L. Peruzzi, M. Geuna, and F. Malavasi. 1990. CD38 molecule: structural and biochemical analysis on human T lymphocytes, thymocytes, and plasma cells. *J Immunol.* 145:878-884.
- Alkhatib, H.M., D.F. Chen, B. Cherney, K. Bhatia, V. Notario, C. Giri, G. Stein, E. Slattery, R.G. Roeder, and M.E. Smulson. 1987. Cloning and expression of cDNA for human poly(ADP-ribose) polymerase. *Proc Natl Acad Sci U S A.* 84:1224-1228.
- Allan, B.B., B.D. Moyer, and W.E. Balch. 2000. Rab1 recruitment of p115 into a cis-SNARE complex: programming budding COPII vesicles for fusion. *Science.* 289:444-448.
- Allured, V.S., R.J. Collier, S.F. Carroll, and D.B. McKay. 1986. Structure of exotoxin A of Pseudomonas aeruginosa at 3.0-Angstrom resolution. *Proc Natl Acad Sci U S A.* 83:1320-1324.
- Alvarez, C., R. Garcia-Mata, E. Brandon, and E. Sztul. 2003. COPI recruitment is modulated by a Rab1b-dependent mechanism. *Mol Biol Cell.* 14:2116-2127.
- Alvarez-Gonzalez, R., and F.R. Althaus. 1989. Poly(ADP-ribose) catabolism in mammalian cells exposed to DNA-damaging agents. *Mutat Res.* 218:67-74.
- Alvarez-Gonzalez, R., and M.K. Jacobson. 1987. Characterization of polymers of adenosine diphosphate ribose generated in vitro and in vivo. *Biochemistry.* 26:3218-3224.
- Ame, J.C., V. Rolli, V. Schreiber, C. Niedergang, F. Apiou, P. Decker, S. Muller, T. Hoger, J. Menissier-de Murcia, and G. de Murcia. 1999. PARP-2, A

novel mammalian DNA damage-dependent poly(ADP-ribose) polymerase. *J Biol Chem.* 274:17860-17868.

- Andrabi, S.A., N.S. Kim, S.W. Yu, H. Wang, D.W. Koh, M. Sasaki, J.A. Klaus, T. Otsuka, Z. Zhang, R.C. Koehler, P.D. Hurn, G.G. Poirier, V.L. Dawson, and T.M. Dawson. 2006. Poly(ADP-ribose) (PAR) polymer is a death signal. *Proc Natl Acad Sci U S A.* 103:18308-18313.
- Audebert, M., B. Salles, and P. Calsou. 2004. Involvement of poly(ADP-ribose) polymerase-1 and XRCC1/DNA ligase III in an alternative route for DNA double-strand breaks rejoining. *J Biol Chem.* 279:55117-55126.
- Audebert, M., B. Salles, and P. Calsou. 2008. Effect of double-strand break DNA sequence on the PARP-1 NHEJ pathway. *Biochem Biophys Res Commun.* 369:982-988.
- Audebert, M., B. Salles, M. Weinfeld, and P. Calsou. 2006. Involvement of polynucleotide kinase in a poly(ADP-ribose) polymerase-1-dependent DNA double-strand breaks rejoining pathway. *J Mol Biol.* 356:257-265.
- Augustin, A., C. Spenlehauer, H. Dumond, J. Menissier-De Murcia, M. Piel, A.C. Schmit, F. Apiou, J.L. Vonesch, M. Kock, M. Bornens, and G. De Murcia. 2003. PARP-3 localizes preferentially to the daughter centriole and interferes with the G1/S cell cycle progression. *J Cell Sci.* 116:1551-1562.
- Barbieri, J.T., and J. Sun. 2004. Pseudomonas aeruginosa ExoS and ExoT. *Rev Physiol Biochem Pharmacol.* 152:79-92.
- Barford, D., A.K. Das, and M.P. Egloff. 1998. The structure and mechanism of protein phosphatases: insights into catalysis and regulation. *Annu Rev Biophys Biomol Struct.* 27:133-164.

- Barlowe, C. 2000. Traffic COPs of the early secretory pathway. *Traffic.* 1:371-377.
- Barnes, C.J., R.K. Vadlamudi, S.K. Mishra, R.H. Jacobson, F. Li, and R. Kumar. 2003. Functional inactivation of a transcriptional corepressor by a signaling kinase. *Nat Struct Biol.* 10:622-628.
- Barth, H., K. Aktories, M.R. Popoff, and B.G. Stiles. 2004. Binary bacterial toxins: biochemistry, biology, and applications of common Clostridium and Bacillus proteins. *Microbiol Mol Biol Rev.* 68:373-402, table of contents.
- Bazan, J.F., and F. Koch-Nolte. 1997. Sequence and structural links between distant ADP-ribosyltransferase families. *Adv Exp Med Biol.* 419:99-107.
- Benchoua, A., C. Couriaud, C. Guegan, L. Tartier, P. Couvert, G. Friocourt, J. Chelly, J. Menissier-de Murcia, and B. Onteniente. 2002. Active caspase-8 translocates into the nucleus of apoptotic cells to inactivate poly(ADP-ribose) polymerase-2. *J Biol Chem.* 277:34217-34222.
- Bergman, L.M., C.N. Birts, M. Darley, B. Gabrielli, and J.P. Blaydes. 2009. CtBPs promote cell survival through the maintenance of mitotic fidelity. *Mol Cell Biol.* 29:4539-4551.
- Boehler, C., L.R. Gauthier, O. Mortusewicz, D.S. Biard, J.M. Saliou, A. Bresson, S. Sanglier-Cianferani, S. Smith, V. Schreiber, F. Boussin, and F. Dantzer. 2011. Poly(ADP-ribose) polymerase 3 (PARP3), a newcomer in cellular response to DNA damage and mitotic progression. *Proc Natl Acad Sci U S A.* 108:2783-2788.
- Bonazzi, M., S. Spano, G. Turacchio, C. Cericola, C. Valente, A. Colanzi, H.S. Kweon, V.W. Hsu, E.V. Polishchuck, R.S. Polishchuck, M. Sallese, T.

Pulvirenti, D. Corda, and A. Luini. 2005. CtBP3/BARS drives membrane fission in dynamin-independent transport pathways. *Nat Cell Biol.* 7:570-580.

- Bortell, R., T. Kanaitsuka, L.A. Stevens, J. Moss, J.P. Mordes, A.A. Rossini, and D.L. Greiner. 1999. The RT6 (Art2) family of ADP-ribosyltransferases in rat and mouse. *Mol Cell Biochem.* 193:61-68.
- Boyd, J.M., T. Subramanian, U. Schaeper, M. La Regina, S. Bayley, and G. Chinnadurai. 1993. A region in the C-terminus of adenovirus 2/5 E1a protein is required for association with a cellular phosphoprotein and important for the negative modulation of T24-ras mediated transformation, tumorigenesis and metastasis. *EMBO J.* 12:469-478.
- Braren, R., G. Glowacki, M. Nissen, F. Haag, and F. Koch-Nolte. 1998. Molecular characterization and expression of the gene for mouse NAD+:arginine ecto-mono(ADP-ribosyl)transferase, Art1. *Biochem J.* 336 (Pt 3):561-568.
- Burnett, G., and E.P. Kennedy. 1954. The enzymatic phosphorylation of proteins. *J Biol Chem.* 211:969-980.
- Caiafa, P., and M. Zampieri. 2005. DNA methylation and chromatin structure: the puzzling CpG islands. *J Cell Biochem.* 94:257-265.
- Carroll, K.S., J. Hanna, I. Simon, J. Krise, P. Barbero, and S.R. Pfeffer. 2001. Role of Rab9 GTPase in facilitating receptor recruitment by TIP47. *Science.* 292:1373-1376.
- Ceresa, B.P. 2006. Regulation of EGFR endocytic trafficking by rab proteins. *Histol Histopathol.* 21:987-993.

- Chambon, P., J.D. Weill, and P. Mandel. 1963. Nicotinamide mononucleotide activation of new DNA-dependent polyadenylic acid synthesizing nuclear enzyme. *Biochem Biophys Res Commun.* 11:39-43.
- Chang, P., M. Coughlin, and T.J. Mitchison. 2005. Tankyrase-1 polymerization of poly(ADP-ribose) is required for spindle structure and function. *Nat Cell Biol.* 7:1133-1139.
- Chang, P., M.K. Jacobson, and T.J. Mitchison. 2004. Poly(ADP-ribose) is required for spindle assembly and structure. *Nature.* 432:645-649.
- Chi, N.W., and H.F. Lodish. 2000. Tankyrase is a golgi-associated mitogen-activated protein kinase substrate that interacts with IRAP in GLUT4 vesicles. *J Biol Chem.* 275:38437-38444.
- Chinnadurai, G. 2003. CtBP family proteins: more than transcriptional corepressors. *Bioessays.* 25:9-12.
- Chinnadurai, G. 2007. Transcriptional regulation by C-terminal binding proteins. *Int J Biochem Cell Biol.* 39:1593-1607.
- Chinnadurai, G. 2009. The transcriptional corepressor CtBP: a foe of multiple tumor suppressors. *Cancer Res.* 69:731-734.
- Chou, H.Y., H.T. Chou, and S.C. Lee. 2006. CDK-dependent activation of poly(ADP-ribose) polymerase member 10 (PARP10). *J Biol Chem.* 281:15201-15207.
- Ciccarone, V.C., D.A. Polayes, and V.A. Luckow. 1998. Generation of Recombinant Baculovirus DNA in E.coli Using a Baculovirus Shuttle Vector. *Methods Mol Med.* 13:213-235.
- Clarke, P.R., and C. Zhang. 2008. Spatial and temporal coordination of mitosis by Ran GTPase. *Nat Rev Mol Cell Biol.* 9:464-477.

- Coburn, J., R.T. Wyatt, B.H. Iglewski, and D.M. Gill. 1989. Several GTP-binding proteins, including p21c-H-ras, are preferred substrates of Pseudomonas aeruginosa exoenzyme S. *J Biol Chem.* 264:9004-9008.
- Cohen-Armon, M., L. Visochek, D. Rozensal, A. Kalal, I. Geistrikh, R. Klein, S. Bendetz-Nezer, Z. Yao, and R. Seger. 2007. DNA-independent PARP-1 activation by phosphorylated ERK2 increases Elk1 activity: a link to histone acetylation. *Mol Cell.* 25:297-308.
- Colanzi, A., C. Hidalgo Carcedo, A. Persico, C. Cericola, G. Turacchio, M. Bonazzi, A. Luini, and D. Corda. 2007. The Golgi mitotic checkpoint is controlled by BARS-dependent fission of the Golgi ribbon into separate stacks in G2. *EMBO J.* 26:2465-2476.
- Collier, R.J. 1975. Diphtheria toxin: mode of action and structure. *Bacteriol Rev.* 39:54-85.
- Cook, B.D., J.N. Dynek, W. Chang, G. Shostak, and S. Smith. 2002. Role for the related poly(ADP-Ribose) polymerases tankyrase 1 and 2 at human telomeres. *Mol Cell Biol.* 22:332-342.
- Corda, D., A. Colanzi, and A. Luini. 2006. The multiple activities of CtBP/BARS proteins: the Golgi view. *Trends Cell Biol.* 16:167-173.
- Corda, D., and M. Di Girolamo. 2003. Functional aspects of protein mono-ADP-ribosylation. *EMBO J.* 22:1953-1958.
- D'Amours, D., S. Desnoyers, I. D'Silva, and G.G. Poirier. 1999. Poly(ADP-ribosyl)ation reactions in the regulation of nuclear functions. *Biochem J.* 342 (Pt 2):249-268.

- Dammer, E.B., and M.B. Sewer. 2008. Phosphorylation of CtBP1 by cAMP-dependent protein kinase modulates induction of CYP17 by stimulating partnering of CtBP1 and 2. *J Biol Chem.* 283:6925-6934.
- Dani, N., A. Stilla, A. Marchegiani, A. Tamburro, S. Till, A.G. Ladurner, D. Corda, and M. Di Girolamo. 2009. Combining affinity purification by ADP-ribose-binding macro domains with mass spectrometry to define the mammalian ADP-ribosyl proteome. *Proc Natl Acad Sci U S A.* 106:4243-4248.
- Dantzer, F., M.J. Giraud-Panis, I. Jaco, J.C. Ame, I. Schultz, M. Blasco, C.E. Koering, E. Gilson, J. Menissier-de Murcia, G. de Murcia, and V. Schreiber. 2004. Functional interaction between poly(ADP-Ribose) polymerase 2 (PARP-2) and TRF2: PARP activity negatively regulates TRF2. *Mol Cell Biol.* 24:1595-1607.
- David, K.K., S.A. Andrabi, T.M. Dawson, and V.L. Dawson. 2009. Parthanatos, a messenger of death. *Front Biosci.* 14:1116-1128.
- De Matteis, M.A., M. Di Girolamo, A. Colanzi, M. Pallas, G. Di Tullio, L.J. McDonald, J. Moss, G. Santini, S. Bannykh, D. Corda, and et al. 1994. Stimulation of endogenous ADP-ribosylation by brefeldin A. *Proc Natl Acad Sci U S A.* 91:1114-1118.
- Deng, Q., and J.T. Barbieri. 2008a. Modulation of host cell endocytosis by the type III cytotoxin, Pseudomonas ExoS. *Traffic.* 9:1948-1957.
- Deng, Q., and J.T. Barbieri. 2008b. Molecular mechanisms of the cytotoxicity of ADP-ribosylating toxins. *Annu Rev Microbiol.* 62:271-288.
- Deng, Q., J. Sun, and J.T. Barbieri. 2005. Uncoupling Crk signal transduction by Pseudomonas exoenzyme T. *J Biol Chem.* 280:35953-35960.

- Di Girolamo, M., N. Dani, A. Stilla, and D. Corda. 2005. Physiological relevance of the endogenous mono(ADP-ribosyl)ation of cellular proteins. *FEBS J.* 272:4565-4575.
- Di Virgilio, F., P. Chiozzi, D. Ferrari, S. Falzoni, J.M. Sanz, A. Morelli, M. Torboli, G. Bolognesi, and O.R. Baricordi. 2001. Nucleotide receptors: an emerging family of regulatory molecules in blood cells. *Blood.* 97:587-600.
- Dolle, C., M. Niere, E. Lohndal, and M. Ziegler. 2010. Visualization of subcellular NAD pools and intra-organellar protein localization by poly-ADP-ribose formation. *Cell Mol Life Sci.* 67:433-443.
- Domenighini, M., C. Magagnoli, M. Pizza, and R. Rappuoli. 1994. Common features of the NAD-binding and catalytic site of ADP-ribosylating toxins. *Mol Microbiol.* 14:41-50.
- Domenighini, M., and R. Rappuoli. 1996. Three conserved consensus sequences identify the NAD-binding site of ADP-ribosylating enzymes, expressed by eukaryotes, bacteria and T-even bacteriophages. *Mol Microbiol.* 21:667-674.
- Doms, R.W., G. Russ, and J.W. Yewdell. 1989. Brefeldin A redistributes resident and itinerant Golgi proteins to the endoplasmic reticulum. *J Cell Biol.* 109:61-72.
- Donaldson, J.G., and C.L. Jackson. 2000. Regulators and effectors of the ARF GTPases. *Curr Opin Cell Biol.* 12:475-482.
- Donaldson, J.G., R.A. Kahn, J. Lippincott-Schwartz, and R.D. Klausner. 1991. Binding of ARF and beta-COP to Golgi membranes: possible regulation by a trimeric G protein. *Science.* 254:1197-1199.

- Donaldson, J.G., J. Lippincott-Schwartz, G.S. Bloom, T.E. Kreis, and R.D. Klausner. 1990. Dissociation of a 110-kD peripheral membrane protein from the Golgi apparatus is an early event in brefeldin A action. *J Cell Biol.* 111:2295-2306.
- Dynek, J.N., and S. Smith. 2004. Resolution of sister telomere association is required for progression through mitosis. *Science.* 304:97-100.
- El-Khamisy, S.F., M. Masutani, H. Suzuki, and K.W. Caldecott. 2003. A requirement for PARP-1 for the assembly or stability of XRCC1 nuclear foci at sites of oxidative DNA damage. *Nucleic Acids Res.* 31:5526-5533.
- Finkel, T., C.X. Deng, and R. Mostoslavsky. 2009. Recent progress in the biology and physiology of sirtuins. *Nature.* 460:587-591.
- Fjeld, C.C., W.T. Birdsong, and R.H. Goodman. 2003. Differential binding of NAD+ and NADH allows the transcriptional corepressor carboxyl-terminal binding protein to serve as a metabolic sensor. *Proc Natl Acad Sci U S A.* 100:9202-9207.
- Flint, A.J., T. Tiganis, D. Barford, and N.K. Tonks. 1997. Development of "substrate-trapping" mutants to identify physiological substrates of protein tyrosine phosphatases. *Proc Natl Acad Sci U S A.* 94:1680-1685.
- Folkers, U., V. Kirik, U. Schobinger, S. Falk, S. Krishnakumar, M.A. Pollock, D.G. Oppenheimer, I. Day, A.S. Reddy, G. Jurgens, and M. Hulskamp. 2002. The cell morphogenesis gene ANGUSTIFOLIA encodes a CtBP/BARS-like protein and is involved in the control of the microtubule cytoskeleton. *EMBO J.* 21:1280-1288.
- Fong, P.C., D.S. Boss, T.A. Yap, A. Tutt, P. Wu, M. Mergui-Roelvink, P. Mortimer, H. Swaisland, A. Lau, M.J. O'Connor, A. Ashworth, J. Carmichael,

S.B. Kaye, J.H. Schellens, and J.S. de Bono. 2009. Inhibition of poly(ADP-ribose) polymerase in tumors from BRCA mutation carriers. *N Engl J Med.* 361:123-134.

- Fowell, D., and D. Mason. 1993. Evidence that the T cell repertoire of normal rats contains cells with the potential to cause diabetes. Characterization of the CD4+ T cell subset that inhibits this autoimmune potential. *J Exp Med.* 177:627-636.
- Fraylick, J.E., E.A. Rucks, D.M. Greene, T.S. Vincent, and J.C. Olson. 2002. Eukaryotic cell determination of ExoS ADP-ribosyltransferase substrate specificity. *Biochem Biophys Res Commun.* 291:91-100.
- Fujiwara, T., K. Oda, S. Yokota, A. Takatsuki, and Y. Ikehara. 1988. Brefeldin A causes disassembly of the Golgi complex and accumulation of secretory proteins in the endoplasmic reticulum. *J Biol Chem.* 263:18545-18552.
- Funaro, A., A.L. Horenstein, L. Calosso, M. Morra, R.P. Tarocco, L. Franco, A. De Flora, and F. Malavasi. 1996. Identification and characterization of an active soluble form of human CD38 in normal and pathological fluids. *Int Immunol.* 8:1643-1650.
- Gagne, J.P., M. Isabelle, K.S. Lo, S. Bourassa, M.J. Hendzel, V.L. Dawson, T.M. Dawson, and G.G. Poirier. 2008. Proteome-wide identification of poly(ADP-ribose) binding proteins and poly(ADP-ribose)-associated protein complexes. *Nucleic Acids Res.* 36:6959-6976.
- Gamble, M.J., and R.P. Fisher. 2007. SET and PARP1 remove DEK from chromatin to permit access by the transcription machinery. *Nat Struct Mol Biol.* 14:548-555.

- Ganesan, A.K., D.W. Frank, R.P. Misra, G. Schmidt, and J.T. Barbieri. 1998. Pseudomonas aeruginosa exoenzyme S ADP-ribosylates Ras at multiple sites. *J Biol Chem.* 273:7332-7337.
- Ganz, T. 2003. Defensins: antimicrobial peptides of innate immunity. *Nat Rev Immunol.* 3:710-720.
- Gao, G., X. Guo, and S.P. Goff. 2002. Inhibition of retroviral RNA production by ZAP, a CCCH-type zinc finger protein. *Science.* 297:1703-1706.
- Garriga-Canut, M., B. Schoenike, R. Qazi, K. Bergendahl, T.J. Daley, R.M. Pfender, J.F. Morrison, J. Ockuly, C. Stafstrom, T. Sutula, and A. Roopra. 2006. 2-Deoxy-D-glucose reduces epilepsy progression by NRSF-CtBP-dependent metabolic regulation of chromatin structure. *Nat Neurosci.* 9:1382-1387.
- Gelman, L., P. Deterre, H. Gouy, L. Boumsell, P. Debre, and G. Bismuth. 1993. The lymphocyte surface antigen CD38 acts as a nicotinamide adenine dinucleotide glycohydrolase in human T lymphocytes. *Eur J Immunol.* 23:3361-3364.
- Gerasimenko, J.V., M. Sherwood, A.V. Tepikin, O.H. Petersen, and O.V. Gerasimenko. 2006. NAADP, cADPR and IP3 all release Ca2+ from the endoplasmic reticulum and an acidic store in the secretory granule area. *J Cell Sci.* 119:226-238.
- Gill, D.M. 1976. The arrangement of subunits in cholera toxin. *Biochemistry.* 15:1242-1248.
- Gill, D.M., A.M. Pappenheimer, Jr., R. Brown, and J.T. Kurnick. 1969. Studies on the mode of action of diphtheria toxin. VII. Toxin-stimulated hydrolysis of

nicotinamide adenine dinucleotide in mammalian cell extracts. *J Exp Med.* 129:1-21.

- Glowacki, G., R. Braren, M. Cetkovic-Cvrlje, E.H. Leiter, F. Haag, and F. Koch-Nolte. 2001. Structure, chromosomal localization, and expression of the gene for mouse ecto-mono(ADP-ribosyl)transferase ART5. *Gene.* 275:267-277.
- Glowacki, G., R. Braren, K. Firner, M. Nissen, M. Kuhl, P. Reche, F. Bazan, M. Cetkovic-Cvrlje, E. Leiter, F. Haag, and F. Koch-Nolte. 2002. The family of toxin-related ecto-ADP-ribosyltransferases in humans and the mouse. *Protein Sci.* 11:1657-1670.
- Goenka, S., and M. Boothby. 2006. Selective potentiation of Stat-dependent gene expression by collaborator of Stat6 (CoaSt6), a transcriptional cofactor. *Proc Natl Acad Sci U S A.* 103:4210-4215.
- Goenka, S., S.H. Cho, and M. Boothby. 2007. Collaborator of Stat6 (CoaSt6)-associated poly(ADP-ribose) polymerase activity modulates Stat6-dependent gene transcription. *J Biol Chem.* 282:18732-18739.
- Gomez, M., J. Wu, V. Schreiber, J. Dunlap, F. Dantzer, Y. Wang, and Y. Liu. 2006. PARP1 Is a TRF2-associated poly(ADP-ribose)polymerase and protects eroded telomeres. *Mol Biol Cell.* 17:1686-1696.
- Gottschalk, A.J., G. Timinszky, S.E. Kong, J. Jin, Y. Cai, S.K. Swanson, M.P. Washburn, L. Florens, A.G. Ladurner, J.W. Conaway, and R.C. Conaway. 2009. Poly(ADP-ribosyl)ation directs recruitment and activation of an ATP-dependent chromatin remodeler. *Proc Natl Acad Sci U S A.* 106:13770-13774.

- Grahnert, A., M. Friedrich, M. Pfister, F. Haag, F. Koch-Nolte, and S. Hauschildt. 2002. Mono-ADP-ribosyltransferases in human monocytes: regulation by lipopolysaccharide. *Biochem J.* 362:717-723.
- Grooteclaes, M., Q. Deveraux, J. Hildebrand, Q. Zhang, R.H. Goodman, and S.M. Frisch. 2003. C-terminal-binding protein corepresses epithelial and proapoptotic gene expression programs. *Proc Natl Acad Sci U S A.* 100:4568-4573.
- Guastafierro, T., B. Cecchinelli, M. Zampieri, A. Reale, G. Riggio, O. Sthandier, G. Zupi, L. Calabrese, and P. Caiafa. 2008. CCCTC-binding factor activates PARP-1 affecting DNA methylation machinery. *J Biol Chem.* 283:21873-21880.
- Guo, X., J. Ma, J. Sun, and G. Gao. 2007. The zinc-finger antiviral protein recruits the RNA processing exosome to degrade the target mRNA. *Proc Natl Acad Sci U S A.* 104:151-156.
- Haag, F., V. Andresen, S. Karsten, F. Koch-Nolte, and H. Thiele. 1995. Both allelic forms of the rat T cell differentiation marker RT6 display nicotinamide adenine dinucleotide (NAD)-glycohydrolase activity, yet only RT6.2 is capable of automodification upon incubation with NAD. *Eur J Immunol.* 25:2355-2361.
- Haas, A.K., S. Yoshimura, D.J. Stephens, C. Preisinger, E. Fuchs, and F.A. Barr. 2007. Analysis of GTPase-activating proteins: Rab1 and Rab43 are key Rabs required to maintain a functional Golgi complex in human cells. *J Cell Sci.* 120:2997-3010.
- Haigis, M.C., and L.P. Guarente. 2006. Mammalian sirtuins--emerging roles in physiology, aging, and calorie restriction. *Genes Dev.* 20:2913-2921.

- Haigis, M.C., R. Mostoslavsky, K.M. Haigis, K. Fahie, D.C. Christodoulou, A.J. Murphy, D.M. Valenzuela, G.D. Yancopoulos, M. Karow, G. Blander, C. Wolberger, T.A. Prolla, R. Weindruch, F.W. Alt, and L. Guarente. 2006. SIRT4 inhibits glutamate dehydrogenase and opposes the effects of calorie restriction in pancreatic beta cells. *Cell.* 126:941-954.
- Haince, J.F., S. Kozlov, V.L. Dawson, T.M. Dawson, M.J. Hendzel, M.F. Lavin, and G.G. Poirier. 2007. Ataxia telangiectasia mutated (ATM) signaling network is modulated by a novel poly(ADP-ribose)-dependent pathway in the early response to DNA-damaging agents. *J Biol Chem.* 282:16441-16453.
- Haince, J.F., D. McDonald, A. Rodrigue, U. Dery, J.Y. Masson, M.J. Hendzel, and G.G. Poirier. 2008. PARP1-dependent kinetics of recruitment of MRE11 and NBS1 proteins to multiple DNA damage sites. *J Biol Chem.* 283:1197-1208.
- Hakme, A., H.K. Wong, F. Dantzer, and V. Schreiber. 2008. The expanding field of poly(ADP-ribosyl)ation reactions. 'Protein Modifications: Beyond the Usual Suspects' Review Series. *EMBO Rep.* 9:1094-1100.
- Hales, C.M., J.P. Vaerman, and J.R. Goldenring. 2002. Rab11 family interacting protein 2 associates with Myosin Vb and regulates plasma membrane recycling. *J Biol Chem.* 277:50415-50421.
- Hallows, W.C., B.N. Albaugh, and J.M. Denu. 2008. Where in the cell is SIRT3?--functional localization of an NAD+-dependent protein deacetylase. *Biochem J.* 411:e11-13.
- Hamada, F., and M. Bienz. 2004. The APC tumor suppressor binds to C-terminal binding protein to divert nuclear beta-catenin from TCF. *Dev Cell.* 7:677-685.

- Han, S., and J.A. Tainer. 2002. The ARTT motif and a unified structural understanding of substrate recognition in ADP-ribosylating bacterial toxins and eukaryotic ADP-ribosyltransferases. *Int J Med Microbiol.* 291:523-529.
- Hans, F., and S. Dimitrov. 2001. Histone H3 phosphorylation and cell division. *Oncogene.* 20:3021-3027.
- Happel, N., and D. Doenecke. 2009. Histone H1 and its isoforms: contribution to chromatin structure and function. *Gene.* 431:1-12.
- Hara, N., M. Tsuchiya, and M. Shimoyama. 1996. Glutamic acid 207 in rodent T-cell RT6 antigens is essential for arginine-specific ADP-ribosylation. *J Biol Chem.* 271:29552-29555.
- Hassa, P.O., M. Covic, S. Hasan, R. Imhof, and M.O. Hottiger. 2001. The enzymatic and DNA binding activity of PARP-1 are not required for NF-kappa B coactivator function. *J Biol Chem.* 276:45588-45597.
- Hassa, P.O., S.S. Haenni, C. Buerki, N.I. Meier, W.S. Lane, H. Owen, M. Gersbach, R. Imhof, and M.O. Hottiger. 2005. Acetylation of poly(ADP-ribose) polymerase-1 by p300/CREB-binding protein regulates coactivation of NF-kappaB-dependent transcription. *J Biol Chem.* 280:40450-40464.
- Hassa, P.O., S.S. Haenni, M. Elser, and M.O. Hottiger. 2006. Nuclear ADP-ribosylation reactions in mammalian cells: where are we today and where are we going? *Microbiol Mol Biol Rev.* 70:789-829.
- Hay, R.T. 2005. SUMO: a history of modification. *Mol Cell.* 18:1-12.
- Helleday, T., H.E. Bryant, and N. Schultz. 2005. Poly(ADP-ribose) polymerase (PARP-1) in homologous recombination and as a target for cancer therapy. *Cell Cycle.* 4:1176-1178.

- Hidalgo Carcedo, C., M. Bonazzi, S. Spano, G. Turacchio, A. Colanzi, A. Luini, and D. Corda. 2004. Mitotic Golgi partitioning is driven by the membrane-fissioning protein CtBP3/BARS. *Science*. 305:93-96.
- Hirata, Y., N. Kimura, K. Sato, Y. Ohsugi, S. Takasawa, H. Okamoto, J. Ishikawa, T. Kaisho, K. Ishihara, and T. Hirano. 1994. ADP ribosyl cyclase activity of a novel bone marrow stromal cell surface molecule, BST-1. *FEBS Lett.* 356:244-248.
- Honjo, T., Y. Nishizuka, and O. Hayaishi. 1968. Diphtheria toxin-dependent adenosine diphosphate ribosylation of aminoacyl transferase II and inhibition of protein synthesis. *J Biol Chem.* 243:3553-3555.
- Hottiger, M.O., M. Boothby, F. Koch-Nolte, B. Luscher, N.M. Martin, R. Plummer, Z.Q. Wang, and M. Ziegler. 2011. Progress in the function and regulation of ADP-Ribosylation. *Sci Signal.* 4:mr5.
- Hottiger, M.O., P.O. Hassa, B. Luscher, H. Schuler, and F. Koch-Nolte. 2010. Toward a unified nomenclature for mammalian ADP-ribosyltransferases. *Trends Biochem Sci.* 35:208-219.
- Houtkooper, R.H., C. Canto, R.J. Wanders, and J. Auwerx. 2010. The secret life of NAD+: an old metabolite controlling new metabolic signaling pathways. *Endocr Rev.* 31:194-223.
- Howard, M., J.C. Grimaldi, J.F. Bazan, F.E. Lund, L. Santos-Argumedo, R.M. Parkhouse, T.F. Walseth, and H.C. Lee. 1993. Formation and hydrolysis of cyclic ADP-ribose catalyzed by lymphocyte antigen CD38. *Science*. 262:1056-1059.
- Hsiao, S.J., and S. Smith. 2008. Tankyrase function at telomeres, spindle poles, and beyond. *Biochimie*. 90:83-92.

- Huang, Q., Y.T. Wu, H.L. Tan, C.N. Ong, and H.M. Shen. 2009. A novel function of poly(ADP-ribose) polymerase-1 in modulation of autophagy and necrosis under oxidative stress. *Cell Death Differ.* 16:264-277.
- Imai, S., C.M. Armstrong, M. Kaeberlein, and L. Guarente. 2000. Transcriptional silencing and longevity protein Sir2 is an NAD-dependent histone deacetylase. *Nature.* 403:795-800.
- Itoh, M., K. Ishihara, H. Tomizawa, H. Tanaka, Y. Kobune, J. Ishikawa, T. Kaisho, and T. Hirano. 1994. Molecular cloning of murine BST-1 having homology with CD38 and Aplysia ADP-ribosyl cyclase. *Biochem Biophys Res Commun.* 203:1309-1317.
- Jager, D., K. Werdan, and U. Muller-Werdan. 2011. Endogenous ADP-ribosylation of elongation factor-2 by interleukin-1beta. *Mol Cell Biochem.* 348:125-128.
- Jeffery, C.J. 2004. Molecular mechanisms for multitasking: recent crystal structures of moonlighting proteins. *Curr Opin Struct Biol.* 14:663-668.
- Jin, L., W. Wei, Y. Jiang, H. Peng, J. Cai, C. Mao, H. Dai, W. Choy, J.E. Bemis, M.R. Jirousek, J.C. Milne, C.H. Westphal, and R.B. Perni. 2009. Crystal structures of human SIRT3 displaying substrate-induced conformational changes. *J Biol Chem.* 284:24394-24405.
- Johansson, M. 1999. A human poly(ADP-ribose) polymerase gene family (ADPRTL): cDNA cloning of two novel poly(ADP-ribose) polymerase homologues. *Genomics.* 57:442-445.
- Jones, E.M., and A. Baird. 1997. Cell-surface ADP-ribosylation of fibroblast growth factor-2 by an arginine-specific ADP-ribosyltransferase. *Biochem J.* 323 (Pt 1):173-177.

- Ju, B.G., V.V. Lunyak, V. Perissi, I. Garcia-Bassets, D.W. Rose, C.K. Glass, and M.G. Rosenfeld. 2006. A topoisomerase IIbeta-mediated dsDNA break required for regulated transcription. *Science*. 312:1798-1802.
- Ju, B.G., and M.G. Rosenfeld. 2006. A breaking strategy for topoisomerase IIbeta/PARP-1-dependent regulated transcription. *Cell Cycle*. 5:2557-2560.
- Ju, B.G., D. Solum, E.J. Song, K.J. Lee, D.W. Rose, C.K. Glass, and M.G. Rosenfeld. 2004. Activating the PARP-1 sensor component of the groucho/ TLE1 corepressor complex mediates a CaMKinase IIdelta-dependent neurogenic gene activation pathway. *Cell*. 119:815-829.
- Juszczynski, P., J.L. Kutok, C. Li, J. Mitra, R.C. Aguiar, and M.A. Shipp. 2006. BAL1 and BBAP are regulated by a gamma interferon-responsive bidirectional promoter and are overexpressed in diffuse large B-cell lymphomas with a prominent inflammatory infiltrate. *Mol Cell Biol*. 26:5348-5359.
- Kahl, S., M. Nissen, R. Girisch, T. Duffy, E.H. Leiter, F. Haag, and F. Koch-Nolte. 2000. Metalloprotease-mediated shedding of enzymatically active mouse ecto-ADP-ribosyltransferase ART2.2 upon T cell activation. *J Immunol*. 165:4463-4469.
- Kaminker, P.G., S.H. Kim, R.D. Taylor, Y. Zebarjadian, W.D. Funk, G.B. Morin, P. Yaswen, and J. Campisi. 2001. TANK2, a new TRF1-associated poly(ADP-ribose) polymerase, causes rapid induction of cell death upon overexpression. *J Biol Chem*. 276:35891-35899.
- Karras, G.I., G. Kustatscher, H.R. Buhecha, M.D. Allen, C. Pugieux, F. Sait, M. Bycroft, and A.G. Ladurner. 2005. The macro domain is an ADP-ribose binding module. *EMBO J*. 24:1911-1920.

- Kassis, S., J. Hagmann, P.H. Fishman, P.P. Chang, and J. Moss. 1982. Mechanism of action of cholera toxin on intact cells. Generation of A1 peptide and activation of adenylate cyclase. *J Biol Chem.* 257:12148-12152.
- Katsanis, N., and E.M. Fisher. 1998. A novel C-terminal binding protein (CTBP2) is closely related to CTBP1, an adenovirus E1A-binding protein, and maps to human chromosome 21q21.3. *Genomics.* 47:294-299.
- Kaufmann, S.H., S. Desnoyers, Y. Ottaviano, N.E. Davidson, and G.G. Poirier. 1993. Specific proteolytic cleavage of poly(ADP-ribose) polymerase: an early marker of chemotherapy-induced apoptosis. *Cancer Res.* 53:3976-3985.
- Kefalas, P., B. Saxty, M. Yadollahi-Farsani, and J. MacDermot. 1999. Chemotaxin-dependent translocation of immunoreactive ADP-ribosyltransferase-1 to the surface of human neutrophil polymorphs. *Eur J Biochem.* 259:866-871.
- Kennedy, B.K., N.R. Austriaco, Jr., J. Zhang, and L. Guarente. 1995. Mutation in the silencing gene SIR4 can delay aging in S. cerevisiae. *Cell.* 80:485-496.
- Kerns, J.A., M. Emerman, and H.S. Malik. 2008. Positive selection and increased antiviral activity associated with the PARP-containing isoform of human zinc-finger antiviral protein. *PLoS Genet.* 4:e21.
- Kickhoefer, V.A., A.C. Siva, N.L. Kedersha, E.M. Inman, C. Ruland, M. Streuli, and L.H. Rome. 1999. The 193-kD vault protein, VPARP, is a novel poly(ADP-ribose) polymerase. *J Cell Biol.* 146:917-928.
- Kim, J.H., E.J. Cho, S.T. Kim, and H.D. Youn. 2005. CtBP represses p300-mediated transcriptional activation by direct association with its bromodomain. *Nat Struct Mol Biol.* 12:423-428.

- Kim, M.Y., S. Mauro, N. Gevry, J.T. Lis, and W.L. Kraus. 2004. NAD+-dependent modulation of chromatin structure and transcription by nucleosome binding properties of PARP-1. *Cell.* 119:803-814.
- Kleine, H., E. Poreba, K. Lesniewicz, P.O. Hassa, M.O. Hottiger, D.W. Litchfield, B.H. Shilton, and B. Luscher. 2008. Substrate-assisted catalysis by PARP10 limits its activity to mono-ADP-ribosylation. *Mol Cell.* 32:57-69.
- Koch-Nolte, F., T. Duffy, M. Nissen, S. Kahl, N. Killeen, V. Ablamunits, F. Haag, and E.H. Leiter. 1999. A new monoclonal antibody detects a developmentally regulated mouse ecto-ADP-ribosyltransferase on T cells: subset distribution, inbred strain variation, and modulation upon T cell activation. *J Immunol.* 163:6014-6022.
- Koch-Nolte, F., and F. Haag. 1997. Mono(ADP-ribosyl)transferases and related enzymes in animal tissues. Emerging gene families. *Adv Exp Med Biol.* 419:1-13.
- Koch-Nolte, F., F. Haag, R. Braren, M. Kuhl, J. Hoovers, S. Balasubramanian, F. Bazan, and H.G. Thiele. 1997. Two novel human members of an emerging mammalian gene family related to mono-ADP-ribosylating bacterial toxins. *Genomics.* 39:370-376.
- Koch-Nolte, F., S. Kernstock, C. Mueller-Dieckmann, M.S. Weiss, and F. Haag. 2008. Mammalian ADP-ribosyltransferases and ADP-ribosylhydrolases. *Front Biosci.* 13:6716-6729.
- Koch-Nolte, F., J. Klein, C. Hollmann, M. Kuhl, F. Haag, H.R. Gaskins, E. Leiter, and H.G. Thiele. 1995. Defects in the structure and expression of the genes for the T cell marker Rt6 in NZW and (NZB x NZW)F1 mice. *Int Immunol.* 7:883-890.

- Koehler, C., L. Carlier, D. Veggi, E. Balducci, F. Di Marcello, M. Ferrer-Navarro, M. Pizza, X. Daura, M. Soriani, R. Boelens, and A.M. Bonvin. 2011. Structural and biochemical characterization of NarE, an iron-containing ADP-ribosyltransferase from Neisseria meningitidis. *J Biol Chem.* 286:14842-14851.
- Kraus, W.L. 2008. Transcriptional control by PARP-1: chromatin modulation, enhancer-binding, coregulation, and insulation. *Curr Opin Cell Biol.* 20:294-302.
- Kraus, W.L., and J.T. Lis. 2003. PARP goes transcription. *Cell.* 113:677-683.
- Krishnakumar, R., M.J. Gamble, K.M. Frizzell, J.G. Berrocal, M. Kininis, and W.L. Kraus. 2008. Reciprocal binding of PARP-1 and histone H1 at promoters specifies transcriptional outcomes. *Science.* 319:819-821.
- Krishnakumar, R., and W.L. Kraus. 2010a. The PARP side of the nucleus: molecular actions, physiological outcomes, and clinical targets. *Mol Cell.* 39:8-24.
- Krishnakumar, R., and W.L. Kraus. 2010b. PARP-1 regulates chromatin structure and transcription through a KDM5B-dependent pathway. *Mol Cell.* 39:736-749.
- Krueger, K.M., and J.T. Barbieri. 1995. The family of bacterial ADP-ribosylating exotoxins. *Clin Microbiol Rev.* 8:34-47.
- Kuimov, A.N., D.V. Kuprash, V.N. Petrov, K.K. Vdovichenko, M.J. Scanlan, C.V. Jongeneel, M.A. Lagarkova, and S.A. Nedospasov. 2001. Cloning and characterization of TNKL, a member of tankyrase gene family. *Genes Immun.* 2:52-55.
- Kumar, V., J.E. Carlson, K.A. Ohgi, T.A. Edwards, D.W. Rose, C.R. Escalante, M.G. Rosenfeld, and A.K. Aggarwal. 2002. Transcription

corepressor CtBP is an NAD(+)-regulated dehydrogenase. *Mol Cell.* 10:857-869.

- Kurosaki, T., H. Ushiro, Y. Mitsuuchi, S. Suzuki, M. Matsuda, Y. Matsuda, N. Katunuma, K. Kangawa, H. Matsuo, T. Hirose, and et al. 1987. Primary structure of human poly(ADP-ribose) synthetase as deduced from cDNA sequence. *J Biol Chem.* 262:15990-15997.
- Landry, J., J.T. Slama, and R. Sternglanz. 2000. Role of NAD(+) in the deacetylase activity of the SIR2-like proteins. *Biochem Biophys Res Commun.* 278:685-690.
- Langelier, M.F., D.D. Ruhl, J.L. Planck, W.L. Kraus, and J.M. Pascal. 2010. The Zn3 domain of human poly(ADP-ribose) polymerase-1 (PARP-1) functions in both DNA-dependent poly(ADP-ribose) synthesis activity and chromatin compaction. *J Biol Chem.* 285:18877-18887.
- Langelier, M.F., K.M. Servent, E.E. Rogers, and J.M. Pascal. 2008. A third zinc-binding domain of human poly(ADP-ribose) polymerase-1 coordinates DNA-dependent enzyme activation. *J Biol Chem.* 283:4105-4114.
- Lee, H.C., and R. Aarhus. 1991. ADP-ribosyl cyclase: an enzyme that cyclizes NAD+ into a calcium-mobilizing metabolite. *Cell Regul.* 2:203-209.
- Lencer, W.I., T.R. Hirst, and R.K. Holmes. 1999. Membrane traffic and the cellular uptake of cholera toxin. *Biochim Biophys Acta.* 1450:177-190.
- Leung, A.K., S. Vyas, J.E. Rood, A. Bhutkar, P.A. Sharp, and P. Chang. 2011. Poly(ADP-ribose) regulates stress responses and microRNA activity in the cytoplasm. *Mol Cell.* 42:489-499.

- Levine, T.P., C. Rabouille, R.H. Kieckbusch, and G. Warren. 1996. Binding of the vesicle docking protein p115 to Golgi membranes is inhibited under mitotic conditions. *J Biol Chem.* 271:17304-17311.
- Liberali, P., E. Kakkonen, G. Turacchio, C. Valente, A. Spaar, G. Perinetti, R.A. Bockmann, D. Corda, A. Colanzi, V. Marjomaki, and A. Luini. 2008. The closure of Pak1-dependent macropinosomes requires the phosphorylation of CtBP1/BARS. *EMBO J.* 27:970-981.
- Liew, C.K., M. Crossley, J.P. Mackay, and H.R. Nicholas. 2007. Solution structure of the THAP domain from Caenorhabditis elegans C-terminal binding protein (CtBP). *J Mol Biol.* 366:382-390.
- Lin, X., B. Sun, M. Liang, Y.Y. Liang, A. Gast, J. Hildebrand, F.C. Brunicardi, F. Melchior, and X.H. Feng. 2003. Opposed regulation of corepressor CtBP by SUMOylation and PDZ binding. *Mol Cell.* 11:1389-1396.
- Lippincott-Schwartz, J., L. Yuan, C. Tipper, M. Amherdt, L. Orci, and R.D. Klausner. 1991. Brefeldin A's effects on endosomes, lysosomes, and the TGN suggest a general mechanism for regulating organelle structure and membrane traffic. *Cell.* 67:601-616.
- Lippincott-Schwartz, J., L.C. Yuan, J.S. Bonifacino, and R.D. Klausner. 1989. Rapid redistribution of Golgi proteins into the ER in cells treated with brefeldin A: evidence for membrane cycling from Golgi to ER. *Cell.* 56:801-813.
- Liu, Q., R. Graeff, I.A. Kriksunov, H. Jiang, B. Zhang, N. Oppenheimer, H. Lin, B.V. Potter, H.C. Lee, and Q. Hao. 2009. Structural basis for enzymatic evolution from a dedicated ADP-ribosyl cyclase to a multifunctional NAD hydrolase. *J Biol Chem.* 284:27637-27645.

- Liu, Q., I.A. Kriksunov, R. Graeff, C. Munshi, H.C. Lee, and Q. Hao. 2005. Crystal structure of human CD38 extracellular domain. *Structure.* 13:1331-1339.
- Liu, Q., I.A. Kriksunov, H. Jiang, R. Graeff, H. Lin, H.C. Lee, and Q. Hao. 2008. Covalent and noncovalent intermediates of an NAD utilizing enzyme, human CD38. *Chem Biol.* 15:1068-1078.
- Liu, Y., B.E. Snow, V.A. Kickhoefer, N. Erdmann, W. Zhou, A. Wakeham, M. Gomez, L.H. Rome, and L. Harrington. 2004. Vault poly(ADP-ribose) polymerase is associated with mammalian telomerase and is dispensable for telomerase function and vault structure in vivo. *Mol Cell Biol.* 24:5314-5323.
- Lonskaya, I., V.N. Potaman, L.S. Shlyakhtenko, E.A. Oussatcheva, Y.L. Lyubchenko, and V.A. Soldatenkov. 2005. Regulation of poly(ADP-ribose) polymerase-1 by DNA structure-specific binding. *J Biol Chem.* 280:17076-17083.
- Lorente-Rodriguez, A., and C. Barlowe. 2011. Entry and Exit Mechanisms at the cis-Face of the Golgi Complex. *Cold Spring Harb Perspect Biol.* 3.
- Loseva, O., A.S. Jemth, H.E. Bryant, H. Schuler, L. Lehtio, T. Karlberg, and T. Helleday. 2010. PARP-3 is a mono-ADP-ribosylase that activates PARP-1 in the absence of DNA. *J Biol Chem.* 285:8054-8060.
- Lowe, M., N. Nakamura, and G. Warren. 1998a. Golgi division and membrane traffic. *Trends Cell Biol.* 8:40-44.
- Lowe, M., C. Rabouille, N. Nakamura, R. Watson, M. Jackman, E. Jamsa, D. Rahman, D.J. Pappin, and G. Warren. 1998b. Cdc2 kinase directly phosphorylates the cis-Golgi matrix protein GM130 and is required for Golgi fragmentation in mitosis. *Cell.* 94:783-793.

- Lupi, R., D. Corda, and M. Di Girolamo. 2000. Endogenous ADP-ribosylation of the G protein beta subunit prevents the inhibition of type 1 adenylyl cyclase. *J Biol Chem.* 275:9418-9424.
- Lyons, R.J., R. Deane, D.K. Lynch, Z.S. Ye, G.M. Sanderson, H.J. Eyre, G.R. Sutherland, and R.J. Daly. 2001. Identification of a novel human tankyrase through its interaction with the adaptor protein Grb14. *J Biol Chem.* 276:17172-17180.
- Ma, Q., K.T. Baldwin, A.J. Renzelli, A. McDaniel, and L. Dong. 2001. TCDD-inducible poly(ADP-ribose) polymerase: a novel response to 2,3,7,8-tetrachlorodibenzo-p-dioxin. *Biochem Biophys Res Commun.* 289:499-506.
- Malanga, M., J.M. Pleschke, H.E. Kleczkowska, and F.R. Althaus. 1998. Poly(ADP-ribose) binds to specific domains of p53 and alters its DNA binding functions. *J Biol Chem.* 273:11839-11843.
- Malavasi, F., S. Deaglio, R. Damle, G. Cutrona, M. Ferrarini, and N. Chiorazzi. 2011. CD38 and chronic lymphocytic leukemia: a decade later. *Blood.*
- Malavasi, F., S. Deaglio, A. Funaro, E. Ferrero, A.L. Horenstein, E. Ortolan, T. Vaisitti, and S. Aydin. 2008. Evolution and function of the ADP ribosyl cyclase/CD38 gene family in physiology and pathology. *Physiol Rev.* 88:841-886.
- Mani-Telang, P., and D.N. Arnosti. 2007. Developmental expression and phylogenetic conservation of alternatively spliced forms of the C-terminal binding protein corepressor. *Dev Genes Evol.* 217:127-135.
- Mann, M., and O.N. Jensen. 2003. Proteomic analysis of post-translational modifications. *Nat Biotechnol.* 21:255-261.

- Mao, Z., C. Hine, X. Tian, M. Van Meter, M. Au, A. Vaidya, A. Seluanov, and V. Gorbunova. 2011. SIRT6 promotes DNA repair under stress by activating PARP1. *Science.* 332:1443-1446.
- Maresso, A.W., M.R. Baldwin, and J.T. Barbieri. 2004. Ezrin/radixin/moesin proteins are high affinity targets for ADP-ribosylation by Pseudomonas aeruginosa ExoS. *J Biol Chem.* 279:38402-38408.
- Masson, M., C. Niedergang, V. Schreiber, S. Muller, J. Menissier-de Murcia, and G. de Murcia. 1998. XRCC1 is specifically associated with poly(ADP-ribose) polymerase and negatively regulates its activity following DNA damage. *Mol Cell Biol.* 18:3563-3571.
- McLauchlan, H., J. Newell, N. Morrice, A. Osborne, M. West, and E. Smythe. 1998. A novel role for Rab5-GDI in ligand sequestration into clathrin-coated pits. *Curr Biol.* 8:34-45.
- Mehrotra, P., J.P. Riley, R. Patel, F. Li, L. Voss, and S. Goenka. 2011. PARP-14 functions as a transcriptional switch for Stat6-dependent gene activation. *J Biol Chem.* 286:1767-1776.
- Mendez, L.M., J.M. Polo, J.J. Yu, M. Krupski, B.B. Ding, A. Melnick, and B.H. Ye. 2008. CtBP is an essential corepressor for BCL6 autoregulation. *Mol Cell Biol.* 28:2175-2186.
- Mendoza-Alvarez, H., and R. Alvarez-Gonzalez. 1993. Poly(ADP-ribose) polymerase is a catalytic dimer and the automodification reaction is intermolecular. *J Biol Chem.* 268:22575-22580.
- Menissier de Murcia, J., M. Ricoul, L. Tartier, C. Niedergang, A. Huber, F. Dantzer, V. Schreiber, J.C. Ame, A. Dierich, M. LeMeur, L. Sabatier, P. Chambon, and G. de Murcia. 2003. Functional interaction between PARP-1

and PARP-2 in chromosome stability and embryonic development in mouse. *EMBO J.* 22:2255-2263.

- Messner, S., M. Altmeyer, H. Zhao, A. Pozivil, B. Roschitzki, P. Gehrig, D. Rutishauser, D. Huang, A. Caflisch, and M.O. Hottiger. 2010. PARP1 ADP-ribosylates lysine residues of the core histone tails. *Nucleic Acids Res.* 38:6350-6362.
- Michan, S., and D. Sinclair. 2007. Sirtuins in mammals: insights into their biological function. *Biochem J.* 404:1-13.
- Michishita, E., J.Y. Park, J.M. Burneskis, J.C. Barrett, and I. Horikawa. 2005. Evolutionarily conserved and nonconserved cellular localizations and functions of human SIRT proteins. *Mol Biol Cell.* 16:4623-4635.
- Mirnezami, A.H., S.J. Campbell, M. Darley, J.N. Primrose, P.W. Johnson, and J.P. Blaydes. 2003. Hdm2 recruits a hypoxia-sensitive corepressor to negatively regulate p53-dependent transcription. *Curr Biol.* 13:1234-1239.
- Misteli, T., and G. Warren. 1994. COP-coated vesicles are involved in the mitotic fragmentation of Golgi stacks in a cell-free system. *J Cell Biol.* 125:269-282.
- Monetta, P., I. Slavin, N. Romero, and C. Alvarez. 2007. Rab1b interacts with GBF1 and modulates both ARF1 dynamics and COPI association. *Mol Biol Cell.* 18:2400-2410.
- Moyer, B.D., B.B. Allan, and W.E. Balch. 2001. Rab1 interaction with a GM130 effector complex regulates COPII vesicle cis--Golgi tethering. *Traffic.* 2:268-276.

- Moynihan, M.R., and A.M. Pappenheimer, Jr. 1981. Kinetics of adenosinediphosphoribosylation of elongation factor 2 in cells exposed to diphtheria toxin. *Infect Immun.* 32:575-582.
- Mroz, E.A., A.H. Baird, W.A. Michaud, and J.W. Rocco. 2008. COOH-terminal binding protein regulates expression of the p16INK4A tumor suppressor and senescence in primary human cells. *Cancer Res.* 68:6049-6053.
- Muramatsu, Y., H. Tahara, T. Ono, T. Tsuruo, and H. Seimiya. 2008. Telomere elongation by a mutant tankyrase 1 without TRF1 poly(ADP-ribosyl)ation. *Exp Cell Res.* 314:1115-1124.
- Nadauld, L.D., R. Phelps, B.C. Moore, A. Eisinger, I.T. Sandoval, S. Chidester, P.W. Peterson, E.J. Manos, B. Sklow, R.W. Burt, and D.A. Jones. 2006. Adenomatous polyposis coli control of C-terminal binding protein-1 stability regulates expression of intestinal retinol dehydrogenases. *J Biol Chem.* 281:37828-37835.
- Nakamura, N., M. Lowe, T.P. Levine, C. Rabouille, and G. Warren. 1997. The vesicle docking protein p115 binds GM130, a cis-Golgi matrix protein, in a mitotically regulated manner. *Cell.* 89:445-455.
- Nardini, M., S. Spano, C. Cericola, A. Pesce, A. Massaro, E. Millo, A. Luini, D. Corda, and M. Bolognesi. 2003. CtBP/BARS: a dual-function protein involved in transcription co-repression and Golgi membrane fission. *EMBO J.* 22:3122-3130.
- Nardini, M., D. Svergun, P.V. Konarev, S. Spano, M. Fasano, C. Bracco, A. Pesce, A. Donadini, C. Cericola, F. Secundo, A. Luini, D. Corda, and M. Bolognesi. 2006. The C-terminal domain of the transcriptional corepressor CtBP is intrinsically unstructured. *Protein Sci.* 15:1042-1050.

- Nardini, M., C. Valente, S. Ricagno, A. Luini, D. Corda, and M. Bolognesi. 2009. CtBP1/BARS Gly172-->Glu mutant structure: impairing NAD(H)-binding and dimerization. *Biochem Biophys Res Commun.* 381:70-74.
- Nguewa, P.A., M.A. Fuertes, B. Valladares, C. Alonso, and J.M. Perez. 2005. Poly(ADP-ribose) polymerases: homology, structural domains and functions. Novel therapeutical applications. *Prog Biophys Mol Biol.* 88:143-172.
- Nibu, Y., H. Zhang, E. Bajor, S. Barolo, S. Small, and M. Levine. 1998. dCtBP mediates transcriptional repression by Knirps, Kruppel and Snail in the Drosophila embryo. *EMBO J.* 17:7009-7020.
- Obritsch, M.D., D.N. Fish, R. MacLaren, and R. Jung. 2005. Nosocomial infections due to multidrug-resistant Pseudomonas aeruginosa: epidemiology and treatment options. *Pharmacotherapy.* 25:1353-1364.
- Oka, S., J. Kato, and J. Moss. 2006. Identification and characterization of a mammalian 39-kDa poly(ADP-ribose) glycohydrolase. *J Biol Chem.* 281:705-713.
- Okazaki, I.J., H.J. Kim, N.G. McElvaney, E. Lesma, and J. Moss. 1996. Molecular characterization of a glycosylphosphatidylinositol-linked ADP-ribosyltransferase from lymphocytes. *Blood.* 88:915-921.
- Okazaki, I.J., and J. Moss. 1998. Glycosylphosphatidylinositol-anchored and secretory isoforms of mono-ADP-ribosyltransferases. *J Biol Chem.* 273:23617-23620.
- Okazaki, I.J., and J. Moss. 1999. Characterization of glycosylphosphatidylinositiol-anchored, secreted, and intracellular vertebrate mono-ADP-ribosyltransferases. *Annu Rev Nutr.* 19:485-509.

- Okazaki, I.J., A. Zolkiewska, M.S. Nightingale, and J. Moss. 1994. Immunological and structural conservation of mammalian skeletal muscle glycosylphosphatidylinositol-linked ADP-ribosyltransferases. *Biochemistry.* 33:12828-12836.
- Ortolan, E., P. Vacca, A. Capobianco, E. Armando, F. Crivellin, A. Horenstein, and F. Malavasi. 2002. CD157, the Janus of CD38 but with a unique personality. *Cell Biochem Funct.* 20:309-322.
- Otto, H., P.A. Reche, F. Bazan, K. Dittmar, F. Haag, and F. Koch-Nolte. 2005. In silico characterization of the family of PARP-like poly(ADP-ribosyl)transferases (pARTs). *BMC Genomics.* 6:139.
- Pan, P.W., J.L. Feldman, M.K. Devries, A. Dong, A.M. Edwards, and J.M. Denu. 2011. Structure and biochemical functions of SIRT6. *J Biol Chem.* 286:14575-14587.
- Panzeter, P.L., and F.R. Althaus. 1990. High resolution size analysis of ADP-ribose polymers using modified DNA sequencing gels. *Nucleic Acids Res.* 18:2194.
- Paone, G., L.A. Stevens, R.L. Levine, C. Bourgeois, W.K. Steagall, B.R. Gochuico, and J. Moss. 2006. ADP-ribosyltransferase-specific modification of human neutrophil peptide-1. *J Biol Chem.* 281:17054-17060.
- Paone, G., A. Wada, L.A. Stevens, A. Matin, T. Hirayama, R.L. Levine, and J. Moss. 2002. ADP ribosylation of human neutrophil peptide-1 regulates its biological properties. *Proc Natl Acad Sci U S A.* 99:8231-8235.
- Pavri, R., B. Lewis, T.K. Kim, F.J. Dilworth, H. Erdjument-Bromage, P. Tempst, G. de Murcia, R. Evans, P. Chambon, and D. Reinberg. 2005. PARP-1

determines specificity in a retinoid signaling pathway via direct modulation of mediator. *Mol Cell.* 18:83-96.

- Pena, C., J.M. Garcia, V. Garcia, J. Silva, G. Dominguez, R. Rodriguez, C. Maximiano, A. Garcia de Herreros, A. Munoz, and F. Bonilla. 2006. The expression levels of the transcriptional regulators p300 and CtBP modulate the correlations between SNAIL, ZEB1, E-cadherin and vitamin D receptor in human colon carcinomas. *Int J Cancer.* 119:2098-2104.
- Peng, G., and S.Y. Lin. 2011. Exploiting the homologous recombination DNA repair network for targeted cancer therapy. *World J Clin Oncol.* 2:73-79.
- Peyroche, A., B. Antonny, S. Robineau, J. Acker, J. Cherfils, and C.L. Jackson. 1999. Brefeldin A acts to stabilize an abortive ARF-GDP-Sec7 domain protein complex: involvement of specific residues of the Sec7 domain. *Mol Cell.* 3:275-285.
- Phan, R.T., and R. Dalla-Favera. 2004. The BCL6 proto-oncogene suppresses p53 expression in germinal-centre B cells. *Nature.* 432:635-639.
- Pleschke, J.M., H.E. Kleczkowska, M. Strohm, and F.R. Althaus. 2000. Poly(ADP-ribose) binds to specific domains in DNA damage checkpoint proteins. *J Biol Chem.* 275:40974-40980.
- Poirier, G.G., G. de Murcia, J. Jongstra-Bilen, C. Niedergang, and P. Mandel. 1982. Poly(ADP-ribosyl)ation of polynucleosomes causes relaxation of chromatin structure. *Proc Natl Acad Sci U S A.* 79:3423-3427.
- Preisinger, C., R. Korner, M. Wind, W.D. Lehmann, R. Kopajtich, and F.A. Barr. 2005. Plk1 docking to GRASP65 phosphorylated by Cdk1 suggests a mechanism for Golgi checkpoint signalling. *EMBO J.* 24:753-765.

- Quinlan, K.G., M. Nardini, A. Verger, P. Francescato, P. Yaswen, D. Corda, M. Bolognesi, and M. Crossley. 2006a. Specific recognition of ZNF217 and other zinc finger proteins at a surface groove of C-terminal binding proteins. *Mol Cell Biol.* 26:8159-8172.
- Quinlan, K.G., A. Verger, A. Kwok, S.H. Lee, J. Perdomo, M. Nardini, M. Bolognesi, and M. Crossley. 2006b. Role of the C-terminal binding protein PXDLS motif binding cleft in protein interactions and transcriptional repression. *Mol Cell Biol.* 26:8202-8213.
- Raval-Fernandes, S., V.A. Kickhoefer, C. Kitchen, and L.H. Rome. 2005. Increased susceptibility of vault poly(ADP-ribose) polymerase-deficient mice to carcinogen-induced tumorigenesis. *Cancer Res.* 65:8846-8852.
- Reale, A., G.D. Matteis, G. Galleazzi, M. Zampieri, and P. Caiafa. 2005. Modulation of DNMT1 activity by ADP-ribose polymers. *Oncogene.* 24:13-19.
- Rechsteiner, M., D. Hillyard, and B.M. Olivera. 1976. Turnover at nicotinamide adenine dinucleotide in cultures of human cells. *J Cell Physiol.* 88:207-217.
- Reeder, R.H., K. Ueda, T. Honjo, Y. Nishizuka, and O. Hayaishi. 1967. Studies on the polymer of adenosine diphosphate ribose. II. Characterization of the polymer. *J Biol Chem.* 242:3172-3179.
- Riefler, G.M., and B.L. Firestein. 2001. Binding of neuronal nitric-oxide synthase (nNOS) to carboxyl-terminal-binding protein (CtBP) changes the localization of CtBP from the nucleus to the cytosol: a novel function for targeting by the PDZ domain of nNOS. *J Biol Chem.* 276:48262-48268.

- Rine, J., J.N. Strathern, J.B. Hicks, and I. Herskowitz. 1979. A suppressor of mating-type locus mutations in Saccharomyces cerevisiae: evidence for and identification of cryptic mating-type loci. *Genetics*. 93:877-901.
- Rippmann, J.F., K. Damm, and A. Schnapp. 2002. Functional characterization of the poly(ADP-ribose) polymerase activity of tankyrase 1, a potential regulator of telomere length. *J Mol Biol*. 323:217-224.
- Rouleau, M., D. McDonald, P. Gagne, M.E. Ouellet, A. Droit, J.M. Hunter, S. Dutertre, C. Prigent, M.J. Hendzel, and G.G. Poirier. 2007. PARP-3 associates with polycomb group bodies and with components of the DNA damage repair machinery. *J Cell Biochem*. 100:385-401.
- Sandkvist, M., M. Bagdasarian, and S.P. Howard. 2000. Characterization of the multimeric Eps complex required for cholera toxin secretion. *Int J Med Microbiol*. 290:345-350.
- Santella, L. 2005. NAADP: a new second messenger comes of age. *Mol Interv*. 5:70-72.
- Satoh, M.S., and T. Lindahl. 1992. Role of poly(ADP-ribose) formation in DNA repair. *Nature*. 356:356-358.
- Sauve, A.A., I. Celic, J. Avalos, H. Deng, J.D. Boeke, and V.L. Schramm. 2001. Chemistry of gene silencing: the mechanism of NAD+-dependent deacetylation reactions. *Biochemistry*. 40:15456-15463.
- Sauve, A.A., C. Wolberger, V.L. Schramm, and J.D. Boeke. 2006. The biochemistry of sirtuins. *Annu Rev Biochem*. 75:435-465.
- Saxena, A., L.H. Wong, P. Kalitsis, E. Earle, L.G. Shaffer, and K.H. Choo. 2002. Poly(ADP-ribose) polymerase 2 localizes to mammalian active

centromeres and interacts with PARP-1, Cenpa, Cenpb and Bub3, but not Cenpc. *Hum Mol Genet.* 11:2319-2329.

- Saxty, B.A., M. Yadollahi-Farsani, P.D. Upton, S.R. Johnstone, and J. MacDermot. 2001. Inactivation of platelet-derived growth factor-BB following modification by ADP-ribosyltransferase. *Br J Pharmacol.* 133:1219-1226.
- Sbodio, J.I., and N.W. Chi. 2002. Identification of a tankyrase-binding motif shared by IRAP, TAB182, and human TRF1 but not mouse TRF1. NuMA contains this RXXPDG motif and is a novel tankyrase partner. *J Biol Chem.* 277:31887-31892.
- Schaeper, U., J.M. Boyd, S. Verma, E. Uhlmann, T. Subramanian, and G. Chinnadurai. 1995. Molecular cloning and characterization of a cellular phosphoprotein that interacts with a conserved C-terminal domain of adenovirus E1A involved in negative modulation of oncogenic transformation. *Proc Natl Acad Sci U S A.* 92:10467-10471.
- Scher, M.B., A. Vaquero, and D. Reinberg. 2007. SirT3 is a nuclear NAD+-dependent histone deacetylase that translocates to the mitochondria upon cellular stress. *Genes Dev.* 21:920-928.
- Scheuplein, F., S. Adriouch, G. Glowacki, F. Haag, M. Seman, and F. Koch-Nolte. 2003. Triggering of T-cell apoptosis by toxin-related ecto-ADP-ribosyltransferase ART2. *Ann N Y Acad Sci.* 1010:296-299.
- Schmitz, F., A. Konigstorfer, and T.C. Sudhof. 2000. RIBEYE, a component of synaptic ribbons: a protein's journey through evolution provides insight into synaptic ribbon function. *Neuron.* 28:857-872.
- Schreiber, V., F. Dantzer, J.C. Ame, and G. de Murcia. 2006. Poly(ADP-ribose): novel functions for an old molecule. *Nat Rev Mol Cell Biol.* 7:517-528.

- Schwer, B., J. Bunkenborg, R.O. Verdin, J.S. Andersen, and E. Verdin. 2006. Reversible lysine acetylation controls the activity of the mitochondrial enzyme acetyl-CoA synthetase 2. *Proc Natl Acad Sci U S A.* 103:10224-10229.
- Schwer, B., B.J. North, R.A. Frye, M. Ott, and E. Verdin. 2002. The human silent information regulator (Sir)2 homologue hSIRT3 is a mitochondrial nicotinamide adenine dinucleotide-dependent deacetylase. *J Cell Biol.* 158:647-657.
- Sciaky, N., J. Presley, C. Smith, K.J. Zaal, N. Cole, J.E. Moreira, M. Terasaki, E. Siggia, and J. Lippincott-Schwartz. 1997. Golgi tubule traffic and the effects of brefeldin A visualized in living cells. *J Cell Biol.* 139:1137-1155.
- Seman, M., S. Adriouch, F. Haag, and F. Koch-Nolte. 2004. Ecto-ADP-ribosyltransferases (ARTs): emerging actors in cell communication and signaling. *Curr Med Chem.* 11:857-872.
- Seman, M., S. Adriouch, F. Scheuplein, C. Krebs, D. Freese, G. Glowacki, P. Deterre, F. Haag, and F. Koch-Nolte. 2003. NAD-induced T cell death: ADP-ribosylation of cell surface proteins by ART2 activates the cytolytic P2X7 purinoceptor. *Immunity.* 19:571-582.
- Shah, G.M., D. Poirier, C. Duchaine, G. Brochu, S. Desnoyers, J. Lagueux, A. Verreault, J.C. Hoflack, J.B. Kirkland, and G.G. Poirier. 1995. Methods for biochemical study of poly(ADP-ribose) metabolism in vitro and in vivo. *Anal Biochem.* 227:1-13.
- Shall, S., and G. de Murcia. 2000. Poly(ADP-ribose) polymerase-1: what have we learned from the deficient mouse model? *Mutat Res.* 460:1-15.

- Shi, Y., J. Sawada, G. Sui, B. Affar el, J.R. Whetstine, F. Lan, H. Ogawa, M.P. Luke, and Y. Nakatani. 2003. Coordinated histone modifications mediated by a CtBP co-repressor complex. *Nature*. 422:735-738.
- Sierra, J., T. Yoshida, C.A. Joazeiro, and K.A. Jones. 2006. The APC tumor suppressor counteracts beta-catenin activation and H3K4 methylation at Wnt target genes. *Genes Dev*. 20:586-600.
- Sims, R.J., 3rd, and D. Reinberg. 2008. Is there a code embedded in proteins that is based on post-translational modifications? *Nat Rev Mol Cell Biol*. 9:815-820.
- Sixma, T.K., S.E. Pronk, K.H. Kalk, E.S. Wartna, B.A. van Zanten, B. Witholt, and W.G. Hol. 1991. Crystal structure of a cholera toxin-related heat-labile enterotoxin from E. coli. *Nature*. 351:371-377.
- Smith, S., and T. de Lange. 1999. Cell cycle dependent localization of the telomeric PARP, tankyrase, to nuclear pore complexes and centrosomes. *J Cell Sci*. 112 (Pt 21):3649-3656.
- Smith, S., and T. de Lange. 2000. Tankyrase promotes telomere elongation in human cells. *Curr Biol*. 10:1299-1302.
- Smith, S., I. Giriat, A. Schmitt, and T. de Lange. 1998. Tankyrase, a poly(ADP-ribose) polymerase at human telomeres. *Science*. 282:1484-1487.
- Spano, S., M.G. Silletta, A. Colanzi, S. Alberti, G. Fiucci, C. Valente, A. Fusella, M. Salmona, A. Mironov, A. Luini, and D. Corda. 1999. Molecular cloning and functional characterization of brefeldin A-ADP-ribosylated substrate. A novel protein involved in the maintenance of the Golgi structure. *J Biol Chem*. 274:17705-17710.

- States, D.J., T.F. Walseth, and H.C. Lee. 1992. Similarities in amino acid sequences of Aplysia ADP-ribosyl cyclase and human lymphocyte antigen CD38. *Trends Biochem Sci.* 17:495.
- Stein, P.E., A. Boodhoo, G.D. Armstrong, S.A. Cockle, M.H. Klein, and R.J. Read. 1994. The crystal structure of pertussis toxin. *Structure.* 2:45-57.
- Stenmark, H. 2009. Rab GTPases as coordinators of vesicle traffic. *Nat Rev Mol Cell Biol.* 10:513-525.
- Stevens, L.A., C. Bourgeois, R. Bortell, and J. Moss. 2003. Regulatory role of arginine 204 in the catalytic activity of rat alloantigens ART2a and ART2b. *J Biol Chem.* 278:19591-19596.
- Streatfield, S.J., M. Sandkvist, T.K. Sixma, M. Bagdasarian, W.G. Hol, and T.R. Hirst. 1992. Intermolecular interactions between the A and B subunits of heat-labile enterotoxin from Escherichia coli promote holotoxin assembly and stability in vivo. *Proc Natl Acad Sci U S A.* 89:12140-12144.
- Sugimura, T., S. Fujimura, S. Hasegawa, and Y. Kawamura. 1967. Polymerization of the adenosine 5'-diphosphate ribose moiety of NAD by rat liver nuclear enzyme. *Biochim Biophys Acta.* 138:438-441.
- Sun, J., and J.T. Barbieri. 2003. Pseudomonas aeruginosa ExoT ADP-ribosylates CT10 regulator of kinase (Crk) proteins. *J Biol Chem.* 278:32794-32800.
- Sutterlin, C., P. Hsu, A. Mallabiabarrena, and V. Malhotra. 2002. Fragmentation and dispersal of the pericentriolar Golgi complex is required for entry into mitosis in mammalian cells. *Cell.* 109:359-369.
- Swanson, J.A., and C. Watts. 1995. Macropinocytosis. *Trends Cell Biol.* 5:424-428.

- Takada, T., K. Iida, and J. Moss. 1995. Conservation of a common motif in enzymes catalyzing ADP-ribose transfer. Identification of domains in mammalian transferases. *J Biol Chem.* 270:541-544.
- Takeyama, K., R.C. Aguiar, L. Gu, C. He, G.J. Freeman, J.L. Kutok, J.C. Aster, and M.A. Shipp. 2003. The BAL-binding protein BBAP and related Deltex family members exhibit ubiquitin-protein isopeptide ligase activity. *J Biol Chem.* 278:21930-21937.
- Tanner, K.G., J. Landry, R. Sternglanz, and J.M. Denu. 2000. Silent information regulator 2 family of NAD- dependent histone/protein deacetylases generates a unique product, 1-O-acetyl-ADP-ribose. *Proc Natl Acad Sci U S A.* 97:14178-14182.
- Tanno, M., J. Sakamoto, T. Miura, K. Shimamoto, and Y. Horio. 2007. Nucleocytoplasmic shuttling of the NAD+-dependent histone deacetylase SIRT1. *J Biol Chem.* 282:6823-6832.
- Tao, Z., P. Gao, and H.W. Liu. 2009. Identification of the ADP-ribosylation sites in the PARP-1 automodification domain: analysis and implications. *J Am Chem Soc.* 131:14258-14260.
- Timinszky, G., S. Till, P.O. Hassa, M. Hothorn, G. Kustatscher, B. Nijmeijer, J. Colombelli, M. Altmeyer, E.H. Stelzer, K. Scheffzek, M.O. Hottiger, and A.G. Ladurner. 2009. A macrodomain-containing histone rearranges chromatin upon sensing PARP1 activation. *Nat Struct Mol Biol.* 16:923-929.
- Tisdale, E.J., J.R. Bourne, R. Khosravi-Far, C.J. Der, and W.E. Balch. 1992. GTP-binding mutants of rab1 and rab2 are potent inhibitors of vesicular transport from the endoplasmic reticulum to the Golgi complex. *J Cell Biol.* 119:749-761.

- Tsuchiya, M., S.R. Price, S.C. Tsai, J. Moss, and M. Vaughan. 1991. Molecular identification of ADP-ribosylation factor mRNAs and their expression in mammalian cells. *J Biol Chem.* 266:2772-2777.
- Uchida, K., S. Hanai, K. Ishikawa, Y. Ozawa, M. Uchida, T. Sugimura, and M. Miwa. 1993. Cloning of cDNA encoding Drosophila poly(ADP-ribose) polymerase: leucine zipper in the auto-modification domain. *Proc Natl Acad Sci U S A.* 90:3481-3485.
- Vaisitti, T., V. Audrito, S. Serra, C. Bologna, D. Brusa, F. Malavasi, and S. Deaglio. 2011. NAD+-metabolizing ecto-enzymes shape tumor-host interactions: the chronic lymphocytic leukemia model. *FEBS Lett.* 585:1514-1520.
- Valente, C., S. Spano, A. Luini, and D. Corda. 2005. Purification and functional properties of the membrane fissioning protein CtBP3/BARS. *Methods Enzymol.* 404:296-316.
- van der Bliek, A.M. 2005. A sixth sense for Rab5. *Nat Cell Biol.* 7:548-550.
- Vassilev, L.T., C. Tovar, S. Chen, D. Knezevic, X. Zhao, H. Sun, D.C. Heimbrook, and L. Chen. 2006. Selective small-molecule inhibitor reveals critical mitotic functions of human CDK1. *Proc Natl Acad Sci U S A.* 103:10660-10665.
- Venkitaraman, A.R. 2002. Cancer susceptibility and the functions of BRCA1 and BRCA2. *Cell.* 108:171-182.
- Verger, A., K.G. Quinlan, L.A. Crofts, S. Spano, D. Corda, E.P. Kable, F. Braet, and M. Crossley. 2006. Mechanisms directing the nuclear localization of the CtBP family proteins. *Mol Cell Biol.* 26:4882-4894.

- Wacker, D.A., D.D. Ruhl, E.H. Balagamwala, K.M. Hope, T. Zhang, and W.L. Kraus. 2007. The DNA binding and catalytic domains of poly(ADP-ribose) polymerase 1 cooperate in the regulation of chromatin structure and transcription. *Mol Cell Biol.* 27:7475-7485.
- Warren, G., T. Levine, and T. Misteli. 1995. Mitotic disassembly of the mammalian Golgi apparatus. *Trends Cell Biol.* 5:413-416.
- Weigert, R., M.G. Silletta, S. Spano, G. Turacchio, C. Cericola, A. Colanzi, S. Senatore, R. Mancini, E.V. Polishchuk, M. Salmona, F. Facchiano, K.N. Burger, A. Mironov, A. Luini, and D. Corda. 1999. CtBP/BARS induces fission of Golgi membranes by acylating lysophosphatidic acid. *Nature.* 402:429-433.
- Wilde, C., and K. Aktories. 2001. The Rho-ADP-ribosylating C3 exoenzyme from Clostridium botulinum and related C3-like transferases. *Toxicon.* 39:1647-1660.
- Williams, G.T., K.M. Lau, J.M. Coote, and A.P. Johnstone. 1985. NAD metabolism and mitogen stimulation of human lymphocytes. *Exp Cell Res.* 160:419-426.
- Wilson, B.S., C. Nuoffer, J.L. Meinkoth, M. McCaffery, J.R. Feramisco, W.E. Balch, and M.G. Farquhar. 1994. A Rab1 mutant affecting guanine nucleotide exchange promotes disassembly of the Golgi apparatus. *J Cell Biol.* 125:557-571.
- Wilson, C., R. Venditti, L.R. Rega, A. Colanzi, G. D'Angelo, and M.A. De Matteis. 2010. The Golgi apparatus: an organelle with multiple complex functions. *Biochem J.* 433:1-9.

- Xiang, Y., J. Seemann, B. Bisel, S. Punthambaker, and Y. Wang. 2007. Active ADP-ribosylation factor-1 (ARF1) is required for mitotic Golgi fragmentation. *J Biol Chem.* 282:21829-21837.
- Yamamoto-Katayama, S., M. Ariyoshi, K. Ishihara, T. Hirano, H. Jingami, and K. Morikawa. 2002. Crystallographic studies on human BST-1/CD157 with ADP-ribosyl cyclase and NAD glycohydrolase activities. *J Mol Biol.* 316:711-723.
- Yang, J.S., S.Y. Lee, S. Spano, H. Gad, L. Zhang, Z. Nie, M. Bonazzi, D. Corda, A. Luini, and V.W. Hsu. 2005. A role for BARS at the fission step of COPI vesicle formation from Golgi membrane. *EMBO J.* 24:4133-4143.
- Ye, B.H., G. Cattoretti, Q. Shen, J. Zhang, N. Hawe, R. de Waard, C. Leung, M. Nouri-Shirazi, A. Orazi, R.S. Chaganti, P. Rothman, A.M. Stall, P.P. Pandolfi, and R. Dalla-Favera. 1997. The BCL-6 proto-oncogene controls germinal-centre formation and Th2-type inflammation. *Nat Genet.* 16:161-170.
- Ye, J.Z., and T. de Lange. 2004. TIN2 is a tankyrase 1 PARP modulator in the TRF1 telomere length control complex. *Nat Genet.* 36:618-623.
- Yeh, T.Y., J.I. Sbodio, Z.Y. Tsun, B. Luo, and N.W. Chi. 2007. Insulin-stimulated exocytosis of GLUT4 is enhanced by IRAP and its partner tankyrase. *Biochem J.* 402:279-290.
- Ying, W. 2006. NAD+ and NADH in cellular functions and cell death. *Front Biosci.* 11:3129-3148.
- Yu, M., S. Schreek, C. Cerni, C. Schamberger, K. Lesniewicz, E. Poreba, J. Vervoorts, G. Walsemann, J. Grotzinger, E. Kremmer, Y. Mehraein, J. Mertsching, R. Kraft, M. Austen, J. Luscher-Firzlaff, and B. Luscher. 2005.

PARP-10, a novel Myc-interacting protein with poly(ADP-ribose) polymerase activity, inhibits transformation. *Oncogene.* 24:1982-1993.

- Zampieri, M., C. Passananti, R. Calabrese, M. Perilli, N. Corbi, F. De Cave, T. Guastafierro, M.G. Bacalini, A. Reale, G. Amicosante, L. Calabrese, J. Zlatanova, and P. Caiafa. 2009. Parp1 localizes within the Dnmt1 promoter and protects its unmethylated state by its enzymatic activity. *PLoS One.* 4:e4717.
- Zhang, C.L., T.A. McKinsey, J.R. Lu, and E.N. Olson. 2001. Association of COOH-terminal-binding protein (CtBP) and MEF2-interacting transcription repressor (MITR) contributes to transcriptional repression of the MEF2 transcription factor. *J Biol Chem.* 276:35-39.
- Zhang, Q., D.W. Piston, and R.H. Goodman. 2002. Regulation of corepressor function by nuclear NADH. *Science.* 295:1895-1897.
- Zhang, Q., S.Y. Wang, A.C. Nottke, J.V. Rocheleau, D.W. Piston, and R.H. Goodman. 2006. Redox sensor CtBP mediates hypoxia-induced tumor cell migration. *Proc Natl Acad Sci U S A.* 103:9029-9033.
- Zhang, R.G., D.L. Scott, M.L. Westbrook, S. Nance, B.D. Spangler, G.G. Shipley, and E.M. Westbrook. 1995. The three-dimensional crystal structure of cholera toxin. *J Mol Biol.* 251:563-573.
- Zhang, Y., C.W. Burke, K.D. Ryman, and W.B. Klimstra. 2007. Identification and characterization of interferon-induced proteins that inhibit alphavirus replication. *J Virol.* 81:11246-11255.
- Zheng, C.L., T. Sumizawa, X.F. Che, S. Tsuyama, T. Furukawa, M. Haraguchi, H. Gao, T. Gotanda, H.C. Jueng, F. Murata, and S. Akiyama. 2005. Characterization of MVP and VPARP assembly into vault ribonucleoprotein complexes. *Biochem Biophys Res Commun.* 326:100-107.

- Zlatanova, J., and P. Caiafa. 2009. CTCF and its protein partners: divide and rule? *J Cell Sci.* 122:1275-1284.
- Zocchi, E., L. Franco, L. Guida, U. Benatti, A. Bargellesi, F. Malavasi, H.C. Lee, and A. De Flora. 1993. A single protein immunologically identified as CD38 displays NAD+ glycohydrolase, ADP-ribosyl cyclase and cyclic ADP-ribose hydrolase activities at the outer surface of human erythrocytes. *Biochem Biophys Res Commun.* 196:1459-1465.
- Zolkiewska, A. 2005. Ecto-ADP-ribose transferases: cell-surface response to local tissue injury. *Physiology (Bethesda).* 20:374-381.
- Zolkiewska, A., and J. Moss. 1993. Integrin alpha 7 as substrate for a glycosylphosphatidylinositol-anchored ADP-ribosyltransferase on the surface of skeletal muscle cells. *J Biol Chem.* 268:25273-25276.
- Zolkiewska, A., and J. Moss. 1997. The alpha 7 integrin as a target protein for cell surface mono-ADP-ribosylation in muscle cells. *Adv Exp Med Biol.* 419:297-303.
- Zolkiewska, A., M.S. Nightingale, and J. Moss. 1992. Molecular characterization of NAD:arginine ADP-ribosyltransferase from rabbit skeletal muscle. *Proc Natl Acad Sci U S A.* 89:11352-11356.

Acknowledgements

I would like to thank my Supervisors Drs. Daniela Corda, Alberto Luini and Daniela Rhodes for their support and helpful discussions during the course of these investigations, and for their help in writing this thesis.

Special thanks go to Drs. Antonino Colanzi and Stefania Mariggiò for all of their precious suggestions and help, and for the incredible strength that they have given me.

Thanks are also due to all of my colleagues in our Laboratory, for the excellent working atmosphere they have brought in our Laboratory. Special thanks go to Carmen, Giuliana and Raman.

Thanks also to my flatmates Romina and Rossella for their scientific and friendly 'discussions'.

I would also like to thank Dr. Chris Berrie for his precious help with my English.

I want to thank the PhD Programme Coordination Team, of Sandro Banfi and Barbara Zimbardi, for their assistance and management throughout my studies.

I would like to thank Roberta and Anna for their friendship.

A great thank you also goes to my family, because they have always supported me during these years.

My final thanks go to Gerardo, for his attempt to understand the incomprehensible life of a scientific researcher.